Telomere dysfunction and senescence in the ageing lung and age-related lung disease

Jodie Birch

A thesis submitted in partial fulfillment of the requirements for the degree of Doctor of Philosophy

Institute of Cellular Medicine and Newcastle University Institute for Ageing, Newcastle University, UK

November 2014

Abstract

Cellular senescence, the irreversible loss of replicative capacity of somatic cells, has been associated with diseases of accelerated lung ageing, including Chronic Obstructive Pulmonary Disease (COPD). However, the mechanisms underlying senescence of airway epithelial cells, particularly the role of telomere dysfunction in this process, are poorly understood. The aim of this work was to investigate senescence and telomere dysfunction in airway epithelial cells from patients with COPD and bronchiectasis, in the ageing murine lung and in the context of cigarette smoke exposure. DNA damage foci (γH2A.X) and foci associated with telomeres (telomere-associated foci (TAF)), along with other senescence-associated markers, were increased in small airway epithelial cells from patients with COPD, without significant telomere shortening. With age, TAF increased in large and small airway epithelial cells of the murine lung and predicted age-dependent lung emphysema, independently of telomere length. Moreover, fourth generation telomerase-null mice showed early-onset emphysema. Exposure to cigarette smoke was found to increase TAF in large and small airway epithelial cells of the murine lung and in epithelial cells and fibroblasts *in vitro*. Cigarette smoke may accelerate telomere dysfunction *via* reactive oxygen species (ROS) and contribute to Ataxia telangiectasia mutated (ATM)-dependent secretion of pro-inflammatory cytokines interleukin (IL)-6 and IL-8. Inhibition of mechanistic target of rapamycin complex 1 (mTORC1) by rapamycin alleviated age-associated increases in TAF *in vivo* and supressed cigarette smoke-induced increases in TAF and inflammatory cytokine release *in vitro*. Cigarette smoke increases mitochondrial-derived ROS, which is supressed by culturing cells at low oxygen pressure and by treating cells with rapamycin. These results suggest that activation of a DNA damage response at telomeres may be induced by oxidative stress from altered mTOR signalling and/or dysfunctional mitochondria. Telomere dysfunction could contribute to inflammatory processes and the functional decline that occurs in the ageing lung and in the context of cigarette smoke-induced accelerated lung ageing.

Acknowledgments

I would like to thank my supervisors Anthony De Soyza, Andrew Fisher, John Taylor and Joao Passos for their guidance and support during my time as a PhD student.

A number of colleagues have contributed to this work and their contributions have been acknowledged throughout the thesis. In particular, I would like to thank Gail Johnson and Kasim Jiwa from The William Leech Centre for Lung Research for assisting with histology and welcoming me into their lab. I would also like to acknowledge Dr Chris Ward for being so very helpful whenever I needed advice.

I would like to thank all members of the Passos lab for their contribution to this work by helping with experiments and engaging in overall discussions. In particular, I would like to thank Rhys Anderson for teaching me immuno-FISH and answering all my annoying questions, Clara Correia Melo for the invaluable experimental discussions and for being a great friend, Graeme Hewitt for being a technology wizard and helping with MacBook queries, Francisco Marques for being a walking PubMed, and Anthony Lagnado for supplying me with copious amounts of coffee and baking tips! I have never been more grateful to a group of (fabulous) scientists – you were all very welcoming when I joined the Passos lab and were always there to help. Thanks for being friendly, fun and hilarious – you are a joy to work with and my final year would have been impossibly difficult without you guys!

To my Gin Club ladies – Nic, Sonya, Liz and Helen; thanks for the famous office buffets, the inspiration and encouragement to keep on running, for being there through the laughs and the cries, the best and worst times. But most of all, thanks for the gin times – it will forever be a Hendricks with basil and Fever-Tree *light*.

To my dearest Mike, you have been amazing. Thanks for your kindness, for your patience and for making me smile every single day - the toughest days were always made brighter by you, for that I am forever grateful.

To my home girls; Becki, Zara, Shona and Rachel, thanks for being there from the beginning – for the walks into school, the sleepovers, the lifts into college and for always showing interest in my endeavours. Thanks for always supporting me.

To my parents Joan and Michael; thank you for always believing in me and showing me lots of love.

List of Abbreviations

4-HNE	4-hydroxy-2-nonenal
4E-BP1	eIF4E-binding protein 1
53BP1	p53 binding protein 1
8-OHdG	8-hydroxy-2'-deoxyguanosine
APES	Aminopropyltriethoxysilane
AT	Ataxia Telangiectasia
ATM	Ataxia telangiectasia mutated
ATR	ATM and Rad3-related
BALF	Broncho-alveolar lavage fluid
Bax	Bcl-2 associated X protein
Bcl-2	B-cell lymphoma 2
BRAF	V-raf murine sarcoma viral oncogene homolog B1
BSA	Bovine serum albumin
CCFs	Cytoplasmic chromatin fragments
CDC25A	Cell division cycle 25A
CDK	Cyclin-dependent kinase
CDKi	Cyclin-dependent kinase inhibitor
Chk1	Checkpoint kinase 1
Chk2	Checkpoint kinase 2
COPD	Chronic Obstructive Pulmonary Disease
CSE	Cigarette smoke extract
DAB	3,3'-diaminobenzidine
DAPI	4',6-diamidino-2-phenylindole
DDR	DNA damage response
DHR	Dihydrorhodamine
DMEM	Dulbecco's Modified Eagle's Medium
DMSO	Dimethyl sulfoxide
DNA-PK	DNA-dependent protein kinase
DNA-SCARS	DNA segments with chromatin alterations reinforcing senescence
DPX	Di-N-Butyle Phthalate in Xylene
DR	Dietary restriction
DSB	Double-strand break
E2F	Transcription factor activating adenovirus E2 gene

ECM	Extracellular matrix
EDTA	Ethylenediaminetetraacetic acid
eIF4E	Eukaryotic initiation factor 4E
EMT	Epithelial-mesenchymal transition
FBS	Foetal bovine serum
FEV_1	Forced expiratory volume in 1 second
GAPDH	Glyceraldehyde-3-phosphate dehydrogenase
GOLD	Global Initiative for Chronic Obstructive Lung Disease
GRO	Growth regulated oncogene
H&E	Haematoxylin and Eosin
H_2O_2	Hydrogen peroxide
HDAi	Histone deacetylase inhibition
HDM2	Human double minute 2
HP-1	Heterochromatin protein-1
HRP	Horseradish peroxidase
IL	Interleukin
IPF	Idiopathic pulmonary fibrosis
MCP	Monocyte chemo-attractant protein
MCP-1	Monocyte chemotactic protein 1
MDC1	Mediator of DNA damage checkpoint 1
MEK	MAPK/ERK kinase
MMPs	Matrix metalloproteinases
MOS	V-mos Moloney murine sarcoma viral oncogene homolog
MRN	MRE11–RAD50–NBS1
mTOR	Mechanistic target of rapamycin
mTORC1/2	Mechanistic target of rapamycin complex 1/2
NAC	N-acetylcysteine
NAD	Nicotinamide adenine dinucleotide
NAO	10-n-nonyl-acridine orange
NF-κB	Nuclear factor kappa B
NFMP	Non-fat milk protein
NGS	Normal goat serum
NHEJ	Non-homologous end joining
OIS	Oncogene-induced senescence
P38MAPK	p38 mitogen-activated protein kinase

PARP	Poly (ADP-ribose) polymerase
PBS	Phosphate buffered saline
PCNA	Proliferating-cell nuclear antigen
PD	Population doubling
PFA	Paraformaldehyde
PGC1- α	Peroxisome proliferator-activated receptor-gamma coactivator
PI	Propidium iodide
PI3K	Phosphatidylinositol 3-kinase
PI3KK	Phosphatidylinositol 3-kinase-like protein kinase
POT1	Protection of telomeres protein 1
PTEN	Phosphatase and tensin homolog deleted on chromosome 10
Q-FISH	Quantitative fluorescence *in situ* hybridisation
RAF	V-raf-1 murine leukemia viral oncogene homolog
Rap1	Telomeric repeat-binding factor 2-interacting protein 1
RAS	Rat sarcoma
ROS	Reactive oxygen species
RPA	Replication protein A
S6K	S6 kinase
SAHF	Senescence-associated heterochromatic foci
SASP	Senescence associated secretory phenotype
Sen-β-Gal	Senescence associated-β-galactosidase
SIPS	Stress-induced premature senescence
SIRT1	Sirtuin 1
SSB	Single-strand break
SSC	Sodium chloride, sodium citrate
TAF	Telomere-associated foci
TBS	Tris-buffered saline
TE	Trypsin-EDTA
TGF-β	Transforming growth factor- β
TIF	Telomere dysfunction-induced foci
TIN2	TERF1-interacting nuclear factor 2
TNF-α	Tumour necrosis factor-α
TPP1	Tripeptidyl peptidase 1
TRF1	Telomeric repeat-binding factor 1
TRF2	Telomeric repeat-binding factor 2

UV	Ultraviolet
VEGF	Vascular endothelial growth factor
γH2A.X	Phospho-histone 2AX

Table of Contents

List of Tables

List of Figures

Chapter 1. Introduction

1.1 Cellular senescence

Cellular senescence is classically defined as the irreversible loss of division potential in somatic cells (Campisi and d'Adda di Fagagna 2007). Hayflick and Moorehead first described cellular senescence more than 50 years ago when they observed that normal human diploid fibroblasts irreversibly lost the ability to divide in culture following extensive passaging (Hayflick and Moorhead 1961). These cells remained viable for prolonged periods of time in culture but failed to proliferate even in the presence of ample space, nutrients and growth factors. This form of senescence was termed "replicative senescence". Subsequently, other groups found that senescence could occur prior to the onset of replicative senescence, which is known as "stress-induced premature senescence" or SIPS (Kuilman, Michaloglou et al. 2010). Two hypotheses were made following these observations. The first hypothesis, based on the fact that transformed cells proliferate indefinitely in culture, was that cellular senescence acts as an anti-cancer or tumour suppressive mechanism. The second hypothesis stemmed from the knowledge that repair and regeneration of tissues declines with age, thus it was suggested that cellular senescence recapitulates cellular ageing *in vivo* (Hayflick 1965). Therefore senescence was considered to be both beneficial and deleterious *in vivo*: on the one hand, protecting organisms against cancer yet on the other hand contributing to age-dependent tissue dysfunction. The concept that cellular senescence can be both beneficial and harmful to organisms can be explained by an evolutionary theory of ageing: antagonistic pleiotropy (Williams 1957; Campisi 2003). Antagonistic pleiotropy, in the ageing context, suggests that senescence is beneficial to young organisms by acting as a tumour suppressor mechanism and therefore promoting survival. However, the senescence process, which is retained into later life, becomes detrimental to older organisms as senescent cells accumulate with age and contribute to age-related deterioration. There is now considerable evidence that senescence is a potent anti-cancer mechanism (Campisi 2001; Dimri 2005) and mounting evidence implicates senescence in the ageing process (Campisi 2013; van Deursen 2014). In fact, cellular senescence is now accepted as a cellular hallmark of ageing (Lopez-Otin, Blasco et al. 2013). Additionally, it is becoming increasingly recognised that senescence is important for many other diverse biological processes, including wound healing, tissue repair and

embryonic development (Krizhanovsky, Yon et al. 2008; Jun and Lau 2010; Munoz-Espin, Canamero et al. 2013; Storer, Mas et al. 2013).

1.2 Causes of cellular senescence

Cellular senescence can be induced by a range of different stimuli (Campisi and d'Adda di Fagagna 2007; Kuilman, Michaloglou et al. 2010), which will be described in detail in the following sections.

1.2.1 Telomere dysfunction

Telomeres are specialised structures at the ends of chromosomes consisting of repetitive DNA (5'-TTAGGG-3') repeats, which function mainly to protect the ends of linear chromosomes from erosion or fusion by DNA repair processes (Blackburn 1991; d'Adda di Fagagna, Teo et al. 2004). Telomeric repeats are reduced during each S-phase due to the so called "end-replication problem" – the inability of standard DNA polymerases to synthesise DNA in a 3'-5' direction leading to incomplete replication of the lagging strand and progressive telomere shortening, which was predicted to explain Hayflick's observations of finite cell division in cells grown in culture (Olovnikov 1971; Watson 1972). It was later demonstrated that telomeres do in fact shorten with serial passaging, however it was unknown whether telomere shortening was causal in replicative senescence (Harley, Futcher et al. 1990). This was confirmed when it was shown that ectopic expression of the catalytic subunit of telomerase, the enzyme responsible for maintaining telomere length, in normal human cells prevents telomere shortening and senescence (Bodnar, Ouellette et al. 1998). Telomeres are stabilised by a complex of proteins, known as shelterin (de Lange 2005). Six proteins constitute shelterin: telomeric repeat-binding factor 1 (TRF1), TRF2 and protection of telomeres protein 1 (POT1), which recognise the telomere repeat sequence, and TERF1-interacting nuclear factor 2 (TIN2), Tripeptidyl peptidase 1 (TPP1) and telomeric repeat-binding factor 2-interacting protein 1 (RAP1) (de Lange 2005), which arrange mammalian telomeres into a loop structure, known as the T-loop, to protect chromosome ends (Griffith, Comeau et al. 1999). During replicative senescence the progressive loss of telomere repeats destabilises T-loops and consequently increases the probability of telomere uncapping *i.e.* loss of shelterin (Griffith, Comeau et al. 1999). Telomere uncapping due to telomere shortening, has been shown to trigger a classical DNA damage response (DDR) similar to double-strand breaks (DSBs), leading to arrest of cell-cycle progression (d'Adda di Fagagna, Reaper et al. 2003; Takai, Smogorzewska

et al. 2003; Herbig, Jobling et al. 2004). Telomere shortening is not solely a result of the end-replication problem, evidenced by the observations that telomere length is very heterogeneous between cells in the same culture and senescent cells isolated from young cultures can have short telomeres (Lansdorp, Verwoerd et al. 1996; Martin-Ruiz, Saretzki et al. 2004). This suggests that replicative senescence can be stress-dependent. Accordingly, it is known that telomeres are more sensitive to oxidative stress, acquiring oxidative single-strand damage at a much faster rate than the bulk of the genome (Petersen, Saretzki et al. 1998). This is possibly due to the fact that telomere repeats contain guanine triplets (Henle, Han et al. 1999), which are particularly sensitive to oxidative modifications, and that repair of single-strand breaks (SSBs) is less efficient at telomeres (Petersen, Saretzki et al. 1998). Thus, telomeres enter DNA replication with higher frequencies of SSBs compared to the rest of the genome, which contributes significantly to telomere erosion (von Zglinicki, Saretzki et al. 1995). In accordance, it has been demonstrated that chronic, low-grade oxidative stress shortens telomeres and reduces replicative lifespan, whereas overexpression of anti-oxidant enzymes or the use of free-radical scavengers reverses it (von Zglinicki, Pilger et al. 2000; von Zglinicki 2002; Serra, von Zglinicki et al. 2003). Additionally, low oxygen has been shown to extend replicative lifespan and reduce telomere shortening rates in human fibroblasts by decreasing reactive oxygen species (ROS) generation (Richter and von Zglinicki 2007). Mitochondrial-derived oxidative stress is thought to contribute to telomere dysfunction (Passos, Saretzki et al. 2007). It was shown that anti-oxidants selectively targeted to the mitochondria counteract telomere shortening and increase lifespan of fibroblasts under mild oxidative stress (Saretzki, Murphy et al. 2003). Similarly, treatments with agents that affect mitochondrial ROS generation extend lifespan and decelerate telomere shortening (Kang, Lee et al. 2006). Additionally, mild chronic uncoupling of mitochondria improves telomere maintenance and extends telomere-dependent lifespan due to a reduction in mitochondrial ROS generation (Passos, Saretzki et al. 2007). Overall, these data suggest that telomere shortening occurs due to the end-replication problem in combination with other factors, such as oxidative stress-induced damage.

Telomere dysfunction is not only contributed to by telomere shortening. Our group recently demonstrated that genotoxic and oxidative damage induces a DDR at both genomic and telomeric regions (referred to as telomere associated DNA damage foci or TAF) and this damage occurs irrespectively of telomerase expression (Hewitt, Jurk et al. 2012). Additionally, it was observed that TAF increase in the murine gut and liver with age but there was no significant difference found between telomere length

distributions in TAF and non-TAF, suggesting that telomere length is not the sole defining factor in TAF induction (Hewitt, Jurk et al. 2012). Similarly, in a murine model for chronic-inflammation where the ageing process is accelerated, telomere dysfunction was not associated with shortened telomere length (Jurk, Wilson et al. 2014). Furthermore, our lab demonstrated that while the great majority of DDR foci were resolved soon after their formation, TAF were relatively long-lived (Hewitt, Jurk et al. 2012). These data were independently confirmed by d'Adda di Fagagna's group (Fumagalli, Rossiello et al. 2012). Additionally, the authors show that DDR activation at telomeres is not associated with loss of TRF2 or telomere shortening. The authors suggest that this persistence of DNA damage foci at telomeres occurs because telomeres resist DNA-damage repair. Consistent with this notion, the authors demonstrated that DSBs induced in budding yeast failed to be repaired when next to telomere repeats due to the supressed recruitment of ligase IV, the enzyme responsible for DNA ligation in non-homologous end joining (NHEJ) (Fumagalli, Rossiello et al. 2012). These findings are supported by earlier reports demonstrating that ligase IV-mediated NHEJ is inhibited at telomeres by components of the shelterin complex, such as TRF2, as a mechanism of preventing end-to-end fusions (Smogorzewska and de Lange 2002; Bae and Baumann 2007). Similarly, it was shown that loss of TRF2 contributes to the activation of a DDR at telomeres and senescence (van Steensel, Smogorzewska et al. 1998). Cesare *et al*. have proposed a three-state model of telomere-end protection. In this model, the 'closed state' is a telomere-length dependent structure (likely the T-loop) that protects chromosome ends against a DDR. The 'intermediate state' is suggested to offer partial protection: a DDR is induced at telomeres but sufficient shelterin is bound to prevent end-to-end fusions. The 'uncapped state' is both DDR positive and fusogenic and might result from insufficient shelterin binding (i.e. telomere uncapping) (Cesare, Kaul et al. 2009). Thus, telomeres that contribute to persistent DDR signalling and senescence are likely in the intermediate state and have sufficient shelterin still bound. In accordance, it has been demonstrated that during replicative senescence of human fibroblasts, DDR positive telomeres retain TRF2 and its binding partner RAP1 and are not associated with end-to-end fusions (Kaul, Cesare et al. 2012).

Taken overall, this suggests that telomere dysfunction, whether due to telomere shortening or damage at longer telomeres, fuels persistent DDR signalling. This highlights the importance of telomeres in both replicative senescence and in SIPS, in response to a variety of stresses (Suram and Herbig 2014).

1.2.2 Non-telomeric DNA damage-induced senescence

Senescence that occurs prior to the stage at which it is induced by telomere shortening is known as SIPS (Kuilman, Michaloglou et al. 2010), which can be induced by telomeric or non-telomeric DNA damage. Genomic DNA damage occurring at non-telomeric sites, if severe enough, may also generate the persistent DDR signalling needed for senescence growth arrest (Nakamura, Chiang et al. 2008). Damage that induces DSBs is usually acute and severe, such as ionizing radiation, and is especially potent at inducing senescence (Di Leonardo, Linke et al. 1994). Many chemotherapeutic drugs, such as bleomycin, cause severe DNA damage and induce senescence in normal cells (Robles and Adami 1998). Furthermore, they also induce senescence in tumour cells both *in vitro* and *in vivo*, a phenomenon known as drug-induced senescence that may be exploited as a cancer therapy (Schmitt, Fridman et al. 2002; te Poele, Okorokov et al. 2002; Roninson 2003). Chronic oxidative stress of low intensity mainly generates oxidative base modifications and base excision repair intermediates, i.e. SSBs. Exposure to hyperoxia, which produces genotoxic ROS, has been shown to cause both SSBs and DSBs, which may induce a persistent DDR and cellular senescence (Roper, Mazzatti et al. ; Helt, Cliby et al. 2005).

1.2.3 Oncogene-induced senescence

Oncogenes may also trigger a robust DDR leading to senescence induction, termed oncogene-induced senescence (OIS). Oncogenes are mutant versions of normal genes that, in conjunction with other mutations, have the potential to transform cells. OIS was first observed when an oncogenic form of RAS, a transducer of mitogenic signals, was expressed in normal human fibroblasts. Serrano and colleagues noted the striking resemblance between these cells and those that had undergone replicative senescence (Serrano, Lin et al. 1997). Other members of the RAS signalling pathway were later implicated in OIS, including RAF, MEK, MOS and BRAF, as well as pro-proliferative nuclear proteins (such as E2F-1) when overexpressed or expressed as oncogenic versions (Lin, Barradas et al. 1998; Zhu, Woods et al. 1998; Dimri, Itahana et al. 2000; Michaloglou, Vredeveld et al. 2005). Evidence suggests that OIS results from oncogene-induced DNA hyper-replication, which leads to prematurely terminated replication forks and DNA damage, such as DSBs, ultimately triggering a DDR (Bartkova, Rezaei et al. 2006; Di Micco, Fumagalli et al. 2006). Experimental downregulation of this DDR prevents senescence and allows cells that have become senescent in response to RAS to re-enter the cell-cycle, demonstrating that it has a

causal role in both initiation and maintenance of OIS (Bartkova, Rezaei et al. 2006; Di Micco, Fumagalli et al. 2006). Interestingly, it has recently been shown that oncogenes can cause transient non-telomeric and persistent telomeric DDR foci in somatic human cells, leading to senescence (Suram, Kaplunov et al. 2012). This suggests that OIS is not telomere-independent and its stability could be due to telomeric DNA damage being irreparable. Thus, similar to replicative and SIPS, OIS may also result from activation of a DDR triggered by DNA damage. In contrast, some forms of OIS are DDR independent, such as senescence caused by E2F-3 or BRAF activation (Lazzerini Denchi, Attwooll et al. 2005; Kaplon, Zheng et al. 2013). Either way, OIS seems to be a mechanism to counteract excessive mitogenic stimulation from oncogenes that induce cell growth, which would otherwise put cells at risk of malignant transformation.

1.2.4 Senescence caused by chromatin perturbation

Chromatin organisation, either compressed (heterochromatin) or loosely configured (euchromatin), determines the extent to which genes are active or silent and depends on histone modifications, such as methylation and acetylation. Generally, heterochromatin is associated with gene silencing, whereas euchromatin is associated with active transcription. Chromatin decompression by exposure to inhibitors of histone deacetylases (HDAi) has been shown to induce senescence (Ogryzko, Hirai et al. 1996; Munro, Barr et al. 2004). The mechanisms by which this occurs are poorly understood and may depend on species and cell type. One study demonstrated that human cells deficient in the cell-cycle inhibitor p16 were resistant to HDAi-induced senescence, suggesting that that the $p16^{INK4A}$-pRb pathway is a major mediator of HDAi-induced senescence (Munro, Barr et al. 2004). In contrast, pathways involving the cell-cycle inhibitor p21 are important for HDAi-induced senescence of mouse embryonic fibroblasts (Romanov, Abramova et al. 2010). Genetic overexpression of Sirtuin 1 (SIRT1), a nicotinamide adenine dinucleotide (NAD)-dependent HDAC involved in many biological processes, protects against SIPS (Yao, Chung et al. 2012). The finding that HDAi causes senescence is surprising and contradictory to the belief that global induction of heterochromatin contributes to the stability of the senescent state (Howard 1996). These distinct heterochromatic structures that accumulate in senescent cells, designated senescence-associated heterochromatic foci (SAHF), are associated with the stable repression of E2F target genes required for cell-cycle progression (Narita, Nunez et al. 2003). This suggests that senescence can be induced by both heterochromatin disruption and formation, a paradox that could be explained by the notion that both

events cause extensive but incomplete changes in chromatin structure and may alter the expression of different critical genes (Campisi and d'Adda di Fagagna 2007).

1.2.5 Other inducers of senescence

Prolonged exposure to anti-proliferative cytokines, such as interferon-β, induces senescence by increasing intracellular ROS leading to activation of a DDR (Moiseeva, Mallette et al. 2006). Similarly, pro-inflammatory mediators released by senescent cells may induce senescence in nearby cells (Acosta, Banito et al. 2013). Senescence can also occur without detectable DDR signaling. "Cell-culture stress" occurs naturally *in vitro* and induces senescence without significant telomere erosion. The causes are unknown but could include inadequate growth conditions (Ramirez, Morales et al. 2001). Cells may also senesce without a DDR by inactivation of various tumour suppressors. For example, inactivation of the tumour suppressor phosphatase and tensin homolog deleted on chromosome 10 (PTEN) rapidly induces DDR-independent senescence (Alimonti, Nardella et al. 2010). Additionally, ectopic expression of the cyclin-dependent kinase (CDK) inhibitors (CDKi) p16 and p21 induces several aspects of the senescence phenotype in young human diploid fibroblasts without an obvious DDR (McConnell, Starborg et al. 1998). Overall, a myriad of senescence-inducing stimuli have, and are still being, identified and may act through the DDR or independently.

1.3 Signalling pathways activated in senescence

Although there are many senescence-inducing stimuli, the senescent cell-cycle arrest is established and maintained by two main pathways: the p53-p21 and p16^{INK4A}-pRb tumour suppressor pathways (Figure 1.1) (Campisi and d'Adda di Fagagna 2007).

1.3.1 The DNA damage response

The DDR can be triggered by both telomeric and non-telomeric DNA damage, including SSBs and DSBs. Three phosphatidylinositol 3-kinase (PI3K)-like protein kinases (PI3KKs) are known to function as the primary transducers of DDR signalling: ataxia-telangiectasia mutated (ATM), ATM and Rad3-related (ATR), and DNA-dependent protein kinase (DNA-PK) (Shiloh 2003). ATM plays a primary role in responding to DSBs, whereas ATR is known to be strongly activated by single-stranded DNA. Nevertheless, ATM and ATR kinase specificities are closely related and their signalling pathways share many components. DNA-PK is recruited to DSBs and plays a role in the NHEJ repair pathway (Shiloh 2003).

DSBs are initially sensed by poly (ADP-ribose) polymerase (PARP) which then recruits the MRE11–RAD50–NBS1 (MRN) complex. The PARP-MRN complex is one of the first factors to be localised to the DNA lesion and enables the assembly of large macromolecular complexes, known as foci, that facilitate repair responses (D'Amours and Jackson 2002; van den Bosch, Bree et al. 2003). NSB1 then recruits ATM (Uziel, Lerenthal et al. 2003; Lee and Paull 2005). ATM then undergoes autophosphorylation, leading to dissociation of the inactive ATM dimer producing active monomers with kinase activity (Bakkenist and Kastan 2003). Active ATM then phosphorylates a host of factors, including the histone variant H2A.X at serine 139 forming phosphorylated H2A.X (γH2A.X) at the site of damage (Rogakou, Pilch et al. 1998; Rogakou, Boon et al. 1999; Burma, Chen et al. 2001). Phosphorylated H2A.X is recognised by a phospho-specific domain of the mediator of DNA damage checkpoint 1 (MDC1). Recruitment of MDC1 stimulates further accumulation of the MRN complex, amplifying local ATM activation and the spreading of γH2A.X along the chromatin from the site of damage (Stucki and Jackson 2006). Phosphorylation of H2A.X spans for megabases around the DSB and corresponds to thousands of nucleosomes, forming the so-called nuclear foci (Rogakou, Boon et al. 1999). γH2A.X is required to maintain factors of the DDR in an active state and this increase in the local concentration of several activated DDR factors at the site of DNA damage generates a positive feedback loop with ATM to maintain the foci, amplifying repair signals. The DNA damage mediator p53 binding protein 1 (53BP1) is one DDR factor that is recruited to the site of damage by exposure to modified histone residues, which further boosts downstream DDR by establishing binding to MDC1 (Huyen, Zgheib et al. 2004; Eliezer, Argaman et al. 2009). 53BP1 is hyperphosphorylated by ATM and localises to nuclear foci (Anderson, Henderson et al. 2001), playing an important role in activating downstream ATM substrates (Wang, Matsuoka et al. 2002). Additionally, 53BP1 is an important DDR factor involved in NHEJ DNA repair (Nakamura, Sakai et al. 2006).

Alternatively, ultraviolet (UV) light damage and replication stress lead to the generation of local regions of replication protein A (RPA)-coated single-stranded DNA, which causes ATR to be recruited to the site of damage (Namiki and Zou 2006). Notably, during the end stages of DSB repair, RPA-coated single-stranded DNA is generated which also activates ATR (Zou and Elledge 2003). ATR binds to DNA by its DNA-binding subunit ATRIP, which activates a less well defined feedback loop through the activation of the RAD9- HUS1-RAD1 (9-1-1) and RAD17-RFC complexes, as well as TOPBP1 (d'Adda di Fagagna 2008). Activated ATR can then phosphorylate

its downstream targets, including H2A.X, forming DNA damage foci, and the checkpoint kinase 1 (Chk1) and 2 (Chk2) (Cortez, Guntuku et al. 2001; Helt, Cliby et al. 2005). Chk1 and Chk2 transiently localise to the DNA damage foci to be phosphorylated by ATR and ATM but once activated they dissociate and freely diffuse throughout the nucleus (d'Adda di Fagagna 2008). Original reports indicated that Chk1 and Chk2 are phosphorylated by ATR and ATM, respectively but it is now known that both ATM and ATR can phosphorylate Chk1 and Chk2 with specificity depending on the form of DNA damage (Helt, Cliby et al. 2005). Chk1 and Chk2 are involved in both S and G2 checkpoints and act by phosphorylating and inactivating the cell division cycle 25A and C (CDC25A/C) proteins, which are key cell-cycle regulators (Bartek and Lukas 2003). CDC25 proteins are phosphatases that are important for cell proliferation as they activate cyclin-dependent kinases (CDKs) but also cause their DDR-mediated inactivation by exclusion from the nucleus or proteolytic degradation (Shen and Huang 2012; Neelsen, Zanini et al. 2013). Ultimately, the checkpoint kinases are the downstream elements of the DDR signalling cascade that connect the DDR to the core of the cell-cycle progression machinery. Therefore, if a DNA damage response is signaled, this leads to cell-cycle arrest *via* activation of tumour suppressor pathways.

1.3.2 Control by the p53-p21 pathway

Stimuli that generate a DDR, which is centered around the ATM kinase, induce senescence primarily through the p53 pathway (Campisi and d'Adda di Fagagna 2007). p53 is a tumour suppressor and a transcriptional activator induced by stress, the basic function of which is to prevent cells with DNA damage from entering S-phase (Toledo and Wahl 2006). p53 controls the expression of various genes implicated in response to genome instability and DNA damage and acts to cease cell proliferation by inducing two main cellular responses: apoptosis (programmed cell death) or senescence (Beausejour, Krtolica et al. 2003; Gao, Shen et al. 2011; Gatta, Dolfini et al. 2011; Rufini, Tucci et al. 2013). When inactive, p53 is associated with the E3 ubiquitin-protein ligase human double minute 2 (HDM2), which both inhibits p53 transcriptional activity and targets it for degradation (Li, Brooks et al. 2003). Activation of the DDR, however, leads to phosphorylation and stabilisation of p53 and prevents HDM2 from binding (Chehab, Malikzay et al. 2000; Webley, Bond et al. 2000). Phosphorylation elevates DNA binding and transcriptional activities of p53 (Vaziri, West et al. 1997). p53 is activated by the Chk1 and Chk2 kinases and can be directly phosphorylated by ATM on Serine 15 (Banin, Moyal et al. 1998; Chehab, Malikzay et al. 2000; Calabrese,

Mallette et al. 2009). However, ATM mainly exerts its effects on p53 indirectly by phosphorylation of Chk2 or modifications of HDM2 (Ahn, Schwarz et al. 2000; Maya, Balass et al. 2001). ATR can also phosphorylate and activate Chk1 and Chk2 and so is also involved in p53 activation (Helt, Cliby et al. 2005; Jazayeri, Falck et al. 2006; Wang, Redpath et al. 2006). As a major transcriptional regulator, p53 has multiple downstream targets that inhibit cell-cycle progression. The main transcriptional target of p53, and mediator of p53-dependent senescence, is the CDKi p21 (also termed CDKN1a, p21Cip1, Waf1 or SDI1) (Brown, Wei et al. 1997; Herbig, Jobling et al. 2004). Indeed, inactivation of p21 prevents mouse embryonic fibroblasts and normal human fibroblasts from undergoing p53-dependent senescence in response to DNA damage (Brugarolas, Chandrasekaran et al. 1995; Brown, Wei et al. 1997). Additionally, inactivation of Chk2 in human fibroblasts leads to decreased p21 expression and increased replicative lifespan due to failure of p53 activation in response to telomere erosion and DNA damage (Gire, Roux et al. 2004). p21 also has multiple targets, in particular it inhibits cyclin-CDK complexes, including cyclin E-CDK2, and proliferating-cell nuclear antigen (PCNA), which are required for passage through the cell cycle (Xiong, Zhang et al. 1992; Harper, Adami et al. 1993; Xiong, Hannon et al. 1993; Waga, Hannon et al. 1994). CDKs stimulate cell-cycle progression by phosphorylating proteins required for transition to the next stage of the cell cycle. The inhibition of cyclin E-CDK2 by p21 prevents the phosphorylation of pRb (the product of the retinoblastoma tumour suppressor gene), which when hyperphosphorylated becomes inactivated and no longer binds and inhibits the activity of E2F transcription factors, which transcribe genes required for G1-S-phase transition (Sherr 1994; Weinberg 1995).

1.3.3 Control by the p16^{INK4A}-pRb pathway

Stimuli that produce a DDR can also engage the p16^{INK4A} (also termed CDKN2a), hereafter referred to as p16, -pRb pathway. p16 is a CDKi that can prevent pRb phosphorylation and inactivation independently of p53 (Alcorta, Xiong et al. 1996). p16 localises to the perinuclear cytoplasm and following activation translocates to the nucleus where it functions as a cyclin D-CDK4/6 inhibitor preventing the phosphorylation of pRb (Serrano, Hannon et al. 1993; Sherr 1994; Weinberg 1995). Some senescence-inducing stimuli act primarily through the p16-pRb pathway, which is particularly true in human epithelial cells, which become senescent with relatively long telomeres and high p16 expression (Kiyono, Foster et al. 1998; Ramirez, Morales et al.

2001). In most cases, engagement of the p16-pRb pathway occurs secondary to the engagement of the p53 pathway, as occurs in fibroblasts (Stein, Drullinger et al. 1999; Beausejour, Krtolica et al. 2003; Jacobs and de Lange 2004). The relative contribution of these two pathways to cell-cycle arrest is also species specific. For example, telomere dysfunction-induced senescence primarily engages the p53 pathway in mouse cells, whereas both pathways are activated in human cells (Smogorzewska and de Lange 2002; Beausejour, Krtolica et al. 2003; Jacobs and de Lange 2004). However, studies suggest that p16 is probably not essential for most types of senescence in humans. Human fibroblasts mutant for p16 still senesce following periods of prolonged replication (Brookes, Rowe et al. 2004). Additionally, mouse embryonic fibroblasts lacking p16 still senesce in response to γ-irradiation, replicative exhaustion and oncogenes (Krimpenfort, Quon et al. 2001). However, overexpression of p16 alone is enough to induce cellular senescence (Coppe, Rodier et al. 2011) and it has been demonstrated in human cells that high levels of p16 at senescence prevents cells from proliferating even after p53 inactivation, whereas cells with low levels of p16 at senescence are able to resume growth following p53 inactivation, suggesting p16 provides an additional barrier in cells that fully engage the p16-pRb pathway (Beausejour, Krtolica et al. 2003). Moreover, loss of p16-pRb activity upregulates p53 and p21 expression in human epithelial cells (Zhang, Pickering et al. 2006), suggesting that there is reciprocal regulation between the two pathways. p16 expression is upregulated gradually with the induction of senescence and coincides with aspects of the senescent phenotype, persisting for months after senescence induction. In contrast, p21 expression is maximal at the initiating stages of senescence and then declines after the cell has become senescent, suggesting that p16 upregulation may be required for maintenance of the senescent cell-cycle arrest (Alcorta, Xiong et al. 1996; Stein, Drullinger et al. 1999; Beausejour, Krtolica et al. 2003). The p16-pRb pathway is involved in the generation of SAHFs, which are ultimately portions of a single condensed chromosome enriched for the histone variant macroH2A that silence genes required for proliferation, namely E2F target genes (Narita, Nunez et al. 2003; Zhang, Chen et al. 2007). The p16-pRb pathway can establish self-maintaining SAHFs, which could be due to the ability of pRb to complex with histone-modifying enzymes that form repressive chromatin, thereby leading to SAHF generation (Macaluso, Montanari et al. 2006). p16 expression is induced by oncogenes, such as oncogenic RAS (Serrano, Lin et al. 1997), oxidative stress (Chen, Stoeber et al. 2004), radiation (Meng, Wang et al. 2003) and telomere dysfunction (Jacobs and de Lange 2004). It is not entirely clear how senescence-causing

stimuli induce p16 expression, however one possibility is that DNA damage signals activate p38MAPK signalling, which then activates p16 (Iwasa, Han et al. 2003; Bulavin, Phillips et al. 2004; Ito, Hirao et al. 2006; Spallarossa, Altieri et al. 2010).

1.3.4 P38MAPK pathway

The p38 mitogen-activated protein kinase (p38MAPK) is important for senescence growth arrest and can activate both p53-p21 and p16-pRb tumour suppressor pathways (Iwasa, Han et al. 2003). Indeed, p38MAPK activity is required for oncogenic RAS-induced senescence and inhibition can delay the onset of replicative senescence (Deng, Liao et al. 2004; Davis and Kipling 2009). X-ray irradiation has been shown to induce p38 with similar dynamics to those of p16, increasing only slightly initially, rising substantially between 2-4 days and peaking at 8-10 days (Freund, Patil et al. 2011), consistent with p38 inducing p16 expression. Additionally, it has been shown that p38MAPK enhances mitochondrial ROS production, which causes cyclic activation of p53 through the replenishment of DNA damage foci, contributing to stabilisation of an ongoing DDR during senescence (Passos, Nelson et al. 2010).

In summary, the main pathways that control induction and maintenance of senescence are the p53-p21 and p16-pRb pathways, which both prevent E2F from transcribing genes that are needed for cell proliferation. It seems that these pathways may interact and have compensatory effects but can act independently. The relative contributions of these pathways to the senescent growth arrest depend on stimuli, species and cell type, reflecting the heterogeneity of the senescence growth arrest.
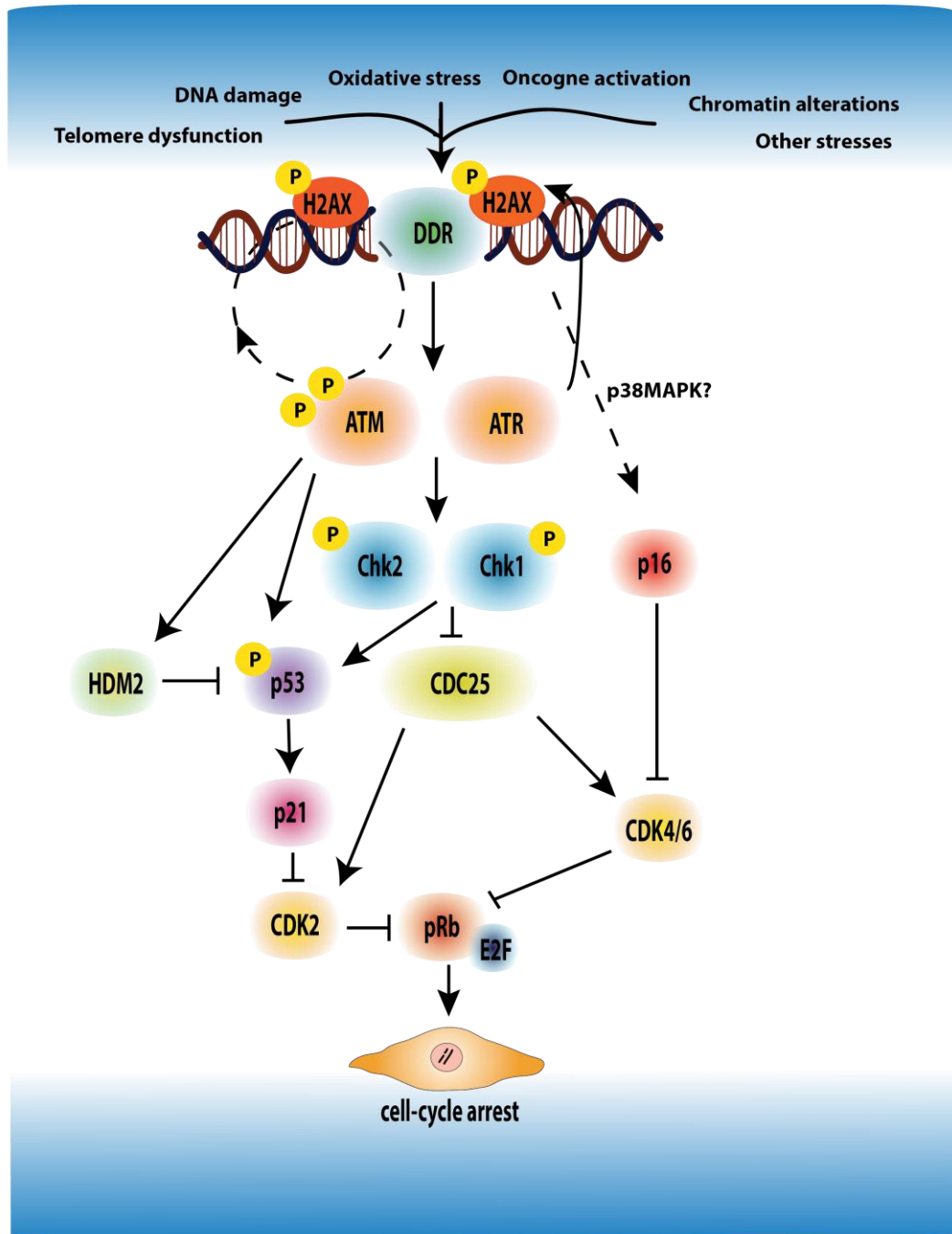
Figure 1.1. Pathways involved in senescence induction. Many signals that induce senescence, such as dysfunctional telomeres and DNA damage, trigger a DNA damage response (DDR) leading to the activation of ataxia-telangiectasia mutated (ATM) and Rad3-related (ATR) kinases and formation of DNA damage foci. Many stressors may also induce senescence, independently of a DDR. Either way, the p53-p21 and p16-retinoblastoma protein (pRb) tumour suppressor pathways are usually engaged. Active p53 establishes senescence, mainly by inducing the expression of the cyclin-dependent kinase (CDK) inhibitor p21, which suppresses the phosphorylation and thus inactivation of pRb. Senescence signals that engage the p16-pRb pathway induce the expression of p16, another CDK inhibitor, which also suppresses pRb inactivation. pRb halts cell proliferation by inhibiting the activation of E2F, a transcription factor required for the expression of cell-cycle progression genes. HDM2, human double minute 2; Chk1/2, checkpoint kinase 1/2; CDC25, cell division cycle 25; p38MAPK, p38 mitogen-activated protein kinase.

13

1.4 Characteristics of senescent cells

Cellular senescence is marked by a number of distinct phenotypic changes. However, no hallmark of senescence identified so far is entirely specific to the senescent state. Furthermore, the phenotype of senescent cells may differ depending on the type of senescence (e.g. replicative senescence vs. SIPS) (Dierick, Eliaers et al. 2002) or stage of senescence development (Baker and Sedivy 2013). Nonetheless, senescent cells display several common characteristics, which in combination, define the senescent state (Figure 1.2) (Rodier and Campisi 2011).

1.4.1 Growth arrest

The initiating step in senescence is the induction of stable cell-cycle arrest, which typically involves prolonged inhibition of cyclin-CDK activity induced by activation of the tumour suppressor pathways (as above). Thus, senescent cells are non-dividing. Senescent cells usually arrest growth with a DNA content that is typical of G1 phase yet they remain metabolically active and have the ability to remain viable in culture for prolonged periods of time (Dulic, Drullinger et al. 1993; Di Leonardo, Linke et al. 1994; Herbig, Jobling et al. 2004). In some cases, the features of the senescence growth arrest may differ, depending on the species, genetic background of the cell and stimuli. For example, a defect in the stress-signalling kinase MKK7 induces a G2-M arrest in mouse fibroblasts (Wada, Joza et al. 2004), loss of ATM in human fibroblasts containing TAF leads to G2 arrest (Herbig, Jobling et al. 2004) and some oncogenes cause cells to arrest with a DNA content that is typical of G2 (Zhu, Woods et al. 1998; Di Micco, Fumagalli et al. 2006). The senescence growth arrest is essentially irreversible, as proliferation cannot be stimulated by known physiological stimuli. However, studies have argued that "escape scenarios" do exist. For example, inactivation of p53 allows senescent cells to re-enter the cell-cycle (Beausejour, Krtolica et al. 2003).

1.4.2 Apoptosis resistance

Apoptosis is a controlled form of cell death, which like senescence, can occur in response to cellular stress and is an important anti-cancer mechanism (Ellis, Yuan et al. 1991; Green and Evan 2002). Whereas senescence prevents the proliferation of damaged cells, apoptosis eliminates them. It is not clear what determines whether cells undergo apoptosis or senescence (Childs, Baker et al. 2014). The nature and intensity of the damage may be important (Seluanov, Gorbunova et al. 2001). The type of cell may also be a factor. For example, fibroblasts and epithelial cells tend to senesce following damage, whereas lymphocytes tend to undergo apoptosis (Campisi and d'Adda di

Fagagna 2007). It is likely that the senescence and apoptosis regulatory systems communicate through the tumour suppressor protein p53, which is strongly involved in both programmes, but the mechanisms are still not entirely understood (Seluanov, Gorbunova et al. 2001). One study demonstrated that both the cellular level of telomere dysfunction and p53 gene status determined whether cells underwent apoptosis or senescence in murine liver cells. This study demonstrated that cells underwent p53-dependent senescence or p53-independent apoptosis, depending on the level of telomere dysfunction in a cell (Lechel, Satyanarayana et al. 2005).

Many cell types, such as fibroblasts, acquire resistance to apoptosis when they become senescent (Wang 1995; Seluanov, Gorbunova et al. 2001; Sanders, Liu et al. 2013). Other cells are less resistant to apoptosis. For example, senescent fibroblasts resist ceramide-induced apoptosis, whereas senescent endothelial cells do not (Hampel, Malisan et al. 2004). Apoptosis resistance may explain the stability of senescent cells for prolonged periods of time in culture and the increasing number of senescent cells with age (Haake, Roublevskaia et al. 1998). The mechanisms governing resistance of apoptosis by senescent cells are not fully understood. In some cells, it could be that p53 preferentially trans-activates genes that arrest proliferation rather than those that promote apoptosis (Jackson and Pereira-Smith 2006). Additionally, it has been shown that histone modifications confer apoptosis resistance to senescent human fibroblasts by regulating altered expression of the anti- and pro-apoptotic genes B-cell lymphoma 2 (Bcl-2) and bcl-2 associated X protein (Bax) (Sanders, Liu et al. 2013). Additionally, data show that p53-dependent apoptotic pathways are specifically blocked in senescent fibroblasts (Seluanov, Gorbunova et al. 2001).

1.4.3 Changes in gene expression

Senescent cells show striking alterations in gene expression, which result in traits associated with the senescence phenotype. For example, changes in gene expression of known cell-cycle inhibitors or activators are responsible for the senescent growth arrest (Shelton, Chang et al. 1999; Chang, Swift et al. 2002; Mason, Jackson et al. 2004; Trougakos, Saridaki et al. 2006). The CDKi p21 and p16 are cell-cycle inhibitors that are often expressed by senescent cells, which act to maintain pRb in a hypophosphorylated and active state (discussed above) (Di Leonardo, Linke et al. 1994; Alcorta, Xiong et al. 1996; Herbig, Jobling et al. 2004; Jacobs and de Lange 2004). Senescent cells also repress genes that promote cell-cycle progression, such as replication-dependent histones, c-FOS, cyclin A, cyclin B and PCNA (Seshadri and

Campisi 1990; Stein, Drullinger et al. 1991; Pang and Chen 1994). Some of these genes are repressed because the transcription factor E2F, which induces them, is also repressed in senescent cells (Dimri, Hara et al. 1994). Senescent cells are unable to express genes required for proliferation, even in the presence of pro-mitogenic factors, which distinguishes them from quiescent cells, which are also non-dividing (Dimri, Hara et al. 1994). Many senescent cells overexpress genes that encode secreted proteins, such as extracellular matrix (ECM) degrading enzymes, inflammatory cytokines and growth factors, which can alter the tissue microenvironment and affect the behaviour of neighbouring and distal cells (Tchkonia, Zhu et al. 2013). This is known as the senescence-associated secretory phenotype (SASP) (discussed below).

1.4.4 Senescence markers

Several markers have been used to identify senescent cells in culture and *in vivo*. Some of these markers reflect the activation of mechanisms that contribute to the senescence program, such as the induction of tumour suppressor pathways, however for others, it is unclear as to what extent they contribute mechanistically (Kuilman, Michaloglou et al. 2010). The first marker to be used for the identification of senescent cells was senescence-associated-β-galactosidase (Sen-β-Gal) activity (Dimri, Lee et al. 1995). Dimri and colleagues demonstrated that Sen-β-Gal, which is histochemically detected in senescent cells at pH 6.0, is active in senescent human fibroblasts and keratinocytes in culture and Sen-β-Gal positive cells age-dependently increase in human skin (Dimri, Lee et al. 1995). It is known that β-Gal is a lysosomal hydrolase enzyme and it has been proposed that Sen-β-Gal probably derives from the lysosomal β-Gal and reflects the increased lysosomal biogenesis that occurs commonly in senescence (Lee, Han et al. 2006). Sen-β-Gal is still not solely specific to the senescent state as prolonged confluence in culture can also lead to Sen-β-Gal positivity (Dimri, Lee et al. 1995). There is currently no evidence pointing to the specific involvement of Sen-β-Gal in the senescence response (Lee, Han et al. 2006).

More obvious markers to use for the identification of senescent cells are those that reflect proliferation arrest and lack of DNA replication. DNA replication is detected by incorporation of 5-bromodeoxyuridine (BrdU) or ^{3}H-thymidine, or by immunostaining for proteins such as PCNA and Ki67 (Muskhelishvili, Latendresse et al. 2003). However, these markers do not distinguish between senescent cells and quiescent or differentiated post-mitotic cells.

As discussed above, the p53-p21 and p16-pRb pathways commonly mediate the induction and maintenance of the senescence program. Consequently, components of these pathways have been used to identify senescent cells. p53 displays increased activity and/or levels in human fibroblasts undergoing replicative or premature senescence (Vaziri, West et al. 1997; Bunz, Dutriaux et al. 1998). Rb also accumulates in its active hypophosphorylated form in senescent cells (Stein, Beeson et al. 1990). In addition, p16, an important regulator of senescence, is expressed by many senescent cells and is used to identify senescent cells both *in vitro* and in *vivo* (Serrano, Lin et al. 1997; Beausejour, Krtolica et al. 2003; Itahana, Zou et al. 2003; Krishnamurthy, Torrice et al. 2004; Herbig, Ferreira et al. 2006; Jeyapalan, Ferreira et al. 2007). p21 also often accumulates in senescent cells and has been used as a marker of senescence, reflecting the activation of this tumour suppressor pathway (Di Leonardo, Linke et al. 1994; Alcorta, Xiong et al. 1996; Herbig, Jobling et al. 2004; Herbig, Ferreira et al. 2006).

Some senescent cells can also be identified using DNA dyes, such as 4'6-diamidino-2-phenylindole (DAPI), which detect alterations in chromatin structure. While cycling or quiescent human cells display overall homogeneous staining patterns, senescent cells often show strikingly different punctate staining patterns. These DNA SAHF are enriched in certain heterochromatin-associated histone variants (for example, histone 3 Lysine 9 methylation, γH2A.X and macro H2A) and proteins (such as, heterochromatin protein-1 (HP1)) (Narita, Nunez et al. 2003). SAHFs also sequester genes involved in cell-cycle control, such as E2F target genes, which is thought to reinforce senescence growth arrest. Indeed, SAHFs have been correlated with the irreversibility of the senescent cell-cycle arrest (Beausejour, Krtolica et al. 2003; Narita, Nunez et al. 2003). When SAHF formation is circumvented, senescence can be bypassed (Narita, Nunez et al. 2003; Zhang, Poustovoitov et al. 2005). As well as transcriptionally silencing genes, chromatin modification leads to the upregulation of genes encoding secreted proteins with pro-inflammatory activity, further linking SAHF formation to progression of the senescence phenotype (Shelton, Chang et al. 1999; Zhang, Pan et al. 2003).

Several reports have described senescence-associated DNA damage foci (SDFs) as markers for senescent cells *in vitro* and *in vivo* (d'Adda di Fagagna, Reaper et al. 2003; Takai, Smogorzewska et al. 2003; Herbig, Jobling et al. 2004; Sedelnikova, Horikawa et al. 2004; Di Micco, Fumagalli et al. 2006). SDFs are subnuclear foci that contain DDR proteins, such as γH2A.X and 53BP1 and represent sites of DNA damage and DDR activity (d'Adda di Fagagna, Reaper et al. 2003). These foci can be detected

by immunofluorescence because chromatin modifications generated by the DDR spread over megabases (Rogakou, Boon et al. 1999). Recently, Rodier and colleagues suggested that persistent DNA damage foci (termed DNA segments with chromatin alterations reinforcing senescence (DNA-SCARS)) are distinguishable from transient foci and act as reservoirs for active DDR signalling, being important for maintaining senescent growth arrest and features of the SASP (Rodier, Munoz et al. 2011). These foci result from both genomic DNA damage, such as DSBs, and dysfunctional telomeres (d'Adda di Fagagna, Reaper et al. 2003; Herbig, Jobling et al. 2004; Sedelnikova, Horikawa et al. 2004). SDFs resulting from telomere shortening/uncapping have been termed telomere dysfunction-induced foci (TIF) (Takai, Smogorzewska et al. 2003; Herbig, Jobling et al. 2004). Recently, it has been demonstrated that SDFs may also be present at longer telomeres and occur independently of telomerase activity and are therefore referred to as telomere-associated foci (TAF) (Fumagalli, Rossiello et al. 2012; Hewitt, Jurk et al. 2012). Senescence induced by telomere dysfunction reflects a DDR that is activated with direct contribution from telomeres and both TIF and TAF have been described as markers of telomere-induced senescence. It has recently been shown that DDR signalling is persistently active months and even years following induction of the senescence state and therefore SDFs may be used to identify senescent cells long after the establishment of senescence (Fumagalli, Rossiello et al. 2014).

Senescence is accompanied by changes in the nucleus, such as increased nuclear size and irregularity and increased density of nuclear pore complexes (Mehta, Figgitt et al. 2007). Additionally, some senescent cells may show alterations in nuclear envelope proteins, such as lamin A and B, which connect the nuclear envelope to the chromatin (Dechat, Pfleghaar et al. 2008). Lamin B1 loss may serve as a biomarker of senescence *in vitro* and *in vivo* as it is lost from both murine and human cells during OIS, SIPS and replicative senescence and in mouse tissues following irradiation, but not in quiescence (Shimi, Butin-Israeli et al. 2011; Freund, Laberge et al. 2012). Data suggests that lamin B1 downregulation is a key trigger of local and global chromatin changes that impact on gene expression, suggesting that this may be an important step in the progression to full senescence (Shah, Donahue et al. 2013).

Sirtuins are conserved NAD-dependent protein and HDACs that play critical roles in a variety of processes, including stress resistance, senescence and ageing (Michan and Sinclair 2007). SIRT1 is the best characterised mammalian sirtuin and is important for maintaining transcriptionally silent chromatin and regulating transcription

of nuclear factor (NF)-κB-dependent genes. Activation or overexpression of SIRT1 has been shown to increase lifespan in yeast, worms and mice (Lin, Defossez et al. 2000; Tissenbaum and Guarente 2001; Howitz, Bitterman et al. 2003; Bordone, Cohen et al. 2007; Satoh, Brace et al. 2013) and decreased SIRT1 expression has been described in the senescence context (Sasaki, Maier et al. 2006; Vassallo, Simoncini et al. 2014).

These markers are associated with, but not exclusive to, the senescent state. Therefore, markers should be investigated in combination in order to identify senescent cells. Lawless and colleagues identified Ki67 negativity in combination with γH2A.X positivity (> 5 per nucleus) as strong criteria for identifying senescent cells in both cell culture and tissue sections (Lawless, Wang et al. 2010).

1.4.5 Morphological changes

Cell senescence is generally associated with changes in cellular morphology. Depending on the inducer of senescence, senescent cells can become large, flat and multinucleated. An increase in cellular volume and a flattened morphology has been noted for human skin fibroblasts undergoing replicative senescence (Bayreuther, Rodemann et al. 1988). A flattened morphology is seen in cells undergoing RAS-induced senescence (Serrano, Lin et al. 1997) and DNA damage-induced senescence (Chen, Prowse et al. 2001). However, human melanocytes undergoing BRAF-induced senescence acquire a more spindle-shaped morphology (Michaloglou, Vredeveld et al. 2005).

1.4.6 The senescence-associated secretory phenotype

Cells undergoing senescence exhibit profound changes in their secretomes (Shelton, Chang et al. 1999). A major consequence of this is the secretion of a plethora of proteins, including pro-inflammatory cytokines and chemokines, growth factors and proteases (Tchkonia, Zhu et al. 2013). Collectively, these factors are referred to as the senescence-associated secretory phenotype (SASP) or senescence messaging secretome (SMS) (Coppe, Patil et al. 2008; Kuilman and Peeper 2009). The SASP is one of the key characteristics that distinguishes senescent cells from quiescent and terminally differentiated cells, therefore SASP components, along with other markers, may also be exploited to identify senescent cells. It has been suggested that development of the SASP reflects progression from transient cell-cycle arrest to full senescence (Correia-Melo, Hewitt et al. 2014; van Deursen 2014), likely due to the triggering of extensive chromatin remodelling and SAHF formation, which are known to regulate SASP production and reinforce senescence (discussed above). Rodier and colleagues demonstrated that for the induction of several of the SASP factors, persistent DNA

damage is required (Rodier, Coppe et al. 2009). Because DNA damage does not accompany all senescent settings, it was suggested that a DDR but not senescence *per se* is required for the SASP (Rodier, Coppe et al. 2009). Consistent with this, primary human fibroblasts overexpressing p21 or p16 undergo senescent growth arrest but fail to activate a DDR and do not produce a SASP (Coppe, Rodier et al. 2011). However, several senescence-inducing stimuli lead to the development of the SASP independently of DNA damage, implying the existence of DDR-independent mechanisms (Munoz-Espin, Canamero et al. 2013; Storer, Mas et al. 2013). SASP factors vary in distinct cell types and under different senescence inducers. It is not surprising then that senescent cells impact various biological processes including cell proliferation, angiogenesis, local inflammation and wound healing (Shelton, Chang et al. 1999; Krtolica, Parrinello et al. 2001; Coppe, Kauser et al. 2006; Jun and Lau 2010). However, pro-inflammatory cytokines and chemokines, such as interleukin IL-6 and IL-8 are among the SASP factors that are highly conserved among different types of cells and types of senescence (Shelton, Chang et al. 1999; Coppe, Patil et al. 2008), suggesting that attracting immune cells and inducing local inflammation are common properties of senescent cells. Recently, it has been discovered that senescent cells can spread the senescence phenotype to healthy neighbouring cells *via* secretion of SASP factors, including transforming growth factor-β (TGF-β) and IL-1α, and so have a "bystander effect" (Acosta, Banito et al. 2013). In addition to affecting the microenvironment and neighbouring cells, secreted SASP factors also affect the cells that produce them and so have autocrine as well as paracrine effects. Indeed, some inflammatory factors establish and maintain senescence arrest. For example, signalling through CXCR2 (a receptor for IL-8) reinforces both replicative and OIS growth arrest through a self-amplifying secretory network and inhibition of this receptor both delays senescence onset and decreases DDR activation (Acosta, O'Loghlen et al. 2008). Similarly, IL-6 is required to induce and maintain OIS in a cell-autonomous fashion (Kuilman, Michaloglou et al. 2008). Mechanistically, it's still not completely understood how the SASP contributes to the reinforcement of cellular senescence (Correia-Melo, Hewitt et al. 2014). However, evidence suggests that positive feedback loops between DDR signalling and components of the SASP, such as inflammatory factors and ROS, lead to new DNA damage and maintain DDR signalling (Passos, Nelson et al. 2010; Jurk, Wilson et al. 2014). The NF-κB family of transcriptional factors regulate expression of many genes involved in stress-responses and inflammation, such as cytokines and enzymes (Pahl 1999), and have been shown to be important in regulating components of senescence

and the SASP (Freund, Patil et al. 2011; Rovillain, Mansfield et al. 2011). Indeed, multiple lines of evidence suggest that NF-κB activity links the DDR with production of SASP components, underscoring the importance of this family of transcription factors in promoting stability and progression of senescence (Passos, Nelson et al. 2010; Osorio, Barcena et al. 2012; Tilstra, Robinson et al. 2012; Jurk, Wilson et al. 2014).

1.4.7 Progression to deep senescence

Senescent cells can remain viable for prolonged periods of time, both in culture and in tissues where they may eventually progress to a stage that has been termed 'late' or 'deep' senescence (Baker and Sedivy 2013). Little is known about this phenomenon but it is thought that 'deep' senescence is maintained by persistent DDR signalling (Passos, Nelson et al. 2010), and is associated with further changes to the cell, including depletion of core histones and extrusion of chromatin into the cytoplasm, resulting in the formation of cytoplasmic chromatin fragments (CCFs) (Ivanov, Pawlikowski et al. 2013). CCFs are strongly positive for H3K27me3 and γH2A.X, contain DNA, and are processed via lysosome-mediated proteolysis, leading to histone loss (Ivanov, Pawlikowski et al. 2013). It has been suggested that these events likely drive transcriptome diversity among senescent cells, even in those resulting from the same inducer, possibly leading to SASP heterogeneity (van Deursen 2014).
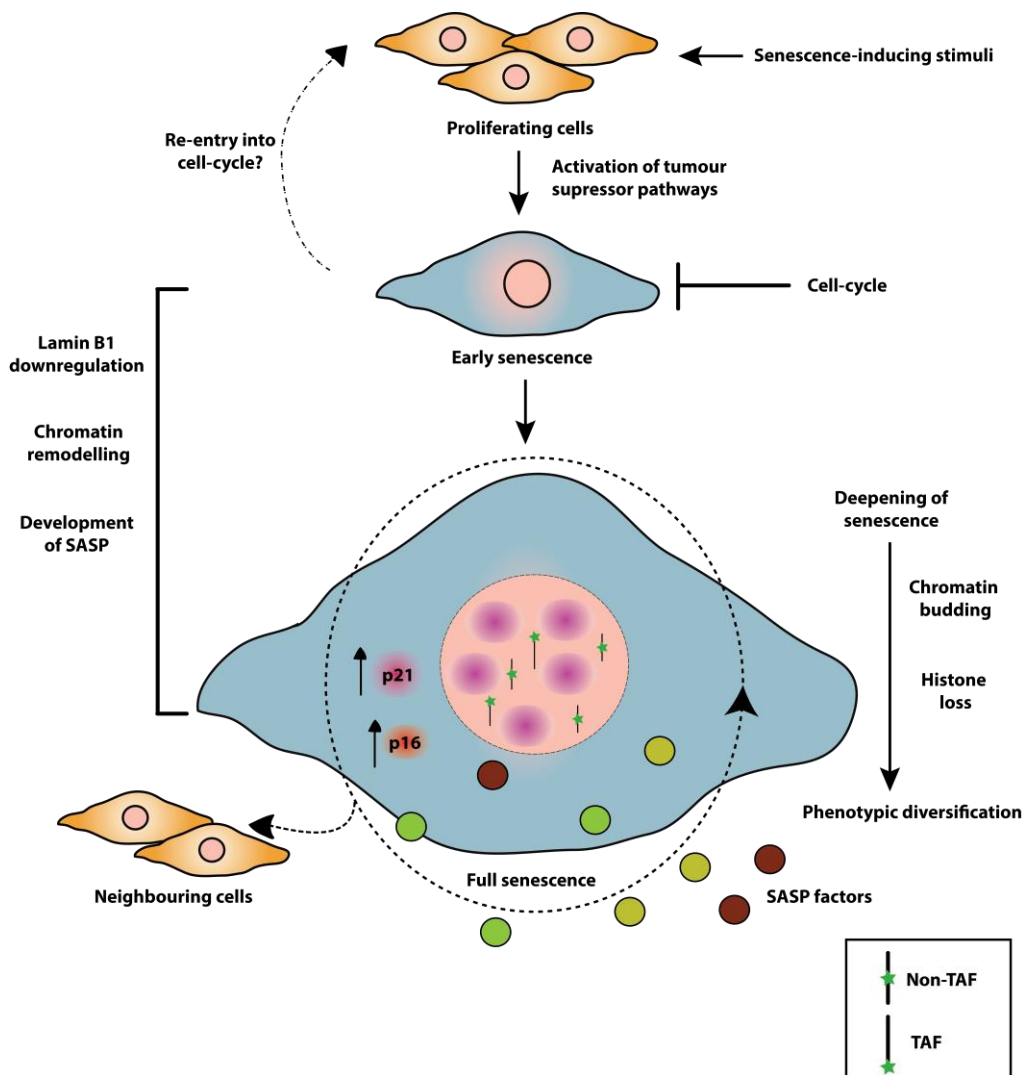
Figure 1.2. Development of the senescence phenotype – a multistep process. Mounting evidence suggests that cellular senescence is a dynamic and evolving process. Initially, stressors can lead to activation of a DNA damage response (DDR) and induction of tumour suppressor pathways resulting in cell-cycle arrest. At this point, it may be possible for cells to re-enter the cell cycle, for example, if damage is repairable. Sustained activation of the p53-p21 and p16-pRb pathways leads to progression from transient to stable cell-cycle arrest and early senescence. Lamin B1 downregulation, triggering extensive chromatin remodelling, leads to progression to full senescence and production of the senescence-associated secretory phenotype (SASP). Secretion of bioactive molecules, such as SASP factors and reactive oxygen species (ROS) acts to reinforce senescence and induce senescence in neighbouring cells by autocrine and paracrine mechanisms, respectively. Further progression of the senescence phenotype may lead to 'deep' senescence, driven by additional changes, such as chromatin budding and histone loss. The development of deep senescence is thought to further drive SASP heterogeneity. Some markers of cellular senescence are shown, including senescence-associated-β-galactosidase (Sen-β-Gal) (blue) expression, formation of senescence-associated heterochromatin foci (SAHF) (pink), the presence of DNA damage foci and telomere-associated foci (TAF) (green) and increased p21 and p16 expression.

1.5 The involvement of reactive oxygen species in induction of telomere dysfunction and senescence

The Free Radical Theory of Ageing suggests that ROS, which are generated inside the cell as by-products of normal redox reactions, react with cellular constituents such as DNA and proteins, the accumulation of which leads to the progressive changes of ageing (Harman 1956). Since mitochondria are the major producers of ROS in cells (Chance, Sies et al. 1979), it was later suggested that mitochondria play an important role in time-dependent cellular ROS generation (Harman 1972). Evidence suggests that ROS are likely to be involved in the induction and stabilisation of cellular senescence. During cellular senescence, it has been shown that mitochondrial dysfunction increases as cells reach the end of their replicative lifespan, leading to increased ROS generation (Passos, Saretzki et al. 2007). Additionally, it has been shown that ROS can accelerate telomere shortening by inducing SSBs at telomeres, with antioxidants and other interventions that reduce ROS being able to prevent telomere shortening and extend replicative lifespan (von Zglinicki, Saretzki et al. 1995; von Zglinicki 2002; Saretzki, Murphy et al. 2003; Serra, von Zglinicki et al. 2003). Elevated ROS levels are also implicated in SIPS and OIS (Saretzki, Murphy et al. 2003; Moiseeva, Bourdeau et al. 2009). Evidence suggests that ROS may act as signalling molecules to stabilise senescence (Passos, Saretzki et al. 2007). For example, activation of pathways downstream of the DDR, such as overexpression of p21 and p16, result in elevated ROS (Macip, Igarashi et al. 2002; Takahashi, Ohtani et al. 2006). It has also been demonstrated that ROS levels increase in senescent cells as a result of mitochondrial dysfunction induced through activation of p21, which in turn replenish short-lived DNA damage foci, maintaining an ongoing DDR and stability of senescence (Passos, Nelson et al. 2010). Additionally, it has been shown that senescent cells can induce a DDR in neighbouring cells *via* gap junctions and processes involving ROS (Nelson, Wordsworth et al. 2012). It is also possible that ROS could lead to bystander effects and impact on tissues, similar to the SASP. In the study by Nelson and colleagues, it was shown that senescent cells can induce senescence in intact bystander cells *in vitro* and that senescent cells are clustered *in vivo*, suggesting that senescent cells induce senescence in nearby cells (Nelson, Wordsworth et al. 2012). Evidence links ROS to reinforcement of senescence by the SASP. In the study by Acosta and colleagues demonstrating that CXCR2 inhibition delays senescence onset and decreases DDR

activation, the authors propose that this could be due to a reduction in ROS (Acosta, O'Loghlen et al. 2008). Interferon-β, a possible component of the SASP, induces senescence by increasing intracellular ROS, which leads to activation of a DDR (Moiseeva, Mallette et al. 2006). TGF-β is known to play a role in the paracrine mechanisms of the SASP (Acosta, Banito et al. 2013) and neutralising antibodies or chemical inhibitors against the TGF-β type II receptor decrease ROS production downstream of the DDR induced in both telomere-dependent and -independent fashions (Passos, Nelson et al. 2010). Another potential link between the SASP and ROS is NF-κB, the main regulator of the SASP, which has roles in the regulation of mitochondrial function and oxidative stress (reviewed in (Correia-Melo, Hewitt et al. 2014)). Finally, the p38MAPK pathway has been shown to be important for ROS generation in both SIPS and replicative senescence and for maintenance of the DDR (Passos, Nelson et al. 2010) and it is known that p38MAPK regulates the SASP mainly through NF-κB transcriptional activity (Freund, Patil et al. 2011).

Therefore, ROS are implicated in, and are important to, multiple steps in the induction and maintenance of senescence as well as the inflammatory processes associated with senescent cells.

1.6 Significance of senescence *in vivo*

Following the discovery of senescence *in vitro,* Hayflick and Moorehead postulated that this program paralleled ageing *in vivo*, likely contributed to the development of age-related disease and supressed the development of cancer (Hayflick 1965). For decades there has been debate between researchers as to whether senescence exists *in vivo* or if it is a phenomenon exclusive to tissue culture and only in the last ten years studies have provided conclusive evidence that senescence occurs and is important *in vivo* (Burton and Krizhanovsky 2014).

1.6.1 Evidence for senescent cells in vivo

Senescence-associated markers have been used to identify senescent cells *in vivo* with the limitation that no marker is exclusive to the senescent state. Senescent cells are found in many renewable tissues in rodents, primates and humans (Krishnamurthy, Torrice et al. 2004; Jeyapalan, Ferreira et al. 2007; Waaijer, Parish et al. 2012). Senescent cells are also found at sites of benign dysplastic or preneoplastic regions *in vivo*, but not at the malignant counterparts, consistent with senescence being an anti-cancer mechanism (Collado, Gil et al. 2005; Michaloglou, Vredeveld et al. 2005; Suram, Kaplunov et al. 2012). The majority of evidence for the presence of senescence *in vivo*,

however, comes from the link between cellular senescence, ageing and age-related disease.

1.6.2 Senescence and ageing

There is considerable evidence that cellular senescence contributes to the ageing process. Using combinations of senescent markers previously mentioned, a number of studies have demonstrated that senescent cells accumulate *in vivo* with age. An age-dependent increase in Sen-β-Gal staining was shown in dermal fibroblasts and epidermal keratinocytes in human skin samples (Dimri, Lee et al. 1995). Interestingly, it has been demonstrated that younger biological age is associated with fewer levels of p16 positive cells in human skin biopsies (Waaijer, Parish et al. 2012). Dermal fibroblasts expressing p16 and harbouring TAF accumulate in the skin of baboons with advancing age (Jeyapalan, Ferreira et al. 2007). Herbig and colleagues also documented previously that senescent fibroblasts increased in the skin of ageing baboons, as indicated by the presence of TAF, which correlated with increased p16 expression (Herbig, Ferreira et al. 2006). The examples mentioned thus far have investigated senescence of mitotic cells. However, evidence also suggests that non-dividing cells undergo senescent-like changes and increase in tissues with age. For example, it was demonstrated that TAF increase in liver hepatocytes and hippocampal neurones in baboons with age (Fumagalli, Rossiello et al. 2012). Consistent with the notion of post-mitotic cell senescence, Jurk *et al*. have described an age-dependent increase in neurones expressing multiple markers of senescence, including Sen-β-Gal, IL-6 and γH2A.X, in the brains of *C57BL/6* mice (Jurk, Wang et al. 2012). These results suggest that the accumulation of senescent cells in tissues with age is not just contributed to by proliferation-competent cells. Other reports have also shown that senescent cells increase in frequency in a range of murine tissues with age. Increased p16 mRNA and protein expression was observed in almost all rodent tissues with advancing age (Krishnamurthy, Torrice et al. 2004). SIRT1 protein expression decreases with age in murine tissues that have declining mitotic activity, such as the thymus and testis (Sasaki, Maier et al. 2006). Increased frequencies of γH2A.X foci-positive cells have been observed in the murine lung, spleen, small intestine, liver hepatocytes and dermis (Wang, Jurk et al. 2009). In line with this, our group reported an exponential increase in number of TAF per cell in murine liver hepatocytes and intestinal crypt enterocytes with age but found no significant increase in non-colocalising foci with age in either tissue (Hewitt, Jurk et al. 2012). This suggests that TAF are persistent and accumulate in tissues with age, whereas non-TAF

do not. Furthermore, in murine models of accelerated ageing, such as the progeroid mouse, the abundance of cells expressing chronically elevated levels of senescence-associated markers, such as p16, is increased in a number of tissues (Baker, Perez-Terzic et al. 2008). Similarly, in a mouse model for chronic inflammation that leads to accelerated ageing, frequencies of senescent cells identified by TAF were increased in the liver and gut (Jurk, Wilson et al. 2014). Interestingly, frequencies of TAF-containing senescent cells were shown to quantitatively predict mean and maximum lifespan in both short- and long-lived mice cohorts (Jurk, Wilson et al. 2014).

It is unknown as to why senescent cells accumulate in tissues and organs with age. Stimuli that induce senescence, such as ROS, increase with age and it is possible that accumulation of ROS-derived damage with age leads to senescent cell accumulation over time (Hamilton, Van Remmen et al. 2001; Chung, Cesari et al. 2009). Moreover, the increasing number of senescent cells can lead to further induction of senescence in surrounding cells *via* SASP factor release (Acosta, Banito et al. 2013). Recent findings suggest that senescent cells can be cleared by host mechanisms, such as activation of the immune system. For example, in a murine model of liver carcinoma, p53-dependent induction of cellular senescence leads to the induction of the innate immune response culminating in tumour cell clearance (Xue, Zender et al. 2007). Other studies also support the notion that senescent cells signal the innate and adaptive immune systems, probably through secretion of SASP factors, leading to their clearance and thus can be responsible for their own elimination (Krizhanovsky, Yon et al. 2008; Kang, Yevsa et al. 2011; Lujambio, Akkari et al. 2013). Therefore, another possibility is that immune surveillance and clearance of senescent cells becomes more inefficient with age (Sagiv and Krizhanovsky 2013). Indeed, immune cells can also become senescent, which may contribute to age-associated immune deficiency (Effros and Pawelec 1997; Lanna, Henson et al. 2014). Additionally, it has been suggested that the development of deeply senescent cells, which are likely to have evolved increasingly heterogeneous SASPs, may allow evasion of immune cell clearance as the efficiency by which immune cells recognise and clear senescent cells may be dependent on SASP composition (van Deursen 2014).

1.6.3 Senescence and age-related disease

Further support for the existence of senescence *in vivo* comes from the extensive evidence linking the age-dependent increase in senescent cell frequency to age-related decline in tissue structure and function and development of age-related disease (Naylor,

Baker et al. 2013; Ovadya and Krizhanovsky 2014). Cells with senescent cell properties are found at sites of chronic age-related pathology, such as osteoarthritis, atherosclerosis, type II diabetes and Alzheimer's disease (McShea, Harris et al. 1997; Vasile, Tomita et al. 2001; Price, Waters et al. 2002; Sone and Kagawa 2005). Direct evidence that senescent cells drive age-related pathologies was provided by one study, which demonstrated that genetic inactivation of p16 in BubR1 insufficient mice prevented cellular senescence in skeletal muscle and fat and attenuated the premature onset of age-related pathologies that are associated with BubR1 insufficiency in these tissues (Baker, Perez-Terzic et al. 2008). In a subsequent study, it was shown in the BubR1 progeroid mouse background that drug-induced elimination of p16-positive senescent cells delayed the onset of age-related pathologies in skeletal muscle, adipose tissue and eye. Furthermore, clearance of p16-positive senescent cells later in life attenuated the progression of already established age-related disorders, suggesting that senescent cells are causally implicated in age-related dysfunction (Baker, Wijshake et al. 2011). Interestingly, it has also been demonstrated that the number of p16 positive cells in human skin is associated with the occurrence of age-related pathologies, such as cardiovascular diseases (Waaijer, Parish et al. 2012). Thus, senescent cells are associated with ageing and age-related diseases *in vivo*.

There are a number of potential mechanisms by which senescent cells may promote age-related tissue dysfunction. One scenario is that the build-up of senescent cells in tissues with age progressively depletes the organism of functional cells critical for maintaining tissue repair and regeneration, such as stem and progenitor cells (Conboy, Conboy et al. 2005; Choudhury, Ju et al. 2007; Wang, Sun et al. 2012; Jurk, Wilson et al. 2014).

Human ageing is characterised by chronic, low-grade inflammation, termed 'inflammaging' (Franceschi, Capri et al. 2007; Chung, Cesari et al. 2009). In accordance, many age-related diseases are characterised by chronic inflammation and therefore one way that senescent cells may drive ageing and age-associated pathology is *via* the SASP (Tchkonia, Zhu et al. 2013; Franceschi and Campisi 2014). Senescent cells secrete a number of SASP factors, including pro-inflammatory growth factors, cytokines and chemokines, such as GROα, IL-1, IL-6, IL-8, and monocyte chemo-attractant proteins (MCPs) (Coppe, Patil et al. 2008; Freund, Orjalo et al. 2010). Therefore, senescent cells, which accumulate with ageing, may promote chronic tissue inflammation, characterised by infiltration of immune cells and thus causally contribute to the development of age-related disease (Freund, Orjalo et al. 2010). Additionally,

SASP components, such as IL-6 and IL-8 may stimulate tissue fibrosis in epithelial tissues by inducing epithelial-mesenchymal transition (EMT) (Laberge, Awad et al. 2012). Furthermore, SASP factors include proteases, such as matrix metalloproteinases (MMPs) and collagenases, which may compromise the structural and functional integrity of surrounding tissue by cleaving components of the extracellular matrix (ECM), promoting disease (West, Pereira-Smith et al. 1989; Millis, Hoyle et al. 1992; Parrinello, Coppe et al. 2005; Coppe, Patil et al. 2008). Although, as previously alluded to, the SASP can have positive consequences, such as promoting clearance of tumour cells and limiting fibrosis (Xue, Zender et al. 2007; Krizhanovsky, Yon et al. 2008), it is also strongly implicated in tumourigenesis. The release of MMPs and pro-inflammatory mediators is thought to promote a microenvironment that favours survival and progression of neoplastic cells and may also induce malignant phenotypes in neighbouring cells through paracrine mechanisms (Krtolica, Parrinello et al. 2001; Martens, Sieuwerts et al. 2003; Bavik, Coleman et al. 2006; Coppe, Patil et al. 2008). Recently, it has been demonstrated that RAS activation in conjunction with mitochondrial dysfunction induces cellular senescence in *Drosophila* imaginal epithelium, leading to activation of the SASP and overgrowth of neighbouring tissue (Nakamura, Ohsawa et al. 2014). Therefore senescent cells, which cannot form tumours themselves, may facilitate the development of cancer in ageing organisms *via* the SASP, which may partially explain why cancer rates increase exponentially beyond middle age (DePinho 2000). Finally, as the SASP can spread from cell to cell through paracrine mechanisms (Nelson, Wordsworth et al. 2012), this may amplify sterile inflammation, age-related tissue deterioration and disease progression (Tchkonia, Zhu et al. 2013).

Therefore, there is abundant evidence to suggest that the accumulation and persistence of senescent cells with age contributes to the ageing process and to the development of age-related diseases. While many correlations have been made, data also suggests that the senescence programme, late in life, is causally implicated in the generation of many age-related pathologies.

1.7 The role of mTOR in senescence and ageing

The mechanistic target of rapamycin (mTOR) is a serine/threonine protein kinase of the PI3K-related family that functions as a regulator of cell growth and metabolism in response to nutrient and hormonal cues (Johnson, Rabinovitch et al. 2013). mTOR can be found in two structurally and functionally distinct complexes: mTOR complex 1 (mTORC1) and mTOR complex 2 (mTORC2), which are defined by their adaptors

Raptor and Rictor, respectively (Laplante and Sabatini 2012). Much more is known about the mTORC1 pathway and its reported functions involve integrating inputs from growth factors, environmental nutrients, stress and cellular energy status to modulate anabolic processes *via* control of translation, protein synthesis, lipid biosynthesis, glucose metabolism and autophagy (Johnson, Rabinovitch et al. 2013). mTORC1 functions through at least two well-described downstream substrates: ribosomal protein S6 kinases (S6Ks) and eukaryotic translation initiation factor 4E (eIF4E)-binding protein 1 (4E-BP1) (Ekim, Magnuson et al. 2011). In contrast, little is known about the role of mTORC2 but it is known that this complex receives signals from growth factors to regulate glucose metabolism, lipogenesis, the actin cytoskeleton and apoptosis (Laplante and Sabatini 2012).

Multiple lines of evidence support a role for mTOR in modulating the ageing process. It has been demonstrated that inhibition of mTOR and components of the mTORC1 pathway through genetic means extends lifespan of yeast, worms and flies (Fabrizio, Pozza et al. 2001; Vellai, Takacs-Vellai et al. 2003; Jia, Chen et al. 2004; Kapahi, Zid et al. 2004; Kaeberlein, Powers et al. 2005). Similarly, dietary restriction (DR) is the most robust intervention able to extend lifespan and slow the progression of age-related diseases in many diverse species from yeast to primates (Fontana, Partridge et al. 2010). It is thought that decreased mTORC1 activity mediates longevity and health benefits resulting from DR interventions, which seems likely given its function in responding to nutrient availability and growth cues (Kenyon 2010). In agreement with this assumption, it has been demonstrated that DR fails to further extend replicative lifespan when combined with mutations in the mTORC1 pathway in yeast and worms (Kaeberlein, Powers et al. 2005; Hansen, Taubert et al. 2007).

Rapamycin, a compound isolated from *Streptomyces hygroscopicus* present in the soil from Rapa Nui island (Vezina, Kudelski et al. 1975), is a chemical inhibitor of mTORC1 (Sabatini, Erdjument-Bromage et al. 1994). Rapamycin (also known as sirolimus) is a widely used immunosuppressant but is now predominantly recognised for its lifespan extending effects, consistent with a beneficial role for inhibiting mTOR signalling to reduce ageing. Indeed, a number of studies have shown that rapamycin extends lifespan in yeast, worms, flies and mice (Powers, Kaeberlein et al. 2006; Harrison, Strong et al. 2009; Bjedov, Toivonen et al. 2010; Anisimov, Zabezhinski et al. 2011; Miller, Harrison et al. 2011; Robida-Stubbs, Glover-Cutter et al. 2012). Interestingly, Harrison and colleagues demonstrated that mTOR inhibition as a result of a rapamycin-supplemented diet lead to increased median and maximum lifespan even

when this intervention was started later in life (600 days of age) (Harrison, Strong et al. 2009). Recent studies have described that chronic treatment with rapamycin may also inhibit mTORC2 in some cell types (Sarbassov, Ali et al. 2006). Emerging evidence suggests that, like DR, mTORC1 inhibition by rapamycin may also have positive effects on age-related pathologies. For example, rapamycin treatment delays disease progression in mouse models of Alzheimer's disease (Spilman, Podlutskaya et al. 2010; Majumder, Richardson et al. 2011). Similarly, rapamycin attenuates cardiomyopathy in mice and improves cardiac and skeletal muscle function in mice lacking A-type lamins (Shioi, McMullen et al. 2003; McMullen, Sherwood et al. 2004; Ramos, Chen et al. 2012). Additionally, rapamycin slows the occurrence of age-related alterations in heart, liver, adrenal glands, endometrium and tendon (Wilkinson, Burmeister et al. 2012) and also reduces the number of cancer-related deaths in mice (Anisimov, Zabezhinski et al. 2011).

Recent data suggest an important role for mTOR in cellular senescence. *In vitro*, progression from transient cell-cycle arrest induced by experimental p21 overexpression to permanent arrest is dependent upon continuous mTOR activation in response to growth factors (Blagosklonny 2012). Additionally, long-term cell-cycle arrest via p21 overexpression may be reversible if mTOR is inhibited (Blagosklonny 2012). Furthermore, evidence suggests that rapamycin treatment can decelerate cellular senescence. For example, it was demonstrated in primary human fibroblasts undergoing either OIS or replicative senescence that mTOR inhibition by rapamycin or depletion of mTORC1 can delay several aspects of the senescence phenotype, including decreased proliferation rate, IL-8, p21 and Sen-β-Gal expression (Kolesnichenko, Hong et al. 2012). Similar effects have been reported in rat embryonic cells (Pospelova, Leontieva et al. 2012). Consistently, rapamycin treatment attenuates drug- and H_2O_2-induced senescence in fibroblast and epithelial cell lines, respectively (Demidenko and Blagosklonny 2008; Demidenko, Zubova et al. 2009). On the other hand, it has been shown that rapamycin promotes OIS in a mouse model of pancreatic cancer (Kennedy, Morton et al. 2011). Nevertheless, mTOR hyper-activation induces senescence, while its inhibition induces quiescence in a p53-dependent manner (Korotchkina, Leontieva et al. 2010). Additionally, it has been shown that mTOR regulates NF-κB activity, suggesting that mTOR may be involved in the control of some senescence-associated inflammatory pathways (Dan, Cooper et al. 2008).

1.8 Cellular senescence and age-related lung disease

The incidence of chronic respiratory diseases increases with age and so the accumulation of senescent cells in lung tissue might play a critical role in the development of a number of lung diseases (Bartling 2013). The biggest link between senescence and age-related lung disease comes from research into chronic obstructive pulmonary disease (COPD) (see below). However, the ageing process and cellular senescence have also been implicated in other pulmonary diseases, such as idiopathic pulmonary fibrosis (IPF), a progressive lung disease characterised by fibrosis of the interstitium, affecting the alveolar walls, with limited airway-centred pathology (Raghu, Weycker et al. 2006; Alder, Chen et al. 2008; Alder, Cogan et al. 2011; Minagawa, Araya et al. 2011). Bronchiectasis is another chronic lung disease, characterised by irreversible dilation of the bronchi and bronchioles, but in contrast to IPF has very limited interstitial aspects (King 2011). Similar to COPD, chronic inflammation is a major component of bronchiectasis that perpetuates disease progression (King 2011). However, cigarette smoking is not a major risk factor, with the majority of cases being labelled as idiopathic or post-infectious (Pasteur, Helliwell et al. 2000). Up to 50% of patients with COPD also have bronchiectasis (Patel, Vlahos et al. 2004). Thus, it is possible that there is overlap in the causative mechanisms underlying COPD and bronchiectasis. Currently there are, to our knowledge, very little data linking senescence to bronchiectasis.

1.8.1 Accelerated lung ageing and senescence in COPD

Chronic obstructive pulmonary disease (COPD) is one of the most common chronic respiratory diseases in the UK and a leading cause of morbidity and mortality globally (Hogg and Timens 2009). COPD is the fifth highest cause of death worldwide and is predicted to be the third highest by 2020 (Mannino and Buist 2007). COPD is characterised by chronic inflammation of both the large and peripheral airways. COPD also affects the lung parenchyma and thus may involve a degree of peri-airway fibrosis, mucous hypersecretion (chronic bronchitis) and destruction of alveolar airspaces (emphysema) (Bourdin, Burgel et al. 2009; Barnes 2013). These processes can and often occur in one individual although some patients may have either an emphysema or chronic bronchitis predominant phenotype.

There are numerous lines of evidence that suggest accelerated ageing processes underlie the pathogenesis of COPD (Ito and Barnes 2009; MacNee 2009; Lee, Sandford et al. 2011). Inflammation is a key feature of COPD and is linked to tissue-remodelling

events and inadequate repair processes that are responsible for the structural changes that occur in the COPD lung (Chung and Adcock 2008). Inhalation of toxic particles drives inflammation and is linked to the pathogenesis of COPD. Thus, the key risk factor for COPD is cigarette smoking (Forey, Thornton et al. 2011). Around 15-20% of smokers develop COPD and almost all patients with COPD have significant smoking histories (Lokke, Lange et al. 2006). The inflammatory response to cigarette smoke that occurs in the COPD lung is enhanced compared to the inflammatory response that occurs in non-COPD smokers. Even after smoking cessation, chronic inflammation still persists (Willemse, ten Hacken et al. 2005). This suggests that inflammation is maintained by feedback loops in the COPD lung. The inflammation in COPD is complex, involving several types of immune cells and multiple inflammatory mediators (Barnes 2004; Fischer, Pavlisko et al. 2011). Levels of neutrophils, macrophages and CD8$^+$ T lymphocytes are elevated in the COPD lung and show positive correlations with disease severity (Finkelstein, Fraser et al. 1995; Keatings, Collins et al. 1996; O'Shaughnessy, Ansari et al. 1997; Saetta, Baraldo et al. 1999). Pro-inflammatory cytokines, including tumour necrosis factor-α (TNF-α) and IL-6 are elevated in blood and sputum from patients with COPD (Di Francia, Barbier et al. 1994; Keatings, Collins et al. 1996; Bhowmik, Seemungal et al. 2000; Song, Zhao et al. 2001) and IL-8 levels are increased in the sputum and broncho-alveolar lavage fluid (BALF) of COPD patients (Keatings, Collins et al. 1996; Pesci, Balbi et al. 1998; Soler, Ewig et al. 1999). Additionally, baseline IL-8 release is increased from alveolar macrophages and epithelial cells from COPD patients (Culpitt, Rogers et al. 2003; Schulz, Wolf et al. 2003). Growth factors, such as TGF-β, are also produced in COPD-associated inflammation and it has been demonstrated that TGF-β expression is increased from small airway epithelial cells and alveolar macrophages in patients with COPD (Takizawa, Tanaka et al. 2001). Finally, release and activity of proteases, such as MMP2 and MMP9, is increased from peripheral blood monocytes and alveolar macrophages from patients with COPD and likely contribute to connective tissue breakdown and reinforcement of inflammatory processes (Russell, Culpitt et al. 2002; Aldonyte, Jansson et al. 2003). Therefore, one way in which accelerated lung ageing is linked to COPD is in the nature of the inflammatory processes that occur in the COPD lung, with many inflammatory cytokines akin to the SASP (Kumar, Seeger et al. 2014). Moreover, the ability of senescent cells to potentially recruit immune cells (Xue, Zender et al. 2007), may also place them as key culprits in the COPD-associated inflammatory process.

The Free Radical Theory of Ageing suggests that ROS react with cellular constituents such as DNA and proteins, the accumulation of which leads to the progressive changes of senescence and ageing (Harman 1956). There is accumulative evidence that oxidative stress is a major driving mechanism in the pathophysiology of COPD. Indeed, there are an estimated $10^{14\text{-}17}$ oxidative particles per puff of cigarette smoke and patients with COPD show increased markers of oxidative stress both systemically and in the lung (MacNee 2001). Levels of 4-hydroxy-2-nonenal (4-HNE) (a lipid peroxidation end-product that reacts with extracellular proteins forming adducts) modified proteins were increased in airway and alveolar epithelial cells, endothelial cells and neutrophils present in lung tissue from patients with COPD (Rahman, van Schadewijk et al. 2002). Both RNA and DNA oxidation has been described in the alveolar wall cells of patients with COPD (Deslee, Woods et al. 2009). A common by-product of guanine oxidation by reactive oxygen and nitrogen species is 8-hydroxy-2'-deoxyguanosine (8-OHdG), which serves as an established marker of oxidative stress (Kasai 1997). It has been shown that 8-OHdG is increased in the peripheral lungs of patients with COPD and smokers without COPD compared to non-smokers and in induced sputum from patients with COPD compared to smokers and non-smokers (Caramori, Adcock et al. 2011; Tzortzaki, Dimakou et al. 2012). Moreover, antioxidant levels are decreased in patients with COPD (Houben, Mercken et al. 2009).

In addition to cigarette smoking, ageing is a major risk factor for COPD. Indeed, the prevalence of COPD increases exponentially with increasing age (Lee, Sandford et al. 2011; Rycroft, Heyes et al. 2012). COPD is characterised by declining lung function, measured by forced expiratory volume in 1 second (FEV_1). The decline in FEV_1 that occurs as COPD progresses resembles that which occurs naturally with age, however, a larger volume is lost per year in COPD patients (Fletcher and Peto 1977). The ageing lung is associated with structural changes, such as alveolar dilatation, distal airspace enlargement and loss of supporting tissue for peripheral airways (Janssens, Pache et al. 1999). These structural changes resemble those that occur in COPD, causing similar physiological consequences, including loss of elastic recoil. Additionally, mouse models of accelerated ageing, such as the homozygous mutant klotho (-/-) mouse, show premature onset of emphysema (Suga, Kurabayashi et al. 2000).

The concept of accelerated lung ageing underlying the pathogenesis of COPD is further strengthened by studies demonstrating the presence of senescence-associated markers in the COPD lung and cells isolated from patients with COPD. For example, there are higher percentages of alveolar type II cells and pulmonary vascular endothelial

cells positive for p16 and p21 expression in lung tissue from patients with COPD compared to smokers without COPD and non-smokers (Tsuji, Aoshiba et al. 2006; Aoshiba and Nagai 2009; Tsuji, Aoshiba et al. 2010; Amsellem, Gary-Bobo et al. 2011). Similarly, there are significantly more γH2A.X and 53BP1 foci in type I and type II alveolar epithelial cells and endothelial cells in the lungs of patients with COPD (Aoshiba, Zhou et al. 2012). The HDAC SIRT1 is present at decreased levels in the peripheral lung tissue of smokers and COPD patients, likely due to increased oxidative stress (Rajendrasozhan, Yang et al. 2008; Nakamaru, Vuppusetty et al. 2009; Caito, Rajendrasozhan et al. 2010; Yao, Chung et al. 2012). Cells isolated from and cultured outside of the COPD lung, such as pulmonary vascular endothelial cells, retain markers of senescence including, Sen-β-Gal positivity and high p21 and p16 mRNA expression (Amsellem, Gary-Bobo et al. 2011). Similarly, lung fibroblasts from patients with advanced COPD appear senescent in culture, exhibiting reduced proliferation capacity and Sen-β-Gal expression (Holz, Zuhlke et al. 2004; Muller, Welker et al. 2006). Moreover, a number of studies report telomere shortening, a known inducer of senescence, in circulating leukocytes from COPD patients (Houben, Mercken et al. 2009; Mui, Man et al. 2009; Savale, Chaouat et al. 2009). Savale *et al.*, have shown that telomere length in circulating leukocytes of patients with COPD negatively correlates with plasma IL-6 levels (Savale, Chaouat et al. 2009). Interestingly, a dose-dependent relationship between smoking history and telomere length of circulating lymphocytes has also been described (Morla, Busquets et al. 2006). In one study of over 40 000 individuals, shorter telomere length was associated with decreased lung function and increased risk of COPD (Rode, Bojesen et al. 2013). However, other studies have failed to find associations between telomere length and FEV_1 or smoking history (Houben, Mercken et al. 2009; Savale, Chaouat et al. 2009).

Cigarette smoking is the major risk factor for COPD and it has been demonstrated that *in vitro* exposure to cigarette smoke extract (CSE) results in senescence-associated phenotypic changes to the cell. In cultured alveolar epithelial cells, exposure to CSE lead to growth arrest, an enlarged morphology, Sen-β-Gal activity and increased p21 expression (Tsuji, Aoshiba et al. 2004). Similar findings have been reported in lung fibroblasts, with CSE exposure leading to an enlarged and flattened morphology, increased Sen-β-Gal activity and increased p16 expression (Nyunoya, Monick et al. 2006; Aoshiba and Nagai 2009). Cigarette smoke exposure also triggers H2A.X phosphorylation in normal bronchial epithelial cells (Albino, Huang et al. 2004) and leads to reduced SIRT1 expression in macrophages and primary

human epithelial cells *in vitro* (Rajendrasozhan, Yang et al. 2008; Caito, Rajendrasozhan et al. 2010).

Therefore, it could be that accumulation of senescent cells, occurring naturally with ageing and as a result of chronic insult from cigarette smoke exposure, contributes to the structural changes and inflammatory processes that occur in the COPD lung.

1.9 Aims of this research

Although there are a number of studies implicating cellular senescence in the pathogenesis of COPD, it is still largely unknown whether telomere dysfunction is a significant contributor to cigarette smoke induced senescence and COPD-associated pathology. Additionally, the role of cellular senescence in bronchiectasis has not been investigated. The overall aim of this work was to investigate cellular senescence and telomere dysfunction in the ageing lung, in age-related lung disease and in the context of cigarette smoke exposure.

Specifically, the aims of this research were:

1) To investigate large and small airway epithelial cell senescence in patients with COPD and patients with bronchiectasis

2) To investigate airway epithelial cell senescence in the ageing murine lung and following cigarette smoke exposure, in particular the role of telomere dysfunction in this process

3) To determine whether long-term cigarette smoke exposure induces telomere dysfunction and senescence *in vitro*, and if so, to uncover the potential mechanisms involved

Chapter 2: Materials and Methods

2.1 Chemicals and Reagents

Unless otherwise stated, all reagents used in this research were obtained from Sigma-Aldrich Company Ltd (Poole, Dorset, UK).

2.2 Buffers and Solutions

A list of buffers and solutions used during this research is provided in Table 2.1.

Solution	Components
Sen-β-Gal staining solution	150mM NaCl, 2mM MgCl$_2$, 40mM citric acid, 12mM sodium phosphate pH6, 400μg/ml X-Gal, 2.1mg/ml Potassium hexacyanoferrat(II)trihydrate, 1.65mg/ml Potassium hexacyanoferrat (III) trihydrate
PBG-Triton	0.2% fish skin gelatin (Sigma, G7765), 0.5% BSA, 0.5% Triton X-100, 1% PBS
Hybridisation buffer for Immuno-FISH	70% deionised formamide (Sigma), 25 mM MgCl$_2$, 1 M Tris pH 7.2, 5% blocking reagent (Roche,Welwyn, UK), 4ng/μL Cy-3 labelled telomere specific (CCCTAA) peptide nuclei acid probe (Panagene, F1002-5), distilled H$_2$O
2 x SSC	17.53g of NaCl, 8.82g of sodium citrate, 1L of H$_2$O (pH7.0)
Citrate buffer (0.01M)	29.41g of trisodium citrate, 1L of distilled H$_2$O (pH 6.0)
1 x EDTA buffer	10 mM Tris-CL, 1 mM EDTA, distilled H$_2$O (pH 7.5)
Haematoxylin	5g Haematoxylin (Sigma, H3136), 300 ml Glycerin (Sigma, G2289), 50g Aluminium potassium sulphate (Sigma, 7210), 0.5g Sodium iodate (Sigma, S4007), 40 ml glacial acetic acid (Sigma, 537020) in 700 ml H$_2$O
1 x TBS	50 mM Tris-Cl, 150 mM NaCl, distilled H$_2$O (pH 7.5)

Table 2.1. **Buffers and solutions used during this research**.

2.3 Cell culture

2.3.1 Cell lines

MRC5 cells (normal human foetal lung fibroblasts) were obtained from European Collection of Cell Cultures (ECACC, #05090501) (Salisbury, UK).

2.3.2 Primary cells

Primary human airway epithelial cells were isolated from bronchial brushings carried out during research bronchoscopy (normal controls) or from explant lung tissue specimens (COPD). COPD patients were characterised by a physician as having COPD according to smoking pack years, FEV_1 measurements and ranked in Global Initiative for Chronic Obstructive Lung Disease (GOLD) criteria. Patients underwent bronchoscopy after a stable phase of at least 4 weeks. Normal controls identified from a volunteer register or local adverts were confirmed not to have COPD by FEV_1 testing-never and ex-smokers were eligible. Further PBECs from explant lung tissue specimens of patients with advanced COPD were collected. Patients and volunteers gave written informed consent prior to inclusion in the study. The work was performed under approval of the Newcastle and North Tyneside 1 Research Ethics Committee (RES-10/H0906/44) and (RES-11/NE/0291).

2.3.3 Routine cell culture

MRC5 cells were cultured in Dulbecco's Modified Eagle's Medium (DMEM) (Sigma, D7596) supplemented with foetal bovine serum (FBS) (10% v/v) (Sigma, 12133C), L-glutamine (2mM) (Sigma, G3126), penicillin (100 units/ml)/streptomycin (100 µg/ml) (Sigma, P4333) and maintained at 37°C, 5% CO_2. Cell culture was carried out using aseptic technique in a class II safety cabinet. Cell passaging included a phosphate buffered saline (PBS) wash, subsequent trypsinisation with pre-warmed Trypsin-EDTA (TE) (0.5% Trypsin, 0.2% EDTA) (Sigma, T3924) at 37°C followed by neutralisation with cell culture medium. Cells were then collected by centrifugation or resuspended in fresh medium at a suitable density and reseeded into tissue culture flasks or dishes.

Primary airway epithelial cells were cultured on 0.5% PureCol® (Invitrogen, Carlsbad, CA)-coated dishes in large or small airway epithelial cell growth medium (L/SABM, CC-3171/19) supplemented with 2% FBS, 100 U ml^{-1} penicillin and 100 mg ml^{-1} streptomycin (Lonza, Basel, Switzerland) and maintained at 37°C, 5% CO_2.

2.3.4. Cryogenic storage

Exponentially growing adherent cells were trypsinised and centrifuged at 800 g for 5 minutes at room temperature. The supernatant was removed and cells were washed in sterile PBS, re-centrifuged and re-suspended in FBS containing 5% (v/v) dimethyl sulfoxide (DMSO) (Sigma, D2650) at a density of 1 x 10^6 cells/ml. Aliquots of 1ml cell suspension were immediately transferred to cryo-vials and placed in a Nalgene^{TM} Cryo freezing container filled with isopropanol. Cells were kept for 24 hours at -80°C to allow them to slowly freeze before being stored long-term in liquid nitrogen.

2.3.5 Resuscitation of frozen cells

Cryo-vials were removed from liquid nitrogen and quickly thawed at 37°C for 1 to 2 minutes. Cells were immediately seeded into a 75 cm^2 with 20 ml pre-warmed medium. Medium was replaced after 24 hours to remove DMSO and cell debris.

2.3.6 Calculation of cell density and population doublings

To determine the concentration of cells within the cell suspension, 20 μl of suspension was added to a Fuchs-Rosenthal 0.2 mm haemocytometer (VWR International UK) and cells manually counted under a standard microscope (DMIL, Leica Microsystems, UK). The average of four counts of 8 squares was taken, which is equivalent to the number of cells x 10^4/ml. Cells within and touching the top and left sides of the square were counted. Total cell number was calculated by multiplying the total volume of cell suspension by the number of cells per ml. With every cell passage, population doubling (PD) was calculated by comparing total cell number with number previously plated, using the following equation:

PD = X + (ln(N1/N2))/ln2

Where:

PD= population doubling

X= previous PD

N1 = number of cells harvested

N2 = number of cells seeded

2.4 Cell treatments

All cell treatments were performed on MRC5 cells at a PD of 20-30 (stress-induced senescence) or after replicative exhaustion (replicative senescence).

Primary airway epithelial cells were treated at P1 and kept for a maximum of 3 days in culture.

2.4.1 Cigarette smoke extract

Cigarette smoke extract (CSE) was generated in a fume hood by burning one research grade cigarette (Tobacco Health Research Institute, University of Kentucky, Lexington, KY, 4A1) and bubbling the smoke produced into 25 ml of DMEM using a vacuum pump (KNF lab, N811KVP) (flow rate: 13l/min). The generated CSE solution was filtered (0.22 μm) for sterility and to remove large particles. The resulting solution was designated 100% CSE. The CSE solution was diluted in DMEM to the appropriate working concentration and used immediately.

Figure 2.1 Set up of equipment used to generate cigarette smoke extract.

2.4.2 CSE treatment

MRC5 cells at PD 20-25 (when 70-80% confluent), grown under normoxia (20% oxygen) were treated with 5% CSE until replicative senescence. Media + 5% CSE was replaced every 48 hours. Controls were grown in the absence of CSE and media was changed every 48 hours. Cells were harvested for analysis at 3, 7, 13, 24, 38 and 60 days after first treatment. At these time points, 5×10^4 cells were seeded per well into 12-well plates containing sterile 16 mm coverslips to be fixed for further analysis. 25×10^4 cells were also seeded into T-25 flasks to harvest media for cytokine analysis. The remaining cells were used for mitochondrial function and reactive oxygen species (ROS)

production assessment using flow cytometry and pelleted for protein and RNA analysis and stored at -80°C.

Primary airway epithelial cells (P1) were grown under normoxia in 12-well plates on sterile coverslips. Cells were treated with 5% CSE on two separate occasions, 48 hours apart. Cells were fixed 8 hours following the final treatment and stored at -80°C until further analysis.

2.4.3 Hypoxia treatment

MRC5 cells at PD 20-25 were cultured under 3% oxygen in combination with 5% CSE or DMEM alone. MRC5 cells cultured under normal conditions were run in parallel. Media + 5% CSE was replaced every 48 hours. Controls were grown in the absence of CSE and media was changed every 48 hours. Cells were harvested for analysis at 14 and 25 days following the initial treatment. At these time points, cells were seeded into 12-well plates, replated for cytokine analysis and analysed using flow cytometry, as described above.

2.5 Treatment with pathway inhibitors

2.5.1 Inhibition of mTORC1

MRC5 fibroblasts (PD 20-25), confluent to 70-80%, were treated with 5% CSE or DMEM alone (control) in combination with rapamycin (100nM, diluted in DMSO) (Sigma, R8781). Rapamycin was replaced every 48 hours along with 5% CSE or fresh DMEM. Controls treated with the same concentration of DMSO were included. Cells were harvested for analysis at 14 and 25 days following the initial treatment. At these time points, cells were seeded into 12-well plates, re-plated for cytokine analysis and analysed using flow cytometry, as described above.

2.5.2 Inhibition of ATM

MRC5 fibroblasts (PD 20-25), confluent to 70-80%, were treated with 5% CSE and treated with the ATM chemical inhibitor KU55933 (10μM, diluted in DMSO) (R&D, 3544). MRC5 cells cultured in DMEM alone were also treated with 10μM of KU55933. The chemical inhibitor KU55933 was replaced every 48 hours along with 5% CSE or fresh DMEM. Controls treated with the same concentration of DMSO were included. Cells were harvested for analysis at 14 and 25 days following the initial treatment. At these time points, cells were seeded into 12-well plates, re-plated for cytokine analysis and analysed using flow cytometry, as described above.

2.6 Flow cytometry

Calibration of the flow cytometer (Partec, http://www.partec.com) was carried out using fluorescent beads to ensure optimum performance and reproducibility. For each independent experiment, measurements were performed in triplicate and 10×10^4 cells were analysed per measurement.

2.6.1 MitoSOX staining

MitoSOX is a red fluorogenic dye used to detect mitochondrial-derived superoxide anions, which are produced in the mitochondrial matrix. MitoSOX permeates live cells and selectively targets mitochondria. It is rapidly oxidised by superoxide, but not by other ROS, resulting in red fluorescence. MRC5 cells were harvested and centrifuged at 1600 RPM for 3 minutes. Supernatant was discarded and cells were resuspended in MitoSOX Red (5 μM, diluted in serum-free DMEM) (Invitrogen, M36008) and incubated for 10 minutes at 37°C in the dark. Cells were centrifuged at 1600 RPM for 3 minutes and supernatant removed. The cell pellet was resuspended in 2ml of serum free DMEM and MitoSOX median fluorescence intensity was measured by flow cytometry (Red − FL3 channel). The population of live cells was defined in a FSC/SSC dotplot and apoptotic cells and debris excluded by gating.

2.6.2 DHR staining

Dihydrorhodamine (DHR) is a cell-permeable dye used to detect ROS, including peroxynitrite and peroxide. Upon oxidation by ROS, the colourless dihydrorhodamine 123 is oxidised to form rhodamine 123, which is highly fluorescent. The fluorescent product accumulates in the mitochondria. MRC5 cells were harvested and centrifuged at 1600 RPM for 3 minutes. Supernatant was discarded and cells were resuspended in DHR (30 μM, diluted in serum-free DMEM) (Invitrogen, D1168) and incubated for 30 minutes at 37°C in the dark. Cells were centrifuged at 1600 RPM for 3 minutes and supernatant removed. The cell pellet was resuspended in 2ml of serum free DMEM and DHR mean fluorescence intensity was measured by flow cytometry (Green − FL1 channel).

2.7 Senescence associated-β-galactosidase (Sen-β-Gal) staining

Cells grown on coverslips were washed with PBS and fixed with 2% PFA in PBS for 10 minutes. Cells were then stained in Sen-β-Gal staining solution (Table 2.1) (pH 6.0) for 24 hours at 37°C. Coverslips were washed two times in PBS and mounted with hardset VectaShield mounting media with 4',6-diamidino-2-phenylindole (DAPI) (Vector lab,

H1200). Cells showing Sen-β-Gal staining (blue staining) and total number of cells (DAPI staining) were counted in 10 randomly chosen fields (20X objective) per experiment using a Leica DM5500B microscope. Images were captured using a Leica DFC420 camera using LASAF software (Leica). Percentage of positive cells was quantified manually using ImageJ.

2.8 Mice

2.8.1 Mice groups and treatments

All work was compiled with the guiding principles for the care and use of laboratory animals.

Male *C57BL/6* mice were split into groups (n=3-5/group) according to age and diet: 6.5 month old mice fed control or rapamycin-supplemented diet for 3.5 months, 15 month old mice fed control or rapamycin-supplemented diet for 12 months and 24 month old mice fed only control diet. Control and rapamycin diets commenced when mice were 3 months of age and continued until time of sacrifice. Mice were randomly assigned to either control or rapamycin diets. Control and rapamycin diets were purchased from TestDiet - Control diet: 5LG6/122 PPM EUDRAGIT 3/8 #1814831 (5AS0) and Encapsulated Rapamycin diet: 5LG6/122 PPM ENCAP RAP 3/8 #1814830 (5ARZ). Mice were fed *ad libitum* and monitored weekly.

$TERC^{-/+}$ mice (obtained from The Jackson Laboratory) were crossed to generate G1 $TERC^{-/-}$ mice. These mice were crossed through successive generations to produce fourth-generation (G4) $TERC^{-/-}$ mice. Mice were maintained on *C57BL/6J* background. Mice were monitored weekly. Lungs from G4 $TERC^{-/-}$ mice sacrificed at 6 months of age were analysed.

The project was approved by the Faculty of Medical Sciences Ethical Review Committee, Newcastle University. Project license number: 60/3864.

In collaboration, lung tissues from mice exposed to either room air or cigarette smoke were a kind gift from Dr Mark Birrell, Imperial College London, UK. Male *C57BL/6* mice (n=5/group) at 10 weeks of age were subjected to a whole body cigarette smoke exposure system or room air, as previously described (Eltom, Stevenson et al. 2011). Briefly, cigarette smoke was generated using 3R4F cigarettes (Cigarette filter removed, University of Kentucky) and pumped into a Teague chamber (136L) for 1 hour, twice daily (500ml/min) for 14 days. Mice were sacrificed 24 hours after the final exposure.

2.8.2 Mice housing

Animal procedures were performed in accordance with the UK Home Office guidelines for animal welfare based on the Animals (Scientific Procedures) Act 1986. Animals were housed in a temperature-controlled room with a 12 hour light/dark cycle. No statistical method was used to predetermine sample size.

2.8.3 Mice tissue collection and preparation

Tissues were collected during necropsy and fixed with 4% formaldehyde aqueous solution (VWR, 9713.9010) and embedded in paraffin for histochemical analysis.

2.9 Subjects

The cross-sectional investigation of senescence-associated markers in lung tissue specimens from patients with COPD, patients with bronchiectasis and smokers without COPD or bronchiectasis (controls) undergoing resection surgery was conducted at the Sir William Leech Centre for Lung Research, Freeman Hospital (Newcastle upon Tyne, UK) with the help of a clinical team. The clinical team (Prof Andrew Fisher, Dr Anthony De Soyza, Dr Syba Sunny, Mr Sasha Stamenkovic, Dr Fiona Black and Gail Johnson) were involved in subject recruitment and the obtaining of lung tissue specimens. Sampling was opportunistic by necessity.

2.9.1 Subject recruitment

Control subjects were recruited prospectively between October 2011 and February 2012 when attending the Freeman Hospital for pulmonary resection for localised lung cancer. Lung tissue from patients with COPD and patients with bronchiectasis was acquired from archived tissue taken from patients at the time of lung transplantation as part of the lung transplant programme at the Freeman Hospital. Where possible, subjects were matched for age and smoking status. Table 3.1 gives an overview of the clinical characteristics of the subjects.

2.9.2 Obtaining and processing of lung tissue specimens

Potentially suitable material was identified from histology reports and requested from either the Royal Victoria Infirmary (RVI) pathology archive (Newcastle upon Tyne) or the Human Tissue Act (HTA) approved Sir William Leech research archive (Freeman Hospital, Newcastle upon Tyne). Tissue blocks containing central airways and blocks containing parenchymal tissue were obtained from each subject. Formalin-fixed, paraffin-embedded lung tissue blocks were cut into sections at a thickness of 5μm using

a Reichert-Jung 2035 rotary microtome (Leica) and mounted onto glass slides. Slides were dried by incubating at 60°C overnight.

2.9.3 Ethical approval

The collection of lung tissue from control subjects and patients with COPD was approved by the County Durham and Tees Valley 2 Research Ethics Committee (RES-11/NE/0291) and patients gave written informed consent prior to inclusion in the study.

2.10 Immunofluorescence

2.10.1 Immunofluorescence staining on fixed cells

Cells grown on sterile coverslips were fixed with 2% paraformaldehyde (PFA) (VWR, 9713.9010) in PBS for 10 minutes at room temperature. PFA was removed and cells were washed two times with PBS. To permeabilise, cells were incubated with 1 ml PBG-Triton for 45 minutes at room temperature. Cells were incubated with diluted primary antibody in PBG-Triton overnight at 4°C or for one hour at room temperature with gentle agitation. Cells were washed three times with PBG-Triton for 5 minutes and incubated for 45 minutes to 1 hour with fluorescein-conjugated secondary antibody diluted 1:4000 in PBG-Triton away from light. Cells were washed two times with PBS for 10 minutes and stained with 400μl of DAPI (Partec, 05-5001) for 10 minutes. Cells were washed three times with PBS before mounting cells on slides with anti-fade VectaSheild mounting medium (Vector lab, H1000). Slides were analysed using a Leica DM5500B microscope and fluorescence images were captured with a DFC360FX camera using LASAF software (Leica).

2.10.2 Immuno-FISH (γH2A.X-TeloFISH) staining on fixed cells

Fluorescence *in situ* hybridization (FISH) utilises fluorescent probes to detect specific DNA sequences. The bound fluorescent probe can then be visualised using a fluorescent microscope.

Cells grown on coverslips were fixed and γH2A.X immuno-staining was performed as described above. Following application of the secondary antibody, cells were washed with PBS and FISH was performed.

Cells were fixed in 1 ml of fixative (methanol: acetic acid, 3:1) for 30 minutes and then dehydrated in graded ethanol solutions (70, 90, 100%) for 2 minutes each. Cells were immersed in PBS at 37°C for 5 minutes and fixed in 4% PFA in PBS at 37°C for 2 minutes. Cells were dehydrated again with cold ethanol solutions (70, 90, 100%) for 2 minutes each and air-dried before being denatured for 10 minutes at 80°C

in hybridisation buffer containing PNA probe (see Table 2.1). Cells were then incubated for 2 hours at room temperature in the dark to allow hybridisation to occur. Cells were washed 3 times for 10 minutes with 70% formamide in 2 x SSC, followed by three 5 minute washes in TBS-Tween 0.05%. Cells were dehydrated in graded ethanol series (70, 90, 100%) for 2 minutes each, air-dried and mounted using VectaSheild mounting medium Antifade + DAPI (Vector labs, H1500). Cells were imaged using a Leica DM5500B fluorescence microscope. In depth Z stacking was used (a minimum of 40 optical slices with 100 x objective) followed by Huygens (SVI) deconvolution. DNA damage foci and telomere-associated foci were analysed blinded by several experienced observers using ImageJ software. The majority of images were quantified by J Birch with confirmatory quantifications carried out in a blinded fashion by R Anderson and C Melo from our lab.

Antibody	Species/Isotype	Specificity	Dilution
Anti-Ki67 (Abcam, ab15580)	Rabbit polyclonal	Human Mouse	1:250
Anti-phospho-histone H2A.X (γH2A.X) (Ser139) (Millipore, 05-636)	Mouse monoclonal	Human	1:200

Table 2.2 Primary antibodies used for immunofluorescence on cells

Antibody	Species/Isotype	Specificity	Dilution
Anti-rabbit Fluorescein-conjugated secondary antibody AlexaFluor 594 (Invitrogen, A21213)	Goat	Rabbit	1:4000
Anti-mouse Fluorescein-conjugated secondary antibody AlexaFluor 488 (Invitrogen, A21042)	Goat	Mouse	1:4000

Table 2.3 Secondary antibodies used for immunofluorescence on cells

2.10.3 Immunofluorescence staining on paraffin embedded tissues

Sections cut at 5μm (human) or 3μm (mouse) thick were deparaffinised in Histoclear (National Diagnostics, HS-200) twice (5 minutes each) and hydrated in graded ethanol solutions: 100% (2 x 5 minutes), 90% (5 minutes) and 70% (5 minutes), before being washed in distilled H_2O (2 x 5 minutes).

To retrieve antigens, sections were incubated in 0.01M citrate buffer (pH 6.0) for 5 minutes at high power (800W) in a microwave oven, followed by 10 minutes at medium power (400W). Sections were allowed to cool to room temperature in an ice bath before being washed in distilled H_2O (2 x 5 minutes).

Sections were incubated for 30 minutes at room temperature in blocking reagent (Normal goat serum (NGS) (Vector lab, PK-6101) diluted 1:60 in 0.1% bovine serum

albumin (BSA) (Sigma, A9418) in PBS). Sections were incubated with the primary antibody (diluted in blocking reagent) overnight at 4°C.

Sections were washed in PBS (3 x 5 minutes) and incubated for 30 minutes with secondary antibody (diluted in blocking reagent) at room temperature. Sections were washed in PBS (3 x 5 minutes). For γH2A.X staining, sections were incubated with Fluorescein Avidin DCS (1:500) (Vector Lab, A-2011) diluted in PBS for 30 minutes at room temperature. Sections were washed in PBS (3 x 5 minutes) followed by counterstaining with DAPI for 10 minutes. Sections were washed in PBS (3 x 10 minutes), before being mounted with an anti-fade VectaShield mounting medium (Vector lab, H-1000). Staining was analysed using a Leica DM5500B microscope and fluorescence images were captured with a DFC360FX camera using LASAF software (Leica).

2.10.4. Immuno-FISH (γH2A.X-TeloFISH) staining on paraffin embedded tissues

Immunofluorescence staining was carried out as described above. Following incubation with Avidin DCS, sections were washed in PBS (3 x 5 minutes) and then samples were crosslinked by incubating in 4% PFA in PBS for 20 minutes. Sections were washed in PBS (3 x 5 minutes) and then dehydrated in graded ethanol solutions (70%, 90% and 100%, 3 minutes each). Tissue sections were air dried and denatured in hybridisation buffer containing PNA probe (see Table 2.1) for 10 minutes at 80°C, followed by hybridisation for 2 hours at room temperature in the dark. Sections were washed for 10 minutes with 70% formamide in 2 x SSC, followed by a 10 minute wash in 2 x SSC and a further 10 minute wash in PBS. Nuclei were counterstained with DAPI for 10 minutes and washed in PBS (3 x 5 minutes) before being mounted in VectaShield mounting medium. Staining was analysed using a Leica DM5500B fluorescence microscope and Z-stack images (a minimum of 40 optical slices with 100 x objective) taken with a DFC360FX camera using LASAF software (Leica). This was followed by Huygens (SVI) deconvolution. The specificity of staining was confirmed by including controls where the primary antibody was omitted. Telomere associated foci were analysed by several observers as above using ImageJ software.

Antibody	Species/Isotype	Specificity	Dilution
Anti-phospho-histone H2A.X (γH2A.X) (Ser139) (Cell Signaling, 9718)	Rabbit monoclonal	Human Mouse	1:400
Anti-p16 (Santa Cruz, SC-81156)	Mouse monoclonal	Human	1:500

Table 2.4 Primary antibodies used for immunofluorescence on tissues

Antibody	Species/Isotype	Specificity	Dilution
Anti-rabbit IgG Biotinylated (VECTASTAIN Elite ABC Kit) (Vector lab, PK-6101)	Goat	Rabbit	1:200
Anti-mouse Fluorescein-conjugated secondary antibody AlexaFluor 647 (Invitrogen, A20173)	Goat	Mouse	1:4000

Table 2.5 Secondary antibodies used for immunofluorescence on tissues

2.11 Immunohistochemistry

2.11.1 Immunohistochemistry staining of human tissue

On aminopropyltriethoxysilane (APES) (Sigma, A3648) treated slides, sections cut at 5μm were deparaffinised in xylene (5 minutes) and rehydrated through graded ethanol solutions (99%, 99%, 95%; 1 minute each). Endogenous peroxidase activity was blocked by immersing sections in 0.3% H_2O_2 (Sigma, H1009), diluted in methanol for 30 minutes. Sections were washed under running tap water for 10 minutes. Antigen retrieval was performed as described (Table 2.6). Sections were rinsed in 1 x Tris-buffered saline (TBS) and blocked in 5% non-fat milk protein (NFMP) diluted in TBS where required (Table 2.6). Primary antibodies were diluted in 3% bovine serum albumin (BSA) in TBS as per the antibody datasheet and 100μl of diluted antibody or isotype control was applied to tissue sections (See Table 2.6 for dilutions). Antigen retrieval and primary antibody concentrations were optimised in collaboration with Gail Johnson from the Sir William Leech Laboratories, Freeman hospital. Sections were incubated in a moist incubating tray for the required time period (Table 2.6). Slides were then gently washed in TBS (2 x 5 minutes). Excess TBS buffer was removed and 100μl of anti-mouse (Dako, K4006) or anti-rabbit (Dako, K4010) secondary antibody conjugated with a horseradish-peroxidase (HRP)- labelled polymer added (Envision+ System-HRP, Dako). Sections were incubated for 30 minutes at room temperature. Slides were gently washed in TBS for 5 minutes and treated with 3,3'-diaminobenzidine (DAB) (1 drop DAB chromogen to 1ml DAB substrate buffer) for 5-10 minutes. The reaction was checked microscopically. Slides were washed under running tap water and nuclei counterstained with Carrazzi Haematoxylin for 1 minute. Sections were washed under running tap water until nuclei appeared blue, dehydrated through graded ethanol solutions: 95%, 99% and 99% (30 seconds each), cleared in xylene and mounted in Di-N-Butyle Phthalate in Xylene (DPX) (Thermo Scientific, LAMB-DPX).

Central and peripheral airway epithelial cell staining was evaluated using a digital camera (MicroPublisher 3.3, QImaging) in a light microscope (Olympus BH-2) at 400 X magnification. Sub-epithelial reticular basement membrane length was measured in order to calculate the number of positive cells/mm basement membrane as previously described (Ward *et al*., 2004). In brief, an image analyser (Image-Pro Plus, 6.3, Silver Spring, MD, USA) was used to score the number of positive epithelial cell nuclei above all of the reticular basement membrane available in the lung tissue sections.

The length of reticular basement membrane in each visual field was confirmed using a measuring tool calibrated at 400 X magnification. Total number of positive nuclei/mm basement membrane was calculated and an average score for each tissue section generated. In order to avoid artefacts introduced by tissue processing, airways were positively identified by the presence of intact, well-orientated airway epithelium and the attachment of the basement membrane to the rest of the tissue.

Level of staining in human tissue was also quantified using a semi-quantitative scoring method, whereby anonymised tissue sections were ordered from lowest to highest level of staining and given a score of 0-3 based on level of positivity in the airway epithelium. Quantifications were carried out in a blinded fashion by two independent scientists (J Birch and K Jiwa (NHS biomedical scientist)). Figure 2.2 shows examples of scores given for SIRT1 expression in the small airway epithelium.
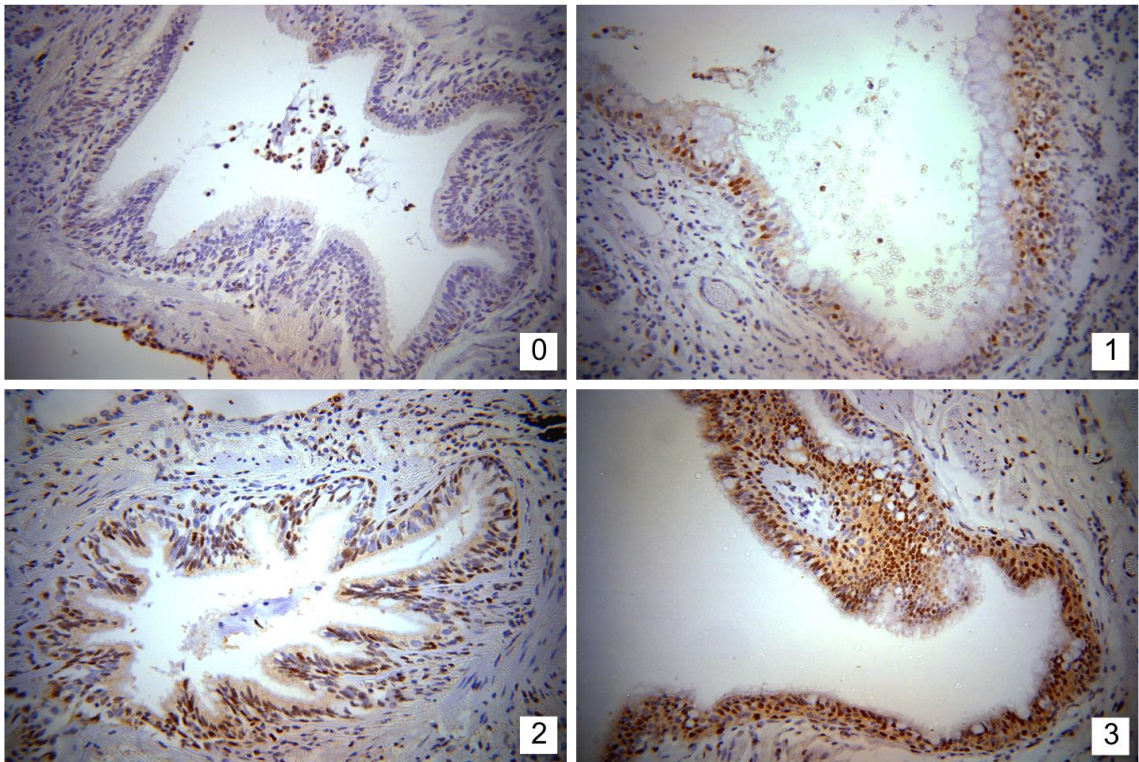
Figure 2.2 Representative images of scores for SIRT1 staining in small airway epithelial cells. Sections were scored from 0-3 based on level of positive staining in the airway epithelium. Scores were determined based on overall staining observed for that marker across all tissue sections. Examples are shown for a score of 0, 1, 2 and 3. Images were captured using X20 objective.

Antibody	Species/Isotype	Dilution	NFMP block	Antigen retrieval	Positive control
Anti-Ki-67 (Novocastra, KI67-MM1-CE)	Mouse monoclonal	1/100 for 45 mins at room temp	No	20 mins EDTA (100% microwave power)	Tonsil
Anti-p21 (Santa Cruz, SC-817)	Mouse monoclonal	1/500 for 24 hours at 4˚C	2 hours	20 mins citrate (100% microwave power)	Placenta
Anti-p16 (Santa Cruz, SC-81156)	Mouse monoclonal	1/500 for 45 mins at room temp	20 mins at room temp	10 mins citrate (100% microwave power)	Lung tissue (internal control)
Anti-Phospho-histone H2A.X (γH2AX) (Ser139) (Cell Signaling, 9718)	Rabbit monoclonal	1/100 for 1 hour at room temp	No	20 mins citrate (100% microwave power)	Lung tissue (internal control)
Anti-SIRT1 (Abcam, ab13749)	Rabbit polyclonal	1/100 for 45 mins at room temp	20 mins at room temp	10 mins EDTA buffer (100%)	Lung tissue (internal control)
Isotype control (Dako, X0931)	Mouse monoclonal	As primary antibody*	As primary antibody*	As primary antibody*	N/A
Isotype control (Dako, X0903)	Rabbit Ig fraction	As primary antibody*	As primary antibody*	As primary antibody*	N/A

Table 2.6 Primary antibodies used for immunohistochemistry on human tissues.
*Isotype controls were diluted to the same protein concentration as the primary antibody. NFMP, non-fat milk protein; Ig, Immunoglobulin; EDTA, Ethylenediaminetetraacetic acid; NA, not applicable.

2.11.2 Immunohistochemistry staining of mouse tissue

On APES treated slides, sections cut at 3μm were deparaffinised in Histoclear (2 x 5 minutes) and hydrated in graded ethanol solutions: 100% (2 x 5 minutes), 90% (5 minutes) and 70% (5 minutes), before being washed in distilled H_2O (2 x 5 minutes).

To retrieve antigens, sections were incubated in 0.01M citrate buffer (pH 6.0) for 5 minutes at high power (800W) in a microwave oven, followed by 10 minutes at medium power (400W). Sections were allowed to cool to room temperature in an ice bath before being washed in distilled H_2O (2 x 5 minutes). Endogenous peroxidase activity was blocked by incubating sections in 0.9% H_2O_2 diluted in distilled H_2O for 30 minutes. Sections were rinsed under running tap water, washed in PBS (5 minutes) and incubated for 30 minutes at room temperature in blocking reagent (NGS diluted 1:60 in 0.1% BSA in PBS). Sections were incubated with the primary antibody (diluted in blocking reagent) overnight at 4°C. Sections were washed in PBS (3 x 5 minutes) and incubated with biotinylated secondary antibody (diluted in blocking reagent) for 30 minutes at room temperature. Sections were washed in PBS (3 x 5 minutes) and secondary antibodies detected using the rabbit peroxidase ABC kit (Vector lab, PK-4001) according to the manufacturer's instructions. Substrate was developed using the NovaRed kit (Vector lab, SK-4800) according to the manufacturer's instructions. Sections were washed in tap water (3 x 1 minute) and nuclei were counterstained with haematoxylin for 15-30 seconds. Sections were washed under running tap water until nuclei appeared blue, dehydrated in graded ethanol solutions: 70%, 90% and 100% (30 seconds each), cleared in Histoclear and mounted in DPX. Slides were analysed with a NIKON ECLIPSE-E800 microscope and images were captured with a Leica DFC420 camera using the LAS software (Leica). Levels of positive staining were determined by quantifying the number of negative and number of positive nuclei and generating an average percentage from 10 randomly captured images for each animal.

Antibody	Species/Isotype	Specificity	Dilution
Anti-p21 (Abcam, ab7960)	Rabbit polyclonal	Human Mouse	1:200
Anti-Neutrophil antibody (NIMP-R14) (Abcam, ab2557)	Rat Monoclonal	Mouse	1: 200

Table 2.7 Primary antibodies used for immunohistochemistry on mouse tissues

Antibody	Species/Isotype	Specificity	Dilution
Anti-rabbit IgG Biotinylated (VECTASTAIN Elite ABC Kit) (Vector lab, PK-6101)	Goat	Rabbit	1:200
Anti-rat IgG (Vector lab, BA-9400)	Goat	Rat	1: 200

Table 2.8 Secondary antibodies used for immunohistochemistry on mouse tissues

2.12 Haematoxylin and eosin (H&E) staining

Sections mounted onto glass slides were de-waxed in xylene (5 mins), rehydrated through graded ethanol solutions (99%, 99%, 95%; 1 min each) and rinsed in water until clear. Sections were immersed in Harris Haematoxylin (6765003; Thermo Scientific) for 1 min. Sections were then rinsed well in running tap water for 2-3 mins. Sections were checked microscopically (Olympus CH-2) and differentiated in 0.1% Acid Alcohol when required. Sections were washed again in running tap water until nuclei appeared blue microscopically. Sections were counterstained in Eosin-Y (6766007; Thermo Scientific) for 2 minutes and washed under running tap water until clear. Sections were dehydrated through graded ethanol solutions (95%, 99%, 99%; 1 min each), cleared in xylene and mounted in DPX.

2.13 Quantification of alveolar airspace size

Following H&E staining, for murine lung tissue sections, alveolar airspace size was quantified by two methods.

2.13.1 Quantification of alveolar airspace size by mean linear intercept

Images were randomly captured (n=10 per animal) using X20 objective of areas of tissue where there were no airways or pulmonary blood vessels contained within the visual field. The mean linear intercept (MLI) was determined for each image and an average calculated per mouse. MLI was determined using ImageJ software, whereby a diagonal line of known length was drawn from the bottom left of each image to the top right and number of intersections (from alveolar wall segments) along that line quantified. The length of the line in microns was divided by the number of intercepts, as previously described (Weibel 1963). Therefore, the fewer the number of intersections, indicative of a reduction in alveolar airspaces or increased airspace size, the higher the MLI value.

2.13.2 Quantification of alveolar airspace size by counting number of airspaces

Changes in alveolar airspace size were also quantified by manually counting the number of airspaces present in each visual field and an average number calculated per animal.

2.14 Analysis of pro-inflammatory cytokine release

2.14.1 Antibody array

A Quantibody Human Cytokine Array for 20 cytokines (RayBiotech, QAH-CYT-1) was performed. Conditional media was collected at a range of time points (mentioned above) for both 5% CSE-exposed and untreated cells following 24h serum deprivation. Conditional media was then sent to RayBiotech for analysis using the Quantibody Human Cytokine Array. Limit of detection for this assay was 10 ρg/ml.

2.14.2 Enzyme-linked immunosorbent assays (ELISA)

IL-6 and IL-8 concentrations in cell culture supernatants were determined using commercially available ELISA kits (Duoset, R&D systems, DY206/DY208), according to the manufacturer's instructions. Conditional media was collected at a range of time points (noted above) for both 5% CSE-exposed and untreated cells following 24h serum deprivation. All assays were carried out at room temperature. Limit of detection for this assay was 10 ρg/ml.

2.15 Protein expression analysis

2.15.1 Protein Extraction

MRC5 cells were washed with ice cold PBS before lysis in ice cold RIPA buffer (150 mM NaCl, 1% NP40, 0.5% NaDoC, 0.1% SDS, 50 mM Tris pH 7.4 and 1x phosphatase

and protease inhibitors cocktail (Thermo Scientific, 78442). Samples were collected into 1.5 ml microcentrifuge tubes and immediately stored at -80°C until further analysis.

2.15.2 Protein quantification

Cell lysates were thawed on ice and centrifuged for 10 minutes at 16100g at 4°C. Protein quantification was performed using a colorimetric Bio-Rad DC Protein Assay (Bio-Rad; Reagent A, 500-0113, Reagent B, 500-0114, Reagent S, 500-0115), according to the manufacturer's instructions. Protein absorbance was measured on the Fluostar Omega plate reader (BMG Labtech). Protein concentration of each sample was then calculated and normalised by mixing adjusted volumes of protein lysate and loading buffer (950 μl of 2xLaemmli buffer (Bio-Rad, 161-0737) plus 50 μl of mercaptoethanol (Sigma, M6250)). Proteins were denatured by incubating samples at 100°C for 5 minutes. Samples were placed on ice after denaturation and used immediately for western blotting.

2.15.3 Western blotting

A running gel was prepared according to the size of the target proteins being analysed and poured into a cassette (Invitrogen, NC2015 or NC2010) (see Table 2.9 for gel preparation). After the running gel had polymerised, a 5% acrylamide staking gel was prepared, poured into the cassette and allowed to polymerise. Gels were placed in a XCell SureLock^{TM} Mini-Cell Electrophoresis System (Invitrogen) covered by Tris-Glycine running buffer (250μM Tris, 1.92mM Glycine and 0.1% SDS). Samples were loaded side by side into wells alongside a protein standard (Bio-Rad, 161-0374) and electrophoresis was performed at 120V, 35mA for 90 minutes.

Proteins were transferred from the gel to a 0.45μm polyvinylidene difluoride (PVDF) membrane (Millipore, IPVH00010). Both the membrane and the gel were placed between transfer pads (VWR, 732-0594), which were soaked in transfer buffer (250μM Tris, 1.92mM Glycine). Transfer was performed using the Trans-Blot® SD Semi-Dry Transfer Cell (BioRad) at 20 volts for 1 hour. The membrane was then stained with Ponceaux red solution (0.5% Ponceaux and 5 % Acetic Acid in H_2O) for detection of protein bands.

The membrane was incubated for 1 hour in blocking buffer (5% Milk in 0.05% PBS-Tween) at room temperature on a shaker. The membrane was then incubated overnight at 4°C while shaking gently with primary antibody diluted in blocking buffer (antibodies against phosphorylated proteins were diluted in 5% BSA in 0.05% PBS-Tween). The membrane was washed 3 times in sterile H_2O before incubation with the

secondary antibody diluted in blocking buffer for 1 hour at room temperature while shaking gently. Membranes were washed 3 times with sterile H_2O followed by a 5 minutes wash in 0.05% PBS-Tween at room temperature while shaking gently, before the final wash in sterile H_2O (5 times).

The blot was incubated with the chemiluminescence agent ClarityTM Western ECL substrate (Bio-Rad, 170-5060) for 5 minutes. The blot was visualised using Fuji film Intelligent Dark box II and Image Reader Las-1000 Software. The protein of interest was confirmed by size comparison of the protein bands to the protein standard loaded during electrophoresis. ImageJ analysis software was used to quantify the intensity of signal. Intensity quantification of the protein of interest was calculated after background subtraction and normalisation to a loading control (GAPDH).

1 X Gel (10ml)	5%	15%
Sterile H$_2$O	6.8 ml	3.3 ml
30% Acrylamide (Severn Biotech, 20- 2100-10)	1.7 ml	4 ml
1.5M Tris pH 8.8 (Sigma, T6066)	2.5 ml	2.5 ml
10% SDS (Sigma, L4390)	100 µl	100 µl
10% Ammonium Persulphate (Sigma, 215589)	100 µl	100 µl
TEMED (Sigma, T9281)	8 µl	100 µl

Table 2.9 Acrylamide gels for western blotting

Antibody	Species/Isotype	Specificity	Dilution
Anti- γ H2A.X (Ser139) (Cell Signalling, #9718)	Rabbit polyclonal	Human Mouse	1:1000
Goat anti-rabbit IgG - HRP conjugated (Sigma, A0545)	Goat	Rabbit	1:5000

Table 2.10 Primary and secondary antibodies used for western blotting

2.16 Telomere length analysis by Real-Time PCR

Total DNA was isolated from small airway epithelial cell pellets using the spin column protocol for the purification of total DNA from the DNeasy® Blood and Tissue Kit according to the manufacturer's instructions (Qiagen, 69506). Telomere length was

measured using RT-PCR in collaboration with the Biomarker lab, Newcastle University. Telomere length was measured as abundance of telomeric template versus a single gene by quantitative real-time PCR (Cawthon, Smith et al. 2003) with modifications as described by Martin-Ruiz *et al*. 2004 (Martin-Ruiz, Saretzki et al. 2004). Measurements were performed in quadruplicate. Three DNA samples with known telomere lengths (3.0, 5.5 and 9.5 kbp) were run as internal standards, allowing us to estimate telomere length in base pairs.

2.17 Statistical analysis

Data are expressed as the mean ± SD, mean ± S.E.M or median ± range, where appropriate. Where data were normally distributed, statistically significant differences between groups were assessed using ANOVA and significant differences between two groups were evaluated using an Independent samples t-test. Where data were not normally distributed, statistically significant differences between groups were assessed using the Kruskal Wallis test and significant differences between two groups were evaluated using the Mann-Whitney U test. P values less than 0.05 were considered significant. Data were analysed using GraphPad Prism version 6.0, GraphPad Software, San Diego California USA, www.graphpad.com and IBM SPSS statistics version 19.

Chapter 3. Airway epithelial cell senescence and telomere dysfunction in COPD

Evidence suggests that senescence is involved in the pathogenesis of age-related lung disease, including IPF and COPD (Faner, Rojas et al. 2012). Previous reports have shown that senescence-associated markers are increased in a number of cells in the COPD lung, mainly in alveolar type II cells, endothelial cells and pulmonary artery smooth muscle cells (Tsuji, Aoshiba et al. 2006; Aoshiba and Nagai 2009; Tsuji, Aoshiba et al. 2010; Amsellem, Gary-Bobo et al. 2011; Noureddine, Gary-Bobo et al. 2011). The airway epithelium likely endures the brunt of environmental insults, such as inhaled toxins present in cigarette smoke, and is one site of the lung most associated with development of cigarette smoke-induced abnormalities (Auerbach, Forman et al. 1957). However, there are very few studies describing senescence-marker expression in the airway epithelium of the COPD lung. Zhou and colleagues found that lung tissue from patients with COPD had increased numbers of p16-positive Clara cells, the progenitors of the distal airway epithelium, as compared to smokers and non-smokers without COPD (Zhou, Onizawa et al. 2011). Similarly, it has been shown that SIRT1 expression is decreased in the small airway epithelium of patients with COPD (Rajendrasozhan, Yang et al. 2008). Nonetheless, studies utilising multiple markers to investigate airway epithelial cell senescence in COPD are lacking, and furthermore, no study has investigated both large and small airway epithelial cell senescence *in situ* in lung specimens from patients with COPD. Bronchiectasis, a chronic respiratory condition characterised by inflammation, occurs more commonly in patients with COPD (Patel, Vlahos et al. 2004). However, there are currently no data, to our knowledge, implicating airway epithelial cell senescence in the bronchiectatic lung.

The aims of this work were to investigate the expression of multiple markers associated with senescence in both the large and small airway epithelium in lung tissue from patients with COPD. Additionally, we aimed to investigate whether expression of senescence-associated markers was altered in the large and small airway epithelium of patients with bronchiectasis.

3.1 Investigating senescence-associated marker expression in the airway epithelium of patients with bronchiectasis and patients with COPD

To determine whether markers associated with the senescence phenotype are increased in the large and small airway epithelium of patients with bronchiectasis and patients

with COPD, we obtained explant lung tissue from patients undergoing transplantation for end-stage bronchiectasis (n=14) or advanced COPD (n=19) and from controls (n=11) undergoing pulmonary resection for localised lung cancer. For each subject, lung tissue containing cartilaginous bronchi (large airways) and lung tissue taken from the sub-pleural parenchyma (containing small airways) was obtained. Expression of the proliferation marker Ki67, the DNA damage response marker γH2A.X, CDK inhibitors p21 and p16 and the HDAC SIRT1 was assessed by immunohistochemistry. Airway epithelial cell expression of markers was quantified in all large (defined in this project as cartilaginous and not completely visible under X4 objective) and small (without cartilage and with an internal diameter of less than 2mm) airways present in lung tissue sections for each subject. Only airways containing intact, well-orientated airway epithelium with basement membrane attachment to underlying tissue were included in analysis. Figure 3.1 shows representative H&E staining of large and small airway sections from subjects in each group.

Control   Bronchiectasis   COPD
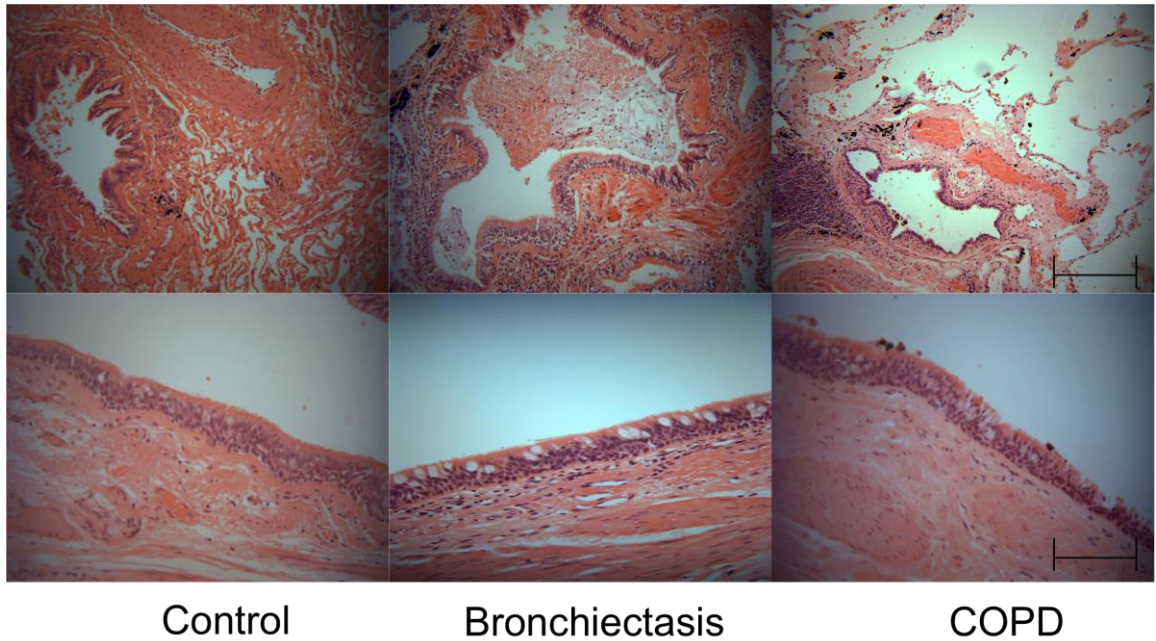
Figure 3.1 Representative H&E staining of human lung tissue containing large and small airway material. Representative H&E staining of lung tissue sections from controls, patients with bronchiectasis and patients with COPD. Upper panel: photomicrographs showing distal airways present in parenchymal tissue sections, captured using X10 objective. Scale bar represents 200 μm. Lower panel: photomicrographs showing representative areas of central airway sections, captured using X20 objective. Scale bar represents 100 μm. H&E, Haematoxylin and Eosin.

3.1.1 Clinical characteristics of the subjects

The clinical characteristics of patients with COPD, patients with bronchiectasis and controls are shown in Table 3.1. Patients with COPD were categorised based upon their GOLD staging, used to classify COPD severity (Rabe, Hurd et al. 2007). All patients in the COPD group were GOLD stage III (FEV_1/FVC <0.70, with 30% $\leq$ FEV_1 < 50% predicted) or IV (FEV_1/FVC <0.70, with FEV_1 < 30% predicted). Although no patients in the control group had written documentation of COPD presence, 4 patients had spirometric patterns in line with mild COPD (GOLD stage I) (FEV_1/FVC <0.70, with $FEV_1 \geq$ 80% predicted) and 3 with moderate COPD (GOLD stage II) (FEV_1/FVC <0.70, with 50% $\leq$ $FEV_1 \leq$ 80% predicted). Patients with bronchiectasis were not categorised using a clinical scoring system. Patients with COPD had lower FEV_1 and FEV_1 % predicted values than patients with bronchiectasis ($p < 0.05$) and controls ($p < 0.001$). The difference in smoking history (measured in cigarette pack-years) between patients with COPD and patients with bronchiectasis was statistically significant ($p = 0.001$). There was no difference in cigarette pack-years between patients with COPD and controls ($p = 0.66$). There was no significant difference in age between patients with COPD and patients with bronchiectasis, however controls were significantly older than patients with COPD and patients with bronchiectasis ($p < 0.001$).

	Controls (n = 11)	Patients with bronchiectasis (n = 14)	Patients with COPD (n = 19)
Sex, M/F	3/8	10/4	11/8
Age, yr	70.45± 7.56	52.51± 6.1	52.84 ± 6.9
FEV$_1$, L	1.79 ± 0.32	0.75 ± 0.21	0.53 ± 0.22
FEV$_1$, %	84.36 ± 9.45	23.5 ± 6.71	17.63 ± 6.99
FVC, L	2.69 ± 0.59	1.89 ± 0.59	1.89 ± 0.51
FVC, %	95.9 ± 16.8	46.57± 14.56	52.05 ± 14.15
Smoking history, pack-years	31.3 ± 17.93	11± 15.24	39.95 ± 27.1
GOLD score, I/II/III/IV	4/3/0/0		0/0/1/18

Table 3.1 Clinical characteristics of subjects used in this research Clinical details of patients with COPD, patients with bronchiectasis and controls. Values are expressed as mean ± SD. FEV$_1$, forced expiratory volume in 1 second; FVC, forced vital capacity; FEV$_1$ %, percentage of predicted FEV$_1$; FVC %, percentage of predicted FVC; GOLD, Global Initiative for Chronic Obstructive Lung Disease; NA, not applicable.

3.1.2 Ki67 expression is decreased in the large airway epithelium of patients with COPD

The absence of Ki67, a proliferation marker expressed in all phases of the cell-cycle, has been used to identify senescent cells (Lawless, Wang et al. 2010). Ki67 expression was assessed in large and small airway epithelial cells present in lung tissue sections from controls, patients with bronchiectasis and patients with COPD by immunohistochemistry. Expression was analysed using both a quantitative (Figure 3.2 A and B) and a semi-quantitative (Figure 3.2 C and D) scoring method. To quantitatively assess the level of Ki67 positivity in the airway epithelium, the number of positive nuclei per mm basement membrane was recorded and an average calculated for the whole tissue section. Using this method, we observed a decreased number of Ki67-positive cells per mm basement membrane in the large airway epithelium of patients with COPD compared to patients with bronchiectasis (2.2-fold) (p = 0.015) and compared to controls (3.6-fold) (p = 0.025) (Figure 3.2A). Using a semi-quantitative scoring approach, whereby each tissue section was given a score from 0-3 based on level of positive staining, we observed a similar pattern of expression (Figure 3.2C). Ki67 expression was decreased in patients with COPD compared to patients with bronchiectasis (2-fold) (p = 0.03) and compared to controls (2-fold) (p = 0.018). In the small airways, we observed no significant difference in expression between the three groups using either method of quantification, with the exception of patients with bronchiectasis, where an increase in Ki67 expression per mm basement membrane was observed compared to controls (2.1-fold) (p = 0.02) (Figure 3.2B). We observed a similar pattern of expression using the semi-quantitative scoring method (Figure 3.1D), with increased Ki67 expression in the epithelium of patients with bronchiectasis compared to controls (1.5-fold) (p = 0.036).

Figure 3.2 Ki67 expression in the large and small airway epithelium of patients with bronchiectasis and patients with COPD. Lung tissue sections were stained for Ki67 expression using immunohistochemistry and levels of expression were quantified in large and small airway epithelial cells using both quantitative and semi-quantitative methods. Dot plots represent the number of Ki67 positive nuclei per mm basement membrane in large (**A**) and small (**B**) airway epithelial cells for each individual subject, generated by quantifying the whole airway epithelium present in one tissue section and calculating an average value. Levels of staining were quantified in a blinded fashion. The horizontal line represents group median. Bar graphs represent the level of positive staining in the large (**C**) and small (**D**) airway epithelium quantified using a semi-quantitative scoring method and in a blinded fashion; each column and error bar represents median + range. (**E**) Representative images of immuno-staining *(brown)* for Ki67 in the large (upper panel) and small (lower panel) airway epithelium in tissue sections from each subject group captured using X40 objective. Lowest panel in control column shows representative image of IgG isotype control. Statistics: Kruskal-Wallis and Mann-Whitney U test. * $p < 0.05$.

3.1.3 γH2A.X expression is increased in the small airway epithelium of patients with COPD

The DDR protein γH2A.X represents sites of DNA damage and DDR activity, with increased γH2A.X foci described in senescent cells (d'Adda di Fagagna, Reaper et al. 2003). γH2A.X expression was assessed in large and small airway epithelial cells present in lung tissue sections from controls, patients with bronchiectasis and patients with COPD by immunohistochemistry. Expression was analysed using a semi-quantitative scoring method (as above). In the large airway epithelium, we observed no significant difference in expression between groups, with the exception of increased expression in patients with bronchiectasis as compared to patients with COPD ($p = 0.03$) (Figure 3.3A). In the small airway epithelium, we observed increased γH2A.X expression in patients with COPD compared to controls (2-fold) ($p = 0.015$) but there was no significant difference compared to patients with bronchiectasis (Figure 3.3B). There was no significant difference in γH2A.X expression in the small airway epithelium of patients with bronchiectasis compared to controls.

3.1.4 There is no change in p21 expression in the COPD epithelium

p21 is a CDK inhibitor and a downstream target of p53, which has been used as a marker for senescence (Di Leonardo, Linke et al. 1994; Alcorta, Xiong et al. 1996; Herbig, Jobling et al. 2004). p21 expression was assessed in large and small airway epithelial cells present in lung tissue sections from controls, patients with bronchiectasis and patients with COPD by immunohistochemistry. Expression was analysed using the semi-quantitative method previously described. In the large airway epithelium, we found the highest levels of p21 expression in the control group and this difference was significant compared to patients with COPD (2-fold) ($p = 0.04$) (Figure 3.4A). In the small airway epithelium, there was no significant difference in p21 expression across all groups (Figure 3.4B).
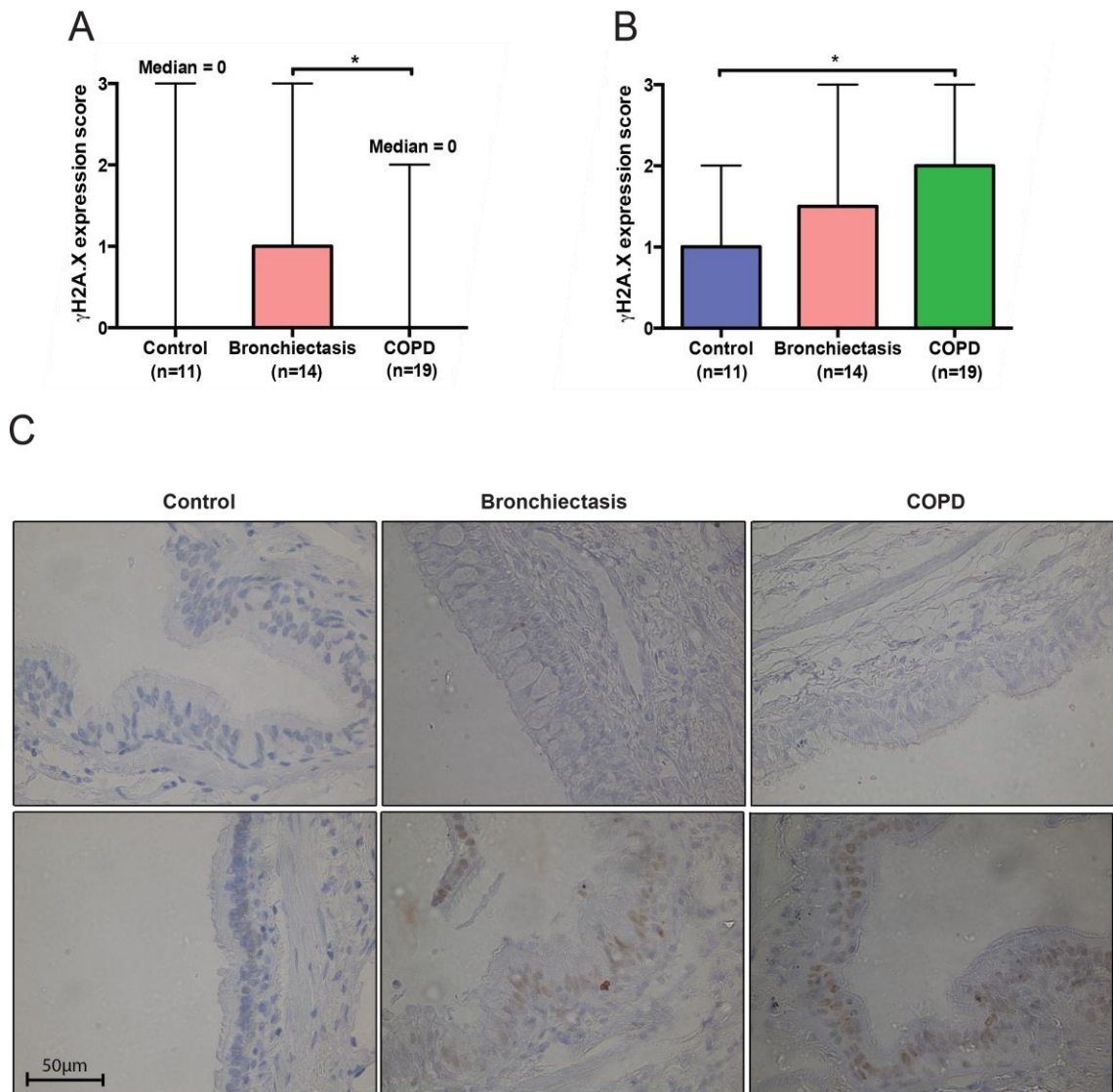
Figure 3.3 γH2A.X expression in the large and small airway epithelium of patients with bronchiectasis and patients with COPD. Lung tissue sections were stained for γH2A.X expression using immunohistochemistry and levels of expression were quantified in large and small airway epithelial cells using a semi-quantitative scoring method and in a blinded fashion. Bar graphs represent the level of positive staining in the large (**A**) and small (**B**) airway epithelium; each column and error bar represents median + range. (**C**) Representative images of immuno-staining *(brown)* for γH2A.X in the large (upper panel) and small (lower panel) airway epithelium in tissue sections from each subject group captured using X40 objective. Statistics: Kruskal-Wallis and Mann-Whitney U test. * $p < 0.05$.
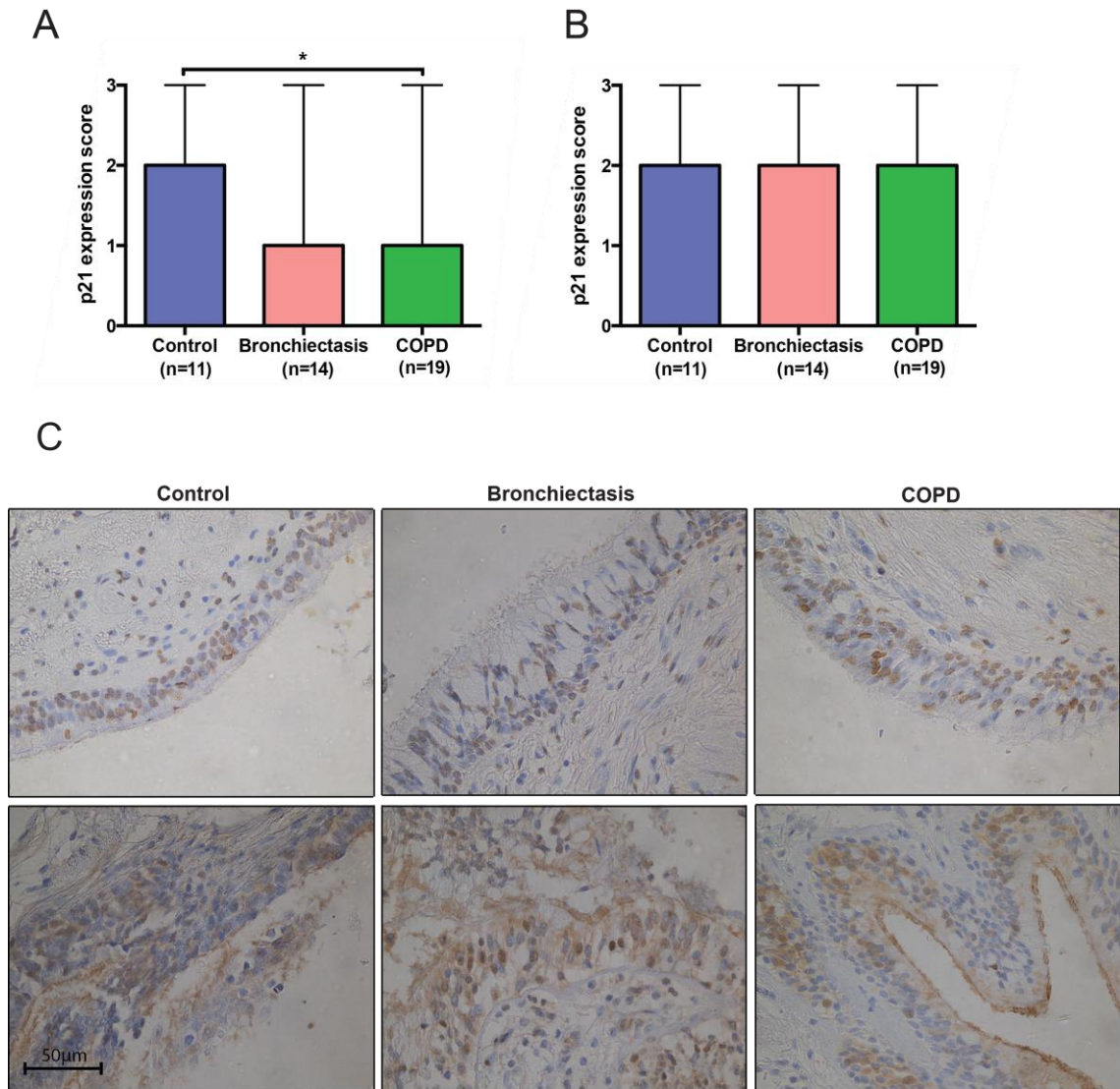
Figure 3.4 p21 expression in the large and small airway epithelium of patients with bronchiectasis and patients with COPD. Lung tissue sections were stained for p21 expression by immunohistochemistry and levels of expression were quantified in large and small airway epithelial cells using a semi-quantitative scoring method and in a blinded fashion. Bar graphs represent the level of positive staining in the large (**A**) and small (**B**) airway epithelium; each column and error bar represents median + range. (**C**) Representative images of immuno-staining *(brown)* for p21 in the large (upper panel) and small (lower panel) airway epithelium in tissue sections from each subject group captured using X40 objective. Statistics: Kruskal-Wallis and Mann-Whitney U test. * p < 0.05.

3.1.5 p16 expression is increased in the small airway epithelium of patients with COPD

The CDK inhibitor p16, an important regulator of senescence, is expressed by many senescent cells and is used to identify senescent cells both *in vitro* and *in vivo* (Serrano, Lin et al. 1997; Beausejour, Krtolica et al. 2003; Herbig, Ferreira et al. 2006; Jeyapalan, Ferreira et al. 2007). Large and small airway epithelial cells present in lung tissue sections from controls, patients with bronchiectasis and patients with COPD were assessed for p16 expression by immunohistochemistry and expression analysed using the semi-quantitative scoring method. In the large airway epithelium, we found no significant difference in p16 expression between the three groups (Figure 3.5A). However, in the small airway epithelium, we observed increased p16 expression in patients with COPD compared to controls (2-fold) (p = 0.04) (Figure 3.5B).

3.1.6 SIRT1 expression is decreased in the large and small airway epithelium of patients with COPD and in the large airway epithelium of patients with bronchiectasis

SIRT1 is a NAD-dependent protein and HDAC that plays critical roles in a variety of processes, including stress resistance, senescence and ageing (Michan and Sinclair 2007) and decreased levels have been described in the senescence context (Sasaki, Maier et al. 2006; Vassallo, Simoncini et al. 2014). SIRT1 expression was assessed in large and small airway epithelial cells present in lung tissue sections from controls, patients with bronchiectasis and patients with COPD by immunohistochemistry and analysed using a semi-quantitative scoring method. In the large airway epithelium, SIRT1 expression was decreased in patients with COPD compared to patients with bronchiectasis (2-fold) (p = 0.02) and compared to controls (2-fold) (p < 0.0001). We also observed a statistically significant decrease in SIRT1 expression in patients with bronchiectasis compared to controls (p = 0.009), although median values are the same (Figure 3.6A). In the small airway epithelium, SIRT1 expression was decreased in patients with COPD compared to patients with bronchiectasis (1.5-fold) (p = 0.04) and compared to controls (2-fold) (p = 0.016) (Figure 3.6B).
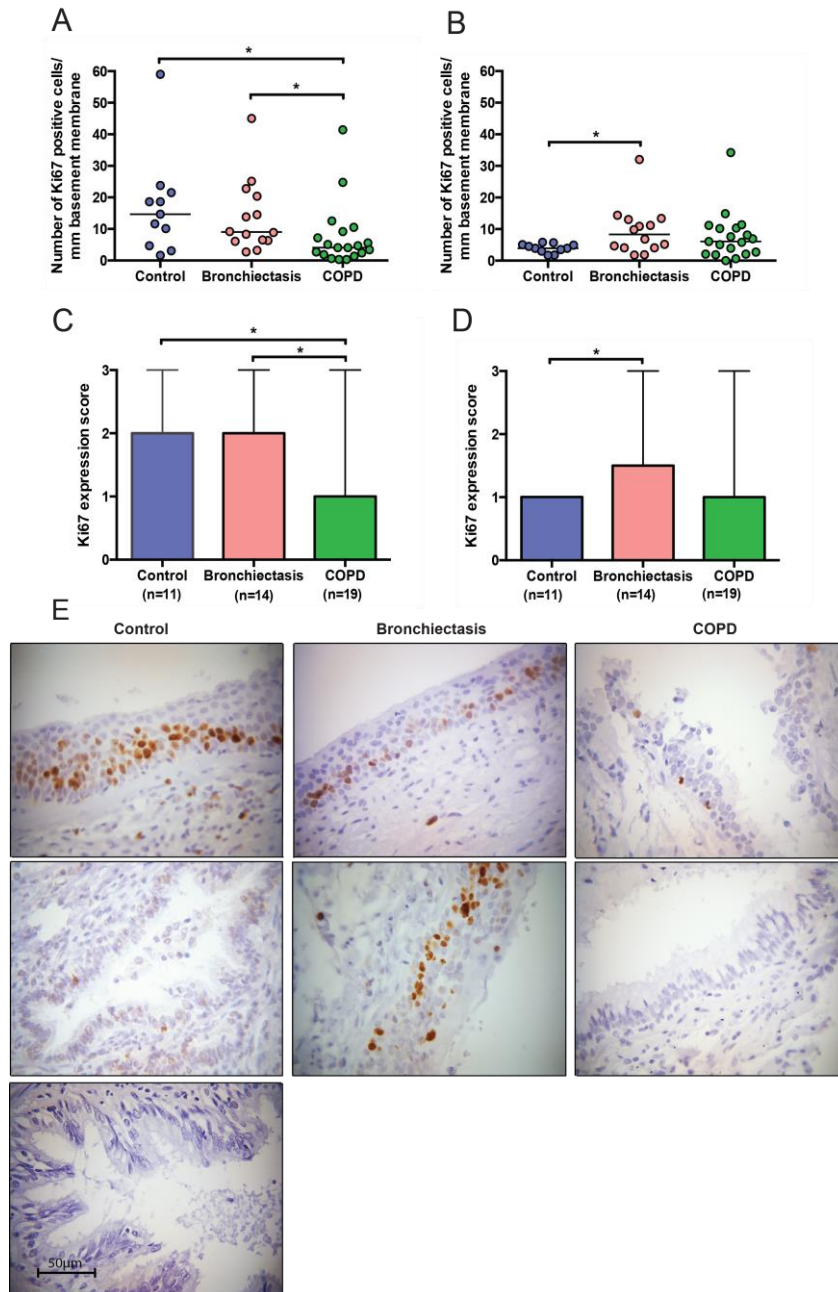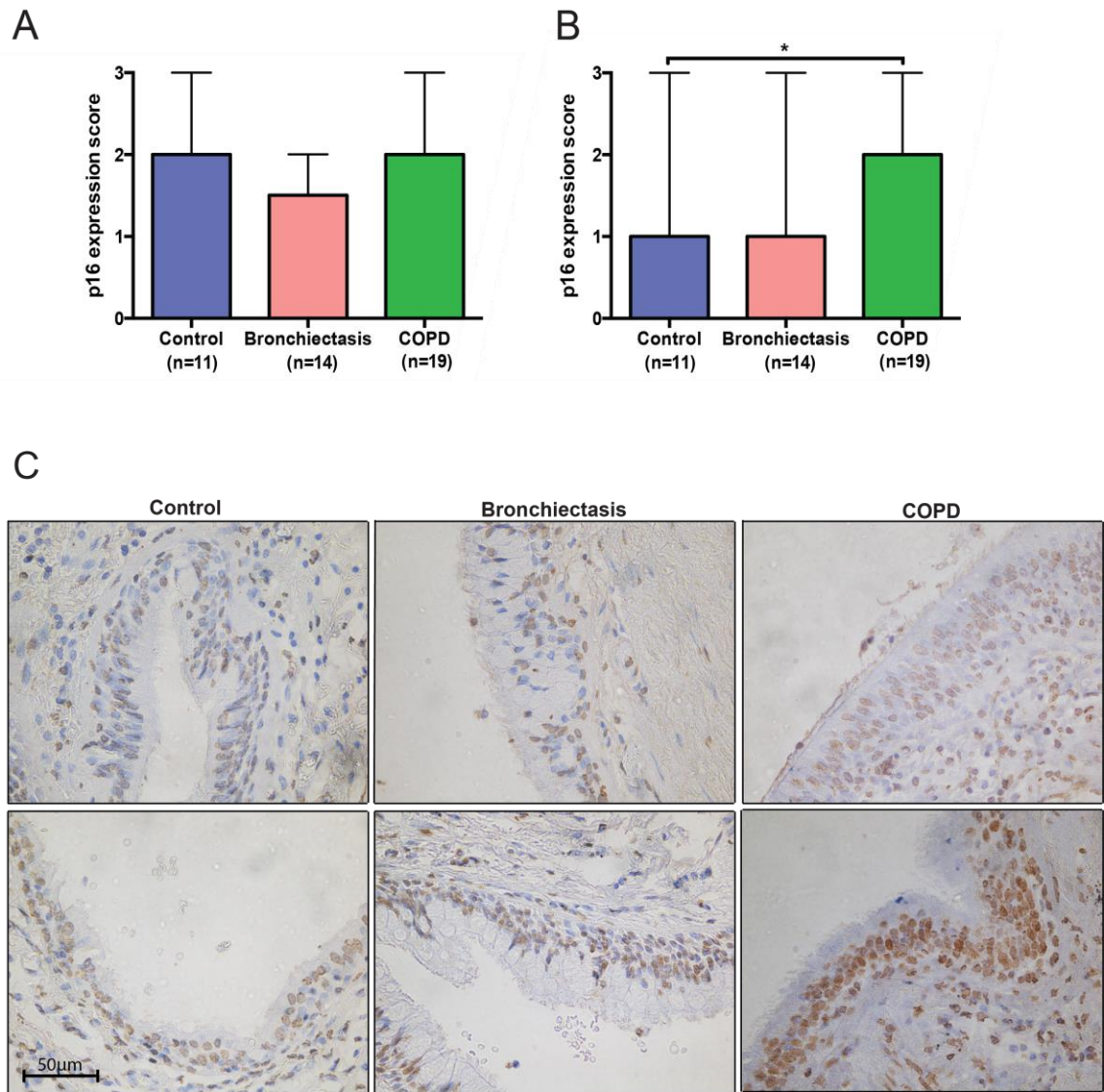
Figure 3.5 p16 expression in the large and small airway epithelium of patients with bronchiectasis and patients with COPD. Lung tissue sections were stained for p16 expression using immunohistochemistry and levels of expression were quantified in large and small airway epithelial cells using a semi-quantitative scoring method and in a blinded fashion. Bar graphs represent the level of positive staining in the large (**A**) and small (**B**) airway epithelium; each column and error bar represents median + range. (**C**) Representative images of immuno-staining *(brown)* for p16 in the large (upper panel) and small (lower panel) airway epithelium in tissue sections from each subject group captured using X40 objective. Statistics: Kruskal-Wallis and Mann-Whitney U test. * p < 0.05.
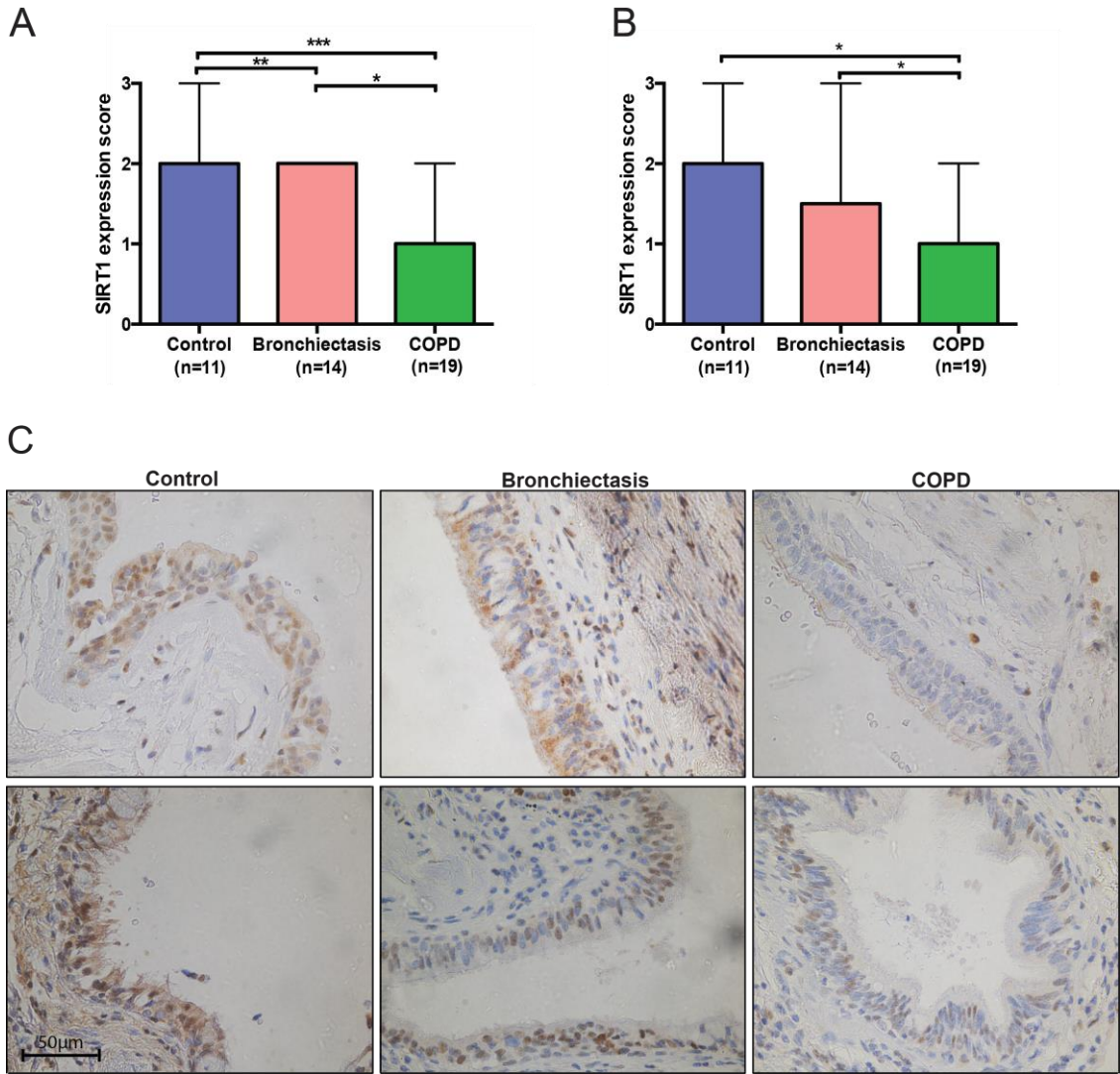
Figure 3.6 SIRT1 expression in the large and small airway epithelium of patients with bronchiectasis and patients with COPD. Lung tissue sections were stained for SIRT1 expression using immunohistochemistry and levels of expression were quantified in large and small airway epithelial cells using a semi-quantitative scoring method and in a blinded fashion. Bar graphs represent the level of positive staining in the large (**A**) and small (**B**) airway epithelium; each column and error bar represents median + range. (**C**) Representative images of immuno-staining *(brown)* for SIRT1 in the large (upper panel) and small (lower panel) airway epithelium in tissue sections from each subject group captured using X40 objective. Statistics: Kruskal-Wallis and Mann-Whitney U test. * p < 0.05, ** p < 0.01, ***p < 0.001.

3.1.7 Senescence-associated markers altered in the COPD lung do not significantly correlate with airflow limitation or smoking history

To determine whether there was a relationship between airway epithelial cell senescence and degree of airflow limitation, we tested the markers altered in the COPD lung for correlations with FEV_1 (% predicted). When subject groups were analysed individually, no significant correlations were found between senescence-marker expression and lung function across all groups. Figure 3.7 shows correlations between markers altered in the COPD lung and FEV_1 (% predicted) for COPD subjects only. However, when correlations were investigated in the overall population, Ki67 expression in the large airway epithelium, assessed using both the quantitative (Figure 3.8A) and semi-quantitative (Figure 3.8B) methods was positively correlated with lung function. Similarly, SIRT1 expression in both the large (Figure 3.8E) and small (Figure 3.8F) airway epithelium was positively correlated with lung function. There were no significant correlations found between γH2A.X (Figure 3.8C) and p16 (Figure 3.8D) expression in the small airway epithelium when assessing the overall population.

To determine whether there was a relationship between airway epithelial cell senescence and cigarette-smoking habits of subjects, we tested the markers altered in the COPD lung for correlations with pack-year number (a clinical tool to indicate smoking history) collected for each subject. When subject groups were analysed individually, there were no significant correlations observed between senescence marker expression and smoking history. Figure 3.9 shows correlations between markers altered in the COPD lung and smoking history (pack-year data) for COPD subjects only. Additionally, when correlations were investigated in the overall population, there were still no significant correlations observed and this finding was true across all markers and for both the large and small airway epithelium (data not shown).
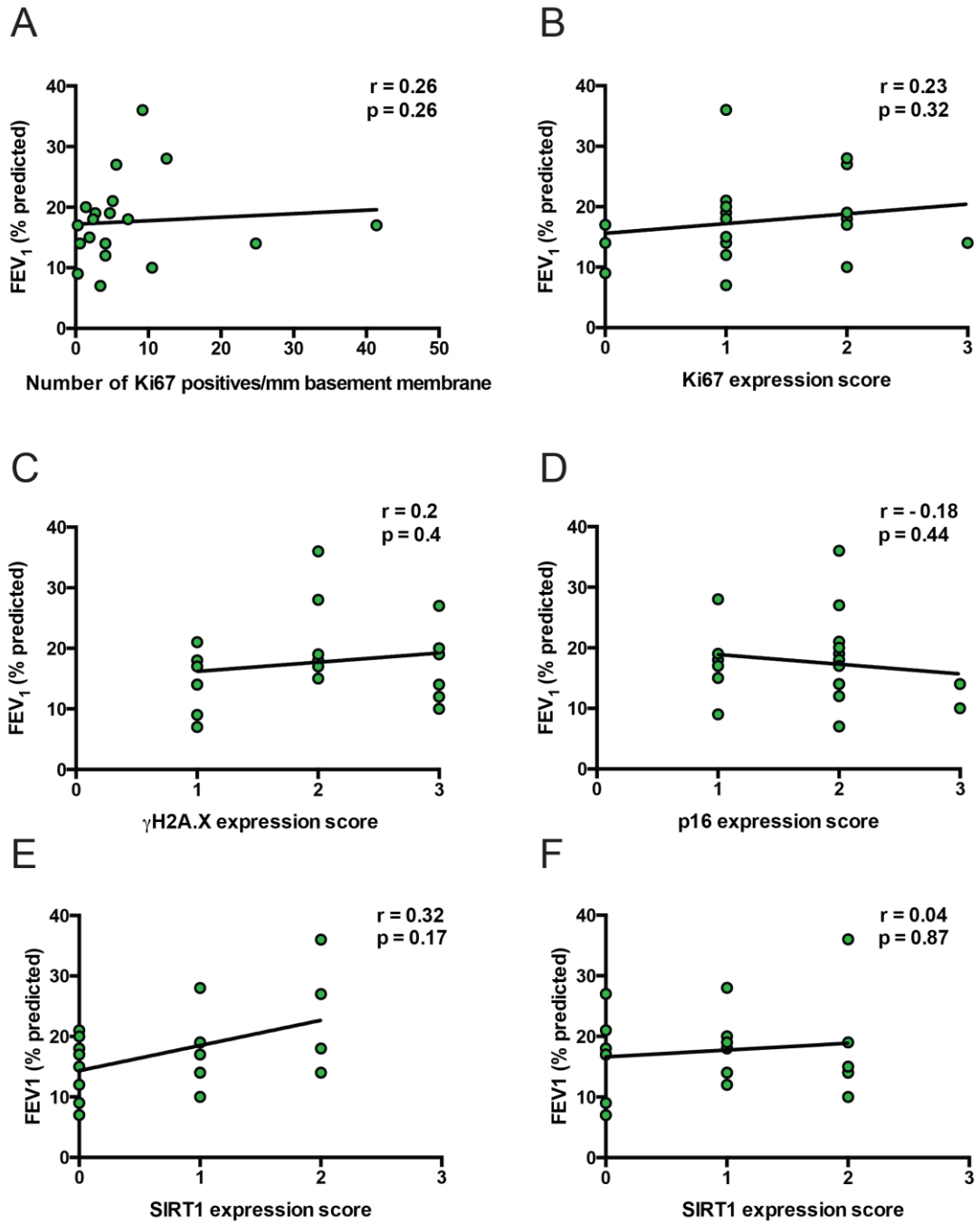
Figure 3.7 Relationship between senescence-associated markers altered in the COPD lung and degree of airflow limitation. Relationship between number of Ki67 positive cells/mm basement membrane (**A**) or Ki67 expression, determined using scoring system, (**B**) in large airway epithelial cells and FEV_1 (% predicted). Relationship between $\gamma H2A.X$ (**C**) and p16 (**D**) expression in small airway epithelial cells and FEV_1 (% predicted). Relationship between SIRT1 expression in the large (**E**) and small (**F**) airway epithelium and FEV_1 (% predicted). Correlations were assessed using Spearman's rank correlation coefficient. Subject groups were analysed individually, only data from COPD group shown. SIRT1, sirtuin 1; FEV_1, forced expiratory volume in 1 second.
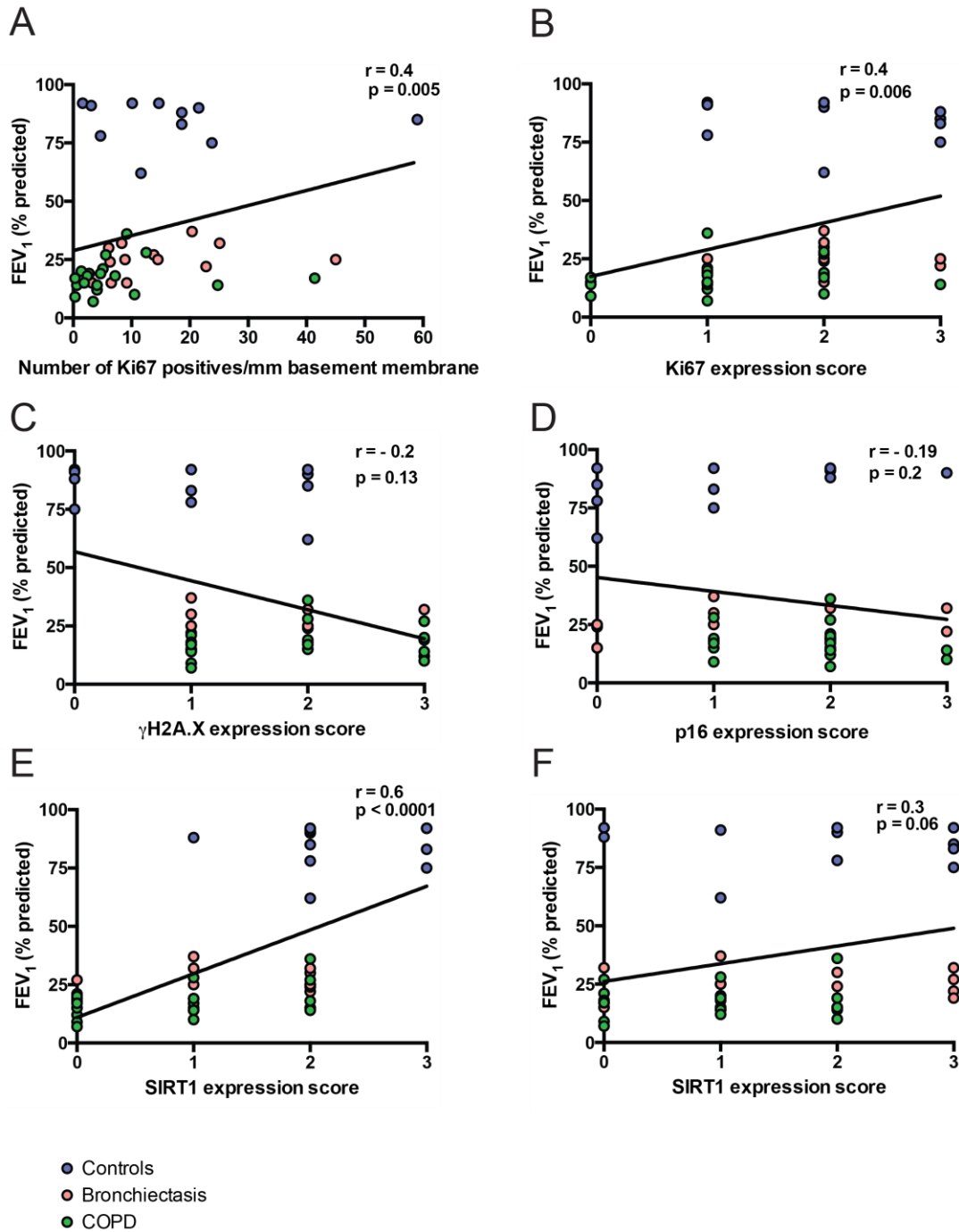
Figure 3.8 Relationship between senescence-associated markers and degree of airflow limitation across overall population. Relationship between number of Ki67 positive cells/mm basement membrane (**A**) or Ki67 expression, determined using scoring system, (**B**) in large airway epithelial cells and FEV_1 (% predicted). Relationship between γH2A.X (**C**) and p16 (**D**) expression in small airway epithelial cells and FEV_1 (% predicted). Relationship between SIRT1 expression in the large (**E**) and small (**F**) airway epithelium and FEV_1 (% predicted). Correlations were assessed using Spearman's rank correlation coefficient. Overall population analysed as one group. P values < 0.05 considered significant. SIRT1, sirtuin 1; FEV_1, forced expiratory volume in 1 second.
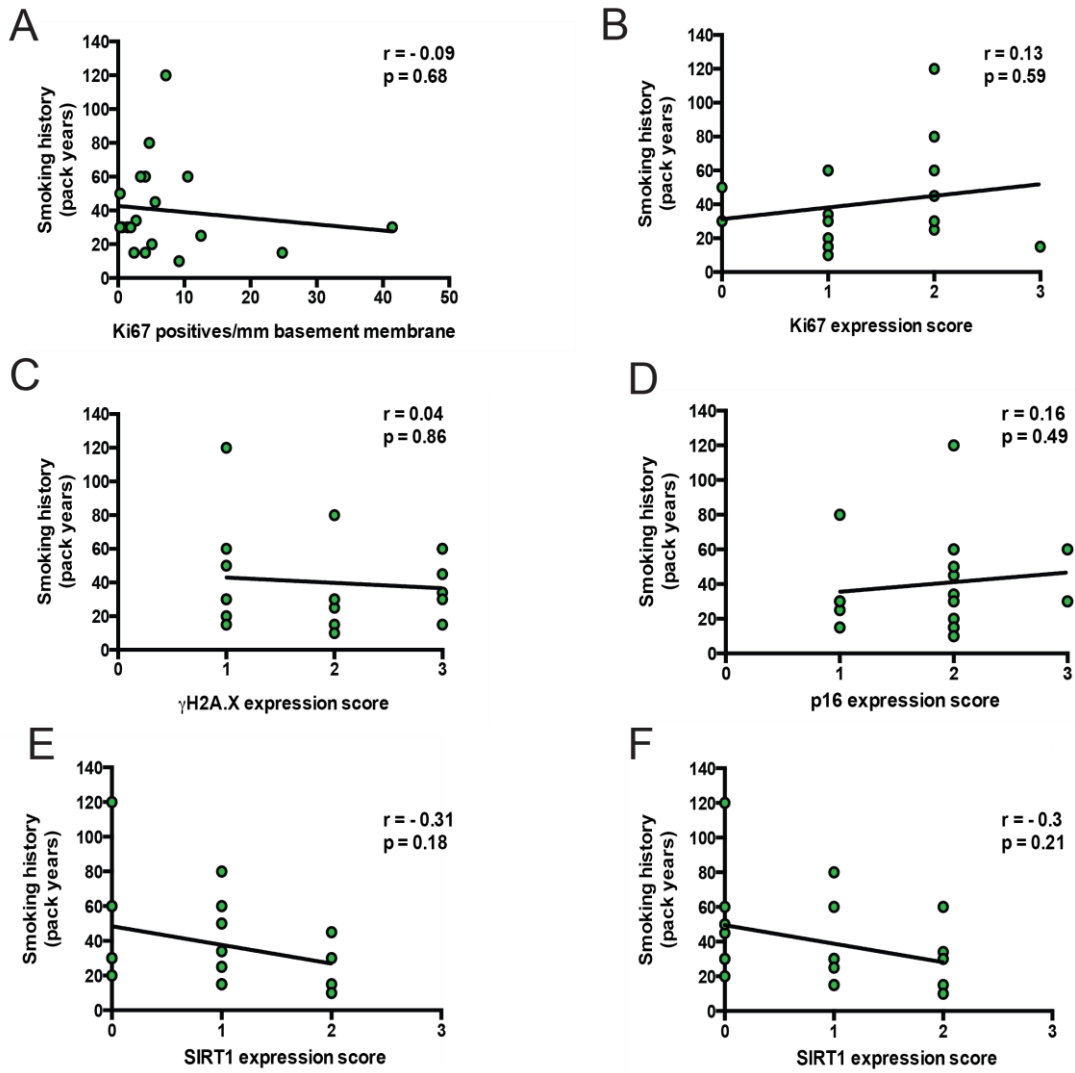
Figure 3.9 Relationship between senescence-associated markers altered in the COPD lung and smoking history. Relationship between number of Ki67 positive cells/mm basement membrane (**A**) or Ki67 expression, determined using scoring system, (**B**) in large airway epithelial cells and smoking history (pack years). Relationship between γH2A.X (**C**) and p16 (**D**) expression in small airway epithelial cells and smoking history (pack years). Relationship between SIRT1 expression in the large (**E**) and small (**F**) airway epithelium and smoking history (pack years). Correlations were assessed using Spearman's rank correlation coefficient. Subject groups were analysed individually, only data from COPD group shown.

3.2 Investigating telomere dysfunction in the small airway epithelium of patients with bronchiectasis and patients with COPD

A number of studies have provided evidence for telomere dysfunction in patients with COPD. Many studies have shown that circulating leukocytes from patients with COPD have shorter telomeres (Morla, Busquets et al. 2006; Houben, Mercken et al. 2009; Mui, Man et al. 2009; Savale, Chaouat et al. 2009). Additionally, accelerated telomere shortening has been described in resident lung cells in patients with COPD, including type II alveolar cells and endothelial cells (Tsuji, Aoshiba et al. 2006). However, there are only very few reports of alterations in telomere length *in situ* in the airway epithelium of patients with COPD. Moreover, the presence of a DDR at telomeres, identified by telomere-associated foci (TAF), has, to our knowledge, not been investigated in human lung tissue or in age-related lung disease. Our lab and others have previously underscored the importance of telomeric DDR signalling in senescence and TAF are believed to be robust markers for senescence and ageing (Herbig, Ferreira et al. 2006; Jeyapalan, Ferreira et al. 2007; Fumagalli, Rossiello et al. 2012; Hewitt, Jurk et al. 2012).

Following our finding that the DDR protein γH2A.X is increased in the small airway epithelium of patients with COPD, along with p16, the importance of which has also recently been emphasised in senescence and ageing (Baker, Wijshake et al. 2011), we aimed to investigate telomere dysfunction in small airway epithelial cells present in lung tissue samples from patients with COPD and patients with bronchiectasis.

3.2.1 Small airway epithelial cells in the COPD lung have increased DNA damage foci and telomere-associated foci without significant telomere shortening

We investigated the presence of γH2A.X foci and TAF in small airway epithelial cells in lung tissue from patients with COPD, patients with bronchiectasis and controls using telomere-specific quantitative fluorescence *in situ* hybridisation (Q-FISH), combined with immunofluorescence against γH2A.X (immuno-FISH). Analysis revealed a significant increase in the mean number of γH2A.X foci per cell in small airway epithelial cells of patients with COPD as compared to controls (2.5-fold) (p = 0.04) (Figure 3.10A), confirming earlier findings using immunohistochemistry (Figure 3.3B). We observed an even greater increase in γH2A.X foci associated with telomeres (TAF) in the small airway epithelium of patients with COPD as compared to controls (3-fold) (p = 0.003) (Figure 3.10B). No significant differences were observed in mean number of γH2A.X foci or mean number of TAF in the small airway epithelium from patients

with bronchiectasis as compared to controls. Analysis of signal intensity from telomeres, which is indicative of telomere length, revealed no significant differences between the three groups (Figure 3.10C). To determine whether there was a difference in signal intensity between non-colocalising telomeres and telomeres that colocalised with γH2A.X, over 500 individual telomeres were analysed in the small airway epithelial cells of patients with COPD. We found no significant difference in telomere intensity between non-colocalising and colocalising telomeres (Figure 3.11A).

3.2.2 γH2A.X foci and telomere-associated foci do not significantly correlate with airflow limitation or smoking history

To determine whether there was a relationship between mean number of γH2A.X foci or mean number of TAF per cell and degree of airflow limitation, we tested these markers for correlations with FEV_1 (% predicted). Individual group analysis revealed no significant correlations between mean number of γH2A.X foci (Figure 3.12A) or mean number of TAF (Figure 3.12B) and FEV_1 (% predicted). Similarly, there was no significant correlation observed between mean number of γH2A.X foci (Figure 3.12C) or mean number of TAF (Figure 3.12D) and smoking history of the subjects (pack-years). When correlations were investigated in the overall population, there was a trend towards a negative correlation between mean number of γH2A.X foci (Figure 3.13A) and mean number of TAF (Figure 3.13B) with FEV_1 (% predicted), however the correlation between mean number of γH2A.X foci was not statistically significant (p = 0.4) and correlations with TAF just failed to reach statistical significance (p = 0.06). There were no correlations observed between mean number of γH2A.X foci (Figure 3.13C) and mean number of TAF (Figure 3.13D) and smoking history of the subjects in the overall population.
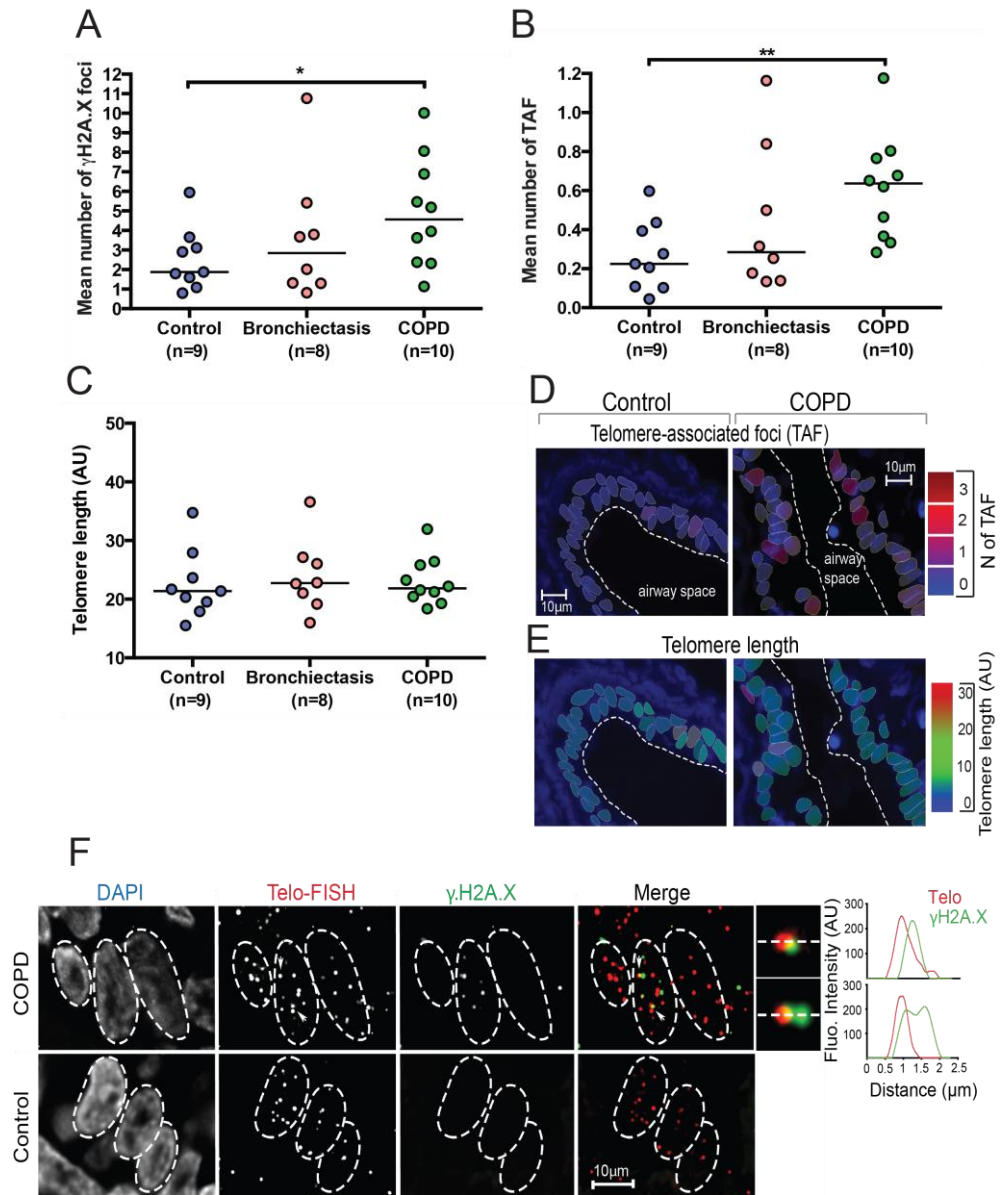
Figure 3.10 γH2A.X foci, telomere-associated foci and telomere length in large and small airway epithelial cells of patients with bronchiectasis and patients with COPD. Explant lung tissue sections from patients with COPD and patients with bronchiectasis, and lung resection specimens from control subjects, containing small airway material were analysed for expression of γH2A.X and TAF by immuno-FISH. Dot plots represent the mean number of γH2A.X foci per cell (**A**), the mean number of TAF per cell (**B**) and mean telomere intensity per cell (**C**) for each individual subject, generated by quantifying Z-stacks of at least 50 cells per subject. The horizontal line represents group median. (**D**) Immuno-FISH images of small airway epithelium in patients with COPD and controls colour coded according to number of TAF (blue: low number; red: high number). (**E**) Immuno-FISH images of small airway epithelium in patients with COPD and controls colour coded according to telomere length (blue: short; red: long). (**F**) Representative images of immuno-FISH staining for γH2A.X *(green)* and telomeres *(red)* in small airway epithelial cells from patients with COPD and controls captured using X100 oil objective and following Huygens (SVI) deconvolution. Arrows point to γH2A.X foci co-localising with telomeres (TAF), depicted by associated histograms and shown at higher magnification on the right (images are from one single Z-plane). Statistics: Mann-Whitney U test *$P < 0.05$, **$P < 0.01$.

Figure 3.11 Telomere length of non-colocalising and colocalising telomeres in small airway epithelial cells of the COPD lung. Explant lung tissue sections from patients with COPD, containing small airway material were analysed for expression of γH2A.X and TAF by immuno-FISH. (**A**) Histogram representing telomere intensity of co-localising and non-co-localising telomeres in small airway epithelial cells of at least four randomly selected COPD patients, generated by quantifying at least 500 individual telomeres; red line indicates median telomere intensity. (**B**) Representative Immuno-FISH (red: telomere PNA probe, green: γH2A.X) of small airway epithelial cell present in COPD lung tissue captured using X100 oil objective and following Huygens (SVI) deconvolution, image is from one single Z-plane. Arrows indicate telomeres of similar length co-localising (**a**) or not (**b**) with γH2A.X in one individual cell. (**C**) Quantification of telomere intensity of co-localising (**a**) or non-co-localising (**b**) telomere. Mann-Whitney U test shows no statistically significant difference.
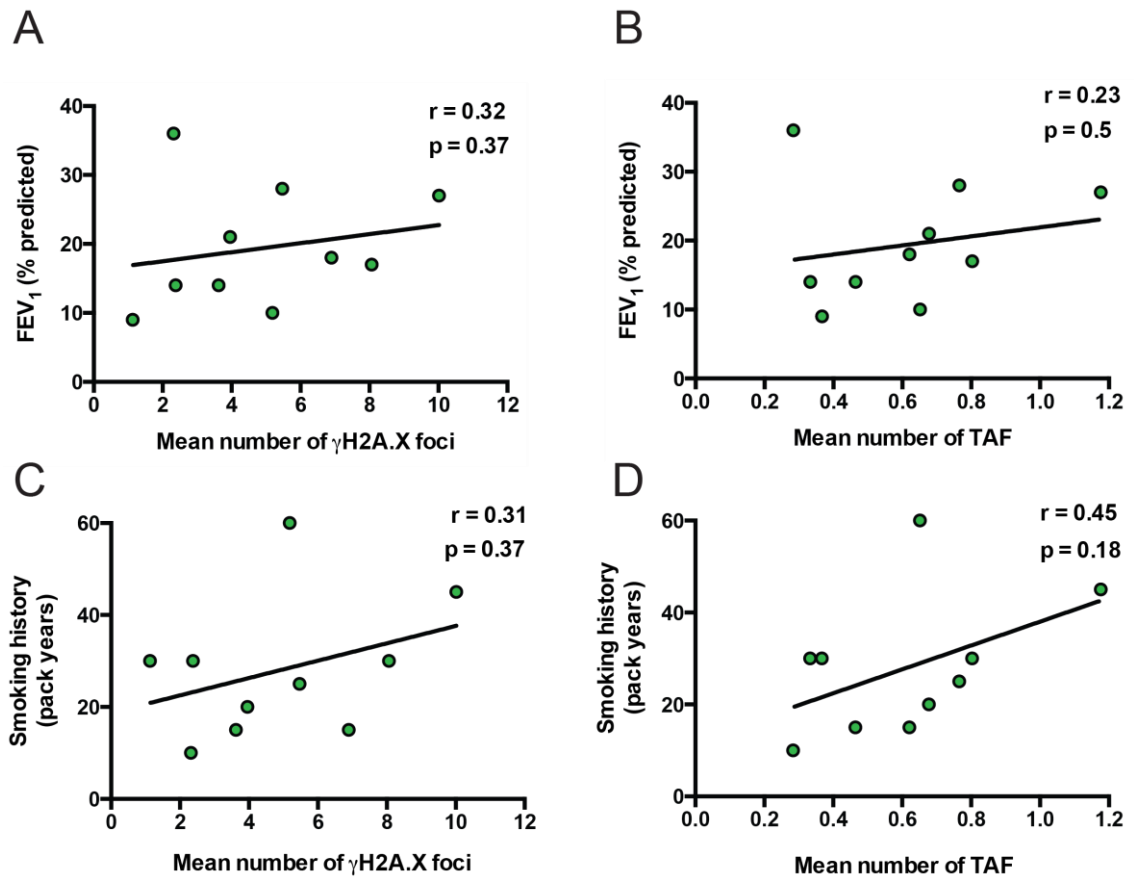
Figure 3.12. Relationship between γH2A.X foci and TAF in the small airway epithelial cells of the COPD lung and degree of airflow limitation and smoking history. Relationship between mean number of γH2A.X foci (**A**) and TAF (**B**) in small airway epithelial cells and FEV$_1$ (% predicted). Relationship between mean number of γH2A.X foci (**C**) and TAF (**D**) in small airway epithelial cells and smoking history (pack years). Correlations were assessed using Spearman's rank correlation coefficient. Subject groups were analysed individually, only data from COPD group shown. TAF, telomere-associated foci; FEV$_1$, forced expiratory volume in 1 second.
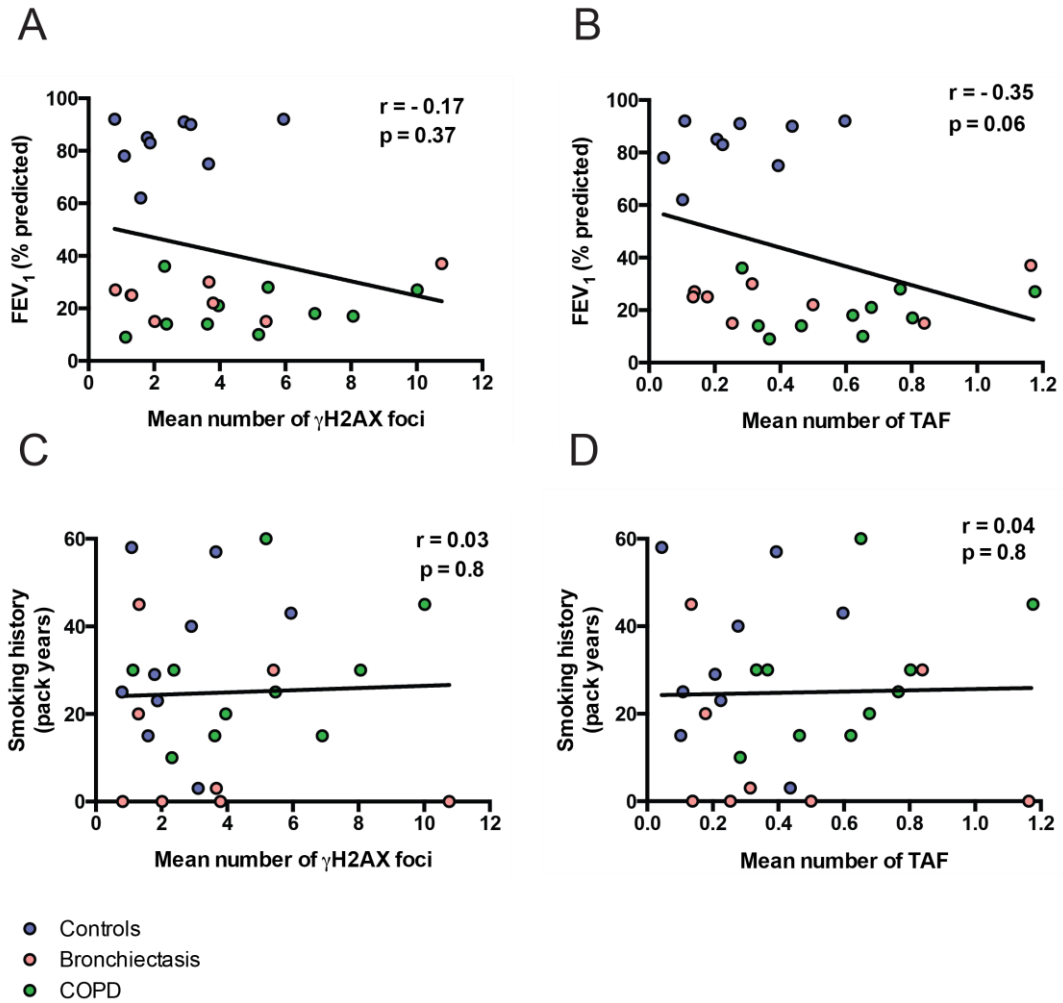
Figure 3.13. Relationship between γH2A.X foci and TAF in small airway epithelial cells and degree of airflow limitation and smoking history across overall population. Relationship between mean number of γH2A.X foci (**A**) and TAF (**B**) in small airway epithelial cells and FEV$_1$ (% predicted). Relationship between mean number of γH2A.X foci (**C**) and TAF (**D**) in small airway epithelial cells and smoking history (pack years). Correlations were assessed using Spearman's rank correlation coefficient. Overall population analysed as one group. TAF, telomere-associated foci; FEV$_1$, forced expiratory volume in 1 second.

3.2.3 p16 positive cells show increased DNA damage foci and TAF in small airway epithelial cells present in COPD lung tissue

To determine whether γH2A.X foci-positive cells and TAF-positive cells were also positive for p16 expression in small airway epithelial cells present in lung tissue from patients with COPD, we carried out double immuno-FISH for p16 and γH2A.X. We observed on average, a higher number of γH2A.X foci per cell in those cells that stained positive for p16 expression compared to those that were negative for p16 (a mean of 2.3 foci/cell compared to 0.8 foci/cell) (p = 0.01) (Figure 3.14A). Additionally, we found that the mean number of TAF per cell was higher in those cells that were also positive for p16 expression compared to p16-negative cells (an average of 0.8 TAF/cell compared to 0.2/cell) (p = 0.008) (Figure 3.14B).
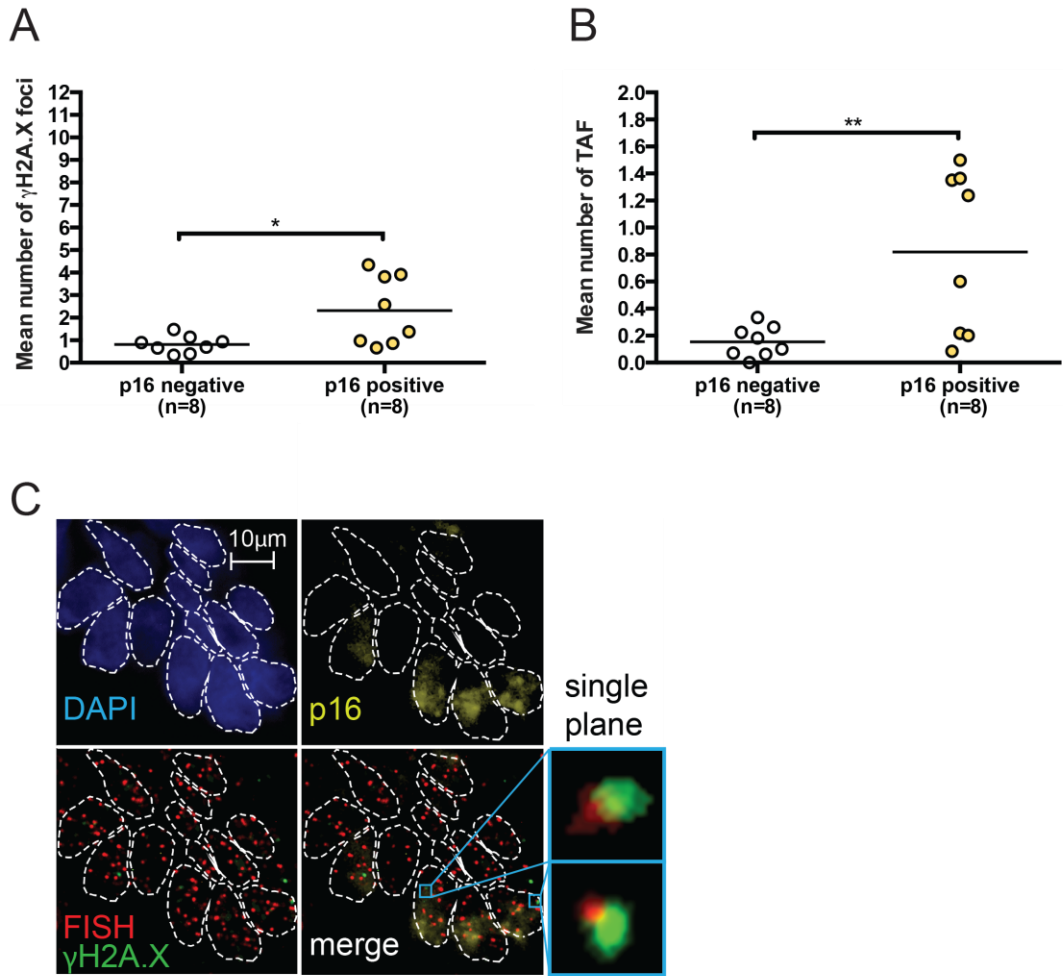
Figure 3.14 Double immuno-FISH staining against p16, γH2A.X and telomeres in small airway epithelial cells present in COPD lung tissue. Explant lung tissue sections from patients with COPD (n=8) containing small airway material were analysed for expression of p16, γH2A.X and TAF by double immuno-FISH to determine whether foci and p16 expression co-localise. Dot plots represent the mean number of γH2A.X foci (**A**) and the mean number of TAF (**B**) per p16-positive and p16-negative cells for each individual subject with the horizontal line representing group mean. Results were generated by quantifying Z-stacks of at least 50 cells per subject. (**C**) Representative image of double immuno-FISH staining for γH2AX *(green)* and p16 *(yellow)* combined with telo-FISH *(red)* captured using X100 oil objective and following Huygens (SVI) deconvolution. γH2A.X foci co-localising with telomeres (TAF) are shown at higher magnification on the right (images are from one single Z-plane). Statistics: Independent samples t-test *$P < 0.05$, **$P < 0.01$.
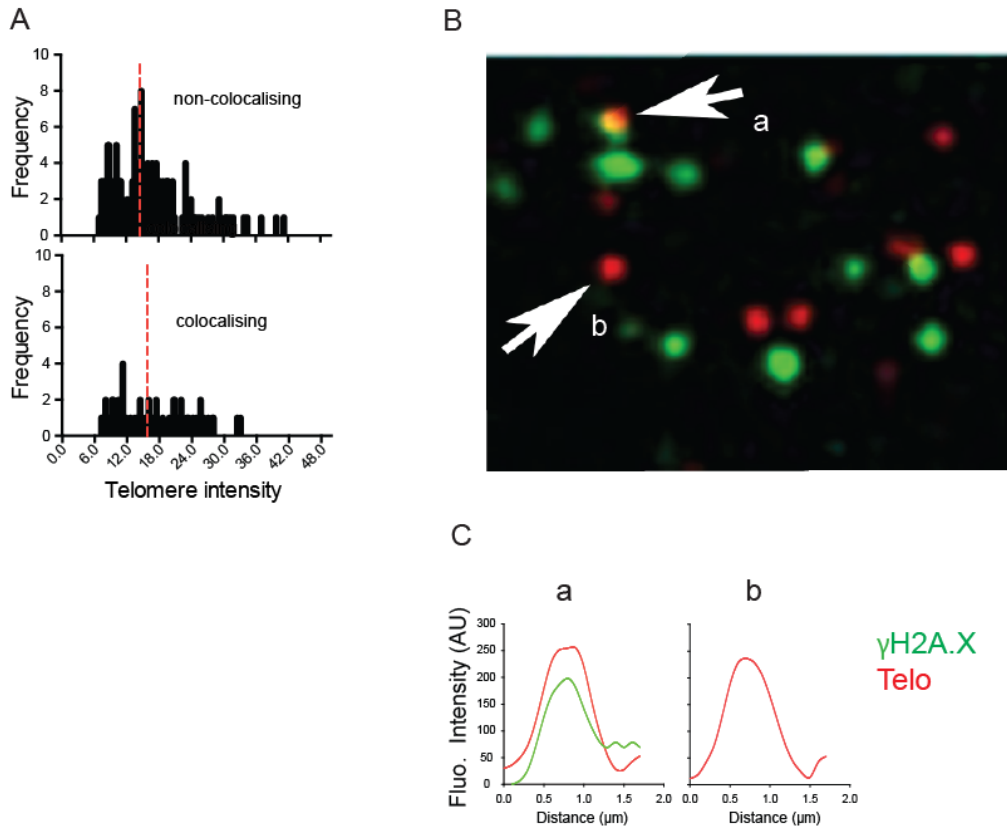
3.2.4 Small airway epithelial cells isolated from the COPD lung have increased telomere-associated foci without significant telomere shortening

Following our observations that TAF were increased in the small airway epithelial cells of lung tissue from patients with COPD compared to controls (who were on average, 20 years older), we aimed to determine whether TAF were increased in small airway epithelial cells isolated and cultured from the COPD lung as compared to healthy aged-matched controls (Table 3.2). Using Immuno-FISH, we evaluated the presence of TAF in small airway epithelial cells isolated from healthy controls during research bronchoscopy or cultured from explant COPD lung tissue. This work was carried out in collaboration with Dr Nicola Green and Dr Elizabeth Moisey from the Lung Immunobiology group, Newcastle University. We found an increase in mean number of TAF per cell in patients with COPD (Figure 3.15A), however this was not statistically significant, whereas the percentage of cells positive for TAF was (Figure 3.15B). We found no significant differences in telomere length between patients with COPD and controls as determined by Q-FISH (Figure 3.15C). We also determined whether differences in telomere length could be detected using the well-established Real-Time PCR method (Cawthon, Smith et al. 2003) in collaboration with the Biomarkers facility (Campus for Ageing and Vitality, Newcastle University), using a slightly larger sample size (Table 3.3). We found no significant differences in telomere length between patients with COPD and controls (Figure 3.15D). We carried out the biochemical assay for detection of Sen-β-Gal activity, an established senescence marker (Dimri, Lee et al. 1995). We observed increased expression of Sen-β-Gal in cells isolated from patients with COPD on average, as compared to controls, however these observations failed to reach statistical significance (Figure 3.16).

	Patients with COPD (n = 3)	Normal controls (n = 3)
Sex, M/F	2/1	2/1
Age, yr	53 ± 8.08	52 ± 7
FEV_1, L	0.42 ± 0.06*	3.53 ± 1.42
FEV_1, %	14.3 ± 3.21**	109.7 ± 20.98
FVC, L	2.1 ± 0.4	4.8 ± 2.32
FVC, %	55.6 ± 5.5*	119 ± 32.14
Smoking history, pack-years	28 ± 10.58*	0
GOLD score, I/II/III/IV	0/0/0/0/3	0/0/0/0

Table 3.2 Clinical characteristics of patients with COPD and normal controls where airway epithelial cells were isolated. COPD, chronic obstructive pulmonary disease; FEV_1, Forced expiratory volume in one second; FEV_1 %, percentage of predicted FEV_1; FVC, forced vital capacity; FVC %, percentage of predicted FVC; GOLD, Global Initiative for Chronic Obstructive Lung Disease. Values are expressed as mean ± SD. Statistics: Independent samples t-test *$p < 0.05$, **$p < 0.01$ as compared to controls.

	Patients with COPD (n = 6)	Normal controls (n = 4)
Sex, M/F	5/1	3/1
Age, yr	54.6 ± 7	49.5 ± 7.59
FEV$_1$, L	0.54 ± 0.17***	3.75 ± 1.24
FEV$_1$, %	15.6 ± 4.13****	111 ± 17.33
FVC, L	2.59 ± 0.95*	5.02 ± 1.96
FVC, %	58.8 ± 19.79**	120.25 ± 26.36
Smoking history, pack-years	38.6 ± 21.67**	0
GOLD score, I/II/III/IV	0/0/0/0/6	0/0/0/0

Table 3.3. Clinical characteristics of patients with COPD and normal controls where airway epithelial cells were isolated for RT-PCR. COPD, chronic obstructive pulmonary disease; FEV$_1$, Forced expiratory volume in one second; FEV$_1$ %, percentage of predicted FEV$_1$; FVC, forced vital capacity; FVC %, percentage of predicted FVC; GOLD, Global Initiative for Chronic Obstructive Lung Disease. Values are expressed as mean ± SD. Statistics: Independent samples t-test. *p < 0.05, **p < 0.01, ***p < 0.001, ****p < 0.0001 as compared to controls.
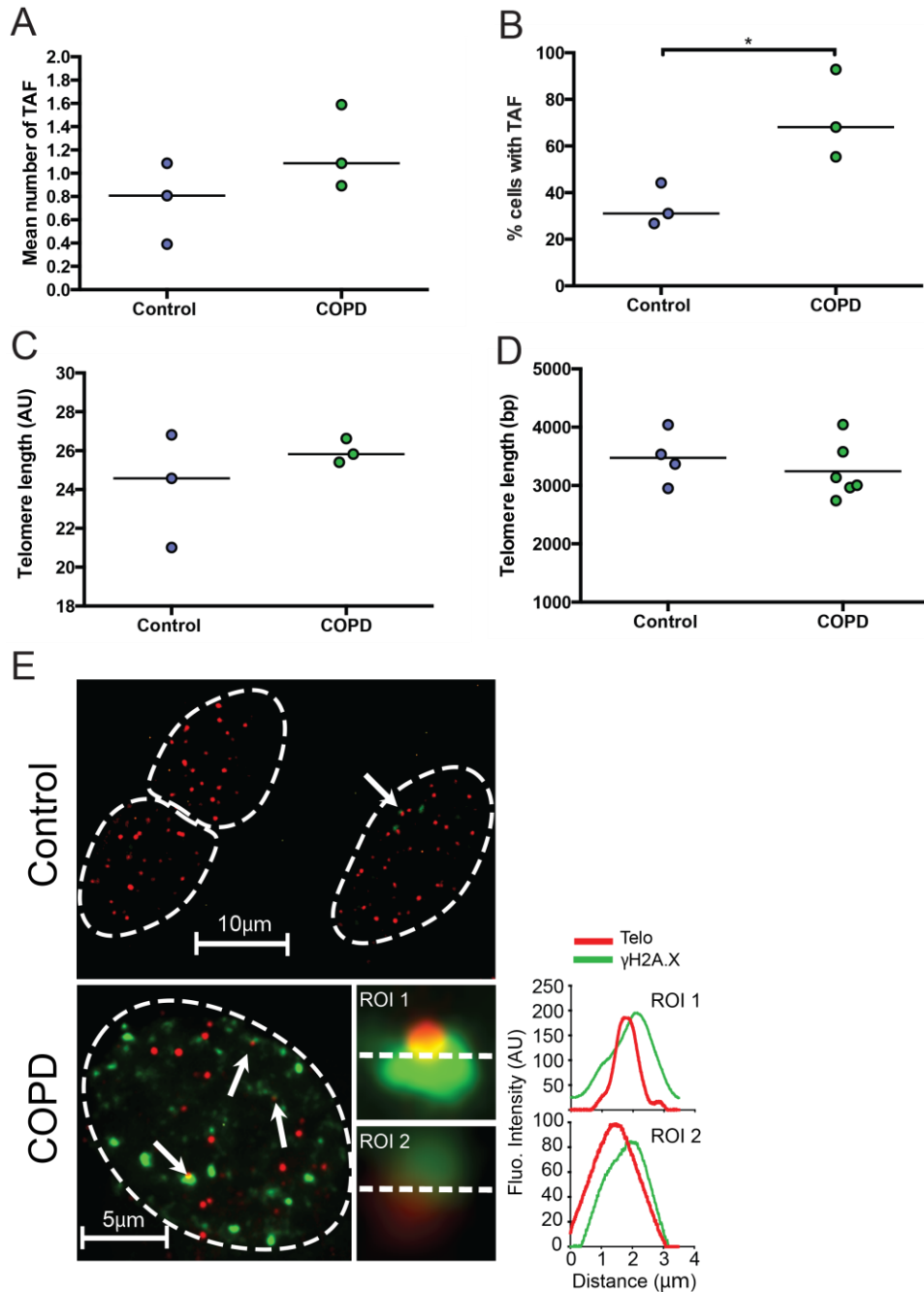
Figure 3.15 Telomere-associated foci and telomere length in small airway epithelial cells cultured from controls and patients with COPD. Small airway epithelial cells (P1-P3) from patients with COPD and aged-matched controls were analysed for γH2A.X and telomeres by immuno-FISH. Dot plots represent mean number of TAF (**A**), percentage of cells containing TAF (**B**) and mean telomere length (**C**) for each individual generated by quantifying Z-stacks of at least 40 cells per subject. Telomere length was also quantified using Real-Time PCR on small airway epithelial cells isolated from a larger number of controls and patients with COPD (**D**). Data are presented as the mean for individual subjects with the horizontal line representing group mean. (**E**) Representative image of immuno-FISH staining for γH2A.X *(green)* and telomeres *(red)* in small airway epithelial cells from patients with COPD and controls, captured using X100 oil objective and following Huygens (SVI) deconvolution. Arrows point to γH2A.X foci co-localising with telomeres (TAF), depicted by associated histograms and shown at higher magnification on the right (images are from one single Z-plane). Statistics: Independent samples t-test *$P < 0.05$.
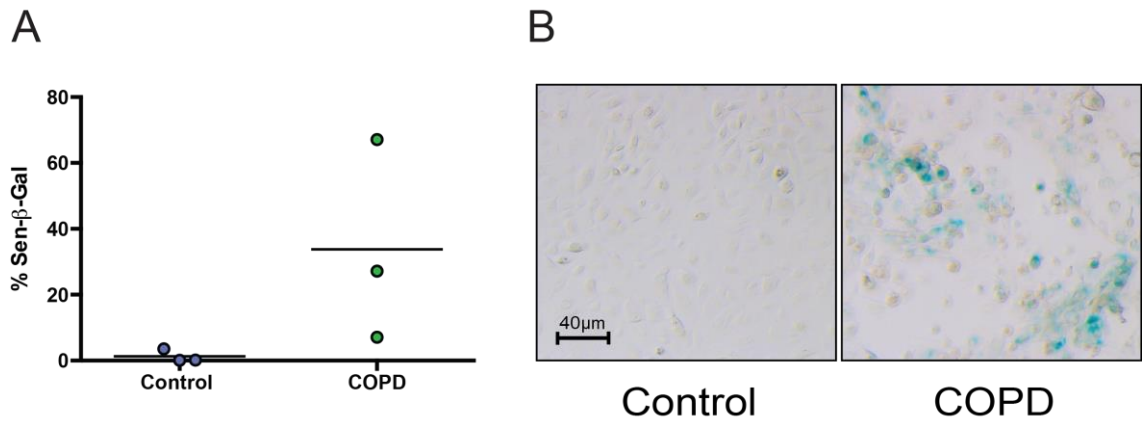
Figure 3.16 Representative images of senescence-associated-β-galactosidase staining in small airway epithelial cells cultured from controls and patients with COPD. Small airway epithelial cells isolated and cultured from the lungs of patients with COPD or healthy aged-matched controls were stained for activity of Sen-β-Gal**.** Dot plot represents percentage of cells positive for Sen-β-Gal staining (**A**), generated by quantifying at least 500 cells per subject. Dots represent mean value per subject with horizontal line representing group mean. Representative images of Sen-β-Gal staining *(blue)* in small airway epithelial cells from patients with COPD and controls captured using X20 objective. Sen-β-Gal staining was carried out in collaboration with Clara Correia Melo from our lab. Sen-β-Gal, senescence-associated-β-galactosidase. Independent samples t-test revealed no statistically significant differences.

3.3 Discussion

While numerous studies have described increased expression of senescence-associated markers in the COPD lung, very few have investigated senescence marker expression in the airway epithelium. Furthermore, very few studies have explored differences in airway epithelial cell senescence in the large and small airway compartments of the COPD lung, both of which are involved in the disease process. In our cohort of subjects, Ki67 and SIRT1 expression was significantly decreased in the large airway epithelium of patients with COPD compared to controls, whereas p21 expression was higher in the large airway epithelium of controls. We found no significant differences in expression of other markers of senescence. We found more evidence for epithelial cell senescence in the small airways of the COPD lung; γH2A.X and p16 were significantly increased in the small airway epithelium of patients with COPD, while SIRT1 expression was decreased. These results confirm previous reports showing that p16-positive Clara cell frequency is higher in the small airways of patients with COPD compared to smokers without COPD and non-smokers (Zhou, Onizawa et al. 2011), while SIRT1 has been shown to be decreased in the small airway epithelium of patients with COPD compared to non-smokers (Rajendrasozhan, Yang et al. 2008). Other studies have described similar findings when investigating senescence of other cell types in the COPD lung. Aoshiba and colleagues note increased γH2A.X foci in type I and type II alveolar epithelial cells and endothelial cells of patients with COPD compared to smokers without COPD and non-smokers (Aoshiba, Zhou et al. 2012) and others have described increased expression of p21 and p16 in these cells in the lungs of patients with COPD (Tsuji, Aoshiba et al. 2006; Amsellem, Gary-Bobo et al. 2011). We failed to find any significant difference in p21 expression in the small airway epithelium between patients with COPD and controls. However, our control tissue was acquired from patients undergoing pulmonary resection for localised lung cancer. Due to the common aetiology of COPD and lung cancer, there was no significant difference in smoking history between subjects with COPD and controls, and although control subjects were non-smokers at time of surgery, they may still be regarded as 'smokers without COPD'. It is not surprising then that we did not see differences in p21 expression. Accordingly, Tsuji and colleagues failed to find significant differences in endothelial cell expression of p21 when comparing patients with COPD to smokers without COPD, with significant differences observed only when comparing to non-smokers (Tsuji, Aoshiba et al. 2006). Similar findings have also been reported for SIRT1 expression when

comparing these subject groups (Rajendrasozhan, Yang et al. 2008). However, the fact that our control and COPD group are matched for smoking history may suggest that the differences in senescence marker expression that we do detect, are an effect of COPD specifically, as opposed to smoking. In fact, in one study where controls and patients with COPD had similar smoking histories, increased p21 expression in pulmonary endothelial cells in COPD lung tissue was still detectable (Amsellem, Gary-Bobo et al. 2011). Nonetheless, the inclusion of life-long never smokers as an additional comparison group would be desirable. It could be that small changes in markers are not detected by our semi-quantitative scoring system, which is likely to be less sensitive than more quantitative methods. This is a subjective and cruder method of quantification and may result in loss of information, as the extent of staining is being forced into a scale of 0-3. However, this method has been well validated and used previously by other groups working in similar fields (Kranenburg, De Boer et al. 2002). Additionally, we internally validated the use of the semi-quantitative scoring method by comparing our results to the levels of Ki67 expression we initially documented using a quantitative method, which involved counting total number of positive nuclei per mm basement membrane. The patterns of expression we observed using the two methods were the same. Re-scoring of a random sample of slides also confirmed that this method is reliable and reproducible, as there was generally a strong agreement between the scores given by two independent observers (data not shown).

A major limitation of this work is that the control group were, on average, 20 years older than patients with COPD. This is of particular importance since senescence markers are known to increase with age (Jeyapalan, Ferreira et al. 2007; Wang, Jurk et al. 2009). This disparity in age between the control and COPD group may explain why increased p21 expression was found in the large airway epithelium of controls compared to patients with COPD and possibly the failure to detect differences in other markers in the large airway epithelium. The fact that some differences in senescence marker expression were still detectable in the small airway epithelium of patients with COPD may reflect a predominance of small airway involvement in the disease process. Indeed, the emphysematous changes that occur in the COPD lung impact on the peripheral airways and are similar to those that occur in the ageing lung (Ito and Barnes 2009). Additionally, it could be that the more harmful oxidants in cigarette smoke reach the lung periphery, causing more damage and cellular senescence. Indeed, early abnormalities and pathology linked to smoking and development of COPD manifest in the small airway epithelium (Auerbach, Forman et al. 1957). Moreover, it has recently

been shown that the small airway epithelium of smokers shows markers of accelerated ageing, including enhanced telomere shortening as compared to non-smokers, which may suggest that molecular changes occur long before the development of COPD in small airway epithelial cells (Walters, De et al. 2014). One caveat of this work is that we did not distinguish between the different cell populations in the airway epithelium but rather studied it as a whole. Most of the normal human airway is lined by a pseudostratified epithelium of ciliated cells, secretory cells and 6–30% basal cells, with proportion varying along the proximal-distal axis (Mercer, Russell et al. 1994; Nakajima, Kawanami et al. 1998). Basal cells are the stem cells of the pseudostratified airway epithelium and a recent review has suggested that disordered basal cell biology following chronic cigarette smoke exposure may lead to accelerated loss of lung function in susceptible individuals that develop COPD (Crystal 2014). It is plausible that basal airway epithelial cell senescence contributes to the development of COPD, which would likely exacerbate both defective cell repopulation and inflammatory processes in the airway epithelium. Therefore targeting of senescent basal cells may be of therapeutic benefit in preventing or slowing COPD progression. Since we did not use markers to specifically identify subpopulations of airway epithelial cells, it is unclear which cells undergo senescence or harbour telomere dysfunction in our cohort of COPD patients. It would be interesting to determine if, and which, cell subsets harbour the most telomere dysfunction in the airway epithelium. One possible explanation for the lack of increased senescent cell frequencies in the large airway epithelium of the COPD lung is that the large and small airway epithelium are made up of differing numbers and types of progenitor cell populations, which may lead to different levels of renewal in these distinct airway compartments. While Clara cells are generally considered the basal cell progenitors of both the large and small airway epithelium, additional epithelial cell progenitors with proliferative capacity have been identified in the large airway epithelium that are believed to contribute to its maintenance (Hong, Reynolds et al. 2004). It is possible therefore that large airway epithelial cells have 'back-up' mechanisms of restoration and are repopulated more frequently or more effectively as compared to small airway epithelial cells. It could be that more damaged or senescent cells are being shed off form the large airway epithelium, which may explain, in part, the inability to detect increased frequencies of senescent cells in the large airways of patients with COPD.

It should also be noted that while none of the subjects in the control group had documented evidence of COPD, some subjects had spirometric patterns in line with

mild obstructive lung function, possibly due to natural lung ageing or the fact that the majority of controls had significant smoking histories. Therefore, caution should be taken when forming conclusions based on this study population. Despite the limitations of our control group, we still observed a significant increase in the majority of senescence-associated markers studied in the small airway epithelium of patients with COPD and so it may be that our findings are an underestimation of the true involvement of small airway epithelial cell senescence in COPD.

Short telomeres, known activators of cellular senescence, have been implicated in in the pathogenesis of COPD, with a number of studies showing accelerated telomere shortening in leukocytes from patients with COPD as compared to smokers and non-smokers (Houben, Mercken et al. 2009; Savale, Chaouat et al. 2009). However, conflicting results have been published with some studies finding no difference in leukocyte telomere length when comparing patients with COPD to smokers without COPD (Morla, Busquets et al. 2006). Similarly, other studies report accelerated telomere shortening in resident cells of the COPD lung when comparisons are made with non-smokers, however this difference is not observed when comparing to smokers without COPD (Tsuji, Aoshiba et al. 2006). In contrast, Q-PCR revealed shorter telomeres in lung tissue extracts from patients with COPD compared to controls with similar smoking histories, however this difference was less than 10% (Amsellem, Gary-Bobo et al. 2011). Using Q-FISH, we found no significant difference in telomere length in the small airway epithelial cells of patients with COPD compared to controls. However, this could be explained by the similar smoking histories and the younger age, on average, of our COPD group. Additionally, our sample size is particularly small (10 patients with COPD, 8 patients with bronchiectasis and 9 controls) compared to previous work demonstrating telomere shortening in COPD as compared to smokers without COPD (Savale, Chaouat et al. 2009). Therefore, it could be that changes in telomere length are subtle, with larger sample sizes required to demonstrate significant differences.

Evidence suggests that senescence can be induced by activation of a DDR at long telomeres in human fibroblasts during stress- (Fumagalli, Rossiello et al. 2012; Hewitt, Jurk et al. 2012), replicative (Kaul, Cesare et al. 2012) and OIS *in vitro* (Suram, Kaplunov et al. 2012) and TAF have been found to increase with age in multiple tissues in mice and primates *in vivo*, irrespective of telomere length (Fumagalli, Rossiello et al. 2012; Hewitt, Jurk et al. 2012). These data suggest that a "critical" telomere length may not be the sole determinant in the activation of a persistent DDR. Although we did not

find significant differences in telomere length, we have shown, for the first time that TAF are significantly increased in the small airway epithelium of patients with COPD compared to controls, suggesting that telomere dysfunction might occur independently of telomere length in COPD. However, we cannot rule out the possibility that telomere shortening has led to TAF accumulation. Our sample size is limited and therefore subtle changes in telomere length may not be detected in tissues by Q-FISH. However, we did analyse intensity of telomere signals from both co-localising and non-co-localising telomeres and found no significant differences in telomere length, suggesting that telomere shortening is not contributing to telomere dysfunction. It is possible, however, that we are not detecting the shortest of telomeres by our method. Analysis of TAF and telomere length, by both Q-FISH and RT-PCR, in small airway epithelial cells isolated from patients with COPD and aged-matched healthy controls confirmed our *in vivo* data. While TAF are increased in cells from patients with COPD, no significant differences in telomere length are observed. However, our sample size is very limited (n=3 per group for Q-FISH analysis and n=4/6 for RT-PCR) and therefore this work should be repeated using more subjects in order to confirm our findings. The limited sample size is also a possible explanation for the failure to detect significant differences in Sen-β-Gal expression between patients with COPD and controls, since there is a lot of variability between subjects. At the very least, our results may suggest that TAF are a more robust marker of senescence compared to other markers, including telomere length, since we find significant differences despite our small sample size. In accordance with our findings, another study also failed to find differences in telomere length between fibroblasts isolated from patients with emphysema and aged-matched controls but found increased expression of other senescence-associated markers (Muller, Welker et al. 2006). Therefore, we cannot exclude the possibility that telomere shortening is not as important to COPD-associated senescence.

The small airways undergo a number of pathological changes in response to chronic cigarette smoke exposure and in respiratory diseases, such as COPD. Airway epithelial hyperplasia (thickening of the airway epithelium) is one such change, caused by enhanced proliferation of airway epithelial cells (Rock, Randell et al. 2010). Proliferation is known to increase content of DNA damage foci and TAF and therefore it is possible that the increase in TAF we observe in the COPD epithelium is due to increased proliferative activity. However, this an unlikely explanation for our observations since we found no significant difference in Ki67 expression in the small airway epithelium of patients with COPD as compared to controls. However, a more

informative approach to this would have been to test directly whether increased γH2A.X foci and TAF occur more commonly in non-proliferating cells by double immuno-FISH staining against γH2A.X and a proliferation marker, such as Ki67 or PCNA. However, we have shown that small airway epithelial cells positive for the CDK inhibitor p16 had more γH2A.X foci and TAF than p16-negative cells in the COPD lung, consistent with cellular senescence. Similar findings have been described in type II alveolar cells of the COPD lung, with those cells expressing high rates of p16 also containing higher numbers of γH2A.X foci (Aoshiba, Zhou et al. 2012).

Bronchiectasis is a chronic lung disease that affects both the large and small airway compartments, the etiopathogenesis of which is still not clear (McShane, Naureckas et al. 2013). Bronchiectasis is characterised by cycles of infection and inflammation, which lead to structural damage to the airways (Cole 1986). Although bronchiectasis is not classed as an age-related disease as such, it is accountable for increasing rates of hospitalisations and subsequent mortality, particularly in the elderly population (Ringshausen, de Roux et al. 2013). To our knowledge, this is the first report describing the investigation of senescence marker expression in the context of bronchiectasis. In the large airway epithelium, we found a significant increase in γH2A.X foci compared to patients with COPD and a significant decrease in SIRT1 expression compared to controls. In the small airway epithelium, we observed a tendency towards decreased SIRT1 expression and increased number of γH2A.X foci/TAF per cell, however these observations were not significant. Unlike COPD, bronchiectasis is not linked with cigarette smoking. However, similar to COPD, there is a strong inflammatory component to the disease. Inflammation has been reported to induce senescence, and senescent cells are thought to perpetuate this inflammatory response via the so-called SASP, thus generating a vicious cycle leading to propagation and maintenance of senescence and aggravation of chronic inflammation (Acosta, O'Loghlen et al. 2008; Coppe, Patil et al. 2008; Kuilman and Peeper 2009). Therefore, the inflammatory processes occurring in bronchiectasis may be contributed to by the presence of senescent cells. Indeed, it has recently been found that airway epithelial cell senescence may play a role in cystic fibrosis (CF), a disease commonly occurring in conjunction with bronchiectasis. Increased expression of p16 and γH2A.X in the large airway epithelium of patients with CF has been described, which the authors suggest could be caused by chronic neutrophilic airway inflammation (Fischer, Wong et al. 2013). CF is not associated with the ageing process but is characterised by chronic cycles of infection and inflammation, similar to bronchiectasis. Interestingly, this study

also reports no difference in telomere length between control and CF subjects, measured by Q-PCR using DNA extracted from isolated airway epithelial cells (Fischer, Wong et al. 2013). Bronchiectasis commonly occurs following early childhood infection, such as pneumonia (Pasteur, Helliwell et al. 2000). Therefore it is possible that severe inflammation in early life leads to development of senescent cells, which accumulate over time and contribute, in part, to the development of bronchiectasis. A recent study using a murine model of low-grade chronic inflammation showed that accelerated senescence and telomere dysfunction occurred in the liver and gut (Jurk, Wilson et al. 2014). The effects of chronic inflammation on the lung were not determined, however it is possible that accelerated lung senescence occurs in this context. Based on our findings, it is not possible to make firm conclusions regarding the presence of airway epithelial cell senescence in bronchiectasis. However, given that there was often tendency for increased expression of senescence associated markers in the airway epithelium in patients with bronchiectasis, or no significant difference at all when compared to controls (who on average were 20 years older), it is likely that a certain degree of airway epithelial cell senescence occurs in bronchiectasis. This is something that should be explored further, with a larger sample size, aged-matched controls and in the context of inflammation-induced senescence, as in the murine model described above.

A number of studies have found correlations between cellular senescence and airflow limitation. Telomere length in lung cells and circulating leukocytes has been found to positively correlate with FEV_1 % predicted (Tsuji, Aoshiba et al. 2006; Mui, Man et al. 2009) and decreased telomere length is associated with increased risk of COPD (Rode, Bojesen et al. 2013). However, some studies have failed to show a correlation between telomere length and lung function (Houben, Mercken et al. 2009; Savale, Chaouat et al. 2009; Noureddine, Gary-Bobo et al. 2011). Similarly, it has been shown that levels of p21 and p16 expression in type II alveolar epithelial cells and endothelial cells negatively correlate with FEV_1 % predicted (Tsuji, Aoshiba et al. 2006). We did not find any significant correlations between expression of senescence markers altered in the COPD lung and degree of airflow limitation in patients with COPD. This could be because our tissue was acquired from patients undergoing lung transplantation for end-stage disease and so the range of FEV_1 % predicted values were very narrow, varying from only 7-36%. When we pooled our subject groups together, we found significant positive correlations between Ki67 and SIRT1 expression and a strong negative trend between mean number of TAF and FEV_1 % predicted (r = -0.35, p

= 0.06). In fact, others have only reported correlations between senescence markers and FEV_1 % predicted when subjects are pooled into one group (Tsuji, Aoshiba et al. 2006). One limitation of our study is that we did not asses levels of TAF in alveolar epithelial cells. While other studies have reported increased frequencies of alveolar epithelial cells expressing p21 and p16 (Tsuji, Aoshiba et al. 2006) and increased content of γH2A.X (Aoshiba, Zhou et al. 2012) in the COPD lung, levels of TAF in alveolar epithelial cells of the COPD lung have never been reported. While we did observe the presence of TAF in both airway epithelial cells and alveolar epithelial cells, we did not image and quantify levels of TAF in alveolar epithelial cells. This is a limitation of our study and it would be important to determine how levels of TAF are altered in the COPD lung. Telomere dysfunction in alveolar epithelial cells may actually be more relevant to lung structural changes in the COPD lung, in particular the development of emphysema. It has been shown that levels of p21 and p16 in alveolar epithelial cells correlate with FEV_1 % predicted (Tsuji, Aoshiba et al. 2006). While we found no significant correlations between mean number of TAF in small airway epithelial cells with lung function, it could be that levels of TAF in alveolar epithelial cells correlate more strongly with changes in lung function and that senescence of alveolar epithelial cells is more relevant to the structural changes that occur in COPD, or at least the emphysematous-like changes.

When investigating the relationship between senescence marker expression and smoking history, measured in pack years, we found no significant correlations irrespective of whether groups were analysed individually or pooled. This is not that surprising; a number of studies have failed to find any association between telomere length of circulating leukocytes and smoking history (Houben, Mercken et al. 2009; Mui, Man et al. 2009; Savale, Chaouat et al. 2009). However, a negative correlation between pack-year exposure and telomere length was reported in a large cohort of women (Valdes, Andrew et al. 2005). One study described an association between p16 expression in circulating T-lymphocytes and tobacco use (Liu, Sanoff et al. 2009), however, other prior studies have not investigated the relationship between senescence marker expression in the lung and smoking history. Our findings could simply be attributed to a limited sample size or may due to the control group having significant smoking histories, similar to COPD patients. However, our pack-year history in the overall cohort did range from 0 to 120, though still no significant associations were found. This could also be explained by the fact that not all smokers develop COPD,

even when smoking histories are extensive, suggesting that a more complex susceptibility component is involved.

Our results suggest that airway epithelial cell senescence and telomere dysfunction occur in the small airway epithelium of the COPD lung. It is possible that telomere shortening plays little role in this process, however we cannot firmly conclude this based on the limitations of our control group and small sample sizes. Future work would be to investigate the occurrence of TAF in a large sample size with aged-matched controls. There are currently no effective therapies for suppressing chronic inflammation in COPD or altering the underlying pathophysiology of the disease and therefore important future work would be to determine whether dysfunctional telomere signalling contributes to inflammatory processes in COPD. Uncovering whether TAF-positive cells are associated with areas of increased inflammation and inflammatory cell recruitment in the COPD lung would be of significant importance and may shed light on whether, and by what mechanisms, telomere dysfunction contributes to COPD pathogenesis. TAF may be a more robust marker for senescence and of therapeutic benefit in COPD. It remains to be elucidated whether TAF could help stratify patients with COPD for example, by predicting subsequent degree of emphysema or by predicting susceptibility to development of COPD in current smokers.

Chapter 4. Airway cell senescence and telomere dysfunction in the ageing murine lung

In the previous chapter, we demonstrated that TAF increase in the small airway epithelial cells of patients with COPD, supporting the range of evidence that suggests that COPD is a disease of accelerated lung ageing. *In situ* investigations into cellular senescence in 'healthy' human lung ageing are lacking, with only studies using whole tissue lysates describing increased senescence-associated makers in the lungs of older humans (Shivshankar, Boyd et al. 2011). Similarly, there is little data describing cellular senescence in resident cells of the ageing murine lung. One study, by Wang and colleagues, previously described an age-dependent increase in DDR foci (γH2A.X) in alveolar epithelial cells of the murine lung (Wang, Jurk et al. 2009). Increased expression of the histone variant mH2A, enriched in SAHF, has also been reported in alveolar epithelial cells and in total lung tissue extracts of old (24 months) as compared to young (4 months) mice (Kreiling, Tamamori-Adachi et al. 2011). Similarly, other studies have described increased senescence marker expression in the murine lung with age, using predominantly lung tissue lysates, however this does not allow us to distinguish between individual cell types (Krishnamurthy, Torrice et al. 2004; Shivshankar, Boyd et al. 2011). Nonetheless, there are limited studies investigating senescence of lung cells during physiological ageing *in situ*, with little focus on airway epithelial cells in particular. Our group have recently demonstrated that TAF accumulate in the liver and intestines of mice with age (Hewitt, Jurk et al. 2012) and TAF have been shown to quantitatively predict mean and maximum lifespan in both short- and long-lived mice cohorts (Jurk, Wilson et al. 2014). While genomic DNA damage can be transient, studies have demonstrated that damage at telomeres is persistent because telomere-binding proteins, such as TRF2, can inhibit DNA repair (Fumagalli, Rossiello et al. 2012; Hewitt, Jurk et al. 2012). Additionally, it has been shown that telomeric DNA repair is not as efficient as repair in the rest of the genome (Petersen, Saretzki et al. 1998). Therefore, analysis of DNA damage foci alone is possibly not a robust enough marker of senescence.

The occurrence of a DDR at telomeres in the ageing lung has not, to our knowledge, previously been investigated. As we have already found an increase in TAF in the small airway epithelial cells of patients with COPD, the aim of this work was to determine whether TAF increased in the airway epithelium of the murine lung with

physiological ageing, and if so, to determine whether telomere dysfunction is contributing to the natural age-related decline in lung structure.

4.1 Telomere dysfunction and senescence in airway epithelial cells of the ageing murine lung

In order to evaluate the role of airway epithelial cell senescence in the lungs of mice during physiological ageing, we studied longitudinal sections, containing both large and small airways, from the left lungs of male *C57BL/6* mice of different ages (6.5, 15 and 24 months), with 3-5 mice analysed per group. Large airways were defined as being 0.5-1 mm in diameter with simple, columnar epithelium and small airways were identified as being less than 100 µm in diameter (Figure 4.1).

Large airway   **Small airway**
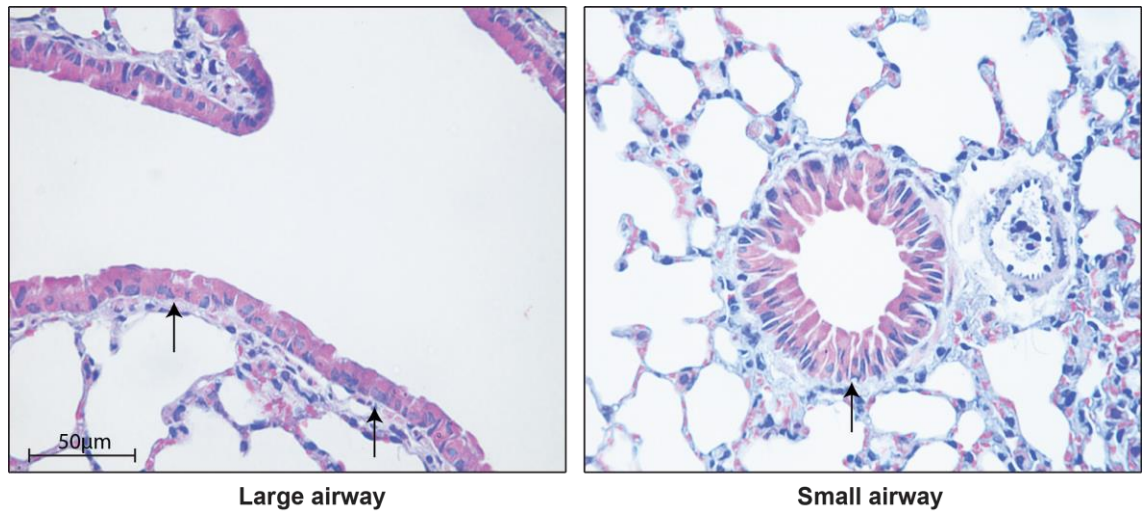
Figure 4.1 Representative images of H&E staining showing large and small airway epithelium of the murine lung. Representative photomicrographs of large and small airway sections in lung tissue from 6.5-month-old mice stained with H&E. Arrows point to airway epithelium, which was focus of this work. Images were captured using X40 objective. H&E, Haematoxylin and Eosin.

4.1.1 p21 expression increases in the large and small airway epithelium of the murine lung with age

p21 expression was assessed in large and small airway epithelial cells present in lung tissue sections from male *C57BL/6* mice of increasing age (6.5, 15 and 24 months) by immunohistochemistry. Expression was analysed by manually counting the total number of negative and positive airway epithelial cells in 10 randomly captured images of both the large and small airway epithelium, for each animal, and percentage positivity then calculated. We observed a slight increase in p21 expression in the large airways (Figure 4.2A) from 6.5 to 15 months, however this was not statistically significant, and a further increase in expression at 24 months as compared to 15- (p = 0.04) and 6.5-month-old (p = 0.02) mice. Similar changes were observed for p21 expression in the small airways (Figure 4.2B). There was no significant difference in expression between 6.5- and 15-month-old mice or 24-month-old mice compared to 15 months (p = 0.058), with significant differences detected only when comparing 6.5- to 24-month-old mice (p = 0.04).

A

B

C

6.5 months   15 months   24 months

Figure 4.2 p21 expression in the large and small airway epithelium of the ageing murine lung. Lung tissue sections from male *C57BL/6* mice of increasing age (6.5-24 months) were stained by immunohistochemistry for p21 expression and levels of expression quantified in the large and small airway epithelium in a blinded fashion. Dot plots represent the percentage of epithelial cells expressing p21 in large (**A**) and small (**B**) airways generated by quantifying 10 random images for each animal. The total number of negative and positive airway epithelial cells per image was quantified manually and percentage positivity calculated from these values before an average was determined for the whole section. (**C**) Representative images of p21 immunostaining *(brown)* in large (*upper panel*) and small (*lower panel*) airway epithelial cells from 6.5-, 15- and 24-month-old mice captured using X40 objective and shown at higher magnification on the right. Arrows point to p21 positive cells. To ensure staining was specific, a control omitting the primary antibody was included (not shown). Data are presented as the mean for individual animals with the horizontal line representing group mean. Statistics: One-way ANOVA and Independent samples t-test *$P < 0.05$.

4.1.2 DNA damage foci and telomere-associated foci increase in the large and small airway epithelial cells of the ageing murine lung, without significant telomere shortening

In order to evaluate DNA damage foci and telomere dysfunction in large and small airway epithelial cells of the ageing murine lung, we performed telomere-specific quantitative fluorescence *in situ* hybridisation (Q-FISH), combined with immunofluorescence against γH2A.X (immuno-FISH). Analysis revealed a significant increase in the mean number of γH2A.X foci per cell in both large (Figure 4.3A) and small (Figure 4.3B) airway epithelial cells from 6.5 until 24 months of age. In the large airways, we found no significant difference in number of γH2A.X foci from 6.5 to 15 months, but found a significant increase from 15 to 24 months ($p = 0.03$) and from 6.5 to 24 months ($p = 0.03$). In the small airways, we found no significant difference in number of γH2A.X foci from 6.5 to 15 months, or from 15 months to 24 months but found a significant increase from 6.5 to 24 months ($p = 0.008$). Analysis of γH2A.X foci associated with telomeres (TAF) revealed a significant increase in mean number of TAF from 15 to 24 months ($p = 0.014$) and from 6.5 to 24 months ($p = 0.002$) in large airway epithelial cells (Figure 4.3C). In the small airways, we observed an increase in mean number of TAF from 6.5 to 15 months ($p = 0.01$) and from 6.5 to 24 months ($p = 0.002$) (Figure 4.3D). The increase in mean number of TAF from 15 to 24 months did not reach statistical significance ($p = 0.06$). Analysis of telomere signal intensity indicated no statistically significant changes between the three age groups in both the large (Figure 4.4A) and small (Figure 4.4B) airway epithelial cells.

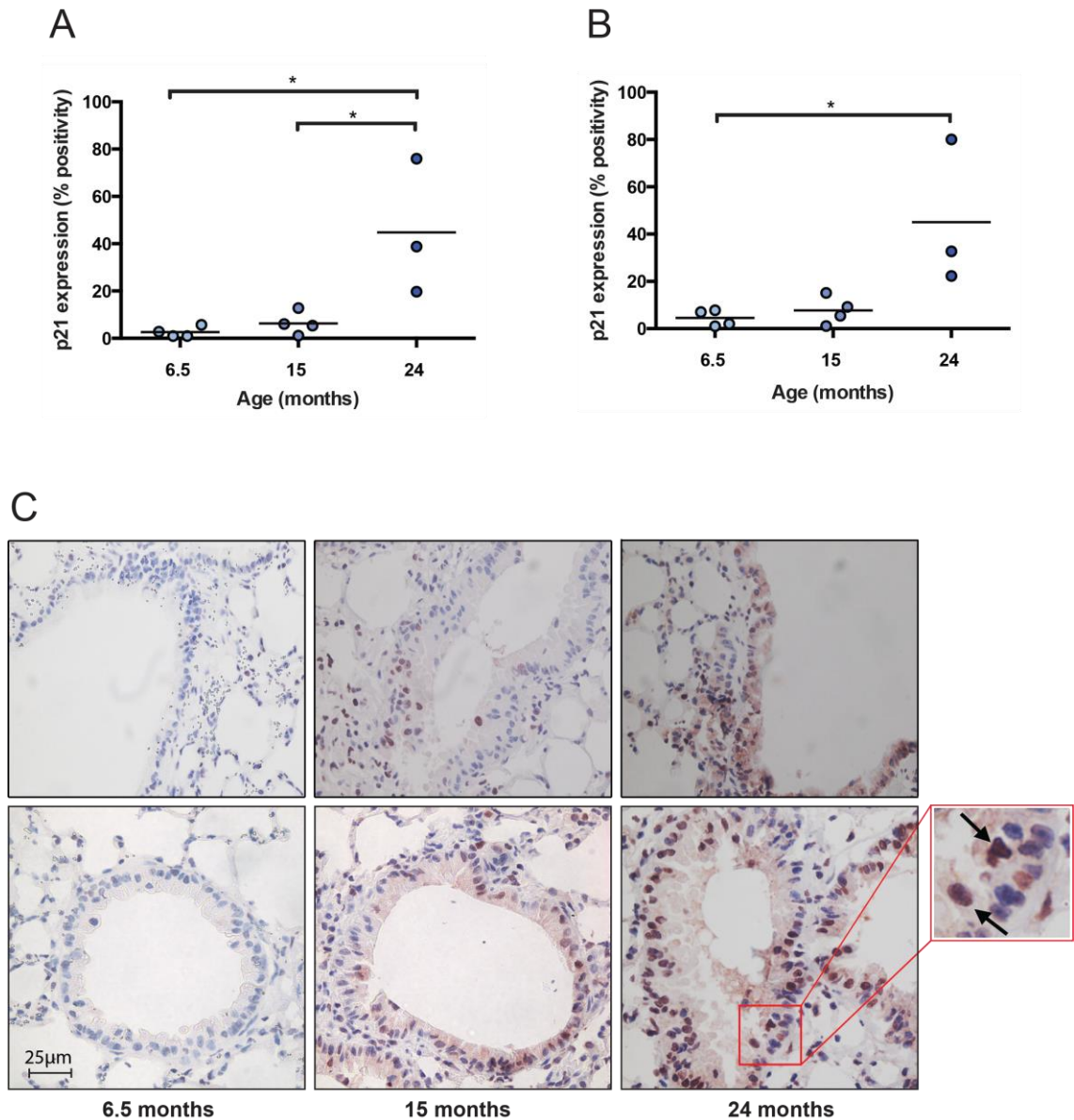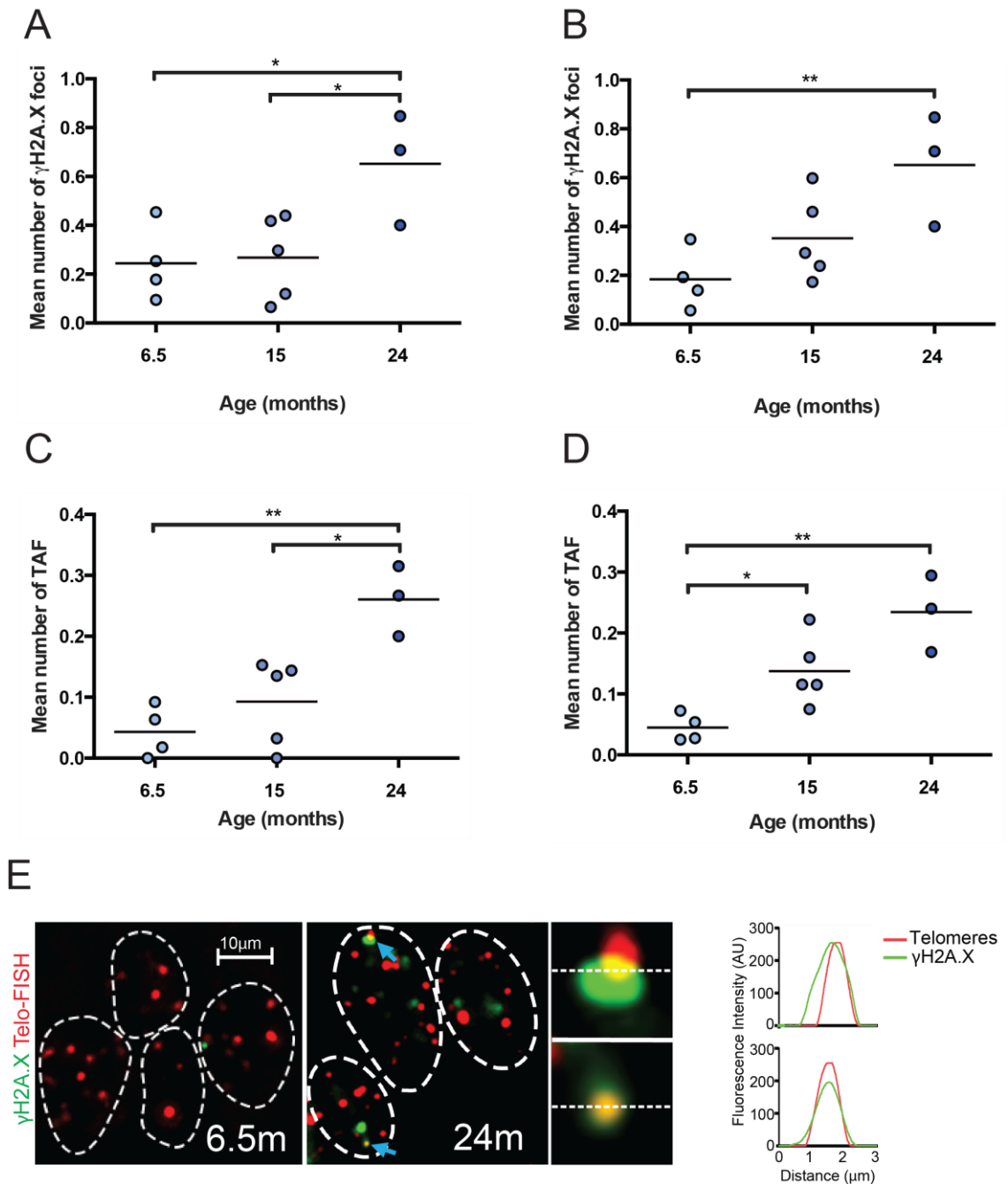**Figure 4.3 γH2A.X foci and telomere-associated foci in large and small airway epithelial cells of the ageing murine lung.** Lung tissue sections from male *C57BL/6* mice of increasing age (6.5-24 months) were analysed for expression of γH2A.X foci and telomere-associated foci (TAF) by immuno-FISH. Dot plots represent the mean number of γH2A.X foci per cell in large (**A**) and small (**B**) airway epithelial cells and the mean number of TAF per cell in large (**C**) and small (**D**) airway epithelial cells for each animal, generated by quantifying Z-stacks of at least 100 cells per mouse. (**E**) Representative image of immuno-FISH for γH2A.X *(green)* and telomeres *(red)* in small airway epithelial cells from 6.5-month and 24-month-old mice captured using X100 oil objective and following Huygens (SVI) deconvolution. Arrows point to γH2A.X foci co-localising with telomeres (TAF), depicted by associated histograms and shown at higher magnification on the right (images are from one single Z-plane). Data are presented as the mean for individual animals with the horizontal line representing group mean. Statistics: One-way ANOVA and Independent samples t-test *$P < 0.05$, **$P < 0.01$.
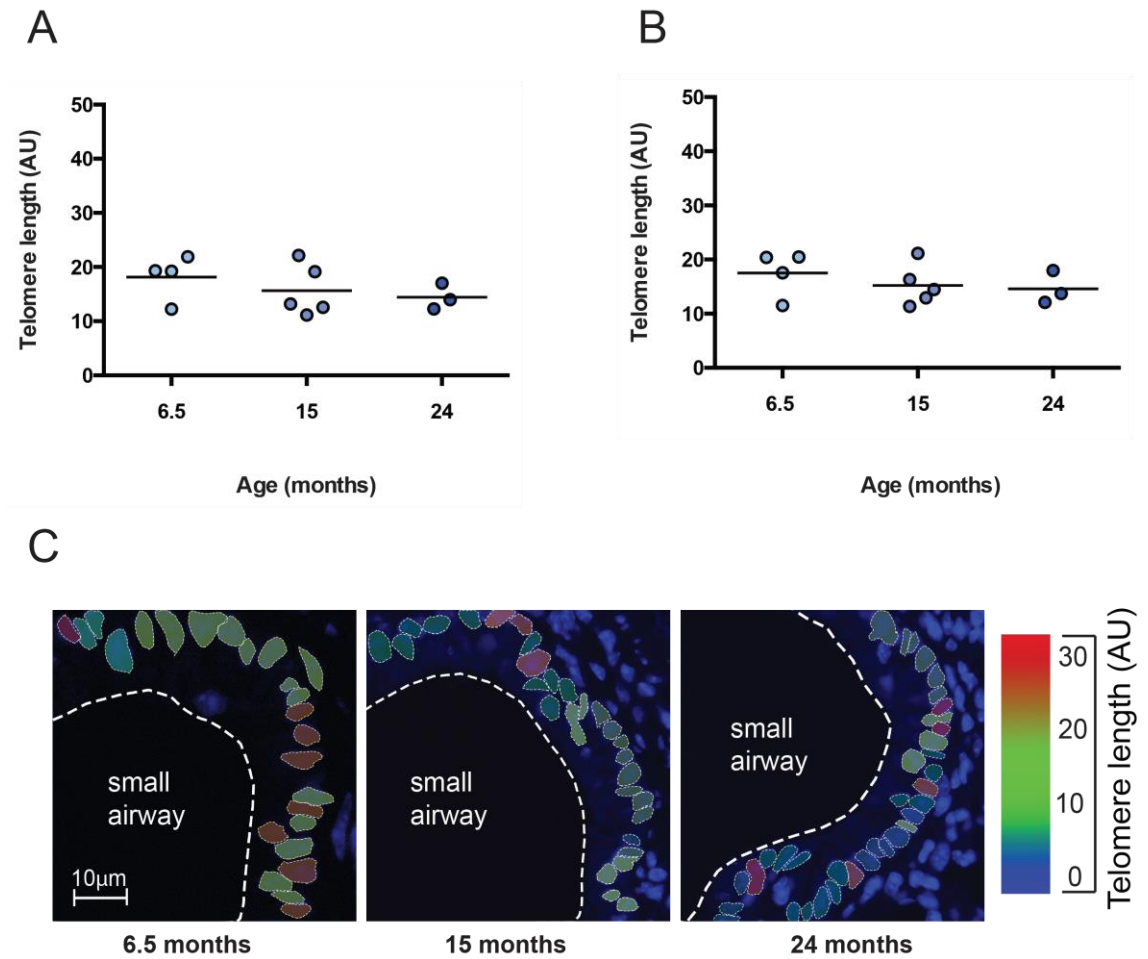
Figure 4.4 Telomere length in large and small airway epithelial cells of the ageing murine lung. Telomere intensity of large and small airway epithelial cells in lung tissue sections from male *C57BL/6* mice of increasing age (6.5-24 months) was assessed by Q-FISH to give an indication of telomere length. Dot plots represent mean telomere length of large (**A**) and small (**B**) airway epithelial cells for each animal generated by quantifying mean intensity of maximum projections of at least 100 cells per animal using a measuring tool on ImageJ analysis software. (**C**) Representative examples of Q-FISH images of small airway sections from 6.5-, 15- and 24-month-old mice, colour coded according to telomere length (blue: short; red: long). Data are presented as the average intensity for individual animals with the horizontal line representing group mean. Statistics: One-way ANOVA and Independent samples t-test. Q-FISH, quantitative-fluorescence *in situ* hybridisation.

4.1.3 Alveolar airspace size increases in the murine lung with age and this correlates with telomere dysfunction and p21 expression

Alveolar airspace size was determined by analysing H&E sections of the murine lung from mice age 6.5, 15 and 24 months of age. Two methods were used to determine changes in alveolar airspace size. The mean linear intercept (MLI) method consists of drawing a line diagonally from the bottom left of each image to the top right and counting the number of intersections (from alveolar wall segments) along that line, before dividing the length of the line in microns by the number of intercepts, as previously described (Weibel 1963). Therefore, the fewer the number of intersections, indicative of a reduction in alveolar airspaces or increased airspace size, the higher the MLI value. We also gathered information about airspace size by manually counting the number of airspaces, with less airspaces per field indicating increased airspace size, and calculating an average number per animal. We gained similar results using both methods, with a significant increase in MLI observed from 6.5 to 24 months (p = 0.003) and from 15 to 24 months (p = 0.004) (Figure 4.5A) and a significant decrease in mean number of airspaces from 6.5 to 24 months (p = 0.0001) and from 15 to 24 months (p = 0.002) (Figure 4.5B).
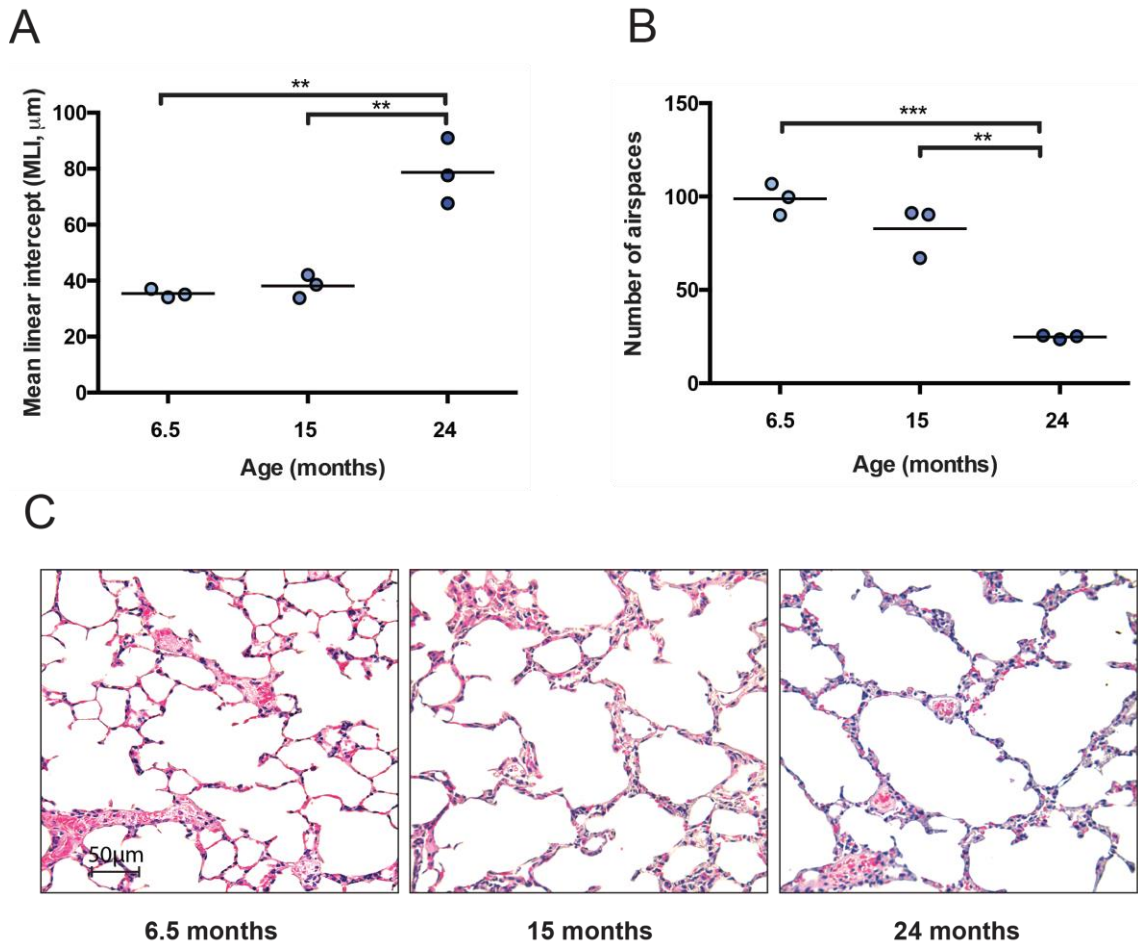
Figure 4.5 Alveolar airspace size in mice of increasing age. Changes in size of alveolar airspaces in the lungs from mice of increasing age were assessed by carrying out H&E staining on lung tissue sections from *C57BL/6* mice in each age group (6.5, 15 and 24 months). 10 random images were captured for each tissue section using X20 objective and images were analysed using one of two methods. Dot plots represent mean linear intercept (MLI) value in microns (**A**) or the mean number of airspaces (**B**) for individual mice calculated as an average of 10 random images. Horizontal line represents group mean. (**C**) Representative images of H&E staining of alveolar airspaces in 6.5-, 15- and 24-month-old mice captured using X20 objective. Statistics: One-way ANOVA and Independent samples t-test. **P < 0.01, ***P < 0.001. H&E, Haematoxylin and Eosin.

We tested correlations between mean number of airspaces and DNA damage foci, telomere length and p21 expression to determine whether a relationship exists between the natural enlargement of alveolar airspaces with age and telomere dysfunction or the presence of senescence markers. We observed no significant correlations between mean number of γH2A.X foci and mean number of airspaces when looking at both large (Figure 4.6A) and small (Figure 4.6B) airway epithelial cell expression. The negative correlations we observed between mean number of TAF and number of airspaces were statistically significant when investigating TAF content in both the large (Figure 4.6C) ($p = 0.03$) and small (Figure 4.6D) ($p = 0.04$) airway epithelial cells. Telomere length did not correlate with number of airspaces in either the large (Figure 4.6E) or small (Figure 4.6F) airway epithelial cells. Interestingly, we observed negative correlations between p21 expression in the large (Figure 4.6G) and small (Figure 4.6H) airway epithelial cells, although only small airway epithelial cell expression of p21 significantly correlated with number of airspaces ($p = 0.005$). As expected, p21 expression positively correlated with mean number of TAF in both the large (Figure 4.7A) ($p = 0.02$) and small (Figure 4.7B) ($p = 0.05$) airway epithelial cells, however this failed to reach significance in the small airways. No correlation was observed between p21 expression and telomere length in either the large (Figure 4.7C) or small (Figure 4.7D) airways.
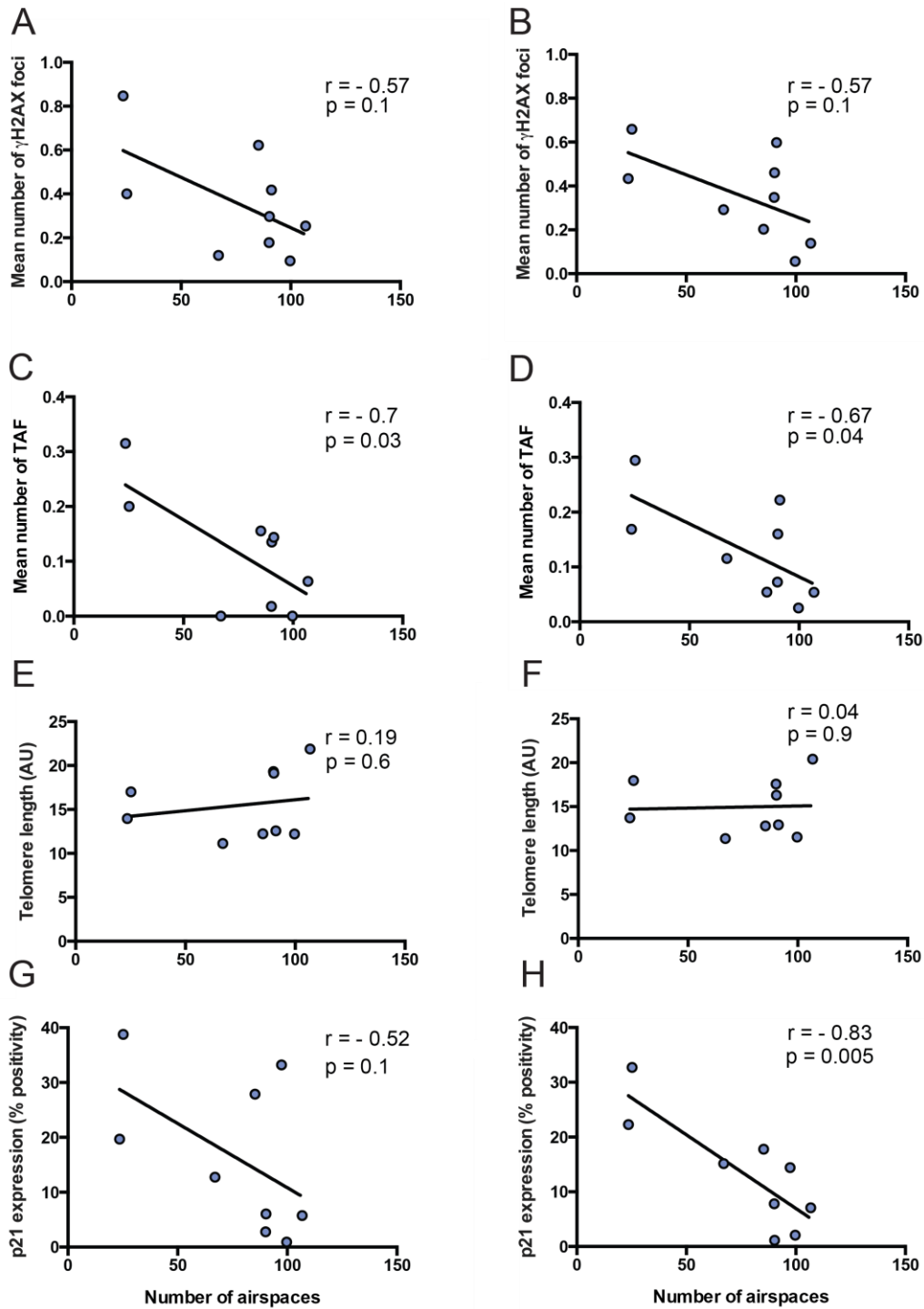
Figure 4.6 Relationship between number of alveolar airspaces and senescence-associated markers in the large and small airway epithelial cells of the ageing murine lung. Relationship between mean number of γH2A.X foci in the large (**A**) and small (**B**) airway epithelial cells, mean number of telomere-associated foci (TAF) in the large (**C**) and small (**D**) airway epithelial cells, telomere length in the large (**E**) and small (**F**) airway epithelial cells and p21 expression in the large (**G**) and small (**H**) airway epithelial cells and number of airspaces in male *C57BL/6* mice aged 6.5-24 months. Not all tissue sections available for analysis of senescence marker expression were suitable for morphological analysis hence inconsistencies in numbers included in correlations. Correlations were assessed using Pearson's correlation coefficient. P values < 0.05 considered significant.
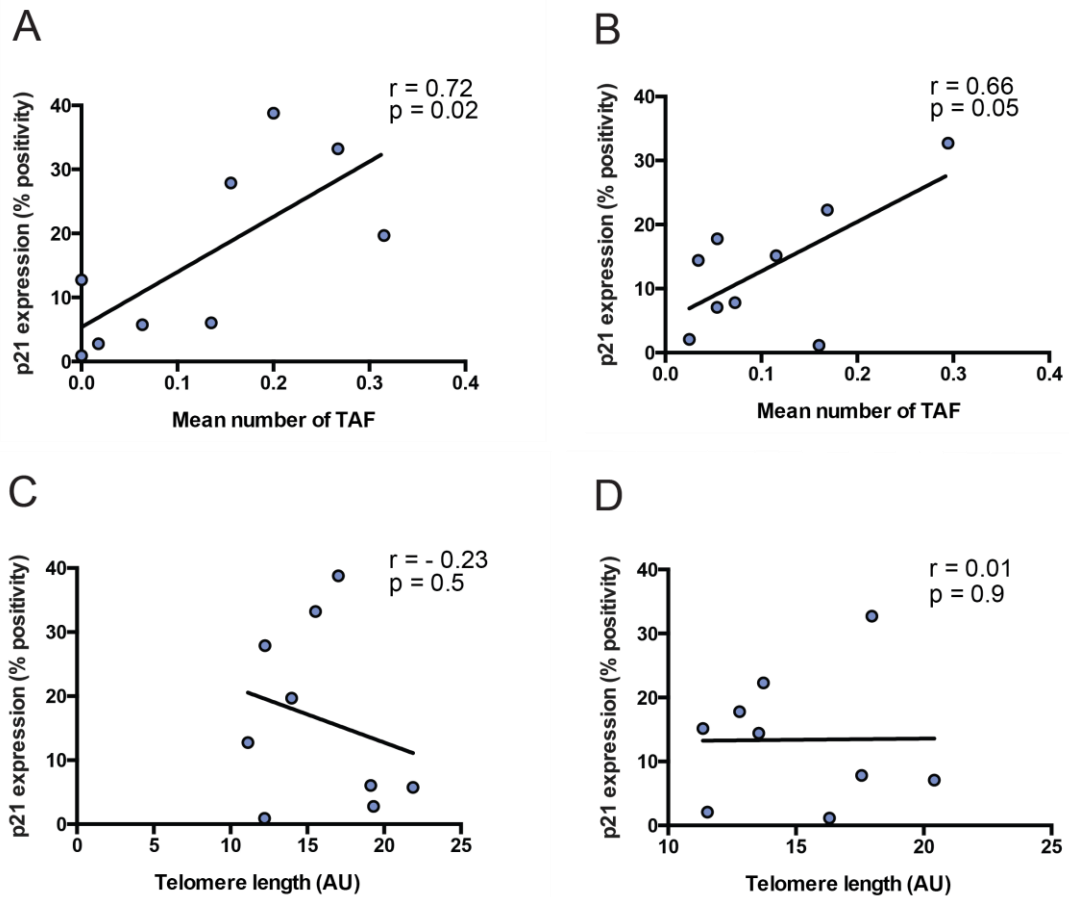
Figure 4.7 Relationship between p21 expression and telomere dysfunction in large and small airway epithelial cells of the ageing murine lung. Relationship between p21 expression and mean number of telomere-associated foci (TAF) in the large (**A**) and small (**B**) airway epithelial cells and telomere length in the large (**C**) and small (**D**) airway epithelial cells in male *C57BL/6* mice aged 6.5-24 months. Not all tissue sections available for analysis of a particular marker were available for analysis of other markers, hence inconsistencies in numbers included in correlations. Correlations were assessed using Pearson's correlation coefficient. P values < 0.05 considered significant.

4.1.4 Late-generation TERC-/- mice show increased telomere-associated foci in small airway epithelial cells and early-onset emphysema

To investigate whether telomere dysfunction contributes directly to loss of alveolar airspaces, we quantified the number of alveolar airspaces in lung tissue sections from mice carrying a homozygous deletion of the RNA component of telomerase (TERC$^{-/-}$), the enzyme responsible for maintaining telomere length, bread until fourth generation (G4) (Blasco, Lee et al. 1997). *G4 TERC$^{-/-}$* mice have severe telomere dysfunction induced by telomere shortening, which results in both cell-cycle arrest and apoptosis (Lee, Blasco et al. 1998), and exhibit a number of phenotypes indicative of premature ageing that are, in part, thought to be due to early onset of senescence (Wong, Maser et al. 2003; Choudhury, Ju et al. 2007). First, we carried out immuno-FISH against γH2A.X and telomeres, to determine whether TAF increase as a result of telomere shortening. We confirmed that at 6.5 months of age, *G4 TERC$^{-/-}$* mice do have critically short telomeres in small airway epithelial cells, as compared to aged-matched wild-types (Figure 4.8A) (p = 0.0005). A significant increase in mean number of TAF in the small airway epithelial cells of *G4 TERC$^{-/-}$* mice compared to age-matched wild-types was also observed (p = 0.008) (Figure 4.8B). Consistent with the hypothesis that telomere dysfunction in airway epithelial cells contributes to airspace enlargement, we found a significant reduction in number of airspaces in *G4 TERC$^{-/-}$* mice (p = 0.0002) (Figure 4.9A). Additionally, the correlation between mean number of TAF in small airway epithelial cells and number of airspaces still holds when *G4 TERC$^{-/-}$* mice are added (p = 0.003) (Figure 4.9B), however telomere intensity still does not show correlations with number of airspaces (p = 0.1) (Figure 4.9C).
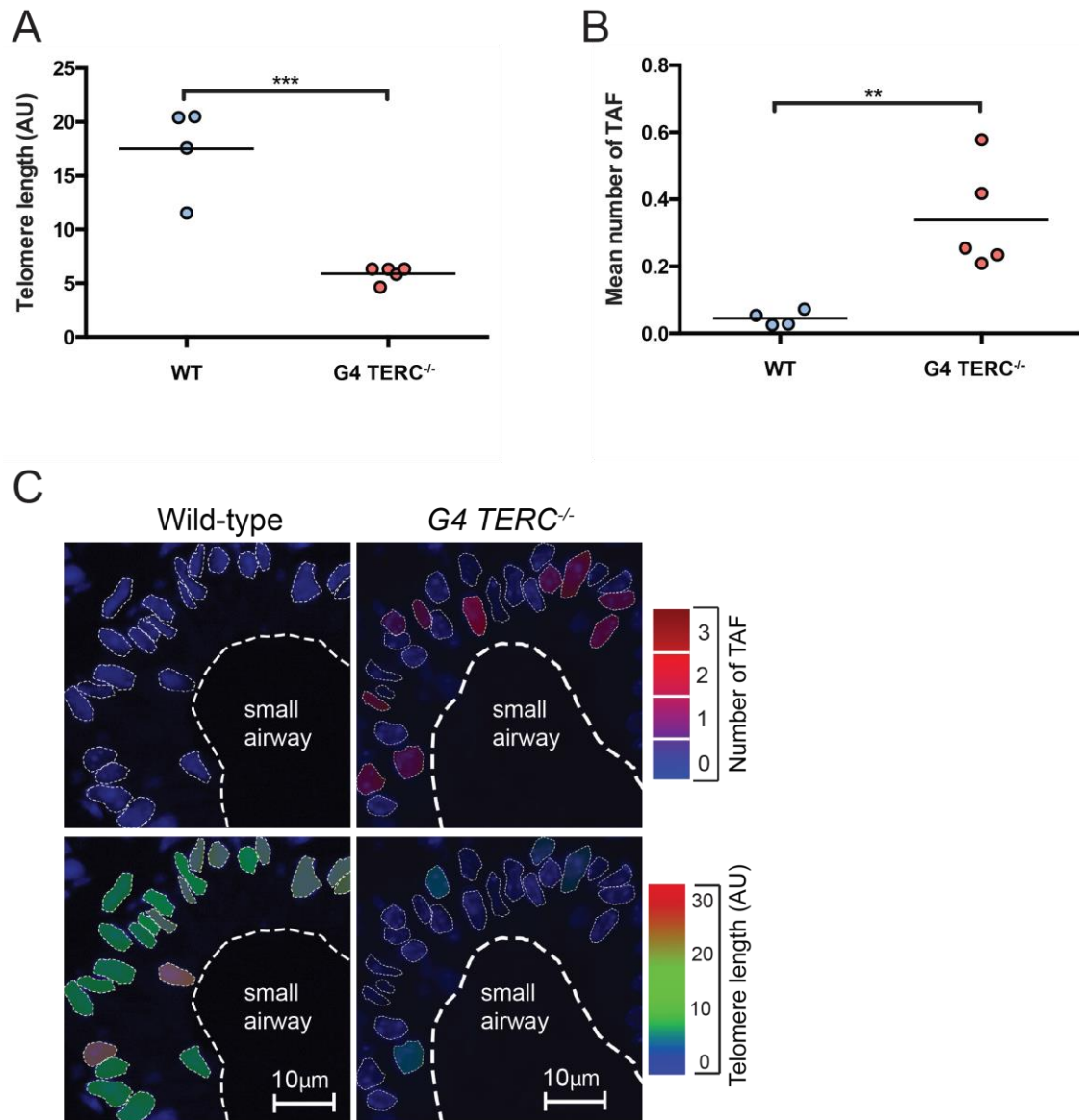
Figure 4.8 Telomere length and telomere-associated foci in small airway epithelial cells of late generation mice lacking telomerase. Immuno-FISH staining for γH2A.X and telomeres was carried out on lung tissue sections from fourth generation telomerase negative (*G4 TERC*^{-/-}) mice and wild type *C57BL/6* mice at 6.5 months of age. Dot plots represent mean telomere length (**A**) and mean number of telomere-associated foci (TAF) (**B**) in small airway epithelial cells for each animal generated by quantifying Z-stacks of at least 100 cells per mouse taken using X100 oil objective. Data are presented as the mean for individual animals with the horizontal line representing group mean. (**C**) Immuno-FISH images of small airway epithelial cells from wild-type and *G4 TERC*^{-/-} mice colour coded according to number of TAF (blue: low number; red: high number) and telomere length (blue: short; red: long). Statistics: Independent samples t-test **$P < 0.01$, ***$P < 0.001$.
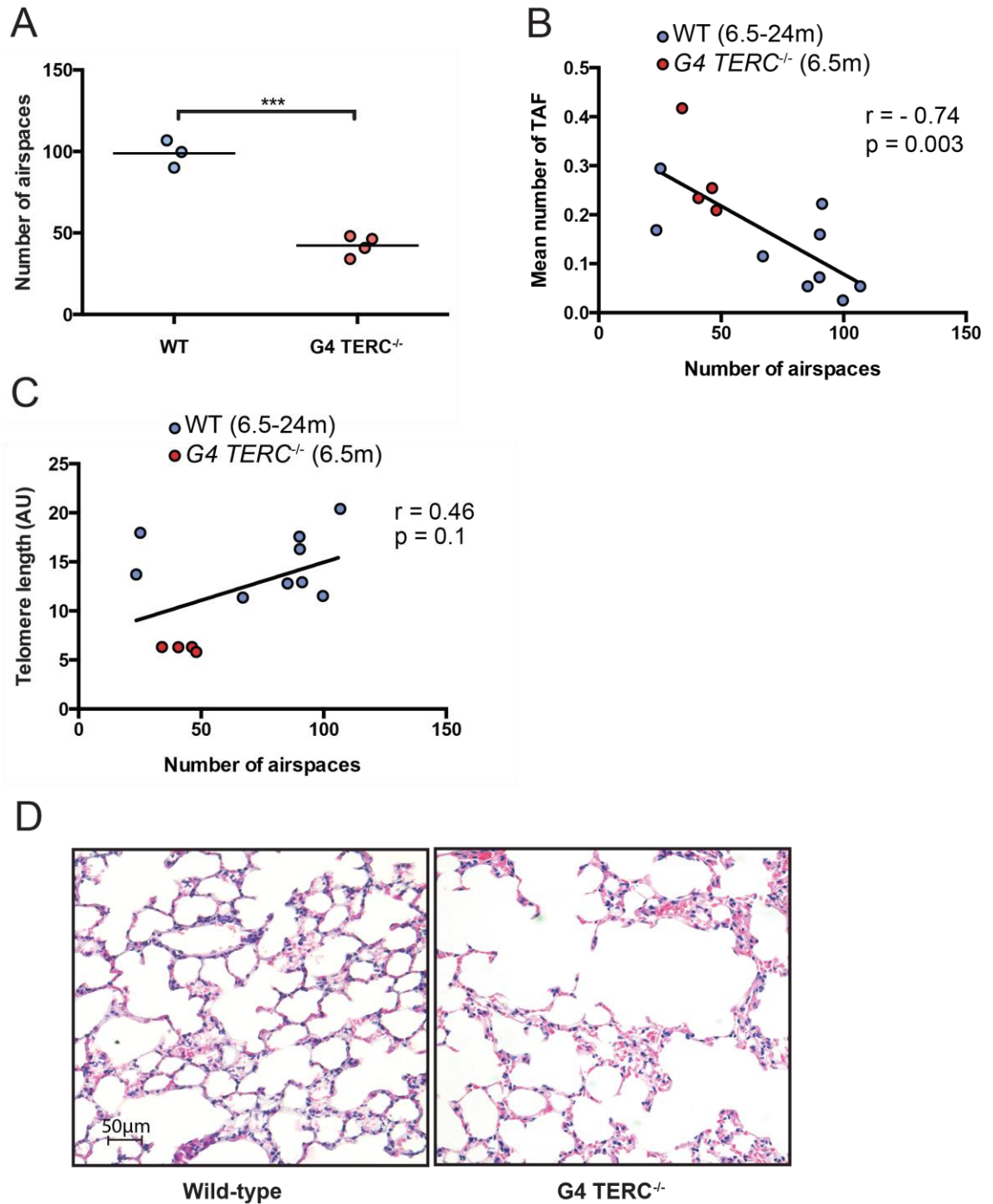
Figure 4.9 Alveolar airspace size and relationship with telomere dysfunction in late generation mice lacking telomerase. H&E staining was carried out on lung tissue sections from fourth generation telomerase negative (*G4 TERC*^{-/-}) mice and wild type *C57BL/6* mice at 6.5 months of age and number of alveolar airspaces manually counted from 10 random images taken using X20 objective for each animal. Dot plot represents mean number of airspaces (**A**). Data are presented as the mean for individual animals with the horizontal line representing group mean. Relationship between mean number of telomere-associated foci (TAF) (**B**) and telomere length (**C**) in small airway epithelial cells and number of airspaces in male *C57BL/6* mice aged 6.5-24 months and *G4 TERC*^{-/-} mice aged 6.5 months. (**D**) Representative images of H&E staining of alveolar airspaces in wild-type and *G4 TERC*^{-/-} mice captured using X20 objective. Statistics: Independent samples t-test, Pearson's correlation ****P* < 0.001. H&E, Haematoxylin and Eosin.

4.2 Telomere dysfunction in the airway epithelial cells of mice exposed to cigarette smoke

Cigarette smoking is the most important risk factor for COPD (Forey, Thornton et al. 2011). In accordance, numerous studies have demonstrated early-onset emphysema and lung inflammation in mice exposed to cigarette smoke (Shapiro, Goldstein et al. 2003; Churg, Wang et al. 2004; Rinaldi, Maes et al. 2012; Yao, Chung et al. 2012; Ganesan, Comstock et al. 2014). Reports also describe increased markers of senescence in the lungs of mice exposed to cigarette smoke. It has been shown that exposure to cigarette smoke for 2 weeks increases Sen-β-Gal staining, p21 expression and lipofuscin accumulation in type II alveolar cells in mice, as compared to air-exposed controls (Tsuji, Aoshiba et al. 2004). Similarly, only 3 days exposure to cigarette smoke has been shown to augment DNA damage (as shown by increased γH2A.X) and increased levels of p21, as detected by immunoblotting in whole lung tissue extracts (Yao, Sundar et al. 2013). SIRT1 is decreased in whole lung tissue extracts and small airway epithelial cells of mice exposed to cigarette smoke (Caito, Rajendrasozhan et al. 2010; Yao, Chung et al. 2012). Additionally, p21 disruption attenuates cigarette smoke-mediated inflammation and airspace enlargement in the murine lung and decreases levels of Sen-β-Gal and γH2A.X in the lungs of mice exposed to cigarette smoke (Yao, Yang et al. 2008; Yao, Chung et al. 2012; Yao, Sundar et al. 2013). Despite these findings, little focus has been given to the effects of cigarette smoke exposure on both large and small airway epithelial cell senescence in the lungs of wild-type mice. Furthermore, the presence of telomere-associated DNA damage has not yet been investigated, to our knowledge, in the context of *in vivo* cigarette smoke exposure.

As we have previously found that TAF are increased in the small airway epithelium in patients with COPD and we show an age-dependent increase in TAF in the large and small airway epithelial cells of the murine lung, we aimed to determine whether cigarette smoke exposure leads to increases in TAF in both large and small airway epithelial cells of the murine lung.

4.2.1 DNA damage foci and telomere-associated foci increase in the large and small airway epithelial cells of mice exposed to cigarette smoke, without significant telomere shortening

To determine whether cigarette smoke exposure lead to induction of TAF in large and small airway epithelial cells of the murine lung, we performed immuno-FISH against telomeres and γH2A.X on lung tissue sections from male *C57BL/6* mice exposed to

cigarette smoke for 1 hour, twice daily, for 2 weeks as compared to air-exposed, aged-matched (3 months of age) controls. We found that cigarette smoke exposure significantly increased mean number of γH2A.X foci in both large (p = 0.02) (Figure 4.10B) and small (p = 0.01) (Figure 4.10C) airway epithelial cells. Similarly, cigarette smoke exposure increased mean number of TAF in the large (p = 0.04) (Figure 4.10D) and small (p = 0.03) (Figure 4.10E) airway epithelial cells, as compared to aged-matched controls. There was no significant differences observed in telomere length in both large (Figure 4.10F) and small (Figure 4.10G) airway epithelial cells of smoke-exposed mice as compared to controls.

4.2.2 Neutrophil infiltration is increased in the lungs of mice exposed to cigarette smoke

It is known that chronic sterile inflammation increases with the ageing process, termed "inflammaging" (Franceschi, Capri et al. 2007). Additionally senescent cells may impact on the innate immune system and attract immune cells, such as neutrophils, *via* activation of the so-called SASP (Xue, Zender et al. 2007). A previous study has shown increased numbers of T-cells, B-cells and macrophages in the lungs of aged (24 months) compared to young (12 month) *Balb/c* mice (Aoshiba and Nagai 2007). We aimed to determine whether cigarette smoke exposure for two weeks increased the number of neutrophils present in murine lung tissue.

In order to evaluate whether cigarette smoke exposure promoted neutrophil recruitment, immunohistochemistry was carried out on lung tissue sections from *C57BL/6* mice exposed to cigarette smoke (as above) and air-exposed, aged-matched controls using an antibody raised against murine neutrophils (NIMP). We observed on average, around a 3-fold increase in the number of neutrophils present per visual field in the lung tissue of mice exposed to cigarette smoke (p = 0.0002) (Figure 4.11A).
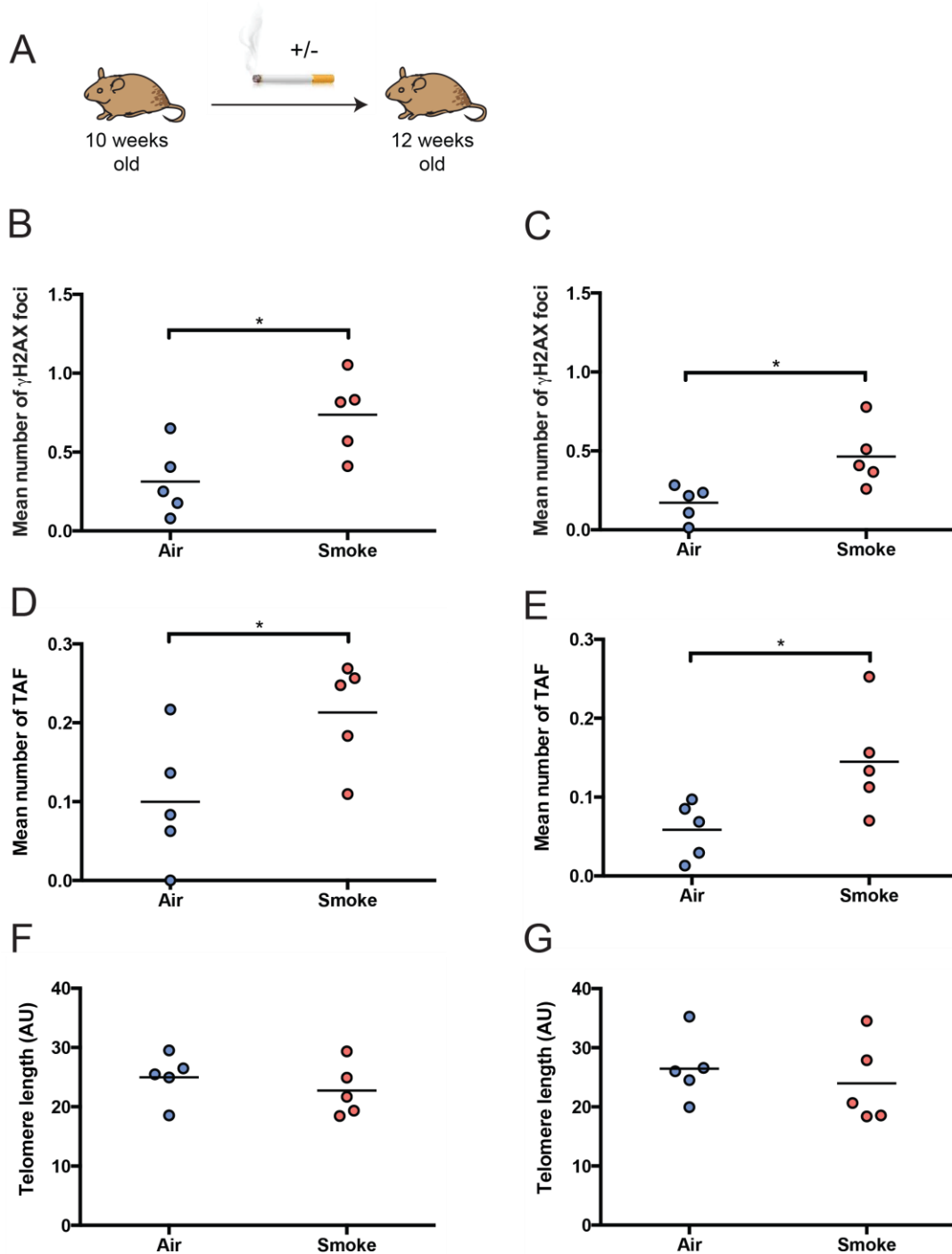
Figure 4.10 γH2A.X foci, telomere-associated foci and telomere length in large and small airway epithelial cells of mice exposed to cigarette smoke. Male *C57BL/6* mice at 10 weeks of age were exposed to cigarette smoke for 1 hour, twice daily, or room air for 14 days (**A**) and sacrificed at 3 months of age, one hour following final exposure. Immuno-FISH against γH2A.X and telomeres was carried out on sections from the left lung. Dot plots represent mean number of γH2A.X foci in large (**B**) and small (**C**) airway epithelial cells, mean number of telomere-associated foci (TAF) in large (**D**) and small (**E**) airway epithelial cells and telomere length in large (**F**) and small (**G**) airway epithelial cells, generated by quantifying Z-stacks of at least 100 cells per animal. Data are presented as the mean for individual animals with the horizontal line representing group mean. Statistics: Independent samples t-test *$P < 0.05$.

A

B
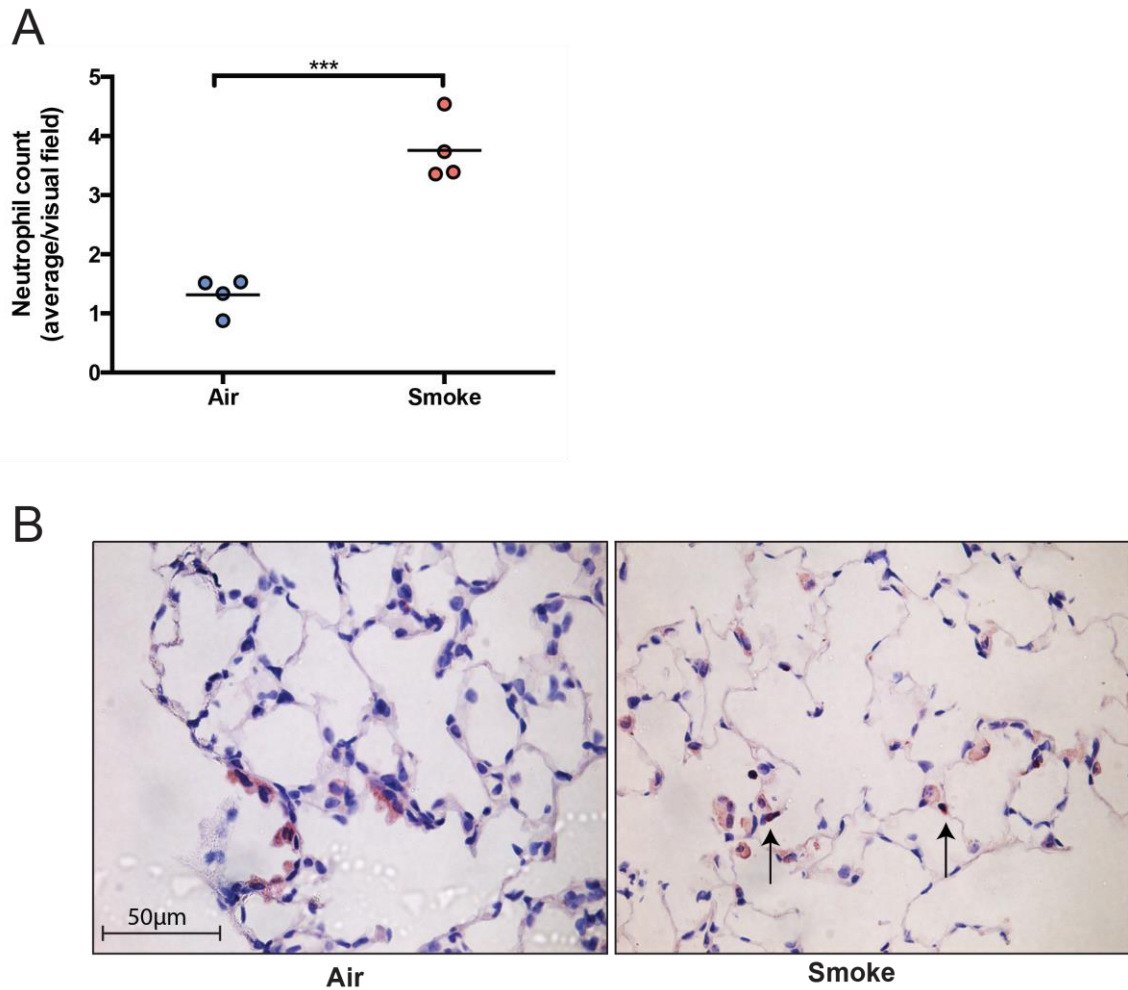
Figure 4.11 Neutrophil infiltration in lung tissue from mice exposed to cigarette smoke. Male *C57BL/6* mice at 10 weeks of age were exposed to cigarette smoke for 1 hour, twice daily, or room air for 14 days and sacrificed at 3 months of age, one hour following final exposure. Immunohistochemistry against murine neutrophils was carried out on sections from the left lung. Dot plots represent mean number of neutrophils per visual field for each animal, generated by quantifying at least 25 randomly captured images, taken using the X40 objective. Black arrows point to neutrophils. Immunohistochemistry was performed in collaboration with Anthony Lagnado from our lab. Data are presented as the mean for individual animals with the horizontal line representing group mean. Statistics: Independent samples t-test ***$P < 0.001$.

4.3 mTORC1 inhibition and ageing of the murine lung

Inhibition of mTOR activity has been shown to extend lifespan in various model systems (Fabrizio, Pozza et al. 2001; Vellai, Takacs-Vellai et al. 2003; Kaeberlein, Powers et al. 2005; Harrison, Strong et al. 2009; Miller, Harrison et al. 2011; Wu, Liu et al. 2013). Rapamycin, a pharmacological inhibitor of mTORC1, attenuates many forms of age-related change in mice, including alterations in heart, liver, adrenal glands, endometrium, and tendon, as well as age-dependent decline in spontaneous activity (Wilkinson, Burmeister et al. 2012). Decreased mTOR expression by genetic means reduces the age-dependent increase in p16 in the kidney and livers of mice as compared to aged-matched wild-types (Wu, Liu et al. 2013). Few studies have investigated the effects of rapamycin treatment on senescent cell accumulation *in vivo*. Furthermore, there are much less data reporting the effects of rapamycin treatment on senescence marker expression in the ageing lung and effects on age-related lung decline.

Our lab has previously shown that rapamycin treatment is able to prevent an age-related increase in TAF in the liver of mice, along with other markers of cellular senescence, including Sen-β-Gal and p21 (unpublished). However, it is unknown as to whether rapamycin treatment affects the age-related increase in TAF in the lung.

We aimed to determine whether a rapamycin-supplemented diet is able to attenuate the age-related increase in telomere dysfunction and other markers of senescence in the large and small airway epithelial cells of the murine lung, along with the loss of alveolar integrity that occurs with age.

In order to evaluate the effects of mTORC1 inhibition on ageing of the murine lung, male *C57BL/6* mice were fed either a control or rapamycin-supplemented diet, as previously described by Harrison and colleagues (Harrison, Strong et al. 2009), and sacrificed at different time points (Figure 4.12).
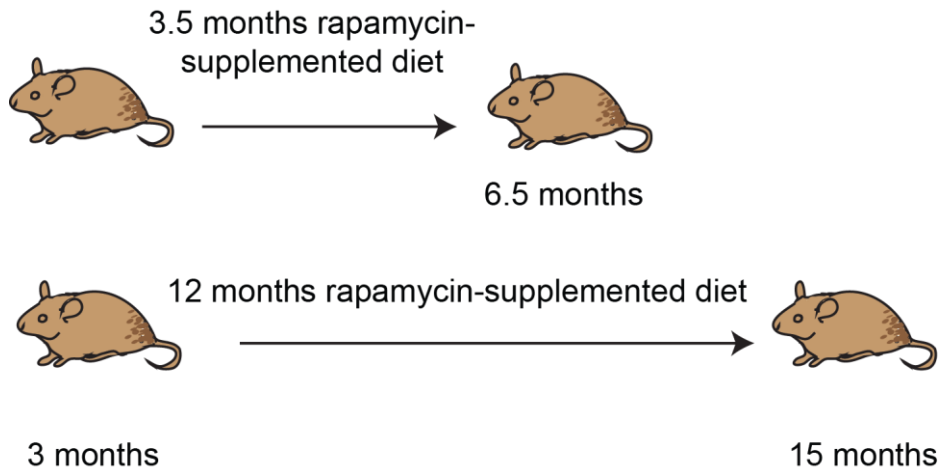
Figure 4.12 Experimental design of rapamycin-supplemented diet study. Male *C57BL/6* mice were fed control or rapamycin-supplemented diets. Diets were begun at 3.5 months of age and mice were sacrificed at either 6.5 months, giving a diet duration of 3.5 months, or 15 months of age, giving a diet duration of 12 months. There were 4-5 animals per group.

4.3.1 Telomere-associated foci are decreased in the small airway epithelial cells of the murine lung following mTORC1 inhibition with rapamycin

In order to elucidate whether a rapamycin-supplemented diet prevented the age-related increase in DNA damage foci and TAF in the airway epithelial cells of the murine lung, we carried out immuno-FISH against telomeres and γH2A.X on lung tissue sections from male *C57BL/6* mice fed a control or rapamycin-supplement diet until 6.5 and 15 months of age. We observed a tendency towards decreased γH2A.X foci in both the large (Figure 4.13A) and small (Figure 4.13B) airway epithelial cells at each time point, however these observations failed to reach statistical significance. Similarly, we observed a tendency towards decreased TAF in both the large (Figure 4.13C) and small (Figure 4.13D) airway epithelial cells at each time point, however these observations also failed to reach significance, with the exception of TAF content in the small airway epithelial cells, which was significantly reduced following 12 months rapamycin treatment (p = 0.02). It is unlikely that changes in TAF in the small airway epithelial cells at 15 months can be attributed to changes in telomere length, since telomere analysis revealed no significant difference in telomere length in either the large (Figure 4.14A) or small (4.14B) airway epithelial cells at all time points following rapamycin supplementation. In order to determine whether rapamycin-supplementation affected other senescence-associated markers, we investigated p21 expression by immunohistochemistry in mice fed control and rapamycin diets at 6.5 and 15 months of age, however no significant changes in p21 expression were found (data not shown).
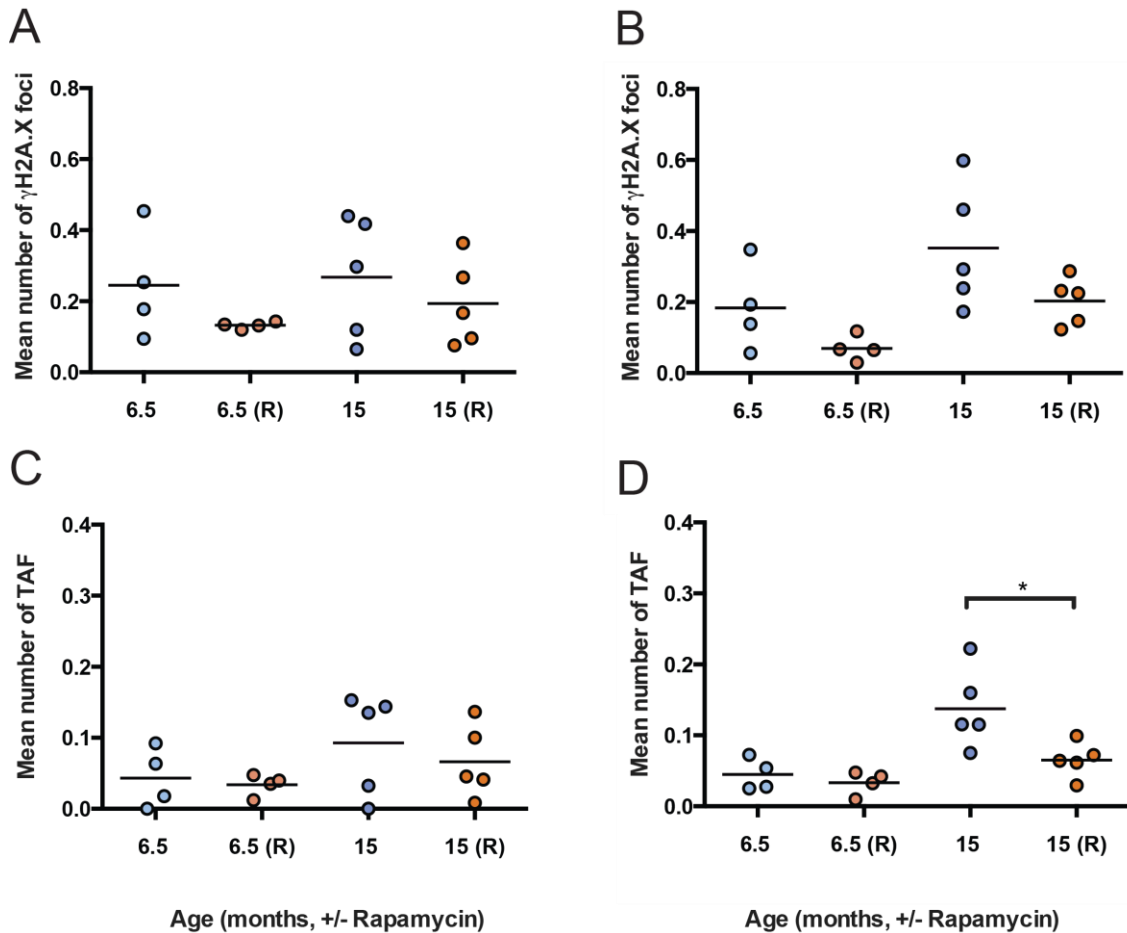
Figure 4.13 Effect of a rapamycin-supplemented diet on DNA damage foci and TAF content in large and small airway epithelial cells of the murine lung. Male *C57BL/6* mice at 3 months of age were fed a control or rapamcin-supplemented diet (R) and sacrificed at either 6.5 or 15 months of age. Immuno-FISH against γH2A.X and telomeres was carried out on sections from the left lung. Dot plots represent mean number of γH2A.X foci in large (**A**) and small (**B**) airway epithelial cells and mean number of telomere-associated foci (TAF) in large (**C**) and small (**D**) airway epithelial cells, generated by quantifying Z-stacks of at least 100 cells per animal. Data are presented as the mean for individual animals with the horizontal line representing group mean. Immuno-FISH staining and imaging was performed in collaboration with Samuel Sharp, a BSc project student in our lab. Statistics: One-way ANOVA and Independent samples t-test *$P < 0.05$.
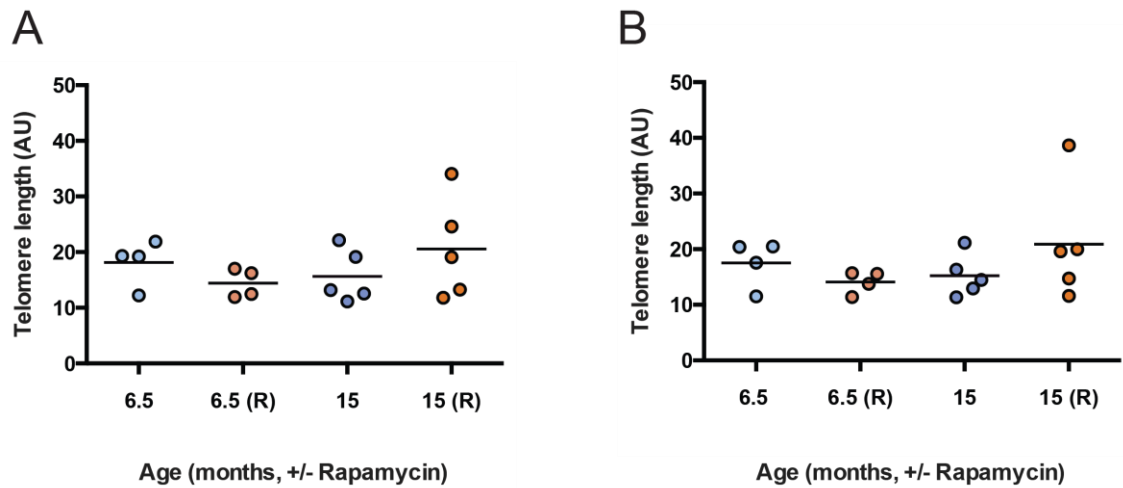
Figure 4.14 Effects of a rapamycin-supplemented diet on telomere length in large and small airway epithelial cells of the murine lung. Male *C57BL/6* mice at 3 months of age were fed a control or rapamcin-supplemented diet (R) and sacrificed at either 6.5 or 15 months of age. Q-FISH analysis was carried out on sections from the left lung. Dot plots represent mean telomere length in large (**A**) and small (**B**) airway epithelial cells, generated by quantifying maximum projections of Z-stack images of at least 100 cells per animal. Data are presented as the mean for individual animals with the horizontal line representing group mean. For all comparisons no statistically significant differences were seen. Statistics: One-way ANOVA and Independent samples t-test. Q-FISH, quantitative-fluorescence *in situ* hybridisation.

4.3.2 mTORC1 inhibition with rapamycin does not significantly affect age-related changes in alveolar airspaces in the murine lung.

To investigate effects of a rapamycin-supplemented diet on alveolar airspace size with age, we carried out H&E staining on lung tissue sections. Ten random images were taken at X20 objective for each tissue section and airspace size was quantified using the MLI method and by manually counting the number of airspaces per visual field, as described previously. Using the MLI method of determining airspace size, we observed no changes following rapamycin treatment at each time point (Figure 4.15A). Similarly, manually counting the number of airspaces revealed no significant changes (Figure 15B).
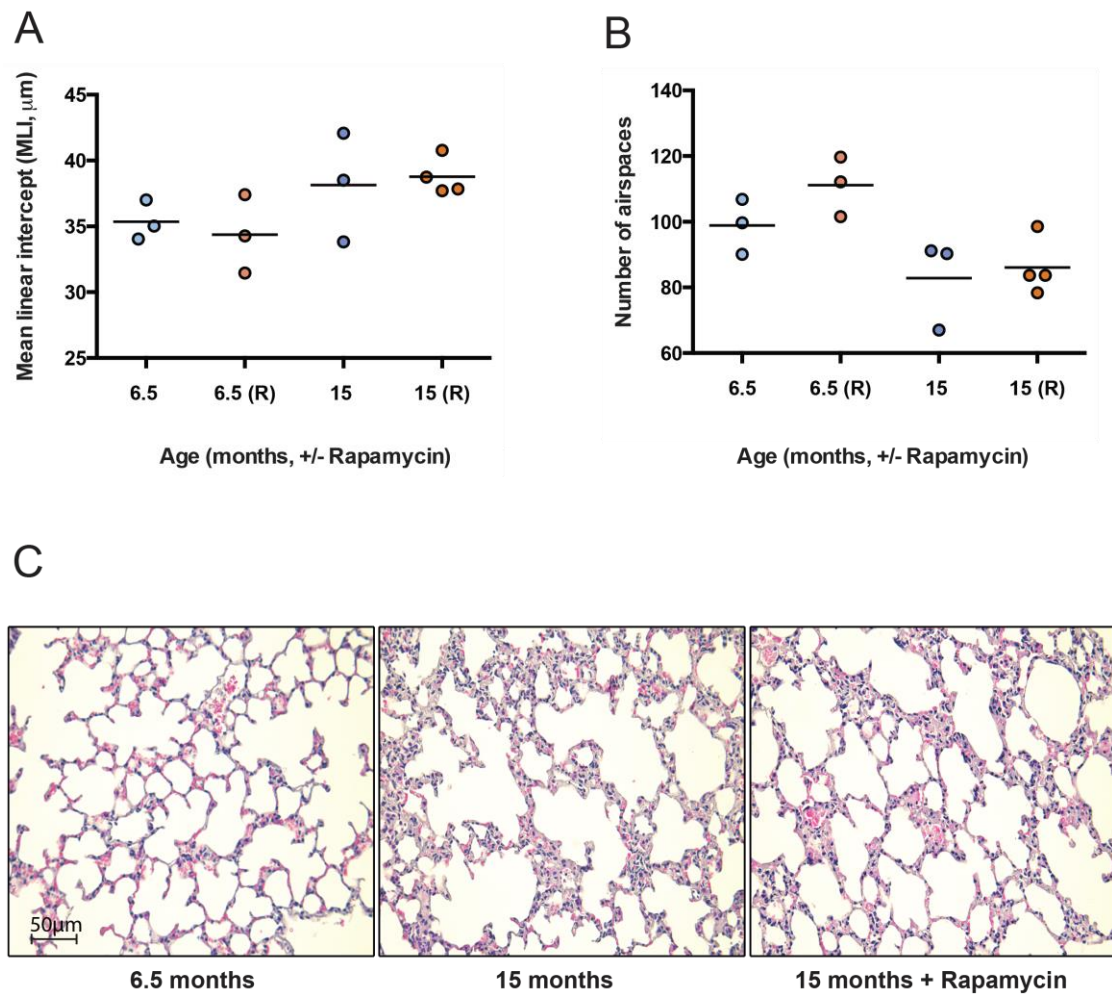
Figure 4.15 Effects of a rapamycin-supplemented diet on alveolar airspace size in the ageing murine lung. Changes in size of alveolar airspaces in the lungs from *C57BL/6* mice fed a control or rapamycin-supplemented diet (R) were assessed by carrying out H&E staining on lung tissue sections from mice in each age group.10 random images were captured for each tissue section using X20 objective and images were analysed using one of two methods. Dot plots represent mean linear intercept (MLI) value (**A**) or the mean number of airspaces (**B**) for individual mice calculated as an average of 10 random images. Horizontal line represents group mean. For all comparisons no statistically significant differences were seen. H&E staining and image analysis was carried out in collaboration with Samuel Sharp. Statistics: One-way ANOVA and Independent samples t-test. H&E, Haematoxylin and Eosin.

4.4 Discussion

Our results show that DNA damage foci (γH2A.X) and TAF age-dependently increase in both large and small airway epithelial cells of the murine lung. These findings corroborate other reports describing increased γH2A.X foci in alveolar epithelial cells of the murine lung with age (Wang, Jurk et al. 2009) and findings from our lab, which demonstrate an age-dependent increase in TAF in the liver and gut of mice (Hewitt, Jurk et al. 2012). Similarly, another study found elevated levels of mH2A, a histone variant present in SAHF, in old (24 month) compared to young (4 month) alveolar epithelial cells of the murine lung (Kreiling, Tamamori-Adachi et al. 2011). A prior study found an increase in γH2A.X foci in mouse lung tissue with age, but rejected the possibility that these foci had a telomeric origin, based on the observation that there was no significant colocalisation of γH2A.X with telomeres in senescent cells *in vitro* (Sedelnikova, Horikawa et al. 2004). Whereas our lab previously found age-related increases in TAF, the number of non-colocalising foci (non-TAF) per cell did not significantly increase with age in these tissues, suggesting that TAF persist and accumulate with age, whereas non-TAF do not (Hewitt, Jurk et al. 2012). We report a significant increase in both colocalising (TAF) and non-colocalising foci (γH2A.X) with age in the large and small airways of the murine lung. However, in all cases we did observe more significant increases in TAF (i.e. a lower p value), which suggests that TAF are a more robust marker for senescence than γH2A.X alone. This is very conceivable, since several groups give evidence which supports that DNA damage at telomeres is irreparable and persistent, therefore potentially preserving the "memory" of the damage accumulated with time (Fumagalli, Rossiello et al. 2012; Hewitt, Jurk et al. 2012). It is unlikely that the observed increase in TAF with age can be explained by telomere shortening, since we found no significant differences in telomere length between mice aged 6.5-24 months, although there was a tendency towards decreasing telomere length with age. Mice have long telomeres and ubiquitously express the enzyme telomerase, hence it was believed that telomere dysfunction did not play a role in cellular senescence in murine tissues (Parrinello, Samper et al. 2003). Our lab previously found no difference in telomere length between TAF and non-TAF in mice intestinal crypts and found a slight increase in telomere length in liver TAF (Hewitt, Jurk et al. 2012). These, coupled with our findings, could suggest that the age-related increase in telomere dysfunction we have observed in the murine lung is independent of telomere length. In accordance, other studies have also described increased senescence

markers with age, without significant telomere shortening. For example, it was shown in hippocampal neurons and liver hepatocytes of baboons that TAF accumulate with age, however telomeres that colocalise with a DDR are not preferentially short (Fumagalli, Rossiello et al. 2012). One study demonstrated an age-related increase in p16 expression in rat kidneys *in vivo*, without significant telomere shortening (Melk, Kittikowit et al. 2003). Interestingly, another study notably reports an inverse correlation between telomere length and lifespan across several mammalian species, which may suggest that longer telomeres are a more probable target for the accumulation of DNA damage (Gomes, Ryder et al. 2011). However, as we did not assess lengths of individual telomeres co-localising or not with DNA damage foci, it is unknown as to whether long or short telomeres are contributing to TAF in this case. In contrast to our findings, Wang and colleagues describe significant telomere shortening with age in mouse intestinal enterocytes (Wang, Jurk et al. 2009). However in this study, a larger age-range (12-42 months) was covered. *C57BL/6* mice have long heterogeneous telomeres, thus it may be difficult to detect subtle changes in telomere length unless extremes of age are compared (Blasco, Lee et al. 1997). Therefore it is possible that we may have detected significant decreases in telomere length had we had access to older mice to include in the analysis. Because mice have long telomeres as compared to humans, it could be that TAF are more relevant to ageing in mice, since longer telomeres may provide a larger area for DNA damage. Whether TAF accumulate in human tissue with age is unknown and in this case, induction of telomere dysfunction could be telomere length-dependent. However, the fact that TAF accumulate in the skin and brains of baboons with age (which are similar to humans in that they have shorter telomeres and lack expression of telomerase), without necessary telomere shortening (Herbig, Ferreira et al. 2006; Jeyapalan, Ferreira et al. 2007; Fumagalli, Rossiello et al. 2012) suggests that TAF are likely to increase in human tissues with age and may be independent of telomere length.

One caveat to this study is that we have not analysed the expression of proliferation markers with age in the murine lung epithelium. γH2A.X staining alone can overestimate frequencies of senescent cells in tissues with high proliferative activity because an active DDR can be initiated by replication stress in dividing cells (Zeman and Cimprich 2014). Therefore, double-staining for γH2A.X and a proliferation marker, such as PCNA or Ki67 should have been conducted. Additionally, some cells containing DNA damage may be repaired or undergo apoptosis, also leading to a possible overestimation of senescent cell number. However, we did evaluate expression

of the CDKi p21 and found that expression increased with age and correlated positively with TAF.

Telomere dysfunction has been associated with increased expression of the CDKi p21 by experiments showing that deletion of p21 prolongs the lifespan of mice with dysfunctional telomeres (Choudhury, Ju et al. 2007). Consistently, we found with increasing age that a greater % of airway epithelial cells stained positive for p21. We document a 16- and 10-fold increase in p21 expression in the large and small airways, respectively, between 6.5 and 24 months of age. Other groups also report increases in p21 in the murine lung and other tissues with age. Krishnamurthy and colleagues report increased expression of p21 mRNA in the lung and other tissues including kidney, uterus and spleen of old (26 months) compared to young (2.5 months) mice, however on average, only a 1.4-fold increase in p21 expression was observed (Krishnamurthy, Torrice et al. 2004). One reason for these discrepancies in our findings could be due to the fact that we analysed protein levels, as opposed to RNA expression, and it could be that p21 expression is upregulated at the translational and post-translational level. The increases we observed in p21 with age, matched those observed for TAF, with no significant changes occurring between 6.5 and 15 months of age in most cases, with significant differences only detected between 15 and 24 months. Mean number of TAF also positively correlated with % p21 expression, suggesting the presence of TAF as a good marker for large and small airway epithelial cell senescence. These findings are in agreement with studies showing that elevation of p21 levels in senescent cells correlate with the accumulation of γH2A.X (Herbig, Wei et al. 2003) and TAF (Herbig, Jobling et al. 2004). On the contrary, telomere length values did not show any correlations with p21 expression. Unfortunately, it was not possible to assess levels of p16 expression in the ageing murine lung. In our hands, it has been technically difficult to get p16 antibodies to work in murine tissue, with other groups in the senescence field reporting similar problems. Ideally the use of RT-PCR to test for mRNA expression of senescence-associated markers, including p21 and p16, should have been carried out on whole tissue lysates. However, this would not be specific to the airway epithelium.

The ageing lung is associated with structural changes similar to those that occur in emphysema, including alveolar dilatation and distal airspace enlargement (Janssens, Pache et al. 1999). We found increases in airspace size (or decreased number of airspaces) in the murine lung with age. Number of airspaces negatively correlated with p21 expression but this was only significant for p21 expression in the small airways. It has been shown that ablation of SIRT1 expression in small airway epithelial cells of the

murine lung aggravates airspace enlargement induced by elastase, due to a lack of protection against development of airway epithelial cell senescence (Yao, Chung et al. 2012). This suggests that small airway epithelial cell senescence may increase susceptibility to stress-induced emphysema. Interestingly, we found that telomere length did not correlate with airspace number, however there was an inverse correlation between mean number of TAF and number of airspaces. To determine whether telomere dysfunction contributes to airspace enlargement, we quantified the number of airspaces in lung tissue sections from *G4 TERC*$^{-/-}$ mice, which have critically short telomeres and increased TAF, as determined in small airway epithelial cells. We found at 6 months of age, that *G4 TERC*$^{-/-}$ mice show a significant reduction in number of airspaces as compared to wild-type controls. In fact, the correlation between TAF and number of airspaces strengthened when *G4 TERC*$^{-/-}$ mice were added, however telomere length still did not correlate with number of airspaces. Contrary to our work, a previous study also using mice null for the RNA component of telomerase at 4th generation report no *de novo* changes in alveolar airspace size as compared to wild-types (Alder, Guo et al. 2011). However, the authors reported surprisingly small differences in telomere length and did not assess telomere dysfunction. In our study, levels of TAF in late *G4 TERC*$^{-/-}$ mice at 6 months were similar to those of wild-types at 24 months of age and telomere length was almost 4-fold shorter. These discrepancies in our findings may be due to difference in technique or strain-specific differences. However, our findings are in concordance with a prior study that identified loss of alveolar integrity in *G4 TERC*$^{-/-}$ mice and this study also reported similar decreases in telomere length to those that we observed (Lee, Reddy et al. 2009). We observed a greater difference in the change in alveolar airspace size than this study reports (2-fold as compared to 1.5-fold). However, this study uses fourth generation wild-type mice that were bred concurrently, to control for effects of inbreeding, whereas we compared to wild-type mice that were not inbred. Thus, the changes in alveolar integrity that we report in *G4 TERC*$^{-/-}$ mice may be overestimated. We have evaluated telomere dysfunction in small airway epithelial cells and found correlations between TAF and airspace size. However, we cannot conclude that dysfunctional telomeres in small airway epithelial cells *per se* are causal to the emphysematous-like changes in the lung in both conditions of stress and with ageing, since telomere dysfunction is global in *TERC*$^{-/-}$ mice. Indeed, we should have investigated whether mean number of TAF in alveolar epithelial cells correlated with number of airspaces, given that alveolar type I and II cells are directly involved in emphysematous-like changes and are therefore likely to be more relevant to these

changes than small airway epithelial cells. Additionally, telomerase has other reported activities, such as protection of mitochondrial function (Ahmed, Passos et al. 2008). Therefore, it is possible that loss of alveolar structural integrity observed in *G4 TERC*^{-/-} mice is caused by mechanisms independent of telomere dysfunction.

A number of studies have shown that cigarette smoke exposure increases senescence-marker expression in the lungs of mice *in vivo* (Tsuji, Aoshiba et al. 2004; Yao, Chung et al. 2012; Yao, Sundar et al. 2013). However, the presence of TAF has not been investigated. We have found that just 2 weeks of cigarette smoke exposure is sufficient to significantly increase both γH2A.X and TAF in the large and small airway epithelial cells of the murine lung. This is in accordance with other studies that have also described increased γH2A.X in the lungs of mice exposed to cigarette smoke in whole tissue lysates (Yao, Sundar et al. 2013) and increased 53BP1 foci in small airway epithelial cells *in situ* (Alder, Guo et al. 2011). In our previous chapter, we found using immunohistochemistry that more markers of senescence were upregulated in the small, as opposed to large airway epithelial cells in the COPD lung, including γH2A.X foci. We observed no obvious differences between the large and small airways of mice exposed to cigarette smoke. The predominance of small airway epithelial cell senescence that we observed in the COPD lung could be a factor of the disease, duration of cigarette smoke exposure or due to differences in breathing technique between mice and humans. Mice are obligatory nasal breathers and so some of the more harmful products that would be inhaled and potentially reach the distal airways of the human lung, may be deposited in the nasal passages of the mice. Additionally, the percentages of different cell subsets that comprise the airway epithelium of the murine lung are different to those that make up the human airway epithelium (Rock, Randell et al. 2010). Therefore the "sensitivities" of the large and small airway epithelial cells to CSE-induced senescence are probably not comparable between the two species. It could be possible that our observations of increased γH2A.X foci and TAF in the airways of mice exposed to cigarette smoke are representative of increased damage, rather than senescence *per se*, since we have not explored other markers of senescence, mainly due to time limitations. However, other studies have shown that senescence markers, such as Sen-β-Gal and p21, are increased in the lungs of mice following 2 weeks of cigarette smoke exposure and following short-term exposures (3 days) (Tsuji, Aoshiba et al. 2004; Yao, Sundar et al. 2013). We did analyse the presence of neutrophils infiltrating lung tissue from mice exposed to cigarette smoke and controls. Similar to previous observations (D'Hulst A, Vermaelen et al. 2005; Doz, Noulin et al. 2008; Nikota, Shen

et al. 2014), we found that cigarette smoke exposure significantly increased the number of neutrophils detected per visual field. We analysed neutrophil number throughout tissue sections and did not focus specifically on the airway compartments. While it is known that cigarette smoke exposure induces acute inflammation, it is still not clear whether senescent cells can be cleared by immune cells or whether senescent cells attract inflammatory cells. Future work would be to determine whether neutrophils are clustered close to senescent cells, or specifically those that contain higher numbers of TAF, and whether interruption of cytokine signalling from the SASP could reduce recruitment of neutrophils. We found no differences in telomere length in mice exposed to cigarette smoke as compared to controls, which coincides with our previous findings of increased TAF, without a necessary decrease in telomere length. However, it could be that after just two weeks of smoke exposure, subtle changes in mean telomere length are difficult to detect (Blasco, Lee et al. 1997). In accordance, another study, also using Q-FISH, failed to detect further shortening of telomeres in small airway epithelial cells of *G4 mTR*^{-/-} mice, following 6 months of cigarette smoke exposure (Alder, Guo et al. 2011). However, it is still possible that minor telomere shortening occurs. There were no obvious changes in alveolar airspace size following cigarette smoke exposure (not shown). However, this was not fully investigated, as many studies have shown that cigarette smoke exposure causes early-onset emphysema in the murine lung, with longer term exposures required for this effect (2-6 months) (Yoshida, Mett et al. 2010; Ganesan, Comstock et al. 2014). Although, there are some studies that show even 6 months of cigarette smoke exposure does not lead to significant airspace disease (Alder, Guo et al. 2011).

To our knowledge, there have been no published studies examining the effects of a rapamycin-supplemented diet on the presence of senescence-associated markers with age in tissues *in situ*. We found a tendency towards decreased γH2A.X and TAF after 3.5 and 12 months of rapamycin treatment in both the large and small airway epithelial cells of the murine lung. However, we only observed statistically significant differences in TAF reduction in small airway epithelial cells following 12 months of rapamycin supplementation. One limitation of our work is that we could only access tissue from mice fed a rapamycin-supplemented diet up to an age of 15 months, despite the majority of senescence-associated markers and age-related changes in the lung only becoming significantly different from young mice at 24 months of age. Therefore, it would be desirable to have included mice at 24 months of age and older. Although, rapamycin-supplementation for 12 months, until 15 months of age, has previously been

shown by our lab to be sufficient to significantly reduce TAF in murine liver hepatocytes *in situ* (unpublished). Despite not reaching statistical significance, our observation of decreased DNA damage foci in rapamycin-fed mice at each time point, and in both large and small airway epithelial cells is still an important one and coincides with previous studies demonstrating the importance of mTORC1 in the maintenance of a DDR *in vivo*. For example, short-term dietary restriction (DR), a known inhibitor of mTOR signalling, in adult mice, significantly reduces the frequencies of γH2A.X foci-positive cells in both intestines and liver and reduces the frequencies of Purkinje cells positive for γH2A.X (Wang, Maddick et al. 2010; Jurk, Wang et al. 2012). In contrast to our findings, one study reports that rapamycin reduces p21 expression in murine lung tissue, as detected by immunoblotting of homogenised tissue, but does not affect expression of the DNA damage/heterochromatin complex marker mH2A and in fact, an increase in mH2A in the lungs of those mice fed a low-dose rapamycin diet was found (Hinojosa, Mgbemena et al. 2012). We did not observe any significant changes in p21 expression in airway epithelial cells of the murine lung following rapamycin treatment (data not shown) and in some cases, we observed a tendency towards increased p21 expression in large and small airway epithelial cells of rapamycin-treated mice. The discrepancies in our findings could be due to the use of different mouse strains and/or different techniques to identify senescence markers. In the study by Hinojosa and colleagues, rapamycin was administered for a similar duration as in ours, however lungs were analysed at 22 months of age and diet was commenced at 9 months, which may also account for some of the differences between our findings. Unpublished data from our lab shows that rapamycin decreases p21 expression in the livers of mice that were harvested from the same cohort we used herein. Interestingly, Krishnamurthy and colleagues report that while DR reduces p16 and p21 expression in several tissues from Fischer 344 rats, there was no attenuation of expression in lung tissue. In fact, although not significant, there was a slight increase in p16 and p21 expression in lung tissue from DR rats (Krishnamurthy, Torrice et al. 2004). Moreover, the genetic overexpression of regulated in development and DNA damage responses (*Redd1*), an inhibitor of mTORC1 signalling, in murine lungs, triggers inflammation, oxidative stress and loss of alveolar integrity and downregulation of Redd1 protects against cigarette smoke-induced lung pathology, such as airspace enlargement (Yoshida, Mett et al. 2010). Furthermore, when authors used rapamycin pretreatment in *Redd1*$^{-/-}$ mice, this protective effect was partially abrogated. Paradoxically, the authors also report that rapamycin protects against acute inflammation induced by cigarette smoke in wild-type

mice (Yoshida, Mett et al. 2010). Therefore, the effects of rapamycin or mTOR inhibition in the lung are somewhat contradictory at present and further research into this area is required. One caveat of our work is that we did not investigate whether rapamycin treatment was decreasing mTORC1 activity, something which should have been confirmed.

A number of studies suggest that because rodents have large telomeres and heavily express telomerase, the signals that induce senescence markers with age are unlikely to be telomere based or telomere shortening may only contribute to cell senescence on a minor scale (Krishnamurthy, Torrice et al. 2004; Wang, Maddick et al. 2010). We observed a tendency towards reduced TAF in the airway epithelial cells of mice fed a rapamycin-supplemented diet and a significant decrease in TAF in the small airway epithelial cells following 12 months rapamycin supplementation. However, despite observing a tendency towards increased telomere length at 15 months of age in those mice fed rapamycin, these observations were not statistically significant. Therefore we believe this reduction in TAF is probably not explained by maintenance of telomere length. Although, there are a number of studies that show DR attenuates age-related telomere erosion. Prior work has shown that long-term DR reduces telomere shortening in various adult mouse tissues, including lung, however these observations were made in alveolar epithelial cells (Vera, Bernardes de Jesus et al. 2013). Similarly, short-term DR, started later in life, also reduces telomere shortening in murine intestinal enterocytes and liver hepatocytes (Wang, Maddick et al. 2010). To our knowledge, there are no studies that have investigated the effects of rapamycin treatment on telomere length *in vivo*.

In summary, we have found that TAF accumulate in the airway epithelial cells of the ageing murine lung and following cigarette smoke exposure. It is possible that TAF are a more robust marker for senescence and may predict loss of lung structural integrity, based on the observation that mice lacking telomerase show early-onset emphysematous-like changes. The preliminary observation that rapamycin appears to have beneficial effects on airway epithelial cell senescence and age-related changes in the lung may suggest that targeting mTORC1 signalling could be of therapeutic benefit in diseases of accelerated lung ageing, such as COPD. Further work is required to elucidate the role of mTOR in lung cellular senescence and in age-related lung disease.

Chapter 5. Cigarette smoke exposure induces telomere dysfunction and cellular senescence

In the preceding chapters, we have shown that DNA damage foci (γH2A.X) and telomere-associated foci (TAF) are increased in small airway epithelial cells from patients with COPD, in the large and small airway epithelium of the ageing murine lung and following cigarette smoke exposure *in vivo*. Cigarette smoking is the greatest risk factor for development of COPD and a number of studies have shown that cigarette smoke exposure induces features of senescence *in vitro* in a range of cell types, including alveolar epithelial cells, lung fibroblasts and bronchial epithelial cells (Tsuji, Aoshiba et al. 2004; Nyunoya, Monick et al. 2006; Hara, Araya et al. 2013; Kanaji, Basma et al. 2014). However, one limitation of most of these studies is that they investigate only the effects of short-term cigarette smoke exposure (48 hours to 14 days). These models, whilst useful for early studies, are models of acute rather than chronic smoke exposure. Moreover, while it has been demonstrated that cigarette smoke exposure leads to increased H2A.X phosphorylation in normal bronchial epithelial cells and human immortalised stromal fibroblasts (Albino, Huang et al. 2004; Salem, Al-Zoubi et al. 2013), the role of telomere dysfunction, specifically the presence of a DDR at telomeres, in cigarette smoke-induced senescence has not been investigated.

The aim of this work was to determine whether long-term cigarette smoke exposure induces telomere dysfunction and consequently other hallmarks of senescence *in vitro*.

5.1 Long-term cigarette smoke exposure induces hallmarks of senescence

In order to determine whether chronic cigarette smoke exposure induces features of senescence *in vitro*, normal human lung fibroblasts (MRC5) at a population doubling (PD) of 25 were exposed to cigarette smoke extract (CSE) at 5% concentration every 48 hours until replicative senescence was reached (around 60 days in culture). At certain stages of the passaging process, cells were analysed for several senescence-associated markers. MRC5 cells were chosen for long-term experiments, as opposed to airway epithelial cells, which would complement the *in vivo* data, due to the fact that prolonged culturing of airway epithelial cells and exposure to cigarette smoke induces EMT in these cells.

5.1.1 Cigarette smoke exposure reduces MRC5 cell proliferation in vitro

MRC5 cells, treated with 5% CSE or normal DMEM (untreated controls), were passaged when cells were around 70% confluent. With each cell passage, cell counts were carried out and PD number calculated as described in Materials and Methods. Initially both CSE-exposed and untreated cells replicated at the same rate, however exposure to 5% CSE induced cellular senescence in MRC5 cells at an earlier time point, evidenced by reduced population doublings as compared to untreated controls (Figure 5.1A). Additionally, expression of the proliferation marker Ki67 was reduced at all time points in cells treated with 5% CSE, however these differences were only significant at day 24 ($p = 0.05$) (Figure 5.1 B and C). Initial viability experiments revealed no significant cell death. Viability was tested 24 hours following initial exposure, using propidium iodide (PI) staining coupled with flow cytometry, which showed that while 5% CSE exposure caused some cell death, viability always remained above 70%, with a mean viability of 80% achieved for untreated cells (n = 3 samples from two independent experiments) (data not shown).
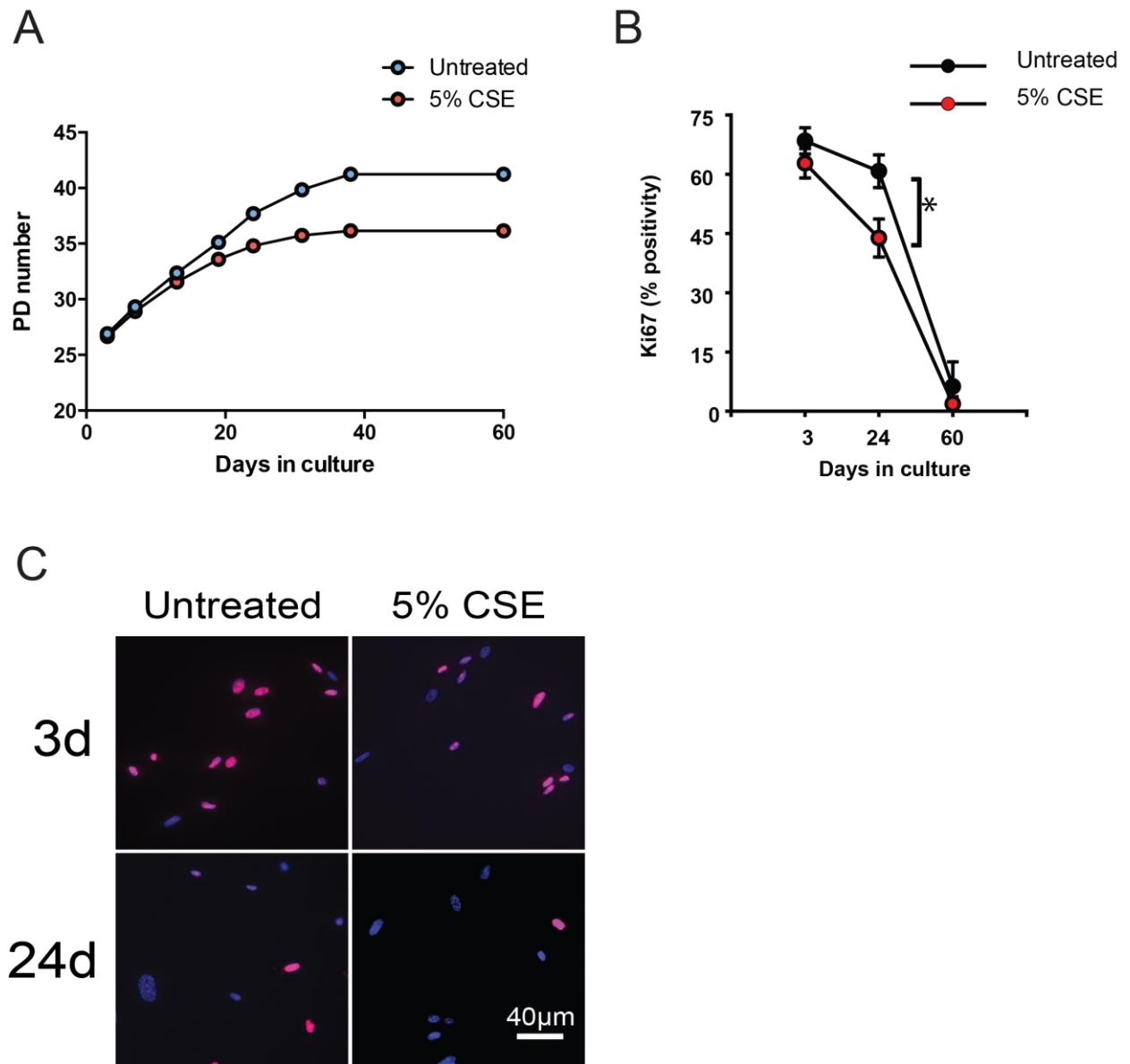
Figure 5.1 Effect of long-term cigarette smoke exposure on growth of MRC5 fibroblasts. MRC5 cells exposed to 5% cigarette smoke extract (CSE) or normal cell culture media every 48 hours were subjected to repeated passaging and cell number counted with each passage. Population doubling (PD) level was calculated for each condition and is plotted against number of days in culture (**A**). Graph A was generated from one experiment and confirmed by an independent experiment (data not shown). Expression of the proliferation marker Ki67 was analysed at a range of time points by immunofluorescence. (**B**) Quantification of Ki67 expression, representative of one experiment; points are mean % Ki67 positivity ± S.E.M of at least 20 random planes. Similar changes in Ki67 expression were confirmed in an independent experiment (not shown). (**C**) Representative images of Ki67 staining (*red*) with DAPI (*blue*) as a nuclear counterstain in MRC5 cells at 3 and 24 days in culture in the presence or absence of 5% CSE. Analysis of Ki67 expression by immunofluorescence was performed in collaboration with Francisco Marques in our lab. Statistics: Two-way ANOVA followed by multiple Independent samples t-test *$P < 0.05$.

5.1.2 Cigarette smoke exposure induces telomere dysfunction in vitro

In order to evaluate DNA damage foci and telomere dysfunction in MRC5 cells exposed to 5% CSE, we performed telomere-specific quantitative fluorescence *in situ* hybridisation (Q-FISH), combined with immunofluorescence against γH2A.X (immuno-FISH) on cells fixed at a range of time points from 3-60 days in culture. Analysis revealed a tendency towards an increase in the mean number of γH2A.X foci per cell in cells exposed to cigarette smoke, which was statistically significant after 24 days in culture ($p = 0.007$) but was no longer significant after 60 days in culture ($p = 0.8$) (Figure 5.2A). Analysis of γH2A.X foci associated with telomeres (TAF) revealed a tendency towards increased TAF in cells exposed to CSE at most time points (Figure 5.2B), however these increases were only significant at day 24 ($p = 0.002$) and day 60 in culture ($p = 0.02$). Analysis of % of cells containing TAF revealed significant differences between CSE-exposed and untreated cells at all time points, except following 60 days in culture where all cells were positive for TAF (Figure 5.2C).
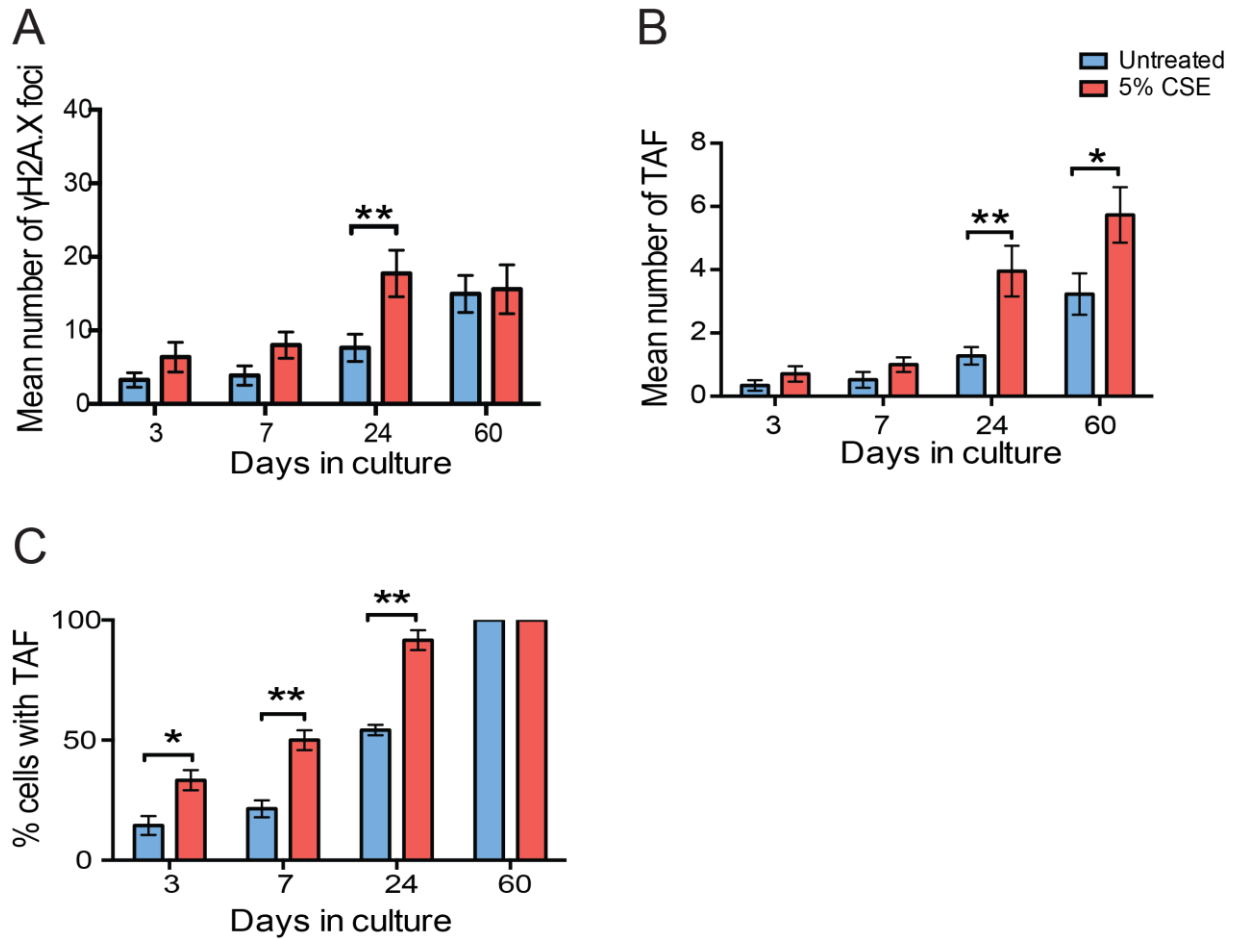
Figure 5.2 DNA damage foci and telomere-associated foci in MRC5 cells in the presence or absence of cigarette smoke. MRC5 cells exposed to 5% cigarette smoke extract (CSE) or normal cell culture media every 48 hours were cultured until replicative senescence and analysed at a range of time points for γH2A.X foci and telomere-associated foci (TAF) by immuno-FISH. Bar graphs represent the mean number of γH2A.X foci per cell (**A**), the mean number of TAF per cell (**B**) and percentage of cells containing TAF (**C**) from one experiment. Data are presented as mean ± S.E.M of 50 cells per condition, generated by quantifying Z-stack images. An independent experiment showed similar results (not shown). Statistics: Two-way ANOVA followed by multiple Independent samples t-test *$P < 0.05$, **$P < 0.01$.
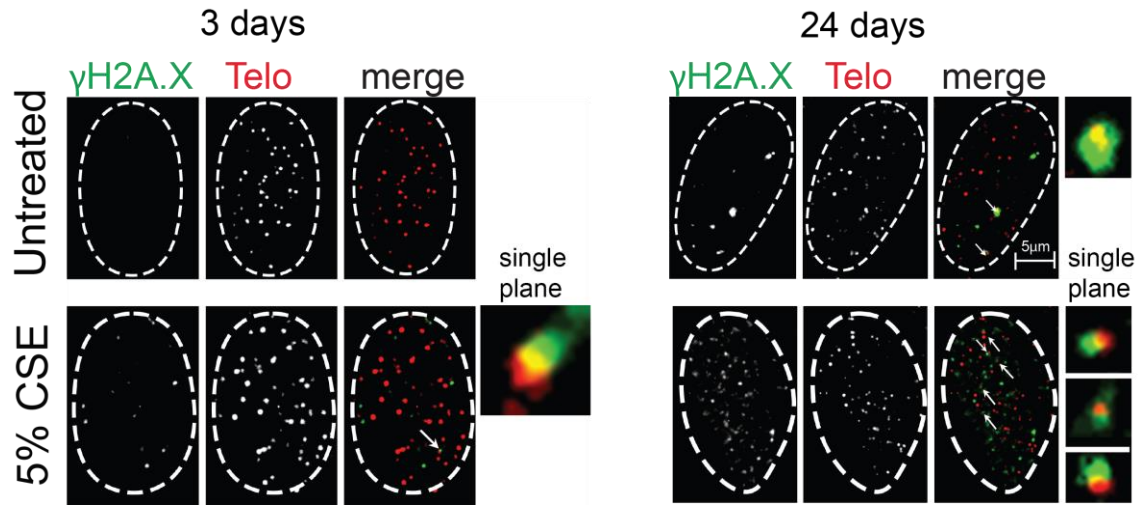
Figure 5.3 Representative images of immunostainings for DNA damage foci and telomere-associated foci in MRC5 cells in the presence or absence of cigarette smoke. Representative image of immuno-FISH for γH2A.X *(green)* and telomeres *(red)* in MRC5 cells at 3 and 24 days in culture in the presence or absence of 5% CSE captured using X100 oil objective and following Huygens (SVI) deconvolution. Arrows point to γH2A.X foci co-localising with telomeres (TAF), shown at higher magnification on the right (images are from one single Z-plane).

Increased cellular volume and increased nuclear size have been described in senescent cells (Bayreuther, Rodemann et al. 1988). Therefore nuclear area of cells exposed to CSE and untreated controls was analysed by DAPI staining. While we observed an increase in nuclear area with time spent in culture for both conditions, there were no significant differences observed between smoke-exposed and untreated cells (Figure 5.4A). Additionally, cells were analysed for expression of the senescence-associated marker Sen-β-Gal. No expression could be detected in either control or smoke-exposed cells until day 24, where cells exposed to 5% CSE had an increased percentage of Sen-β-Gal positive cells (p = 0.0003). This difference in expression of Sen-β-Gal was no longer observed when cells reached replicative senescence (Figure 5.4B).

In order to determine whether cigarette smoke exposure also induced telomere dysfunction in small airway epithelial cells *in vitro*, primary human small airway epithelial cells were exposed to 5% CSE. Cells were exposed to CSE (two exposures, 48 hours apart) or to normal cell culture media and were fixed 24 hours following the final exposure. Immuno-FISH analysis revealed an increase in mean number of γH2A.X foci per cell in those cells exposed to CSE, however this was not statistically significant (p = 0.057) (Figure 5.5A). However, there was a significant increase in mean number of TAF in cells exposed to CSE (p = 0.04) (Figure 5.5B). Interestingly, not all cells analysed had significant increases in TAF, suggesting that patient-specific differences in response to cigarette smoke exposure may occur (Figure 5.5C). There were no significant differences in telomere length between untreated and smoke-exposed cells (p = 0.2). Sen-β-Gal staining revealed low levels of positivity in both untreated and CSE-exposed cells (less than 5%). No significant differences in positive staining were observed between untreated and CSE exposed small airway epithelial cells when compared as a group (p = 0.6) (Figure 5.7A), suggesting that 48 hours exposure is too short to induce Sen-β-Gal activity. However, comparisons between untreated and smoke exposed cells isolated from the same subject revealed slight, but significant, increases in Sen-β-Gal positivity for two subjects (Figure 5.7B), suggesting that induction of Sen-β-Gal may also be subject-dependent.
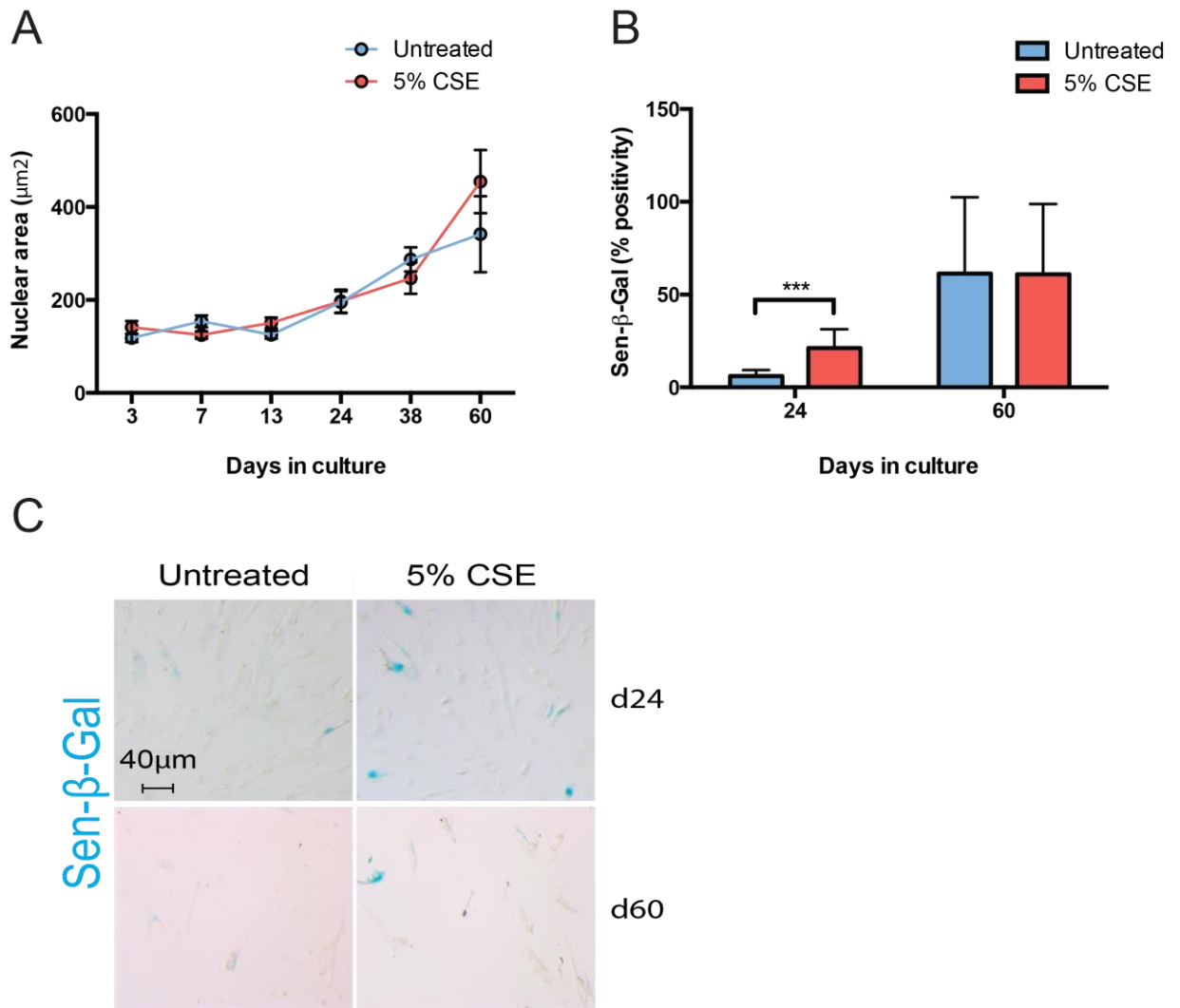
Figure 5.4 Nuclear area and Sen-β-Gal positivity in MRC5 cells cultured in the presence or absence of cigarette smoke. MRC5 cells exposed to 5% cigarette smoke extract (CSE) or normal cell culture media every 48 hours were cultured until replicative senescence and nuclear size measured at a range of time points following DAPI staining. (**A**) Changes in nuclear size over time generated from one experiment. Data are presented as mean ± S.E.M of 50 cells per condition. An independent experiment showed the same pattern (not shown). (**B**) Sen-β-Gal positivity in cells exposed to 5% CSE and untreated controls. Data are presented as mean + SD of at least 10 random planes and are representative of one experiment. An independent experiment confirmed these findings (not shown). (**C**) Representative images of Sen-β-Gal staining in CSE exposed and untreated cells following 24 and 60 days in culture, captured using X20 objective. Sen-β-Gal staining was carried out in collaboration with Clara Correia Melo from our lab. Statistics: Two-way ANOVA followed by multiple Independent samples t-test ***$P < 0.001$.
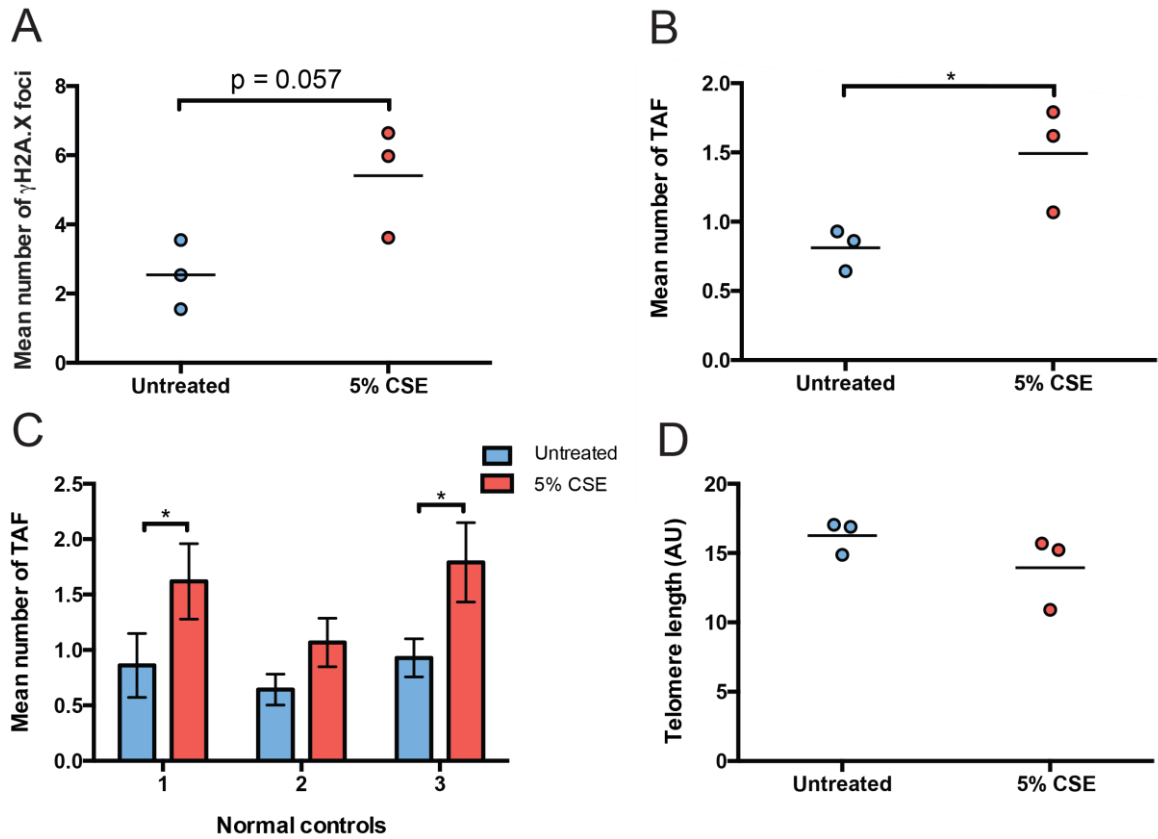
Figure 5.5 DNA damage foci and telomere-associated foci in small airway epithelial cells exposed to cigarette smoke *in vitro*. Primary human small airway epithelial cells isolated from the lung during research bronchoscopy (passage 1-2) were exposed to 5% CSE (two exposures, 48 hours apart) or normal cell culture media (untreated control) and fixed 24 hours following the final exposure. Cells were analysed for γH2A.X foci and telomere-associated foci (TAF) content by immuno-FISH. Dot plots represent the mean number of γH2A.X foci per cell (**A**) and the mean number of TAF per cell (**B**) in small airway epithelial cells exposed to 5% CSE or normal media, generated by quantifying Z-stacks of at least 50 cells per subject. Data are presented as the mean for individual subjects with the horizontal line representing group mean. (**C**) Bar graph showing mean number of TAF per cell for each individual subject when cells were exposed to 5% CSE or left untreated. Data are presented as mean ± S.E.M of 50 cells per condition. (**D**) Dot plot representing telomere length for each subject when cells are left untreated or exposed to 5% CSE. Data are presented as the mean for individual subjects with the horizontal line representing group mean. Statistics: One-way ANOVA and Independent samples t-test *$P < 0.05$.
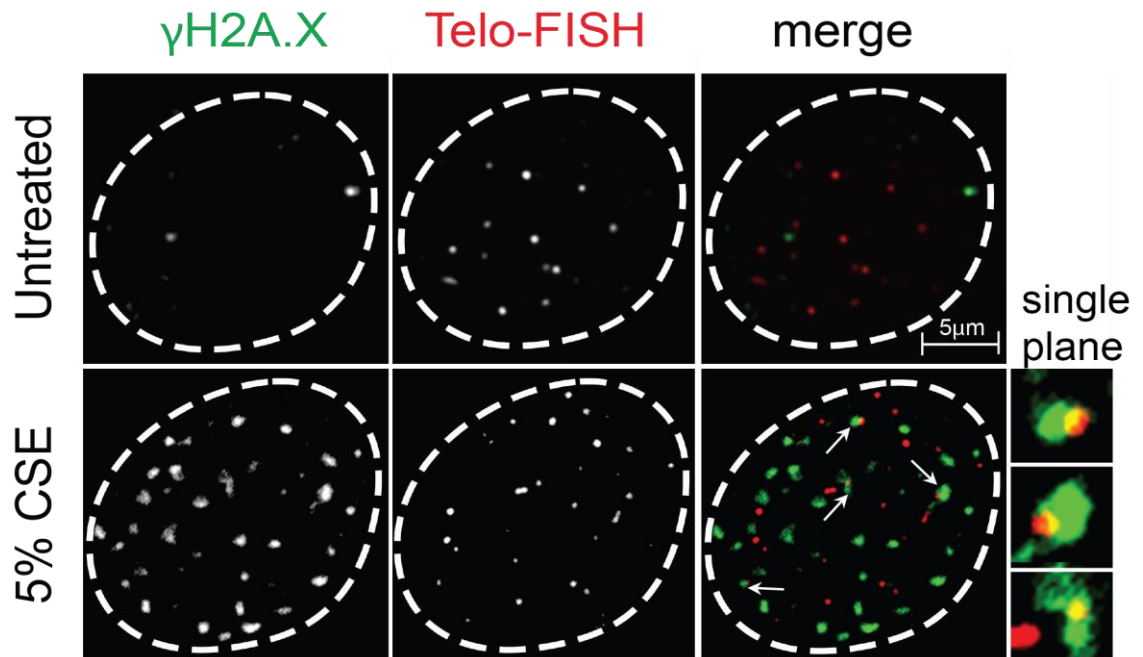
Figure 5.6 Representative images of immunostainings for DNA damage foci and telomere-associated foci in small airway epithelial cells exposed or not to cigarette smoke. Representative image of immuno-FISH for γH2A.X *(green)* and telomeres *(red)* in small airway epithelial cells exposed to CSE or untreated, captured using X100 oil objective and following Huygens (SVI) deconvolution. Arrows point to γH2A.X foci co-localising with telomeres (TAF), shown at higher magnification on the right (images are from one single Z-plane).
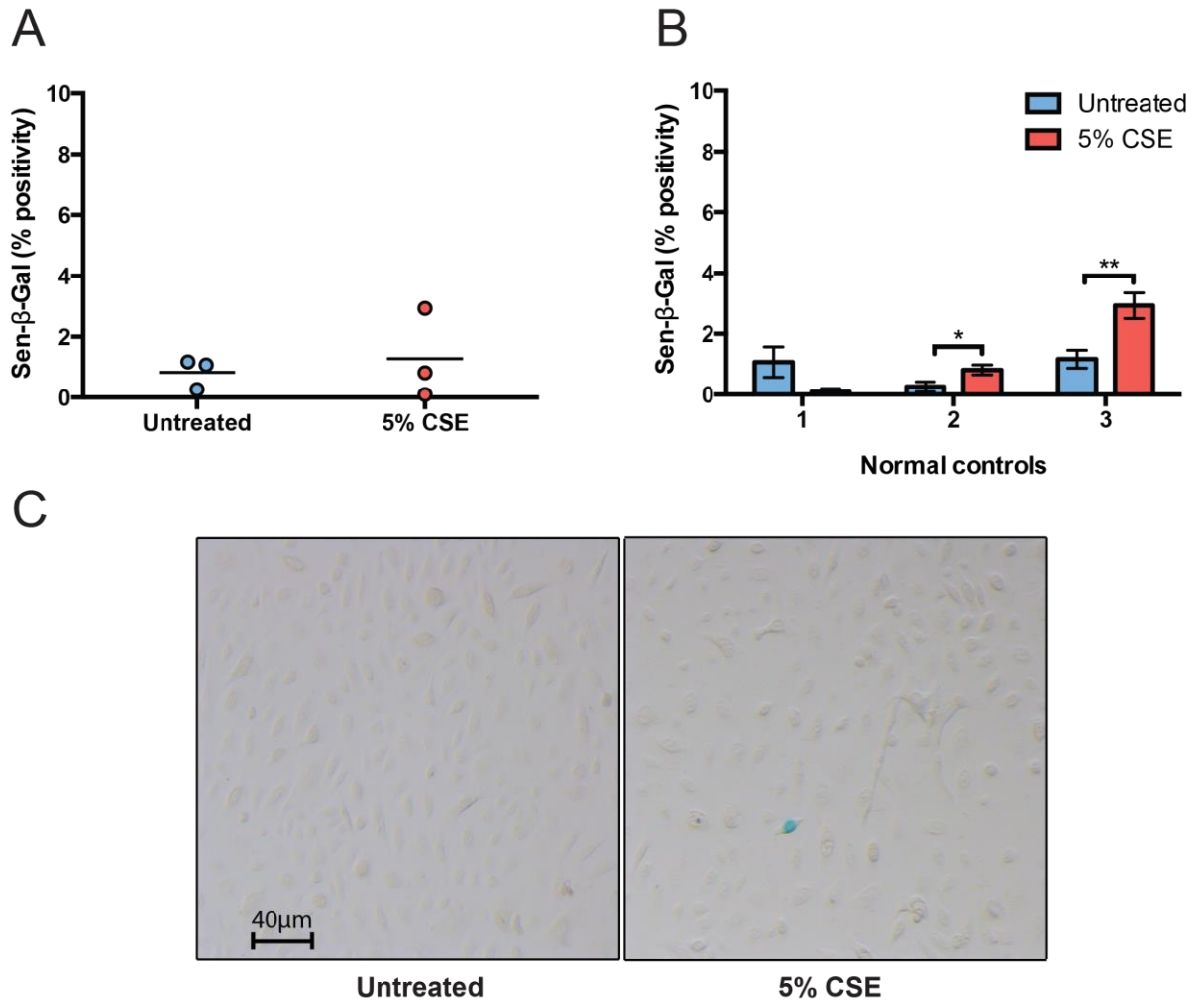
Figure 5.7 Sen-β-Gal positivity in small airway epithelial cells exposed to cigarette smoke *in vitro*. Primary human small airway epithelial cells isolated from healthy volunteers during research bronchoscopy (passage 1-2) were exposed to 5% CSE (two exposures, 48 hours apart) or normal cell culture media (untreated control) and fixed 24 hours following the final exposure. Cells were stained for senescence-associated-β-galactosidase (Sen-β-Gal) activity. **(A)** Dot plot representing percentage positivity for Sen-β-Gal staining, generated by quantifying at least 10 random fields per subject. Data are presented as the mean for individual subjects with the horizontal line representing group mean. **(B)** Bar graph showing Sen-β-Gal levels (percentage positivity) for each individual subject when cells were exposed to 5% CSE or left untreated. Data are presented as mean ± S.E.M of at least 10 random planes. **(C)** Representative image of Sen-β-Gal staining in small airway epithelial cells exposed to CSE or untreated, captured using X20 objective. Sen-β-Gal staining was carried out in collaboration with Clara Correia Melo from our lab Statistics: One-way ANOVA and Independent samples t-test $*P < 0.05$, $** P < 0.01$.

5.1.3 Cigarette smoke exposure promotes SASP factor release in vitro

In order to determine whether long-term cigarette smoke exposure promotes SASP factor release from MRC5 cells, conditioned media was harvested from cells at all time points. For technical reasons, we were unable to harvest media from cells that had been cultured until 60 days, therefore our last time point was 38 days. We first conducted an array analysis of 20 pro-inflammatory mediators. Of all mediators analysed only IL-6, IL-8, vascular endothelial growth factor (VEGF), growth regulated oncogene (GRO) and monocyte chemotactic protein 1 (MCP-1) were upregulated following 5% CSE exposure for 38 days (Figure 5.8A and B). However, only IL-6 (p = 0.03) and IL-8 (p = 0.01) secretion were significantly increased. Most other cytokines or growth factors analysed were secreted below detection level. Since IL-6 and IL-8 release were significantly increased, we conducted ELISAs for IL-6 and IL-8 detection at all time points, which independently confirmed the findings of the cytokine array (Figure 5.8C and D). The rise in cytokine secretion following CSE exposure was evident at all time points, however differences only became statistically significant after 13 days in culture, which became enriched after 38 days. We also observed increasing concentrations of cytokine release in untreated MRC5 fibroblasts with increasing PD, consistent with the onset of replicative senescence (not shown).
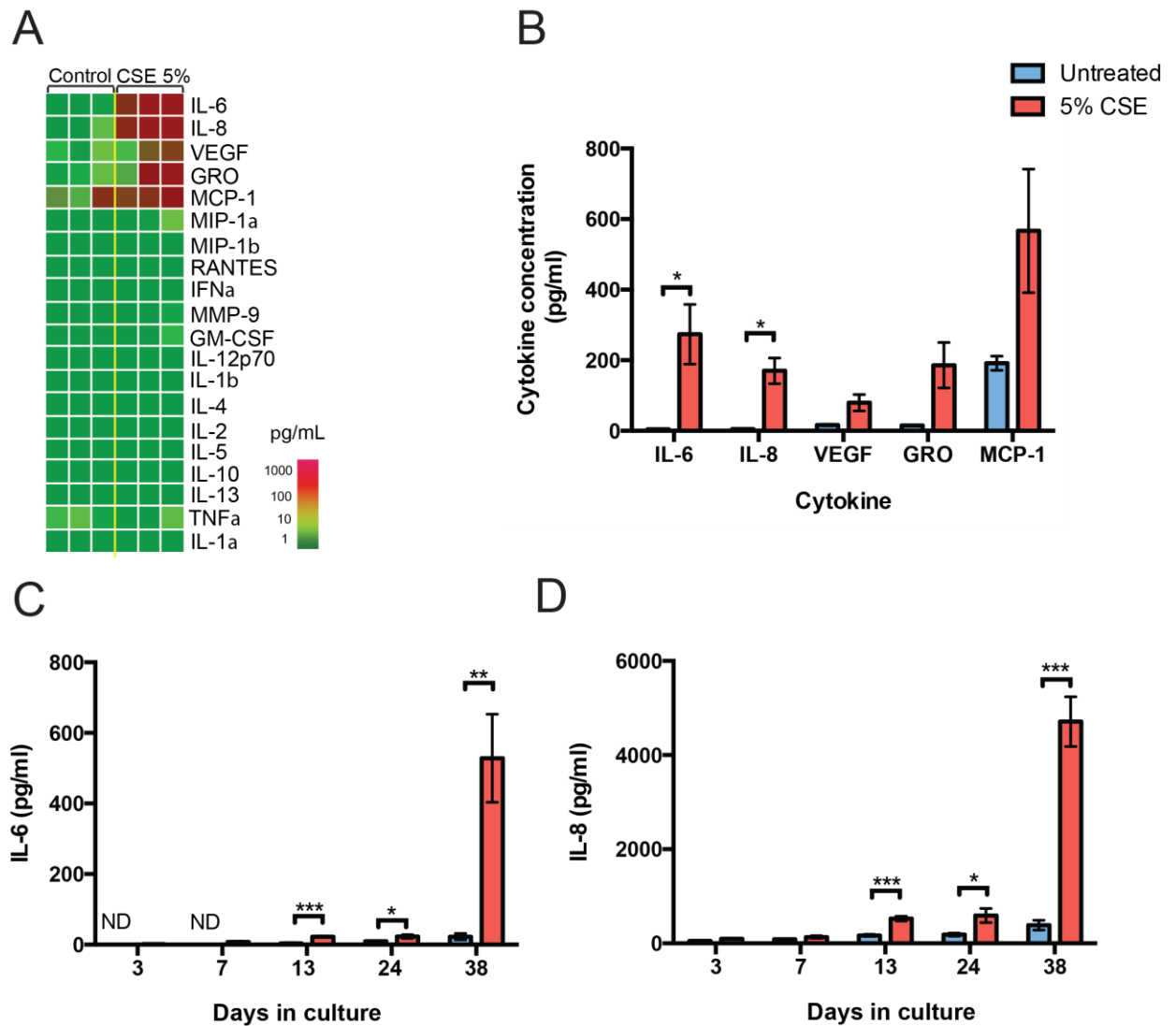
Figure 5.8 Effect of long-term cigarette smoke exposure on cytokine release from MRC5 cells. MRC5 cells exposed to 5% cigarette smoke extract (CSE) or normal cell culture media every 48 hours were cultured until replicative senescence and conditioned media collected at a range of time points and analysed for the presence of pro-inflammatory cytokines. Cells were serum starved 24 hours prior to media collection. (**A**) Secreted protein array (RayBiotech) of a variety of inflammatory proteins 38 days following 5% CSE exposure, colour coded according to levels of protein detected for each pro-inflammatory mediator. (**B**) Bar graph representing concentrations of those pro-inflammatory mediators detected by protein array. Data are mean ± S.E.M of 3 independent experiments. Bar graph representing concentrations of IL-6 (**C**) and IL-8 (**D**) in cell culture media from MRC5 cells exposed to 5% CSE or untreated media measured by ELISA. Data are presented as mean ± SEM of 4 independent experiments. Statistics: Two-way ANOVA followed by multiple Independent samples t-test *$P < 0.05$, **$P < 0.01$, ***$P < 0.001$.

5.2 ROS-dependent telomere dysfunction may be involved in cigarette smoke-induced senescence

Mechanistically, it is still unclear how CSE induces telomere dysfunction. Evidence suggests that oxidative stress is likely to be involved in the induction and maintenance of senescence and a number of studies have shown that ROS can directly damage DNA, inducing a DDR and cellular senescence (Chen, Fischer et al. 1995; Rai, Onder et al. 2009). Telomeres are highly sensitive to oxidative stress compared to the bulk of the genome (Petersen, Saretzki et al. 1998). This is possibly due to the fact that telomere repeats contain guanine triplets, which are remarkably susceptible to oxidative modifications (Henle, Han et al. 1999). In accordance, mild-oxidative stress has been shown to accelerate telomere shortening, whereas overexpression of anti-oxidant enzymes, the use of free-radical scavengers and low oxygen have been shown to extend replicative lifespan and reduce telomere shortening rates in human fibroblasts by decreasing ROS generation (von Zglinicki 2002; Serra, von Zglinicki et al. 2003; Richter and von Zglinicki 2007). Oxidative stress has been implicated in the pathogenesis of COPD. Patients with COPD show increased markers of oxidative stress both systemically and in the lung, as well as imbalanced antioxidant defence (Rahman, van Schadewijk et al. 2002; Igishi, Hitsuda et al. 2003; Houben, Mercken et al. 2009; Caramori, Adcock et al. 2011). Additionally, exposure to cigarette smoke has been shown to increase markers of oxidative stress in the lungs of mice *in vivo* and in human lung fibroblasts *in vitro* (Aoshiba, Koinuma et al. 2003; Deslee, Adair-Kirk et al. 2010). Therefore it is possible that TAF are induced by oxidative stress generated by exposure to cigarette smoke.

To determine whether telomere dysfunction, in the context of cigarette smoke-induced senescence, was caused by oxidative stress, MRC5 fibroblasts were cultured under conditions of low (3% O_2) or normal (20% O_2) oxygen pressure and exposed to 5% CSE or normal cell culture media every 48 hours for 25 days (Figure 5.9A). We found that low oxygen pressure increased MRC5 cell proliferation, evidenced by a higher cumulative cell number being reached as compared to cells cultured under 20% O_2 (Figure 5.9B and C). Similarly, the difference in number of cells between those exposed to CSE and untreated controls was supressed when cells were cultured under 3% O_2.

Consistent with a causal role for oxidative stress in induction of telomere dysfunction, we found by immuno-FISH that low oxygen pressure was able to supress CSE-induced increases in TAF (Figure 5.10B). As shown previously, 5% CSE

increased mean number of γH2A.X foci per cell (p = 0.018) and this increase was reduced slightly when cells were cultured at 3% O_2, but this was not statistically significant (p = 0.1) (Figure 5.10A). However, the increase in TAF observed following CSE exposure (p = 0.015) was significantly reduced when cells were cultured at low oxygen pressure (p = 0.02).

Analysis of Sen-β-Gal expression revealed that 5% CSE exposure increased the percentage of cells positive for Sen-β-Gal at 20% O_2 (p = 0.001), as shown previously. However, cultivation of cells at 3% O_2 drastically reduced frequencies of Sen-β-Gal positive cells to undetectable levels, in both cells cultured with normal media and 5% CSE (Figure 5.11A).

Telomere-dysfunction and resulting DDR activation result in increased expression of IL-6 and IL-8 (Rodier, Coppe et al. 2009). To determine whether ROS contribute to development of the SASP, ELISAs were carried out for detection of IL-6 and IL-8 in cell culture media from MRC5 cells cultured at normal and low oxygen pressure exposed, or not, to CSE. As previous, we found that 25 days of exposure to 5% CSE lead to increased release of IL-6 (p = 0.03) (Figure 5.12A), with cultivation at 3% O_2 reducing levels of IL-6 release in both untreated cells (p = 0.0002) and cells exposed to 5% CSE (p = 0.016) (Figure 5.12A). Similarly, we found that exposure to 5% CSE lead to increased release of IL-8 (p = 0.006) with cultivation at 3% O_2 both decreasing release of IL-8 from untreated cells (p = 0.0002) and cells exposed to CSE (p = 0.0009) (Figure 5.12B).

In order to determine whether CSE exposure led to increased ROS and mitochondrial-derived ROS, we measured intracellular ROS levels (measured by DHR fluorescence) and levels of mitochondrial-derived superoxide production (measured by MitoSOX fluorescence). CSE increased intracellular ROS levels, which was suppressed when culturing cells under 3% O_2 (Figure 5.13A). Increases in mitochondrial-derived ROS observed when cells are treated with 5% CSE were also reduced when cells were cultured at 3% O_2 (Figure 5.13B).
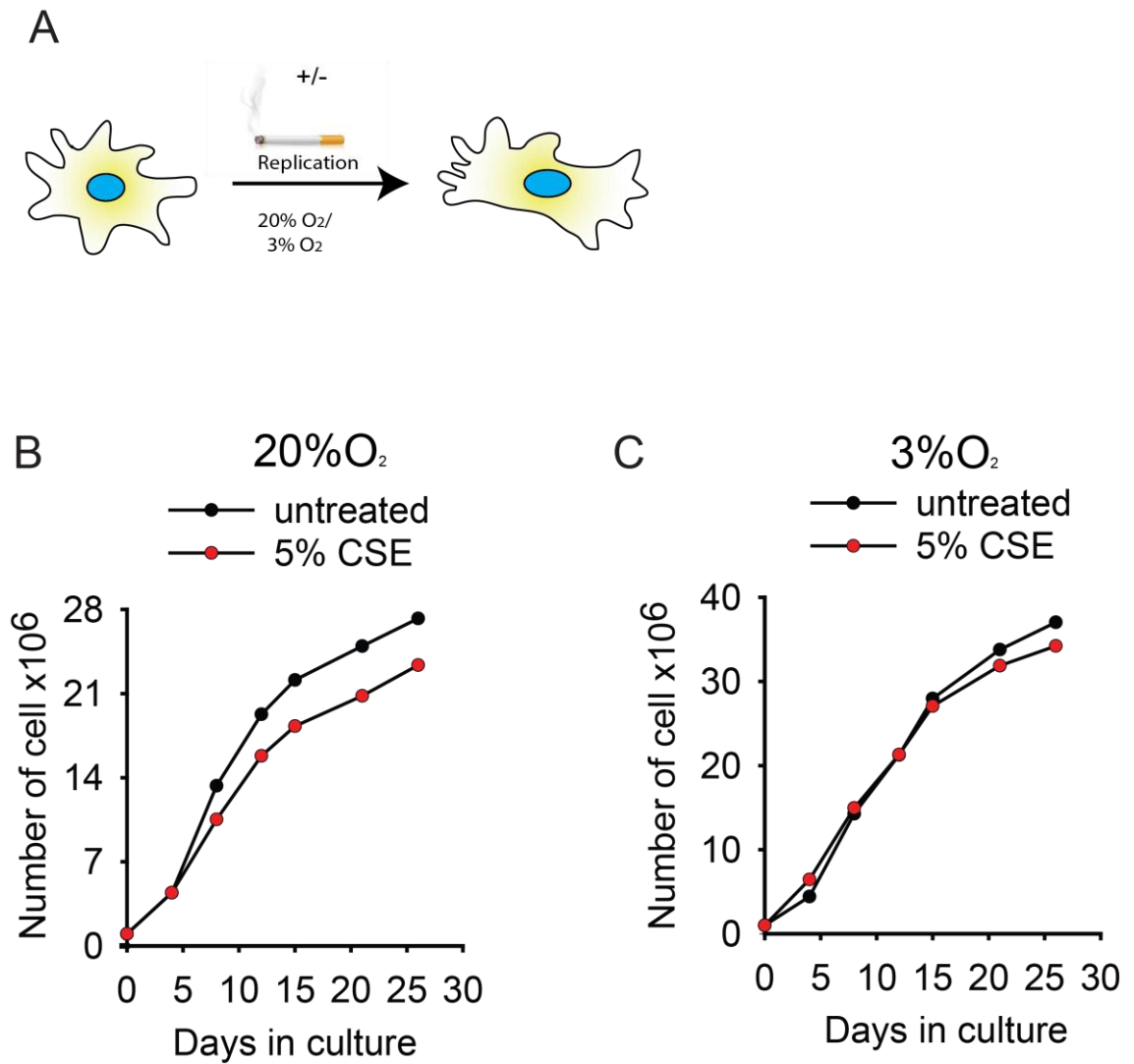
Figure 5.9 Effect of oxygen pressure and cigarette smoke exposure on growth of MRC5 fibroblasts. MRC5 cells (PD 25) cultured under normoxia (20% O_2) or hypoxia (3% O_2) were exposed to 5% cigarette smoke extract (CSE) or normal cell culture media every 48 hours for 25 days (**A**). With every cell passage, cell number was quantified and is plotted against days in culture (**B** and **C**). Graphs are generated from one experiment.
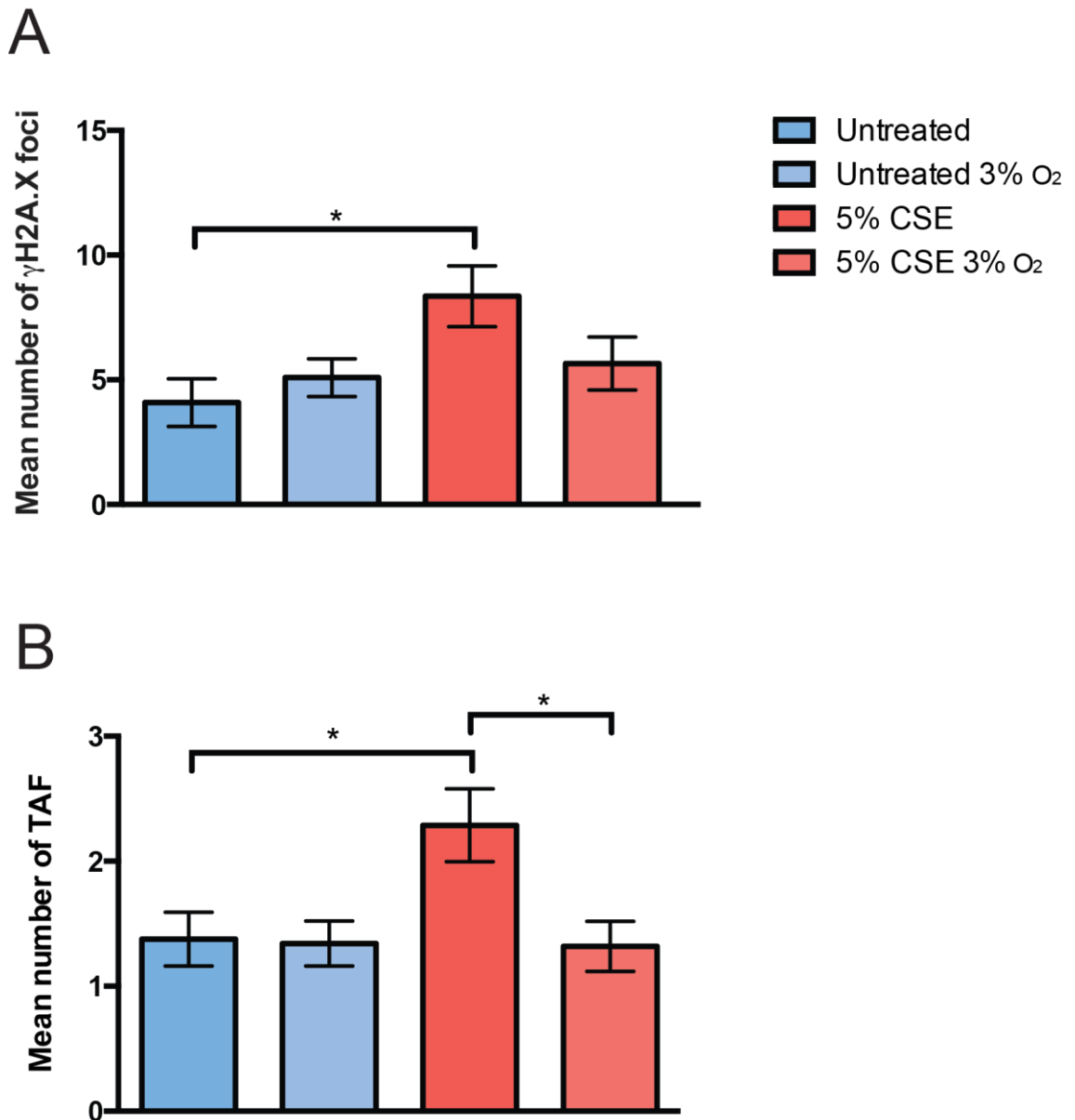
Figure 5.10 Effect of oxygen pressure on cigarette smoke-induced DNA damage foci and telomere-associated foci in MRC5 cells. MRC5 cells cultured under 3% O_2 or 20% O_2 were exposed to 5% cigarette smoke extract (CSE) or normal cell culture media every 48 hours for 25 days and γH2A.X foci and telomere-associated foci (TAF) expression evaluated by immuno-FISH. Bar graphs represent the mean number of γH2A.X foci per cell (**A**) and the mean number of TAF per cell (**B**) from one experiment. Data are presented as mean ± S.E.M of 50 cells per condition, generated by quantifying Z-stack images. Statistics: One-way ANOVA followed by Independent samples t-test *$P < 0.05$.
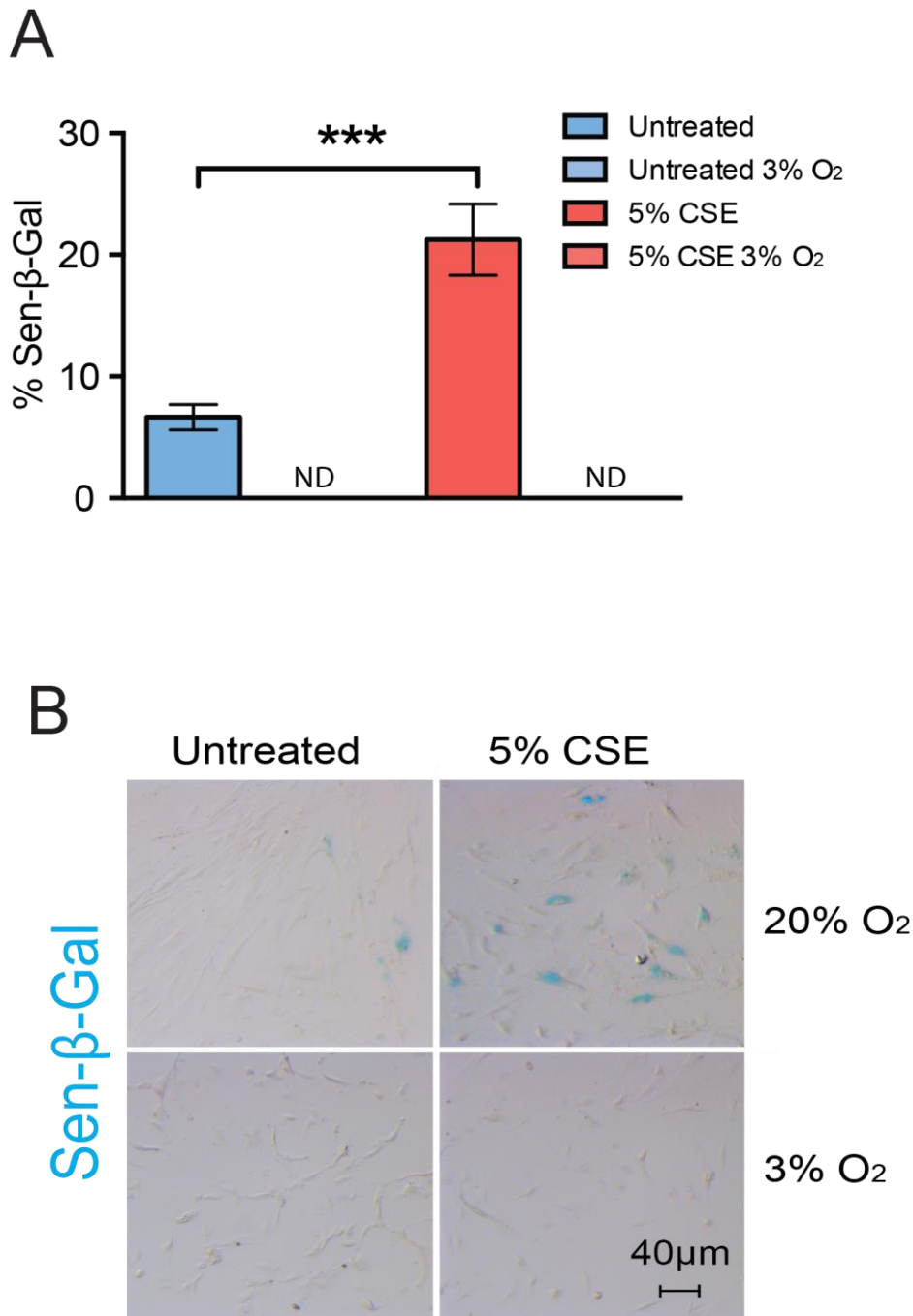
Figure 5.11 Effect of oxygen pressure and cigarette smoke exposure on Sen-β-Gal expression in MRC5 cells. MRC5 cells cultured under 3% O_2 or 20% O_2 were exposed to 5% cigarette smoke extract (CSE) or normal cell culture media every 48 hours for 25 days and stained for senescence-associated-β-galactosidase (Sen-β-Gal) expression. (**A**) Bar graph represents Sen-β-Gal expression (percentage positivity) per condition from one experiment. Data are presented as mean ± S.E.M of 10 random planes per condition. (**B**) Representative image of Sen-β-Gal staining in MRC5 cells exposed to CSE or normal cell culture media and cultured at 3% O_2 or 20% O_2, captured using X20 objective. Sen-β-Gal staining was carried out in collaboration with Clara Correia Melo from our lab. Statistics: One-way ANOVA and Independent samples t-test *** $P < 0.001$.
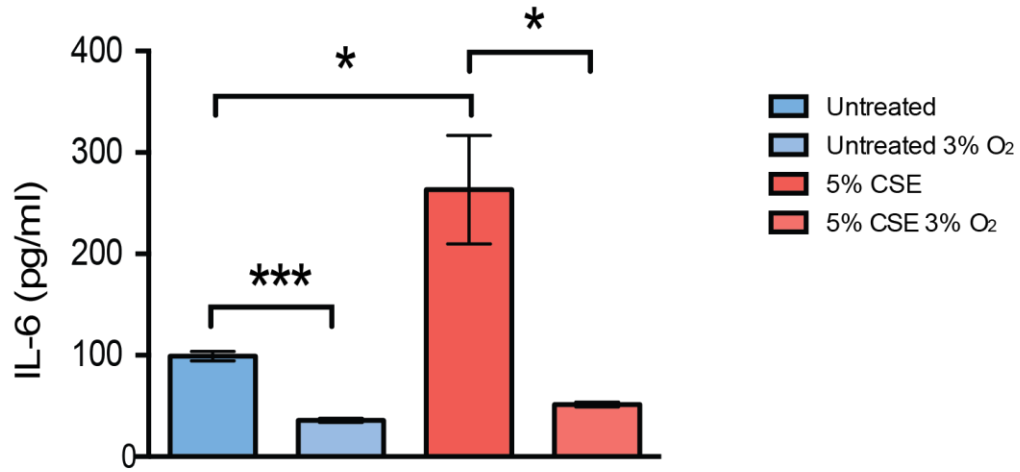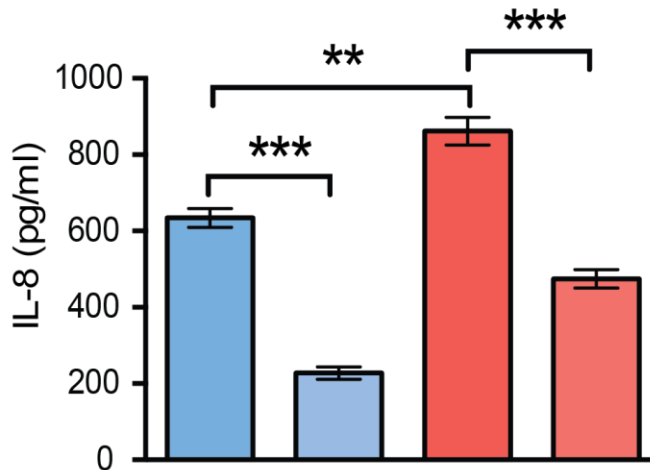
Figure 5.12 Effect of oxygen pressure and cigarette smoke exposure on cytokine secretion from MRC5 cells. MRC5 cells cultured under 3% O_2 or 20% O_2 were exposed to 5% cigarette smoke extract (CSE) or normal cell culture media every 48 hours for 25 days and conditioned media collected and analysed for the presence of pro-inflammatory cytokines. Cells were serum starved 24 hours prior to media collection. Bar graph represents concentrations of IL-6 (**A**) and IL-8 (**B**) in cell culture media measured by ELISA. Data are presented as mean ± SEM of 3 independent experiments. Statistics: One-way ANOVA and Independent samples t-test *$P < 0.05$, ** $P < 0.01$, *** $P < 0.001$.
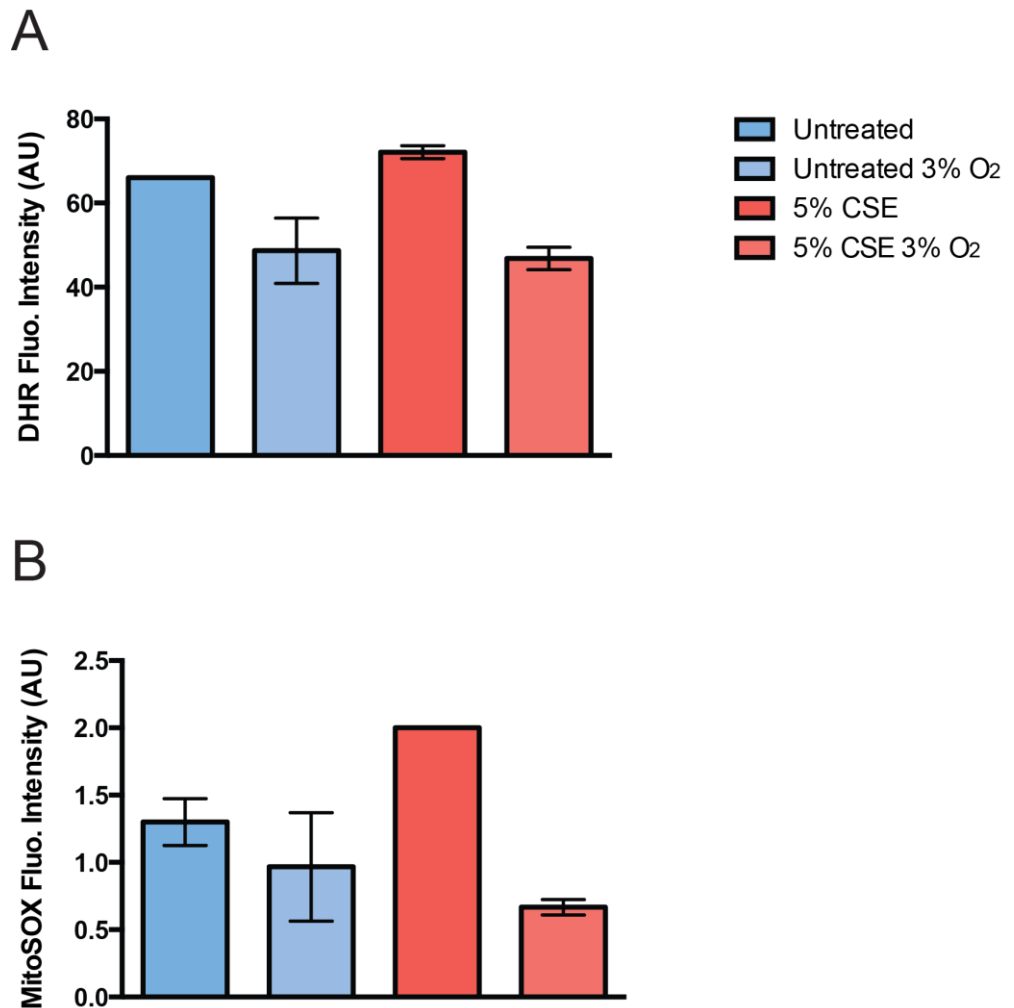
Figure 5.13 Effect of oxygen pressure and cigarette smoke exposure on intracellular ROS levels and mitochondrial-derived ROS in MRC5 cells. MRC5 cells (PD 25) cultured under normoxia (20% O_2) or hypoxia (3% O_2) were exposed to 5% cigarette smoke extract (CSE) or normal cell culture media every 48 hours for 25 days and Dihydrorhodamine (DHR) (**A**) and MitoSOX (**B**) staining coupled with FACS analysis used to measure ROS levels, and mitochondrial ROS generation, respectively. Bar graphs represent mean fluorescence intensity; each column and error bar represents mean ± SD of 3 technical repeats of one experiment. One-way ANOVA revealed no statistically significant differences between conditions.

5.3 ATM inhibition suppresses cigarette smoke-induced telomere dysfunction and the SASP

A number of groups report that persistent DDR activation is required for development and stability of senescence (Rodier, Coppe et al. 2009; Passos, Nelson et al. 2010; Fumagalli, Rossiello et al. 2014). ATM, a key sensor of DNA damage and transducer of the DDR, can trigger activation of NF-κB, the main transcriptional activator of the SASP (McCool and Miyamoto 2012). Moreover, persistent ATM activation is necessary for induction of the SASP (Rodier, Coppe et al. 2009). The effect of inhibiting the DDR in the context of cigarette smoke-induced senescence has not yet been explored.

To determine whether suppression of ATM activity affects cigarette-smoke induced telomere dysfunction and other senescence-associated phenotypes, MRC5 cells exposed to 5% CSE were treated with an inhibitor of ATM (KU55933) or DMSO (untreated control) (see methods section 2.5.2). 5% CSE or normal cell culture media, along with DMSO or the ATM inhibitor, were replaced every 48 hours and cells cultured for 25 days (Figure 5.14A). We first demonstrated that KU55933 supresses phosphorylation of H2A.X (a target of ATM kinase) by treating MRC5 cells exposed to 20Gy X-ray irradiation with the same concentration of the ATM inhibitor used in the *in vitro* experiments and carried out Western blotting for γH2A.X, confirming its role in DDR inhibition (Figure 5.14B). Culturing cells in the presence of the ATM inhibitor severely affected cell proliferation, evidenced by only small increases in PD value over time, as compared to cells treated with DMSO (not shown). Although cells were cultured until 25 days, analysis was carried out only following 14 days in culture because long-term culture with the ATM inhibitor leads to significant cell death.

To determine whether ATM inhibition decreased cigarette smoke-induced telomere dysfunction, immuno-FISH was carried out following 14 days in culture. As expected, ATM inhibition was able to reduce mean number of γH2A.X foci per cell in CSE exposed cells ($p = 0.001$) (Figure 5.15A). Similarly, ATM inhibition reduced mean number of TAF in CSE exposed cells ($p < 0.0001$) (Figure 5.15B).

In order to test the hypothesis that CSE-dependent activation of a DDR results in increased IL-6 and IL-8, ELISAs were carried out for detection of IL-6 and IL-8 in cell culture media from MRC5 cells cultured in the presence of DMSO or the ATM inhibitor and exposed, or not, to 5% CSE. It was found that 14 days of exposure to the ATM inhibitor significantly reduced levels of IL-6 release from both untreated ($p = 0.01$)

and CSE exposed MRC5 cells (p = 0.001) (Figure 5.16A). ATM inhibition also reduced IL-8 release from smoke-exposed MRC5 cells (p = 0.03) (Figure 5.16B), supporting the hypothesis that smoked-induced DDR activation results in increased SASP.
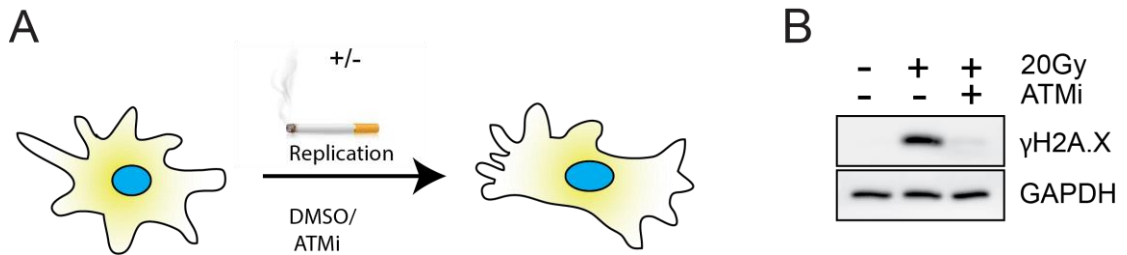
Figure 5.14 Set up of ATM inhibition experiments and effect on H2A.X phosphorylation. MRC5 cells (PD 25) were exposed to 5% cigarette smoke extract (CSE) or normal cell culture media every 48 hours along with DMSO or 10μM of the ATM inhibitor KU55933 (ATMi), diluted in DMSO for 25 days (**A**). (**B**) Representative western blot of γH2A.X expression in MRC5 cells one day after 20Gy X-ray irradiation when treated with the same concentration of the ATM inhibitor. Blot is representative of one experiment. Western blot analysis was carried out in collaboration with Graeme Hewitt from our lab.
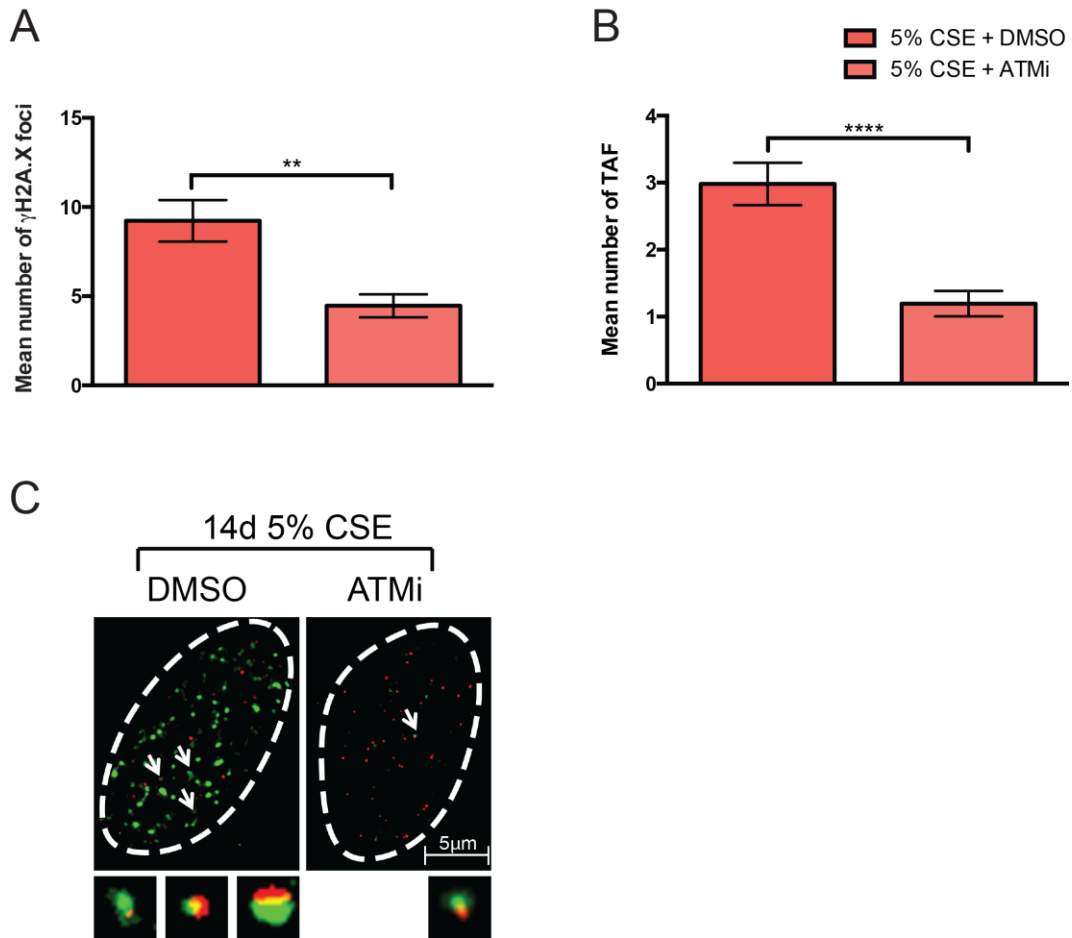
Figure 5.15 Effect of ATM inhibition on cigarette smoke-induced increases in γH2A.X foci and TAF. MRC5 cells were exposed to 5% cigarette smoke extract (CSE) or normal cell culture media (data not shown) every 48 hours along with DMSO or the ATM inhibitor KU55933 (ATMi), diluted in DMSO for 14 days. γH2A.X foci and telomere-associated foci (TAF) expression were evaluated by immuno-FISH. Bar graphs represent the mean number of γH2A.X foci per cell (**A**) and the mean number of TAF per cell (**B**) from one experiment. Data are presented as mean ± S.E.M of 50 cells per condition, generated by quantifying Z-stack images. (**C**) Representative image of immuno-FISH for γH2A.X (*green*) and telomeres (*red*) in MRC5 cells at 14 days in culture in the presence of 5% CSE and DMSO or 5% CSE and KU55933 captured using X100 oil objective and following Huygens (SVI) deconvolution. Arrows point to γH2A.X foci co-localising with telomeres (TAF), shown at higher magnification at the bottom (images are from one single Z plane). Statistics: One-way ANOVA followed by Independent samples t-test ** $P < 0.01$, **** $P < 0.0001$.
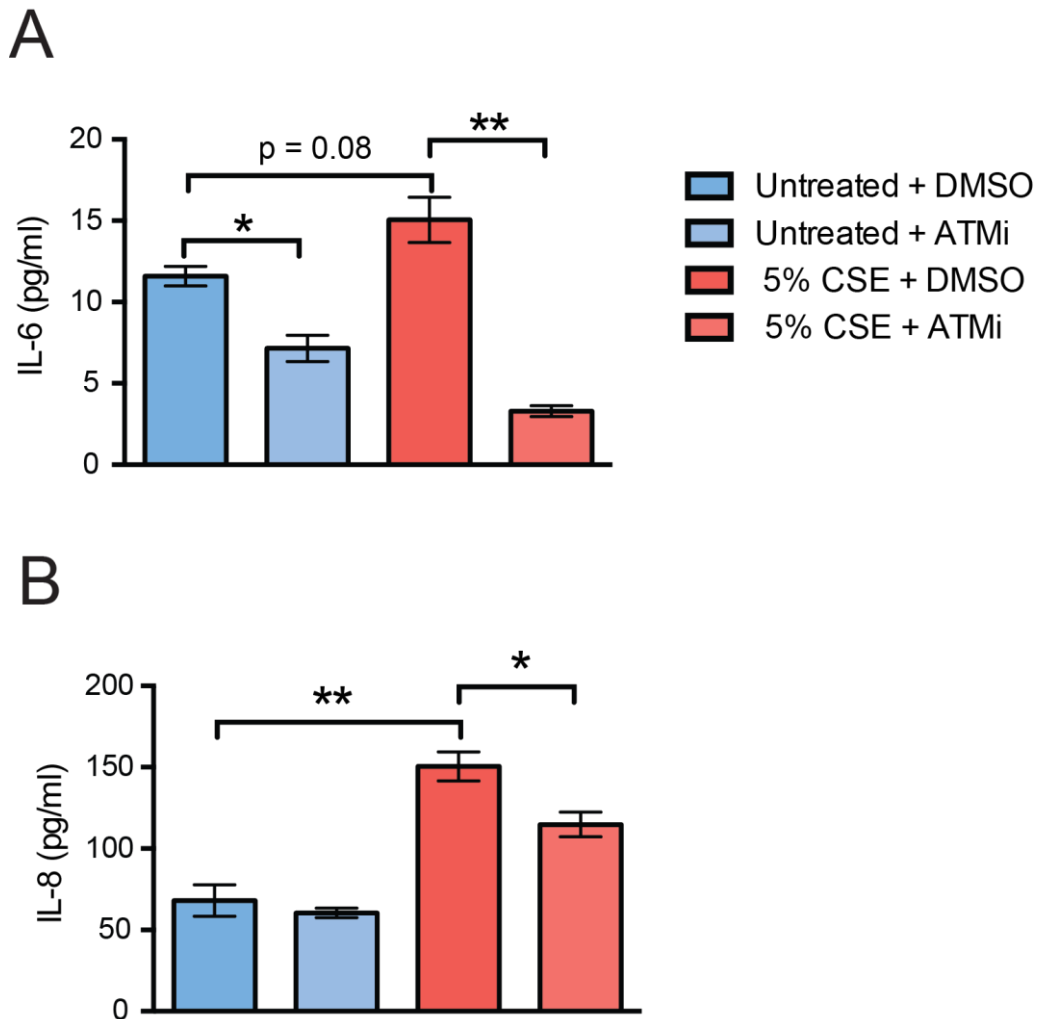
Figure 5.16 Effect of ATM inhibition on cigarette smoke-induced cytokine release in MRC5 cells. MRC5 cells were exposed to 5% cigarette smoke extract (CSE) or normal cell culture media every 48 hours along with DMSO or the ATM inhibitor KU55933 (ATMi), diluted in DMSO for 14 days and conditioned media collected and analysed for the presence of pro-inflammatory cytokines. Cells were serum starved 24 hours prior to media collection. Bar graph represents concentrations of IL-6 (**A**) and IL-8 (**B**) in cell culture media measured by ELISA. Data are presented as mean ± SEM of 3 independent experiments. Statistics: One-way ANOVA and Independent samples t-test *$P < 0.05$, ** $P < 0.01$.

5.4 mTORC1 inhibition suppresses cigarette smoke-induced telomere dysfunction and the SASP

In the previous chapter, we found that mTORC1 inhibition by rapamycin decreased the age-related increase in TAF in the small airway epithelial cells of the murine lung. A number of DNA damaging agents have been shown to activate mTORC1, including X-ray irradiation (unpublished work from our group), UV light (Brenneisen, Wenk et al. 2000) and chemotherapeutic agents (Demidenko and Blagosklonny 2008). However, it is unknown whether cigarette smoke exposure also activates mTORC1. One group have shown that inhibition of mTOR by Torin1 supresses CSE-induced cellular senescence and decline in autophagy activity in human bronchial epithelial cells (HBECs) (Fujii, Hara et al. 2012). Our group have also shown that inhibition of mTORC1 by rapamycin alleviates features of the senescence phenotype in both replicative and stress-induced senescence (unpublished). The effect of mTORC1 inhibition by rapamycin on the induction of senescence, and telomere dysfunction in particular, by cigarette smoke has not yet been investigated.

In order to test the impact of mTORC1 inhibition on cigarette smoke-induced telomere dysfunction and features of the senescence phenotype, MRC5 cells exposed to 5% CSE smoke were treated with rapamycin or DMSO (untreated control). 5% CSE or normal cell culture media, along with DMSO or rapamycin, were replaced every 48 hours and cells cultured for 25 days (Figure 5.17A). Similarly to ATM inhibition, we found that culturing cells in the presence of rapamycin severely affected cell proliferation, evidenced by only small increases in PD value over time, as compared to cells treated with DMSO (Figure 5.17B).

To determine whether mTORC1 inhibition by rapamycin decreased cigarette smoke-induced telomere dysfunction, immuno-FISH was carried out following 25 days in culture (a time point in which we start observing a shift towards senescence). As previous, we found that treatment with CSE increased mean number of γH2A.X foci ($p < 0.0001$) and mean number of TAF per cell ($p < 0.0001$) (Figure 5.18). Rapamycin treatment was able to reduce mean number of γH2A.X foci per cell in cells exposed to CSE ($p < 0.0001$) (Figure 5.18A). Similarly, rapamycin treatment reduced mean number of TAF in CSE exposed cells ($p < 0.0001$) (Figure 5.18B). There was no significant effect of rapamycin treatment on mean number of foci and TAF in untreated cells.

In order to determine whether treatment with rapamycin affected development of the SASP in CSE-induced senescence, ELISAs for detection of major SASP factors IL-6 and IL-8 were carried out using cell culture media from MRC5 cells cultured in the presence of DMSO or rapamycin and exposed, or not, to 5% CSE. We found that 25 days of exposure to rapamycin significantly reduced levels of IL-6 release from both untreated ($p < 0.0001$) and CSE exposed MRC5 cells ($p < 0.0001$) (Figure 5.19A). Rapamycin treatment also reduced IL-8 release from untreated ($p < 0.0001$) and smoke-exposed MRC5 cells ($p < 0.0001$) (Figure 5.19B), suggesting that mTORC1 over-activation may contribute to features of the cigarette smoke-induced senescence phenotype.

Analysis of intracellular ROS levels (measured by DHR fluorescence) revealed that rapamycin treatment reduced these levels in both untreated and CSE exposed cells (Figure 5.20A). Levels of mitochondrial-derived superoxide anions (measured by MitoSOX fluorescence) were also reduced in CSE exposed cells treated with rapamycin (Figure 5.20B). There was also a reduction in mitochondrial-derived ROS in untreated cells cultured with rapamycin (Figure 5.20B).
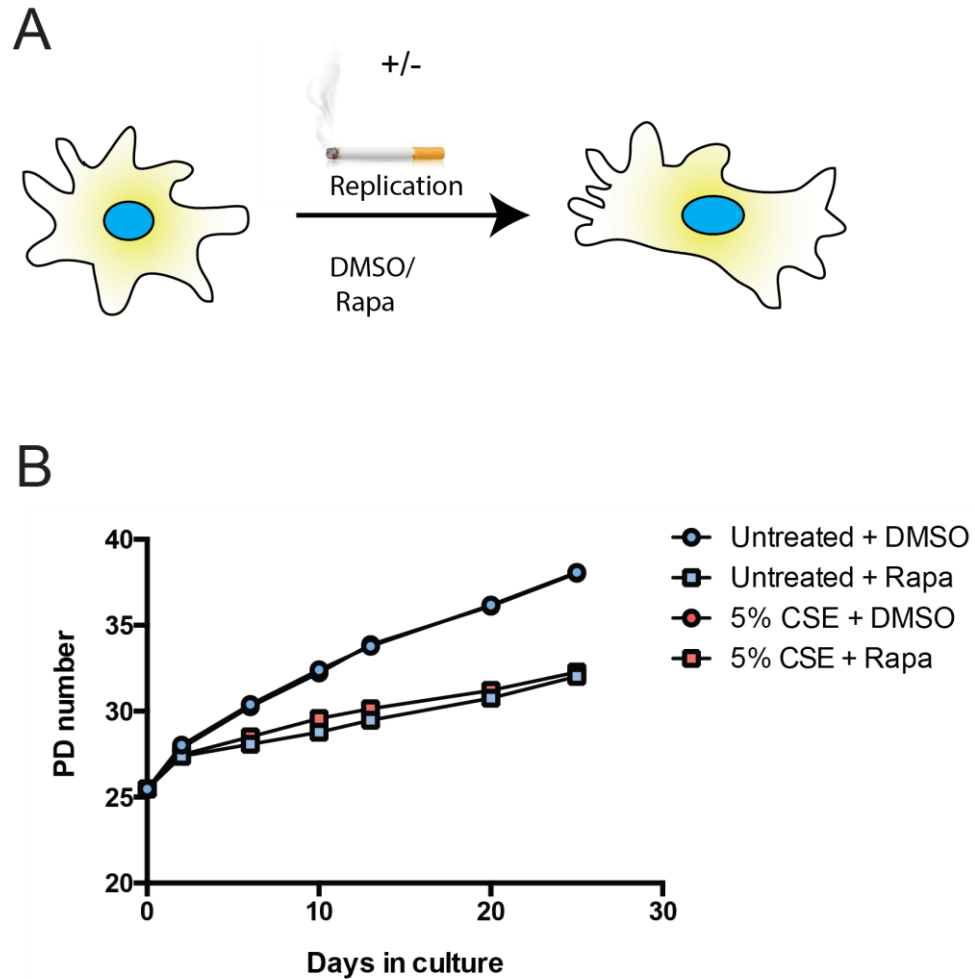
Figure 5.17 Effect of mTORC1 inhibition by rapamycin and cigarette smoke exposure on growth of MRC5 fibroblasts. MRC5 cells (PD 25) were exposed to 5% cigarette smoke extract (CSE) or normal cell culture media every 48 hours along with DMSO or 100nM of rapamycin (Rapa), diluted in DMSO for 25 days (**A**). With every cell passage, cell number was quantified and changes in population doubling (PD) level calculated for each condition. (**B**) Changes in PD plotted against number of days in culture. Graph was generated from one experiment.
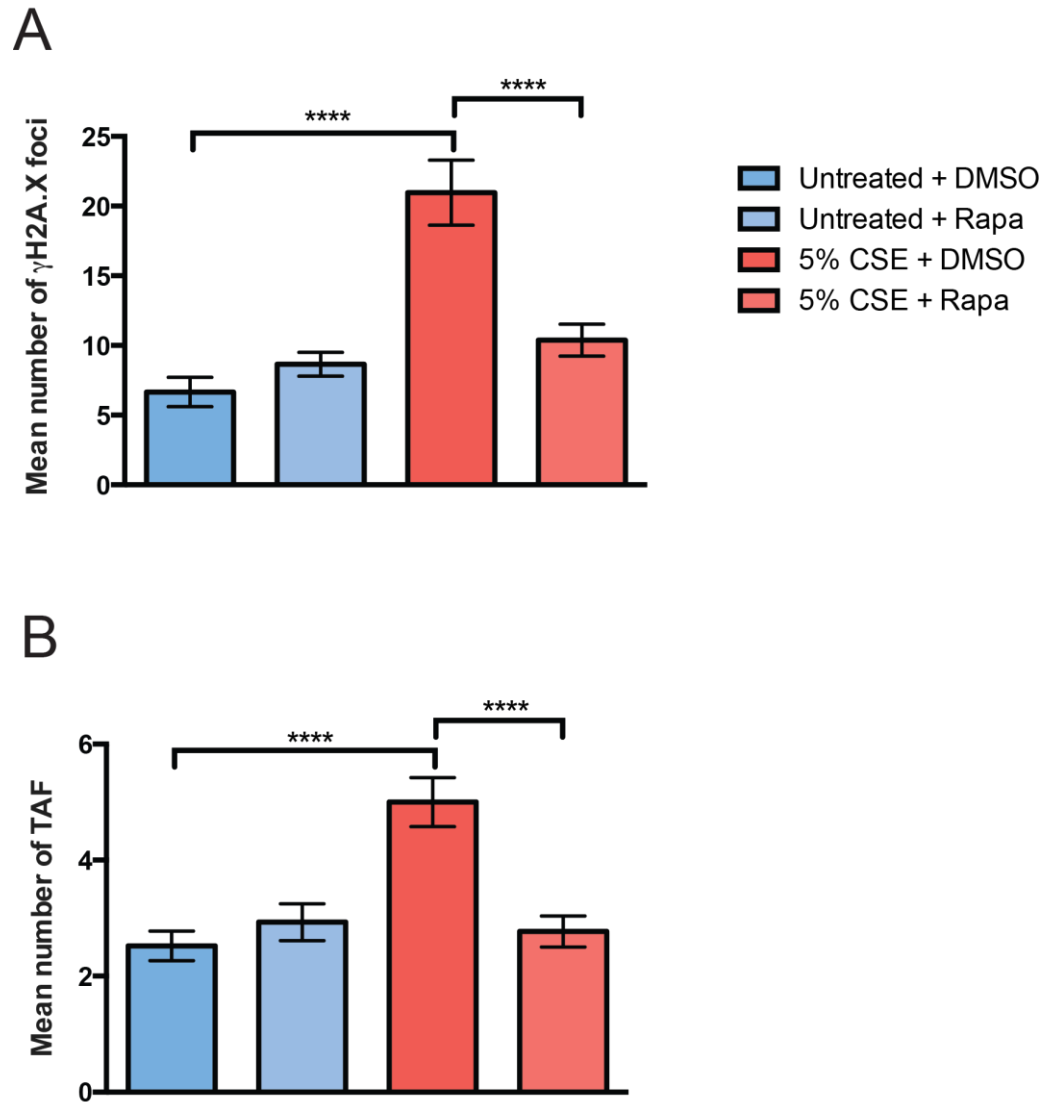
Figure 5.18 Effect of mTORC1 inhibition by rapamycin on cigarette smoke-induced increases in DNA damage foci and TAF. MRC5 cells were exposed to 5% cigarette smoke extract (CSE) or normal cell culture media every 48 hours along with DMSO or rapamycin (Rapa), diluted in DMSO for 25 days. γH2A.X foci and telomere-associated foci (TAF) were evaluated by immuno-FISH. Bar graphs represent the mean number of γH2A.X foci per cell (**A**) and the mean number of TAF per cell (**B**) from 1 independent experiment. Data are presented as mean ± S.E.M of 50 cells per condition, generated by quantifying Z-stack images. Statistics: One-way ANOVA followed by Independent samples t-test *$P < 0.05$, ** $P < 0.01$, **** $P < 0.0001$.
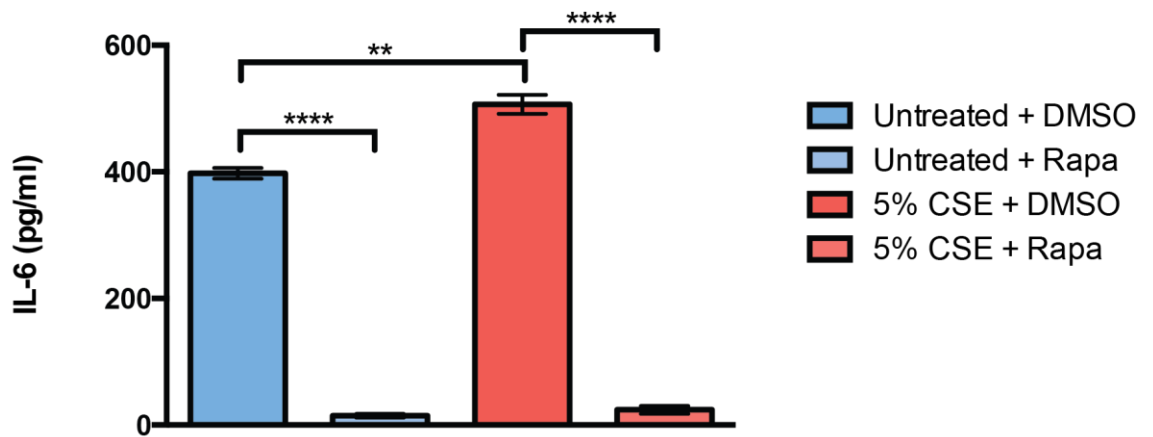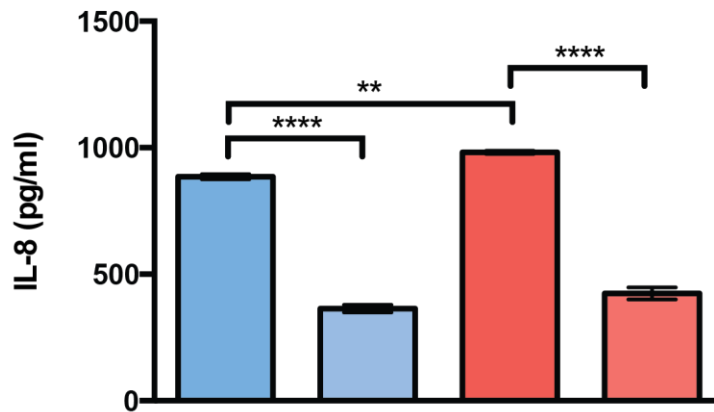
Figure 5.19 Effect of mTORC1 inhibition by rapamycin on cigarette smoke-induced cytokine release in MRC5 cells. MRC5 cells were exposed to 5% cigarette smoke extract (CSE) or normal cell culture media every 48 hours along with DMSO or rapamycin (Rapa), diluted in DMSO for 25 days and conditioned media collected and analysed for the presence of pro-inflammatory cytokines. Cells were serum starved 24 hours prior to media collection. Bar graph represents concentrations of IL-6 (**A**) and IL-8 (**B**) in cell culture media measured by ELISA. Data are presented as mean ± S.E.M of 3 independent experiments. Statistics: One-way ANOVA and Independent samples t-test *$P < 0.05$, ** $P < 0.01$.
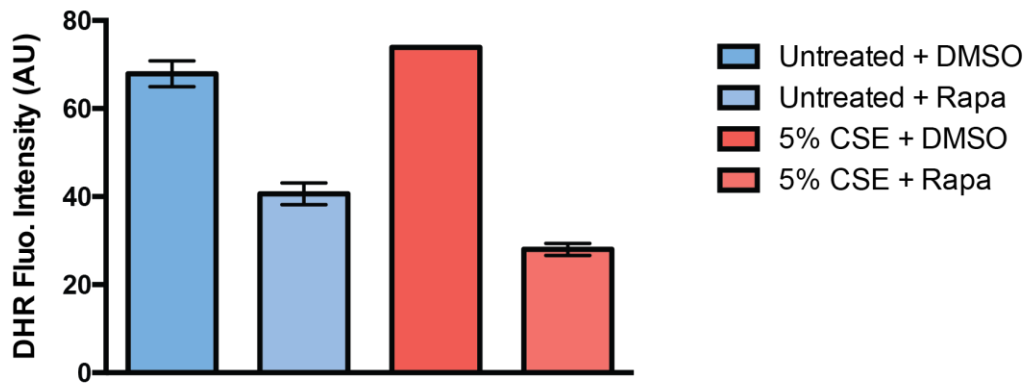
Figure 5.20 Effect of mTORC1 inhibition by rapamycin on cigarette smoke-induced increases in intracellular ROS and mitochondrial-derived ROS levels in MRC5 cells. MRC5 cells were exposed to 5% cigarette smoke extract (CSE) or normal cell culture media every 48 hours along with DMSO or rapamycin (Rapa), diluted in DMSO for 25 days and Dihydrorhodamine (DHR) (**A**) and MitoSOX (**B**) staining coupled with FACS analysis used to measure ROS levels and mitochondrial ROS generation, respectively. Bar graphs represent mean fluorescence intensity; each column and error bar represents mean ± SD of 3 technical repeats of one experiment.

5.5 Discussion

We have found that long-term exposure to 5% CSE limits the proliferative capacity of MRC5 cells following 25 days in culture. These findings are in line with previous studies, showing that exposure of lung fibroblasts to cigarette smoke significantly inhibits fibroblast proliferation (Nakamura, Romberger et al. 1995; Nobukuni, Watanabe et al. 2002; Nyunoya, Monick et al. 2006; Nyunoya, Monick et al. 2009). Similar results have also been described in alveolar epithelial cells (Tsuji, Aoshiba et al. 2004). One study showed that exposure of human lung fibroblasts (HLF-1) to 3.5% CSE for 14 days almost completely inhibited cell growth (Nyunoya, Monick et al. 2006). In contrast, we showed only a modest decrease in cell growth over time and small reductions in Ki67 expression with CSE exposure. This could be due to differences in sensitivity of these cell types to cigarette smoke. We found an increase in Sen-β-Gal activity following 25 days in culture with 5% CSE, which is in line with reports from previous groups showing increased Sen-β-Gal activity in human lung fibroblasts following CSE exposure, however other studies have detected differences after just 7 days (Nyunoya, Monick et al. 2006; Nyunoya, Monick et al. 2009). Similar effects of CSE exposure have also been described in alveolar epithelial cells after just 36 hours (Tsuji, Aoshiba et al. 2004). The differences we observed in Sen-β-Gal activity between CSE-exposed and untreated cells were no longer significant after 60 days in culture. Following 60 days in culture, the majority of cells will have reached replicative senescence, by which point there may be no detectable differences between CSE-exposed and untreated cells, therefore these results are not that surprising. Nyunoya and colleagues report an increase in cell size with a flat an enlarged morphology (Nyunoya, Monick et al. 2006), similar to previous reports following cigarette smoke exposure (Tsuji, Aoshiba et al. 2004). While we did not assess changes in cellular morphology, area of the nucleus was calculated following DAPI staining. We observed increasing nuclear size with time spent in culture, consistent with replicative senescence, however, in our hands, no significant differences were found between untreated and CSE-exposed cells.

It has been shown that CSE exposure induces DNA damage in a number of cell types, including human lung fibroblasts, (Kim, Liu et al. 2004; Nyunoya, Monick et al. 2009), bronchial epithelial cells (Albino, Huang et al. 2004; Liu, Conner et al. 2005; Fujii, Hara et al. 2012), human immortalised stromal fibroblasts (Salem, Al-Zoubi et al. 2013) and vascular endothelial cells (Csiszar, Labinskyy et al. 2008) *in vitro*. In

accordance, we report increases in mean number of γH2A.X foci in both CSE-exposed MRC5 cells and primary small airway epithelial cells. While changes in number of γH2A.X foci following CSE exposure were not significant following 60 days in culture or in small airway epithelial cells, the increases we observed in mean number of TAF were statistically significant. To or knowledge, this is the first time that TAF have been observed following cigarette smoke exposure in human cells. We did not evaluate telomere length in this instance, however a prior study has described decreased telomere length, measured by Q-FISH, in mouse embryonic stem cells following 2 weeks of exposure to low dose cigarette smoke condensate (CSC) (Huang, Okuka et al. 2013). Currently there is little data describing the effects of cigarette-smoke exposure on telomere length in lung cells *in vitro*. However one study by Nyunoya and colleagues failed to find differences in telomere length, as measured by RT-PCR, between HLF-1 cells exposed to 3.5% CSE or left untreated for 14 days in culture (Nyunoya, Monick et al. 2006). Our previous data suggests that telomere dysfunction can occur independently of telomere length and therefore measurements by Q-FISH and RT-PCR should be conducted on our samples. While our data suggests that cigarette smoke exposure induces telomere dysfunction (i.e. TAF) in human lung fibroblasts *in vitro*, there are limitations of this work. Due to time constraints and the extended nature of these experiments, it was only possible to conduct two independent experiments for the majority of this work. Therefore, our results should be further confirmed with additional repeats. The use of other cell lines and primary human fibroblasts should also be considered, to determine whether CSE induces TAF in other systems. Ideally, we would want to conduct these experiments using airway epithelial cells to complement our *in vivo* data. However, it is not possible to test the effects of chronic cigarette smoke exposure on airway epithelial cells as prolonged culture leads to fibroblastic changes in these cells. Nevertheless, a more thorough characterisation of airway epithelial cells following short-term CSE exposure should be carried out. Additionally, investigating other DDR markers, such as 53BP1 and phosphorylated ATM, should also be included in conjunction with γH2A.X to further confirm our findings.

It is known that cigarette smoke can induce apoptosis *in vitro* and increased apoptosis has been documented in the lungs of patients with COPD (Kasahara, Tuder et al. 2001; Hodge, Hodge et al. 2005; Demedts, Demoor et al. 2006). We chose 5% CSE for our experiments based on previous work conducted in our lab, whereby concentrations up to 10% were found not to be cytotoxic. Prior studies have also shown that a concentration range of between 1 and 5% CSE induces DNA damage but not

apoptosis in human lung fibroblasts (Kim, Liu et al. 2004), with much higher concentrations (above 20%) required to cause apoptosis (Ishii, Matsuse et al. 2001). Furthermore, initial viability experiments using PI staining coupled with flow cytometry, revealed that while 5% CSE exposure caused some cell death, viability always remained above 70%, with averages of 80% viability achieved for untreated cells.

In order to determine whether CSE exposure induced TAF in primary human small airway epithelial cells, we carried out a short-term exposure to CSE for 48 hours, which was based on evidence suggesting that CSE exposure can induce features of EMT in airway epithelial cells following periods of CSE exposure longer than 48 hours (Eurlings, Reynaert et al. 2014). While we observed overall increases in TAF in CSE-exposed cells, interestingly we observed that not all cells had significantly increased TAF, suggesting that patient-specific differences may occur. Different responses to cigarette smoke were also observed in the context of Sen-β-Gal activity, with cells isolated from two individuals showing an increase in expression following CSE exposure, with one individual showing no significant change. Overall, there were no significant changes in Sen-β-Gal activity when the two groups were compared and level of staining observed was very low overall (0.8% in untreated compared to 1.3% in CSE-exposed cells). This is in contrast to previous studies, which report roughly a 10% level of Sen-β-Gal positivity in HBECs at baseline, increasing to 30% positivity following exposure to 1% CSE for 48 hours (Fujii, Hara et al. 2012; Hara, Araya et al. 2012). However, because we are using primary human cells there is a lot of variation between individuals and therefore experiments would need to be repeated using a greater sample size in order to confirm our findings.

Senescence is characterised by increased secretion of bioactive, frequently pro-inflammatory peptides, known collectively as the senescence-associated secretory phenotype (SASP). Pro-inflammatory cytokines IL-6 and IL-8 are increased during senescence and contribute to maintenance of senescence in autocrine and paracrine fashions (Acosta, O'Loghlen et al. 2008; Kuilman, Michaloglou et al. 2008; Acosta, Banito et al. 2013). The similarities between pro-inflammatory mediators that comprise the SASP and those involved in COPD pathogenesis are becoming increasingly acknowledged (Kumar, Seeger et al. 2014). Indeed, the chemokine IL-8, which is highly secreted by senescent cells (Coppe, Patil et al. 2008) and known for its ability to activate neutrophils and other immune cells (Baggiolini and Loetscher 2000), is purported to be one of the most important cytokines playing a critical role in COPD and in cigarette smoke-induced airway disease (Nocker, Schoonbrood et al. 1996; Mio,

Romberger et al. 1997). Similarly, IL-6 is also a major SASP factor (Coppe, Patil et al. 2008) and is elevated in the plasma from patients with COPD (Savale, Chaouat et al. 2009). It has previously been shown that exposure to 1% CSE for 48 hours leads to increased IL-8 release in HBECs (Fujii, Hara et al. 2012; Hara, Araya et al. 2012) and after just 4 hours, 10% CSE was reported to increase IL-8 release from HBECs (Moon, Zheng et al. 2013). 10% CSE also increases release of IL-8 from airway smooth muscle cells after 72 hours (Chen, Ge et al. 2014). However, the effect of long-term cigarette smoke exposure on SASP induction *in vitro* has not previously been investigated. Compared to untreated cells, we observed an increase in both IL-6 and IL-8 release in CSE exposed cells at all time points, however this difference only became significant following 13 days in culture. After 39 days in culture, IL-6 and IL-8 release from MRC5 cells treated with CSE was increased 23-fold and 12–fold, respectively, consistent with early onset of senescence. Previous reports have suggested that the SASP is activated 7-10 days following the induction of a DDR (Coppe, Patil et al. 2008), which suggests that chronic cigarette smoke exposure is likely required to lead to a sufficient level of senescence for SASP induction. It could be that a threshold level of DNA damage, or indeed TAF, is required before the SASP is activated. The mechanisms behind activation of the SASP in response to telomere dysfunction are still poorly understood. Data suggests that active ATM can directly activate NF-κB following induction of a DDR by NEMO-dependent degradation of the NF-κB inhibitor IκB (Wu, Shi et al. 2006). It has also been shown that SASP factor release can occur independently of a DDR via p38MAPK-dependent increase in NF-κB transcriptional activity (Freund, Patil et al. 2011). Epigenetic mechanisms may also be involved in the regulation of SASP factor release in response to chronic cigarette smoke exposure. It has been shown that SIRT1 inhibits transcriptional activity of NF-κB by deacetylating the RelA/p65 subunit of NF-κB on lysine 310, a site critical for NF-κB transcriptional activity (Yeung, Hoberg et al. 2004). In lungs of patients with COPD and following chronic cigarette smoke exposure both *in vitro* and *in vivo*, SIRT1 levels are decreased (Yang, Wright et al. 2007; Rajendrasozhan, Yang et al. 2008), thought to be due to cigarette smoke-associated oxidative alterations and subsequent degradation of SIRT1. Therefore, reductions in SIRT1 following chronic cigarette smoke exposure may be partly responsible for increased SASP factor release due to increased RelA/p65 acetylation and NF-κB activity.

In order to mechanistically understand how CSE exposure causes telomere dysfunction *in vitro*, cells were cultured under atmospheric (20%) or low (3%) O_2. Culturing under 20% O_2 can lead to early-onset senescence due to supraphysiological oxygen levels causing oxidative damage, whereas culturing under 3% O_2 is more physiological (Parrinello, Samper et al. 2003). Consistent with a role for oxidative stress in inducing CSE-associated senescence, we found that low O_2 was able to increase proliferative capacity of MRC5 cells and supress CSE-induced increases in DNA damage foci, TAF, Sen-β-Gal positivity and IL-6 and IL-8 release. These results suggest that oxidative stress induced by cigarette smoke exposure may be responsible for CSE-associated telomere dysfunction, which contributes to induction of other senescence-associated phenotypes, such as Sen-β-Gal activity and activation of the SASP. Other studies have also implicated ROS in CSE-induced senescence. The use of the antioxidant N-acetylcysteine (NAC) has been shown to reduce CSE-induced increases in Sen-β-Gal activity in alveolar epithelial cells (Tsuji, Aoshiba et al. 2004) and HBECs (Hara, Araya et al. 2013), and CSE-induced DNA damage in HLF-1 cells (Kim, Liu et al. 2004). Additionally, NAC reduces CSE-associated reduction in SIRT1 expression and activity in human lung epithelial cells by reducing ROS-mediated oxidative modifications including carbonylation (Caito, Rajendrasozhan et al. 2010). Cigarette smoke is a rich source of ROS, containing 10^{15} free radicals and 4700 different chemical compounds per puff. Therefore, cigarette smoke may cause damage to DNA directly or indirectly, through the generation of endogenous ROS from inflammatory and structural cells (Rahman and Adcock 2006). The precise source of ROS involved in CSE-induced telomere dysfunction remains to be clearly elucidated. We found that 5% CSE exposure resulted in increased ROS generation and an increase in mitochondrial-derived ROS. Mitochondria are the major source of endogenous ROS (Kowald and Kirkwood 2011). Hence, numerous studies have shown that cellular senescence is characterised by mitochondrial dysfunction, contributing to elevated ROS (Saretzki, Murphy et al. 2003; Hutter, Renner et al. 2004; Passos, Saretzki et al. 2007). Mitochondria are susceptible to damage from cigarette smoke and a higher level of oxidative mitochondrial DNA damage has been observed in smokers (Ballinger, Bouder et al. 1996). Moreover, it has been shown that cigarette smoke exposure enhances mitochondrial ROS production from vascular endothelial cells and lung epithelial cells and also leads to mitochondrial fragmentation (Csiszar, Labinskyy et al. 2008; Hara, Araya et al. 2013). Additionally, CSE-induced increases in mitochondrial ROS can be inhibited by NAC (Hara, Araya et al. 2013), which coincide with our findings of

decreased mitochondrial ROS generation when culturing cells at low O_2. A positive feedback loop has been described by our lab, whereby both telomere-dependent and –independent DDR signalling cause mitochondrial dysfunction and ROS production, leading to continued replenishment of short-lived DDR foci and continued DDR signalling (Passos, Nelson et al. 2010). Therefore, it is possible that initial cell-cycle arrest caused by cigarette smoke-induced DNA damage leads to mitochondrial dysfunction, increased ROS and further DNA damage leading to persistent DDR signalling. Thus telomere dysfunction could be induced both directly and indirectly. However, other experiments would need to be carried out in order to directly implicate mitochondria in CSE-induced telomere dysfunction, such as the use of mitochondrial-targeted antioxidants or mitochondrial elimination in combination with CSE. One interesting consideration is the numerous reports showing that oxidative stress shortens telomeres (von Zglinicki 2002). In previous chapters, we have failed to find significant differences in telomere length in the context of cigarette smoke exposure and COPD. Therefore, if oxidative stress was playing a role in telomere dysfunction then one would expect to find significant decreases in telomere length. Although, it has been shown that other oxidant stresses, such as hydrogen peroxide and UV light did not lead to telomere erosion in cultured human fibroblasts (Gorbunova, Seluanov et al. 2002). The SASP is dependent on persistent DNA damage signalling (Rodier, Coppe et al. 2009), such as that created by a positive feedback loop between DDR signalling and ROS. Accordingly we found that low O_2 reduced levels of DNA damage markers and SASP factors, regardless of cigarette smoke exposure. Mechanistically, it has been shown that ATM activation in response to DNA damage can trigger NEMO-dependent activation of NF-κB, the main transcriptional activator of the SASP (McCool and Miyamoto 2012). In addition, CSE has been shown to significantly increase NF-κB activation both *in vitro* and *in vivo* (Yang, Wright et al. 2007; Csiszar, Labinskyy et al. 2008). We found that inhibition of ATM significantly reduced CSE-associated increases in DNA damage, TAF and IL-6 and IL-8 release, supporting the hypothesis that cigarette smoke-induced DDR signalling results in increased SASP. However, we cannot conclude that dysfunctional telomere signalling, specifically, results in SASP activation since ATM inhibition was not targeted to telomeres. While these preliminary results are interesting, further repeats are required in order to confirm our findings. The majority of this data is generated from technical repeats of one biological experiment, which is a limitation of this work. Additionally, it would be interesting to determine whether these findings could be reproduced using other cell lines or in primary cells from the lung. Moreover,

CSE experiments carried out using cells derived from patients with Ataxia Telangiectasia (AT), where ATM is mutated, should be conducted to support our data. Other means of reducing oxidative stress in CSE-induced senescence should also be considered, such as the use of NAC, which has proved promising in suppressing senescence markers but the effect on telomere dysfunction and SASP induction is unknown.

A number of studies suggest a role for mTOR in promoting cellular senescence. As previously mentioned, mTOR activity is enhanced by a number of known inducers of senescence. In the previous chapter, we showed that mTORC1 inhibition by rapamycin attenuates the age-related increases in TAF in small airway epithelial cells of the murine lung. However, the role of mTOR in CSE-associated senescence and COPD is currently unknown. We questioned whether inhibition of mTORC1 by rapamycin could supress some of the senescence-associated changes observed following CSE treatment. Due to limited time availability, it was not possible to characterise all aspects of the senescence phenotype, however we did find that rapamycin was able to supress CSE-induced increases in DNA damage foci and TAF and decreased the release of SASP factors IL-6 and IL-8. Our findings are in accordance with other studies, showing that mTORC1 inhibition by rapamycin alleviates features of the senescence phenotype. For example, in normal human lung fibroblasts (WI-38), rapamycin treatment attenuates senescence induced by chemotherapeutic drug doxorubicin (Demidenko and Blagosklonny 2008) and decreases H_2O_2-induced senescence in human retinal pigment epithelial cells (Demidenko, Zubova et al. 2009). Short-term rapamycin treatment supresses the induction of IL-8 and p21 in replicative-senescent human skin fibroblasts (BJ cells) and reduces levels of p21 in RAS-induced senescent BJ cells (Kolesnichenko, Hong et al. 2012). The authors also showed that long-term rapamycin treatment starting in the pre-senescent stages, similar to our experimental design, prevented loss of proliferation potential and increases in Sen-β-Gal staining that occur with replicative senescence. Cells also retained their pre-senescent levels of p21, p53 and IL-8. Similar findings were also gained when treating RAS-induced senescent BJ cells from the pre-senescent stage (Kolesnichenko, Hong et al. 2012). In our experience, cells treated with rapamycin proliferated much slower than cells treated with DMSO, something that was also described previously in rat embryonic cells (Pospelova, Leontieva et al. 2012). Similar to our findings, Pospelova and colleagues report a reduction in DNA damage foci (γH2A.X and 53BP1) with rapamycin treatment in the context of replicative senescence (Pospelova, Leontieva et al. 2012). Our lab have also shown that rapamycin

treatment supresses increases in DNA damage foci in MRC5 cells and mouse embryonic fibroblasts in the context of stress-induced senescence (X-ray irradiation), but has negative effects on cell proliferation (unpublished). It is possible then that the reductions in γH2A.X foci and TAF we observe are due to the fact that there is less proliferation, which is known to increase cellular content of DNA damage foci due to replication stress (Zeman and Cimprich 2014). It could be that the concentration of rapamycin used in these experiments was too high and a lower dose, that does not affect proliferation, should be tested to determine whether DNA damage content would still be reduced. Another caveat of this work is that we did not assess mTOR activity following cigarette smoke exposure and treatment with rapamycin. This should be explored to confirm that rapamycin is reducing mTORC1 activity and to indicate whether CSE does in fact increase signalling from mTOR.

It is unknown how mTOR activity may regulate the SASP. mTOR plays a critical role in maintaining nutrient and energy status through a pathway that regulates many essential biological processes, including autophagy, a lysosomal degradation pathway (Laplante and Sabatini 2012). mTOR positively regulates protein synthesis and negatively regulates autophagy. Therefore, enhanced activity of mTOR during senescence may increase protein content of senescent cells due to increased protein synthesis and decreased autophagy, which could possibly impact on the cell secretome. The impact of autophagy in CSE-induced cellular senescence is poorly defined and current findings are conflicting. It has been shown in primary HBECs that autophagy is impaired following CSE exposure, which is in line with increased mTOR activity (Fujii, Hara et al. 2012), however other studies have found that CSE enhances autophagy in a range of different lung cell types (Chen, Kim et al. 2008; Hwang, Chung et al. 2010) and in stromal fibroblasts (Salem, Al-Zoubi et al. 2013), which may suggest that cigarette smoke exposure inhibits mTOR activity. There may be time-dependent effects of acute vs. chronic cigarette smoke exposure, with short-term exposure likely inducing autophagy, which might become impaired with prolonged exposure. However, one group has observed increased autophagy in lung tissue from patients with COPD (Chen, Kim et al. 2008). Further work is required to determine whether altered mTOR signalling and autophagy contribute to the development of senescence and the SASP in the context of cigarette smoke exposure.

Mitochondrial dysfunction has been implicated in cellular senescence (Passos, Saretzki et al. 2007; Moiseeva, Bourdeau et al. 2009). Mitochondrial biogenesis is essential for maintaining functional mitochondria in the cell and mTOR has been linked

to mitochondrial biogenesis through the regulation of peroxisome proliferator-activated receptor-gamma coactivator (PGC1- α), an activator of transcription and regulator of mitochondrial metabolism and biogenesis (Cunningham, Rodgers et al. 2007). Moreover, mice fed with a rapamycin-supplemented diet have lower mitochondrial content (Harrison, Strong et al. 2009) and show enhanced survival and attenuated disease progression in a mouse model of mitochondrial disease (Johnson, Yanos et al. 2013). Similarly, our lab has shown that rapamycin reduces age-related increases in mitochondrial content in the murine liver (unpublished). Our findings suggest that mTOR signalling impacts on mitochondria, since rapamycin reduced mitochondrial-derived ROS, which are increased following CSE exposure. Supporting this finding, a previous study showed that rapamycin treatment enhances mitochondrial membrane potential, reduces ROS levels and increases replicative lifespan of normal human fibroblasts (Lerner, Bitto et al. 2013). Our lab has also demonstrated that rapamycin inhibits increases in mitochondrial mass in the context of stress-induced senescence (unpublished). It is possible therefore that the effects of rapamycin treatment on the SASP are mediated through the effects of mTOR inhibition on mitochondrial function, which when dysfunctional may contribute to a positive feedback loop between ROS generation and the DDR, as aforementioned, leading to increased SASP activity (Passos, Nelson et al. 2010). Additionally, mechanisms of inflammatory activation by mTOR, independent of mitochondria, have also been described. For example, it was shown in PTEN-null/inactive prostate cancer cells that activation of mTOR downstream of Akt regulates activity of NF-κB *via* stimulation of IKK activity (Dan, Cooper et al. 2008), which may also explain how mTOR may regulate the SASP.

The precise role of mTOR in the context of CSE-induced senescence and COPD needs to be clearly elucidated. While our preliminary results are interesting, further experiments are required to confirm our findings. Additional repeats and a more detailed characterisation of the effects of mTORC1 inhibition on cigarette smoke-induced senescence are needed. Alternative methods of supressing mTOR activity, such as knockdown by siRNA should also be considered as well as enhancing mTOR activity alongside CSE exposure to determine whether the ability of CSE to induce senescence is altered.

In summary, our data suggests that chronic cigarette smoke exposure induces telomere dysfunction and senescence-associated phenotypes, including Sen-β-Gal positivity and SASP activity. The mechanisms behind CSE-induced telomere dysfunction are still unclear. While our preliminary data may suggest an involvement

for mitochondrial dysfunction and altered mTOR signalling, further work is required in order to elucidate the mechanisms behind telomere dysfunction in the context of cigarette smoke exposure and COPD.

Chapter 6. General discussion and conclusions

Senescence has been firmly implicated in the ageing process and has been shown to impact on a number of age-related diseases (van Deursen 2014). A wealth of data has linked cellular senescence with COPD (Aoshiba and Nagai 2009; MacNee 2009). However, the role played by telomeres in this process is still unclear. Moreover, whether senescence has significant impact on the lung during natural ageing and in other chronic lung diseases has been poorly studied so far. The aim of this work was to investigate airway epithelial cell senescence, and telomere dysfunction in particular, during physiological lung ageing, in age-related lung disease and in the context of cigarette smoke exposure. We also aimed to explore some of the potential mechanisms underlying these processes.

While there have been many associations found between cellular senescence and COPD, the underlying mechanisms of how cellular senescence occurs and promotes the development of COPD are still not clear. The role of telomere dysfunction in COPD appears to be more complex than simple telomere attrition, based on the many conflicting findings from telomere length analysis of smokers and patients with COPD. We have found in lung tissue and isolated airway epithelial cells from patients with COPD, and from *in vitro* and *in vivo* conditions of cigarette smoke exposure, that telomere dysfunction (i.e. the co-localisation of DDR proteins at telomeres) is increased, without significant changes in telomere length. These findings are in line with previous studies demonstrating that TAF can occur irrespective of telomere length (Fumagalli, Rossiello et al. 2012; Hewitt, Jurk et al. 2012). An inefficiency of DNA repair has been purported to occur in patients with COPD and patients show markers of oxidative DNA modifications in the lung, including 8-OHdG, a product of guanine oxidation (Caramori, Adcock et al. 2011). Telomeres are particularly susceptible to oxidative damage compared to the bulk of the genome, which is thought to be due to the fact that telomere repeats contain guanine triplets (Petersen, Saretzki et al. 1998; Henle, Han et al. 1999). Moreover, evidence suggests that damage at telomeres is irreparable (Fumagalli, Rossiello et al. 2012; Hewitt, Jurk et al. 2012). This may suggest that TAF, given their persistence, are excellent markers for senescence and are important to COPD pathogenesis. It could be that irreparable damage at telomeres, caused by cigarette smoke exposure, may lead to persistent DDR signalling and sustained downstream effects, such as activation of the SASP. Moreover, the observation that even after

176

smoking cessation, chronic inflammation still persists in the lungs of patients with COPD (Willemse, ten Hacken et al. 2005) suggests that there may be a feedback loop maintaining inflammatory signalling processes, such as the one between the DDR and SASP factor signalling (Rodier, Coppe et al. 2009), which may be maintained via ROS (Acosta, O'Loghlen et al. 2008; Jurk, Wilson et al. 2014). All of these observations point to telomeres as one of the key players in cigarette smoke-induced senescence and COPD pathogenesis.

In the majority of systems used in this work, increases in TAF were always more clear than increases in γH2A.X foci alone, suggesting that TAF are a more robust marker for senescence (Table 6.1). Moreover, TAF correlated with other senescence-associated markers, including p21, and changes in alveolar airspaces in the murine lung with age. This coupled with the observation that *G4 TERC$^{-/-}$* mice show enhanced telomere dysfunction and early onset emphysema could suggest that TAF may be able to predict decline in lung structural integrity in the context of ageing and age-related lung disease. Further studies using a larger number of patients (at different stages of the disease) and excluding confounding factors such as age and history of cigarette smoke exposure need to be done in order to determine if TAF may be used as an indicator of COPD disease severity or susceptibility of smokers to develop COPD. Since we continually observe significant increases in TAF, both with age and in the context of cigarette smoke exposure, despite particularly small sample sizes (n=3-5 mice or 5-10 patients) this further strengthens the use of TAF as both a biomarker for ageing and potentially for COPD. From this work, we still do not know whether telomere shortening is causing increases in TAF. While our results suggest that telomere attrition may not be the sole determinant of TAF induction, some experimental limitations of our work cannot allow us to make a definite conclusion about the relative contributions of telomere shortening and telomere damage occurring irrespectively of length. Currently, this work is limited by resolution of imaging. In some instances, TAF could simply be a telomere and a DDR signal in close proximity, rather than a DDR occurring specifically at telomeres. One study reports that in around 70% of senescent nuclei, multiple telomeres co-localised with one γH2A.X foci, suggesting that dysfunctional telomeres aggregate in senescent cells (Kaul, Cesare et al. 2012). This potential aggregation may affect values gained for telomere signal intensity analysis when measured by Q-FISH, leading to inaccurate conclusions regarding telomere length. Furthermore, it is likely that some TAF are not detected at all, since the shortest of telomeres may generate a very weak FISH signal. Telomere shortening may also progress to the almost complete

disappearance of telomere repeats (Baird, Rowson et al. 2003), which may affect PNA probe binding. Therefore, we still do not know for sure whether telomere shortening is inducing TAF. Nevertheless, using well-established methods, we found no significant decreases in telomere length and found robust increases in TAF in most system studied, suggesting that telomere dysfunction does occur, whether induced by shortening or damage at longer telomeres. It is currently unknown how many dysfunctional telomeres are required to signal senescence. Since TAF also appeared in young or control conditions, this suggests that a certain level of telomere dysfunction can be tolerated by the cell and that a threshold level of telomere dysfunction may be required to induce senescence. Using cohorts of mice that differed in their maximum and median lifespan, it was found that the minimum number of TAF associated with cellular senescence is between 2 and 3 in liver hepatocytes and intestinal enterocytes (Jurk, Wilson et al. 2014). In contrast another report claims that 5 dysfunctional telomeres precede the onset of replicative senescence in cells in culture (Kaul, Cesare et al. 2012). Dysfunctional telomere aggregation in senescent cells may lead to miscalculations in the number of TAF a cell contains, leading to inconsistencies between the numbers of TAF reported to be associated with onset of the senescent phenotype. Moreover, it may be difficult to compare absolute numbers in 5 μm sections of tissue, as compared to whole cells grown in culture. In fact, in some instances, just one dysfunctional telomere has been reported to be sufficient for the induction of a persistent DDR and permanent cell-cycle arrest (Hemann, Strong et al. 2001; Herbig, Jobling et al. 2004).

The mechanisms driving CSE-induced telomere dysfunction are still unclear. Oxidative stress has been widely implicated in COPD (Rahman and Adcock 2006) and our preliminary data suggest that ROS may contribute to CSE-induced telomere dysfunction, given that culturing cells under low levels of oxygen pressure reduced CSE-associated increases in TAF and other features of senescence, including Sen-β-Gal positivity and release of major SASP factors IL-6 and IL-8. Hypoxia also appeared to reduce levels of intracellular ROS and mitochondrial-derived superoxide anions, suggesting that mitochondrial dysfunction could be partially responsible for the increased oxidative stress and telomere dysfunction following cigarette smoke exposure. The role of mTOR signalling in COPD and in the context of cigarette smoke exposure is largely understudied. Our preliminary data suggest that decreasing mTORC1 activity by rapamycin reduces CSE-induced increases in TAF, SASP factor release and both ROS and mitochondrial-derived superoxide anions. This may suggest a causal link between altered mTOR signalling, ROS, activation of a DDR at telomeres and the pro-

inflammatory phenotype characteristic of senescence and COPD. A positive feedback loop has been described by our lab, whereby DDR signalling causes mitochondrial dysfunction and ROS production, leading to further DNA damage and continued DDR signalling (Passos, Nelson et al. 2010). It is possible that initial cell-cycle arrest caused by cigarette smoke-induced DNA damage leads to mitochondrial dysfunction, increased ROS and further DNA damage leading to persistent DDR signalling. It is unknown how mTOR activity may regulate the SASP. mTOR signalling has been linked to the control of mechanisms that regulate mitochondrial homeostasis, such as mitophagy and mitochondrial biogenesis, which may affect mitochondrial function during ageing (Laplante and Sabatini 2012). Our findings suggest that mTOR signalling impacts on mitochondria, since rapamycin reduced mitochondrial-derived ROS, which are increased following CSE exposure. It is possible therefore that the effects of rapamycin treatment on the SASP are mediated through the effects of mTOR inhibition on mitochondrial function, which when dysfunctional may contribute to a positive feedback loop between ROS generation and the DDR, as aforementioned, leading to increased SASP activity (Passos, Nelson et al. 2010). The speculation that altered mTOR signalling and mitochondrial dysfunction may be involved in cigarette smoke-induced telomere dysfunction requires further investigation. Our data are preliminary and additional work is required to elucidate the role of mitochondria and mTOR in COPD-associated senescence. We also observed that rapamycin treatment *in vivo* reduces age-related increases in TAF in small airway epithelial cells and appeared to have positive effects on alveolar airspace size. This is in line with recent data from our lab showing that rapamycin treatment reduces a number of senescence-associated markers in the murine liver, including age-related increases in TAF (unpublished). It is not inconceivable then that targeting mTOR activity may be of therapeutic benefit in COPD, but this will require further investigation.

It is still not clear whether there is a causal link between telomere dysfunction and the SASP. However, we found that inhibition of ATM, a key initiator of the DDR, represses CSE-induced secretion of IL-6 and IL-8 and increases in TAF. IL-6 and IL-8 have been described in multiple publications as the major and more abundant SASP components and both have been shown to play roles in stabilisation of senescence (Acosta, O'Loghlen et al. 2008; Kuilman, Michaloglou et al. 2008) and induction of paracrine effects (Acosta, Banito et al. 2013). Effective targeting of inflammatory processes is one of the key therapeutic goals in COPD, since there are currently no effective anti-inflammatory treatments that impact on disease progression (Barnes 2013).

Patients with COPD are at increased risk of lung cancer (Papi, Casoni et al. 2004; Young and Hopkins 2010) and evidence suggests that the SASP can promote malignant transformation and progression (Krtolica, Parrinello et al. 2001). Therefore, suppression of the SASP could be therapeutically beneficial, not only by reducing inflammatory processes that promote progressive lung decline in COPD, but by potentially decreasing incidences of lung cancer in patients with COPD.

Collectively, our data suggest that telomere dysfunction increases in large and small airway epithelial cells during normal ageing and in conditions of cigarette smoke-induced accelerated lung ageing, which may be independent of telomere length. Our data proposes that telomere dysfunction may contribute to changes in lung architecture and the pro-inflammatory environment that occurs during lung ageing and in COPD. Hence, TAF may be more robust markers for senescence and indicators of accelerated lung ageing following cigarette smoke exposure. It is possible that TAF could be used as markers to predict susceptibility to developing COPD in smokers, to stratify and predict disease severity in existing COPD patients and to also predict the efficacy of a certain therapy for COPD. Our data suggest a causal link between ROS, activation of a DDR at telomeres and the pro-inflammatory phenotype characteristic of senescence (Figure 6.1). However, the mechanisms underlying cigarette smoke-induced telomere dysfunction are still unclear and may involve altered mTOR signalling and mitochondrial dysfunction. Further work is required to elucidate the role of mTOR signalling and mitochondrial function in COPD. Targeting of senescent cells may be of therapeutic benefit for patients with COPD, which is currently an incurable disease.

Condition	Mean no. γH2A.X foci (control)	Mean no. γH2A.X foci	P value	Mean no. TAF (control)	Mean no. TAF	P value	Figure
Control vs. COPD SAECs	2.37	3.95	0.28	0.78	1.18	0.2	3.15
5% CSE-exposed SAECs	2.5	5.4	0.057	0.8	1.49	0.04	5.5
COPD vs. control tissue (small airways)	1.8	4.5	0.04	0.22	0.63	0.003	3.10
MRC5 cells 25 days 5% CSE	7.68	17.75	0.007	1.28	3.95	0.002	5.2
Smoke-exposed mice (large airways, small airways)	0.3 0.17	0.7 0.46	0.02 0.01	0.1 0.05	0.2 0.14	0.04 0.036	4.10
6.5 vs 24 month mice (large airways, small airways)	0.24 0.18	0.65 0.57	0.03 0.008	0.04 0.04	0.26 0.23	0.002 0.002	4.3

Table 6.1 Comparisons between γH2A.X foci and γH2A.X foci co-localised with telomeres in a range of systems. Changes in γH2A.X foci compared to changes in telomere-associated foci (TAF) in treated/COPD as compared to untreated/control group.
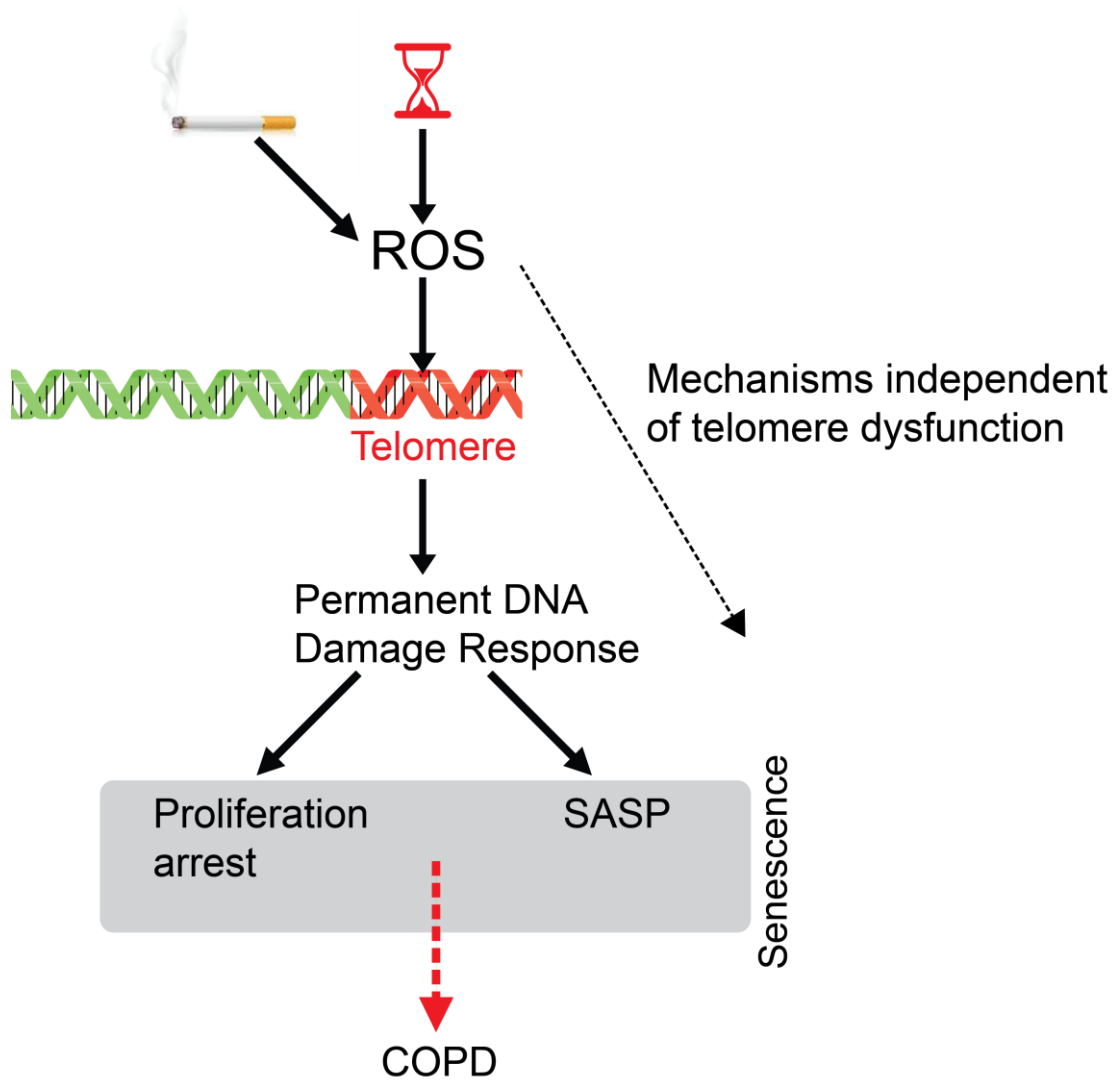
Figure 6.1 Potential links between reactive oxygen species, activation of a permanent DNA damage response at telomeres and induction of senescence in development of COPD. Activation of a persistent DNA damage response (DDR) at telomeres may be driven by time and/or cigarette smoke exposure. Persistent DDR signalling at telomeres may contribute to the loss of cellular regenerative capacity and pro-inflammatory conditions that occur in the lung with physiological ageing and in the context of COPD. Mechanisms independent of a telomeric DDR may also be contributing to the development of senescence in the context of cigarette smoke exposure and COPD.

References

Acosta, J. C., A. Banito, et al. (2013). "A complex secretory program orchestrated by the inflammasome controls paracrine senescence." Nat Cell Biol **15**(8): 978-990.

Acosta, J. C., A. O'Loghlen, et al. (2008). "Chemokine signaling via the CXCR2 receptor reinforces senescence." Cell **133**(6): 1006-1018.

Ahmed, S., J. F. Passos, et al. (2008). "Telomerase does not counteract telomere shortening but protects mitochondrial function under oxidative stress." J Cell Sci **121**(Pt 7): 1046-1053.

Ahn, J. Y., J. K. Schwarz, et al. (2000). "Threonine 68 phosphorylation by ataxia telangiectasia mutated is required for efficient activation of Chk2 in response to ionizing radiation." Cancer Res **60**(21): 5934-5936.

Albino, A. P., X. Huang, et al. (2004). "Induction of H2AX phosphorylation in pulmonary cells by tobacco smoke: a new assay for carcinogens." Cell Cycle **3**(8): 1062-1068.

Alcorta, D. A., Y. Xiong, et al. (1996). "Involvement of the cyclin-dependent kinase inhibitor p16 (INK4a) in replicative senescence of normal human fibroblasts." Proc Natl Acad Sci U S A **93**(24): 13742-13747.

Alder, J. K., J. J. Chen, et al. (2008). "Short telomeres are a risk factor for idiopathic pulmonary fibrosis." Proc Natl Acad Sci U S A **105**(35): 13051-13056.

Alder, J. K., J. D. Cogan, et al. (2011). "Ancestral mutation in telomerase causes defects in repeat addition processivity and manifests as familial pulmonary fibrosis." PLoS Genet **7**(3): e1001352.

Alder, J. K., N. Guo, et al. (2011). "Telomere length is a determinant of emphysema susceptibility." Am J Respir Crit Care Med **184**(8): 904-912.

Aldonyte, R., L. Jansson, et al. (2003). "Circulating monocytes from healthy individuals and COPD patients." Respir Res **4**: 11.

Alimonti, A., C. Nardella, et al. (2010). "A novel type of cellular senescence that can be enhanced in mouse models and human tumor xenografts to suppress prostate tumorigenesis." J Clin Invest **120**(3): 681-693.

Amsellem, V., G. Gary-Bobo, et al. (2011). "Telomere dysfunction causes sustained inflammation in chronic obstructive pulmonary disease." Am J Respir Crit Care Med **184**(12): 1358-1366.

Anderson, L., C. Henderson, et al. (2001). "Phosphorylation and rapid relocalization of 53BP1 to nuclear foci upon DNA damage." Mol Cell Biol **21**(5): 1719-1729.

Anisimov, V. N., M. A. Zabezhinski, et al. (2011). "Rapamycin increases lifespan and inhibits spontaneous tumorigenesis in inbred female mice." Cell Cycle **10**(24): 4230-4236.

Aoshiba, K., M. Koinuma, et al. (2003). "Immunohistochemical evaluation of oxidative stress in murine lungs after cigarette smoke exposure." Inhal Toxicol **15**(10): 1029-1038.

Aoshiba, K. and A. Nagai (2007). "Chronic lung inflammation in aging mice." FEBS Lett **581**(18): 3512-3516.

Aoshiba, K. and A. Nagai (2009). "Senescence hypothesis for the pathogenetic mechanism of chronic obstructive pulmonary disease." Proc Am Thorac Soc **6**(7): 596-601.

Aoshiba, K., F. Zhou, et al. (2012). "DNA damage as a molecular link in the pathogenesis of COPD in smokers." Eur Respir J **39**(6): 1368-1376.

Auerbach, O., J. B. Forman, et al. (1957). "Changes in the bronchial epithelium in relation to smoking and cancer of the lung; a report of progress." N Engl J Med **256**(3): 97-104.

Bae, N. S. and P. Baumann (2007). "A RAP1/TRF2 complex inhibits nonhomologous end-joining at human telomeric DNA ends." Mol Cell **26**(3): 323-334.

Baggiolini, M. and P. Loetscher (2000). "Chemokines in inflammation and immunity." Immunol Today **21**(9): 418-420.

Baird, D. M., J. Rowson, et al. (2003). "Extensive allelic variation and ultrashort telomeres in senescent human cells." Nat Genet **33**(2): 203-207.

Baker, D. J., C. Perez-Terzic, et al. (2008). "Opposing roles for p16Ink4a and p19Arf in senescence and ageing caused by BubR1 insufficiency." Nat Cell Biol **10**(7): 825-836.

Baker, D. J. and J. M. Sedivy (2013). "Probing the depths of cellular senescence." J Cell Biol **202**(1): 11-13.

Baker, D. J., T. Wijshake, et al. (2011). "Clearance of p16Ink4a-positive senescent cells delays ageing-associated disorders." Nature **479**(7372): 232-236.

Bakkenist, C. J. and M. B. Kastan (2003). "DNA damage activates ATM through intermolecular autophosphorylation and dimer dissociation." Nature **421**(6922): 499-506.

Ballinger, S. W., T. G. Bouder, et al. (1996). "Mitochondrial genome damage associated with cigarette smoking." Cancer Res **56**(24): 5692-5697.

Banin, S., L. Moyal, et al. (1998). "Enhanced phosphorylation of p53 by ATM in response to DNA damage." Science **281**(5383): 1674-1677.

Barnes, P. J. (2004). "Mediators of chronic obstructive pulmonary disease." Pharmacol Rev **56**(4): 515-548.

Barnes, P. J. (2013). "New anti-inflammatory targets for chronic obstructive pulmonary disease." Nat Rev Drug Discov **12**(7): 543-559.

Bartek, J. and J. Lukas (2003). "Chk1 and Chk2 kinases in checkpoint control and cancer." Cancer Cell **3**(5): 421-429.

Bartkova, J., N. Rezaei, et al. (2006). "Oncogene-induced senescence is part of the tumorigenesis barrier imposed by DNA damage checkpoints." Nature **444**(7119): 633-637.

Bartling, B. (2013). "Cellular senescence in normal and premature lung aging." Z Gerontol Geriatr **46**(7): 613-622.

Bavik, C., I. Coleman, et al. (2006). "The gene expression program of prostate fibroblast senescence modulates neoplastic epithelial cell proliferation through paracrine mechanisms." Cancer Res **66**(2): 794-802.

Bayreuther, K., H. P. Rodemann, et al. (1988). "Human skin fibroblasts in vitro differentiate along a terminal cell lineage." Proc Natl Acad Sci U S A **85**(14): 5112-5116.

Beausejour, C. M., A. Krtolica, et al. (2003). "Reversal of human cellular senescence: roles of the p53 and p16 pathways." EMBO J **22**(16): 4212-4222.

Bhowmik, A., T. A. Seemungal, et al. (2000). "Relation of sputum inflammatory markers to symptoms and lung function changes in COPD exacerbations." Thorax **55**(2): 114-120.

Bjedov, I., J. M. Toivonen, et al. (2010). "Mechanisms of life span extension by rapamycin in the fruit fly Drosophila melanogaster." Cell Metab **11**(1): 35-46.

Blackburn, E. H. (1991). "Structure and function of telomeres." Nature **350**(6319): 569-573.

Blagosklonny, M. V. (2012). "Cell cycle arrest is not yet senescence, which is not just cell cycle arrest: terminology for TOR-driven aging." Aging (Albany NY) **4**(3): 159-165.

Blasco, M. A., H. W. Lee, et al. (1997). "Telomere shortening and tumor formation by mouse cells lacking telomerase RNA." Cell **91**(1): 25-34.

Blasco, M. A., H. W. Lee, et al. (1997). "Mouse models for the study of telomerase." Ciba Found Symp **211**: 160-170; discussion 170-166.

Bodnar, A. G., M. Ouellette, et al. (1998). "Extension of life-span by introduction of telomerase into normal human cells." Science **279**(5349): 349-352.

Bordone, L., D. Cohen, et al. (2007). "SIRT1 transgenic mice show phenotypes resembling calorie restriction." Aging Cell **6**(6): 759-767.

Bourdin, A., P. R. Burgel, et al. (2009). "Recent advances in COPD: pathophysiology, respiratory physiology and clinical aspects, including comorbidities." Eur Respir Rev **18**(114): 198-212.

Brenneisen, P., J. Wenk, et al. (2000). "Activation of p70 ribosomal protein S6 kinase is an essential step in the DNA damage-dependent signaling pathway responsible for the ultraviolet B-mediated increase in interstitial collagenase (MMP-1) and stromelysin-1 (MMP-3) protein levels in human dermal fibroblasts." J Biol Chem **275**(6): 4336-4344.

Brookes, S., J. Rowe, et al. (2004). "Contribution of p16(INK4a) to replicative senescence of human fibroblasts." Exp Cell Res **298**(2): 549-559.

Brown, J. P., W. Wei, et al. (1997). "Bypass of senescence after disruption of p21CIP1/WAF1 gene in normal diploid human fibroblasts." Science **277**(5327): 831-834.

Brugarolas, J., C. Chandrasekaran, et al. (1995). "Radiation-induced cell cycle arrest compromised by p21 deficiency." Nature **377**(6549): 552-557.

Bulavin, D. V., C. Phillips, et al. (2004). "Inactivation of the Wip1 phosphatase inhibits mammary tumorigenesis through p38 MAPK-mediated activation of the p16(Ink4a)-p19(Arf) pathway." Nat Genet **36**(4): 343-350.

Bunz, F., A. Dutriaux, et al. (1998). "Requirement for p53 and p21 to sustain G2 arrest after DNA damage." Science **282**(5393): 1497-1501.

Burma, S., B. P. Chen, et al. (2001). "ATM phosphorylates histone H2AX in response to DNA double-strand breaks." J Biol Chem **276**(45): 42462-42467.

Burton, D. G. and V. Krizhanovsky (2014). "Physiological and pathological consequences of cellular senescence." Cell Mol Life Sci.

Caito, S., S. Rajendrasozhan, et al. (2010). "SIRT1 is a redox-sensitive deacetylase that is post-translationally modified by oxidants and carbonyl stress." FASEB J **24**(9): 3145-3159.

Calabrese, V., F. A. Mallette, et al. (2009). "SOCS1 links cytokine signaling to p53 and senescence." Mol Cell **36**(5): 754-767.

Campisi, J. (2001). "Cellular senescence as a tumor-suppressor mechanism." Trends Cell Biol **11**(11): S27-31.

Campisi, J. (2003). "Cancer and ageing: rival demons?" Nat Rev Cancer **3**(5): 339-349.

Campisi, J. (2013). "Aging, cellular senescence, and cancer." Annu Rev Physiol **75**: 685-705.

Campisi, J. and F. d'Adda di Fagagna (2007). "Cellular senescence: when bad things happen to good cells." Nat Rev Mol Cell Biol **8**(9): 729-740.

Caramori, G., I. M. Adcock, et al. (2011). "Unbalanced oxidant-induced DNA damage and repair in COPD: a link towards lung cancer." Thorax **66**(6): 521-527.

Cawthon, R. M., K. R. Smith, et al. (2003). "Association between telomere length in blood and mortality in people aged 60 years or older." Lancet **361**(9355): 393-395.

Cesare, A. J., Z. Kaul, et al. (2009). "Spontaneous occurrence of telomeric DNA damage response in the absence of chromosome fusions." Nat Struct Mol Biol **16**(12): 1244-1251.

Chance, B., H. Sies, et al. (1979). "Hydroperoxide metabolism in mammalian organs." Physiol Rev **59**(3): 527-605.

Chang, B. D., M. E. Swift, et al. (2002). "Molecular determinants of terminal growth arrest induced in tumor cells by a chemotherapeutic agent." Proc Natl Acad Sci U S A **99**(1): 389-394.

Chehab, N. H., A. Malikzay, et al. (2000). "Chk2/hCds1 functions as a DNA damage checkpoint in G(1) by stabilizing p53." Genes Dev **14**(3): 278-288.

Chen, J. H., K. Stoeber, et al. (2004). "Loss of proliferative capacity and induction of senescence in oxidatively stressed human fibroblasts." J Biol Chem **279**(47): 49439-49446.

Chen, L., Q. Ge, et al. (2014). "Effects of cigarette smoke extract on human airway smooth muscle cells in COPD." Eur Respir J **44**(3): 634-646.

Chen, Q., A. Fischer, et al. (1995). "Oxidative DNA damage and senescence of human diploid fibroblast cells." Proc Natl Acad Sci U S A **92**(10): 4337-4341.

Chen, Q. M., K. R. Prowse, et al. (2001). "Uncoupling the senescent phenotype from telomere shortening in hydrogen peroxide-treated fibroblasts." Exp Cell Res **265**(2): 294-303.

Chen, Z. H., H. P. Kim, et al. (2008). "Egr-1 regulates autophagy in cigarette smoke-induced chronic obstructive pulmonary disease." PLoS One **3**(10): e3316.

Childs, B. G., D. J. Baker, et al. (2014). "Senescence and apoptosis: dueling or complementary cell fates?" EMBO Rep **15**(11): 1139-1153.

Choudhury, A. R., Z. Ju, et al. (2007). "Cdkn1a deletion improves stem cell function and lifespan of mice with dysfunctional telomeres without accelerating cancer formation." Nat Genet **39**(1): 99-105.

Chung, H. Y., M. Cesari, et al. (2009). "Molecular inflammation: underpinnings of aging and age-related diseases." Ageing Res Rev **8**(1): 18-30.

Chung, K. F. and I. M. Adcock (2008). "Multifaceted mechanisms in COPD: inflammation, immunity, and tissue repair and destruction." Eur Respir J **31**(6): 1334-1356.

Churg, A., R. D. Wang, et al. (2004). "Tumor necrosis factor-alpha drives 70% of cigarette smoke-induced emphysema in the mouse." Am J Respir Crit Care Med **170**(5): 492-498.

Cole, P. J. (1986). "Inflammation: a two-edged sword--the model of bronchiectasis." Eur J Respir Dis Suppl **147**: 6-15.

Collado, M., J. Gil, et al. (2005). "Tumour biology: senescence in premalignant tumours." Nature **436**(7051): 642.

Conboy, I. M., M. J. Conboy, et al. (2005). "Rejuvenation of aged progenitor cells by exposure to a young systemic environment." Nature **433**(7027): 760-764.

Coppe, J. P., K. Kauser, et al. (2006). "Secretion of vascular endothelial growth factor by primary human fibroblasts at senescence." J Biol Chem **281**(40): 29568-29574.

Coppe, J. P., C. K. Patil, et al. (2008). "Senescence-associated secretory phenotypes reveal cell-nonautonomous functions of oncogenic RAS and the p53 tumor suppressor." PLoS Biol **6**(12): 2853-2868.

Coppe, J. P., F. Rodier, et al. (2011). "Tumor suppressor and aging biomarker p16(INK4a) induces cellular senescence without the associated inflammatory secretory phenotype." J Biol Chem **286**(42): 36396-36403.

Correia-Melo, C., G. Hewitt, et al. (2014). "Telomeres, oxidative stress and inflammatory factors: partners in cellular senescence?" Longev Healthspan **3**(1): 1.

Cortez, D., S. Guntuku, et al. (2001). "ATR and ATRIP: partners in checkpoint signaling." Science **294**(5547): 1713-1716.

Crystal, R. G. (2014). "Airway Basal Cells: The "Smoking Gun" of COPD." Am J Respir Crit Care Med.

Csiszar, A., N. Labinskyy, et al. (2008). "Vasoprotective effects of resveratrol and SIRT1: attenuation of cigarette smoke-induced oxidative stress and proinflammatory phenotypic alterations." Am J Physiol Heart Circ Physiol **294**(6): H2721-2735.

Culpitt, S. V., D. F. Rogers, et al. (2003). "Impaired inhibition by dexamethasone of cytokine release by alveolar macrophages from patients with chronic obstructive pulmonary disease." Am J Respir Crit Care Med **167**(1): 24-31.

Cunningham, J. T., J. T. Rodgers, et al. (2007). "mTOR controls mitochondrial oxidative function through a YY1-PGC-1alpha transcriptional complex." Nature **450**(7170): 736-740.

d'Adda di Fagagna, F. (2008). "Living on a break: cellular senescence as a DNA-damage response." Nat Rev Cancer **8**(7): 512-522.

d'Adda di Fagagna, F., P. M. Reaper, et al. (2003). "A DNA damage checkpoint response in telomere-initiated senescence." Nature **426**(6963): 194-198.

d'Adda di Fagagna, F., S. H. Teo, et al. (2004). "Functional links between telomeres and proteins of the DNA-damage response." Genes Dev **18**(15): 1781-1799.

D'Amours, D. and S. P. Jackson (2002). "The Mre11 complex: at the crossroads of dna repair and checkpoint signalling." Nat Rev Mol Cell Biol **3**(5): 317-327.

D'Hulst A, I., K. Y. Vermaelen, et al. (2005). "Time course of cigarette smoke-induced pulmonary inflammation in mice." Eur Respir J **26**(2): 204-213.

Dan, H. C., M. J. Cooper, et al. (2008). "Akt-dependent regulation of NF-{kappa}B is controlled by mTOR and Raptor in association with IKK." Genes Dev **22**(11): 1490-1500.

Davis, T. and D. Kipling (2009). "Assessing the role of stress signalling via p38 MAP kinase in the premature senescence of ataxia telangiectasia and Werner syndrome fibroblasts." Biogerontology **10**(3): 253-266.

de Lange, T. (2005). "Shelterin: the protein complex that shapes and safeguards human telomeres." Genes Dev **19**(18): 2100-2110.

Dechat, T., K. Pfleghaar, et al. (2008). "Nuclear lamins: major factors in the structural organization and function of the nucleus and chromatin." Genes Dev **22**(7): 832-853.

Demedts, I. K., T. Demoor, et al. (2006). "Role of apoptosis in the pathogenesis of COPD and pulmonary emphysema." Respir Res **7**: 53.

Demidenko, Z. N. and M. V. Blagosklonny (2008). "Growth stimulation leads to cellular senescence when the cell cycle is blocked." Cell Cycle **7**(21): 3355-3361.

Demidenko, Z. N., S. G. Zubova, et al. (2009). "Rapamycin decelerates cellular senescence." Cell Cycle **8**(12): 1888-1895.

Deng, Q., R. Liao, et al. (2004). "High intensity ras signaling induces premature senescence by activating p38 pathway in primary human fibroblasts." J Biol Chem **279**(2): 1050-1059.

DePinho, R. A. (2000). "The age of cancer." Nature **408**(6809): 248-254.

Deslee, G., T. L. Adair-Kirk, et al. (2010). "Cigarette smoke induces nucleic-acid oxidation in lung fibroblasts." Am J Respir Cell Mol Biol **43**(5): 576-584.

Deslee, G., J. C. Woods, et al. (2009). "Oxidative damage to nucleic acids in severe emphysema." Chest **135**(4): 965-974.

Di Francia, M., D. Barbier, et al. (1994). "Tumor necrosis factor-alpha levels and weight loss in chronic obstructive pulmonary disease." Am J Respir Crit Care Med **150**(5 Pt 1): 1453-1455.

Di Leonardo, A., S. P. Linke, et al. (1994). "DNA damage triggers a prolonged p53-dependent G1 arrest and long-term induction of Cip1 in normal human fibroblasts." Genes Dev **8**(21): 2540-2551.

Di Micco, R., M. Fumagalli, et al. (2006). "Oncogene-induced senescence is a DNA damage response triggered by DNA hyper-replication." Nature **444**(7119): 638-642.

Dierick, J. F., F. Eliaers, et al. (2002). "Stress-induced premature senescence and replicative senescence are different phenotypes, proteomic evidence." Biochem Pharmacol **64**(5-6): 1011-1017.

Dimri, G. P. (2005). "What has senescence got to do with cancer?" Cancer Cell **7**(6): 505-512.

Dimri, G. P., E. Hara, et al. (1994). "Regulation of two E2F-related genes in presenescent and senescent human fibroblasts." J Biol Chem **269**(23): 16180-16186.

Dimri, G. P., K. Itahana, et al. (2000). "Regulation of a senescence checkpoint response by the E2F1 transcription factor and p14(ARF) tumor suppressor." Mol Cell Biol **20**(1): 273-285.

Dimri, G. P., X. Lee, et al. (1995). "A biomarker that identifies senescent human cells in culture and in aging skin in vivo." Proc Natl Acad Sci U S A **92**(20): 9363-9367.

Doz, E., N. Noulin, et al. (2008). "Cigarette smoke-induced pulmonary inflammation is TLR4/MyD88 and IL-1R1/MyD88 signaling dependent." J Immunol **180**(2): 1169-1178.

Dulic, V., L. F. Drullinger, et al. (1993). "Altered regulation of G1 cyclins in senescent human diploid fibroblasts: accumulation of inactive cyclin E-Cdk2 and cyclin D1-Cdk2 complexes." Proc Natl Acad Sci U S A **90**(23): 11034-11038.

Effros, R. B. and G. Pawelec (1997). "Replicative senescence of T cells: does the Hayflick Limit lead to immune exhaustion?" Immunol Today **18**(9): 450-454.

Ekim, B., B. Magnuson, et al. (2011). "mTOR kinase domain phosphorylation promotes mTORC1 signaling, cell growth, and cell cycle progression." Mol Cell Biol **31**(14): 2787-2801.

Eliezer, Y., L. Argaman, et al. (2009). "The direct interaction between 53BP1 and MDC1 is required for the recruitment of 53BP1 to sites of damage." J Biol Chem **284**(1): 426-435.

Ellis, R. E., J. Y. Yuan, et al. (1991). "Mechanisms and functions of cell death." Annu Rev Cell Biol **7**: 663-698.

Eltom, S., C. S. Stevenson, et al. (2011). "P2X7 receptor and caspase 1 activation are central to airway inflammation observed after exposure to tobacco smoke." PLoS One **6**(9): e24097.

Eurlings, I. M., N. L. Reynaert, et al. (2014). "Cigarette Smoke Extract Induces a Phenotypic Shift in Epithelial Cells; Involvement of HIF1alpha in Mesenchymal Transition." PLoS One **9**(10): e107757.

Fabrizio, P., F. Pozza, et al. (2001). "Regulation of longevity and stress resistance by Sch9 in yeast." Science **292**(5515): 288-290.

Faner, R., M. Rojas, et al. (2012). "Abnormal lung aging in chronic obstructive pulmonary disease and idiopathic pulmonary fibrosis." Am J Respir Crit Care Med **186**(4): 306-313.

Finkelstein, R., R. S. Fraser, et al. (1995). "Alveolar inflammation and its relation to emphysema in smokers." Am J Respir Crit Care Med **152**(5 Pt 1): 1666-1672.

Fischer, B. M., E. Pavlisko, et al. (2011). "Pathogenic triad in COPD: oxidative stress, protease-antiprotease imbalance, and inflammation." Int J Chron Obstruct Pulmon Dis **6**: 413-421.

Fischer, B. M., J. K. Wong, et al. (2013). "Increased expression of senescence markers in cystic fibrosis airways." Am J Physiol Lung Cell Mol Physiol **304**(6): L394-400.

Fletcher, C. and R. Peto (1977). "The natural history of chronic airflow obstruction." Br Med J **1**(6077): 1645-1648.

Fontana, L., L. Partridge, et al. (2010). "Extending healthy life span--from yeast to humans." Science **328**(5976): 321-326.

Forey, B. A., A. J. Thornton, et al. (2011). "Systematic review with meta-analysis of the epidemiological evidence relating smoking to COPD, chronic bronchitis and emphysema." BMC Pulm Med **11**: 36.

Franceschi, C. and J. Campisi (2014). "Chronic inflammation (inflammaging) and its potential contribution to age-associated diseases." J Gerontol A Biol Sci Med Sci **69 Suppl 1**: S4-9.

Franceschi, C., M. Capri, et al. (2007). "Inflammaging and anti-inflammaging: a systemic perspective on aging and longevity emerged from studies in humans." Mech Ageing Dev **128**(1): 92-105.

Freund, A., R. M. Laberge, et al. (2012). "Lamin B1 loss is a senescence-associated biomarker." Mol Biol Cell **23**(11): 2066-2075.

Freund, A., A. V. Orjalo, et al. (2010). "Inflammatory networks during cellular senescence: causes and consequences." Trends Mol Med **16**(5): 238-246.

Freund, A., C. K. Patil, et al. (2011). "p38MAPK is a novel DNA damage response-independent regulator of the senescence-associated secretory phenotype." EMBO J **30**(8): 1536-1548.

Fujii, S., H. Hara, et al. (2012). "Insufficient autophagy promotes bronchial epithelial cell senescence in chronic obstructive pulmonary disease." Oncoimmunology **1**(5): 630-641.

Fumagalli, M., F. Rossiello, et al. (2012). "Telomeric DNA damage is irreparable and causes persistent DNA-damage-response activation." Nat Cell Biol **14**(4): 355-365.

Fumagalli, M., F. Rossiello, et al. (2014). "Stable Cellular Senescence Is Associated with Persistent DDR Activation." PLoS One **9**(10): e110969.

Ganesan, S., A. T. Comstock, et al. (2014). "Combined exposure to cigarette smoke and nontypeable Haemophilus influenzae drives development of a COPD phenotype in mice." Respir Res **15**: 11.

Gao, W., Z. Shen, et al. (2011). "Upregulation of human autophagy-initiation kinase ULK1 by tumor suppressor p53 contributes to DNA-damage-induced cell death." Cell Death Differ **18**(10): 1598-1607.

Gatta, R., D. Dolfini, et al. (2011). "NF-Y joins E2Fs, p53 and other stress transcription factors at the apoptosis table." Cell Death Dis **2**: e162.

Gire, V., P. Roux, et al. (2004). "DNA damage checkpoint kinase Chk2 triggers replicative senescence." EMBO J **23**(13): 2554-2563.

Gomes, N. M., O. A. Ryder, et al. (2011). "Comparative biology of mammalian telomeres: hypotheses on ancestral states and the roles of telomeres in longevity determination." Aging Cell **10**(5): 761-768.

Gorbunova, V., A. Seluanov, et al. (2002). "Expression of human telomerase (hTERT) does not prevent stress-induced senescence in normal human fibroblasts but protects the cells from stress-induced apoptosis and necrosis." J Biol Chem **277**(41): 38540-38549.

Green, D. R. and G. I. Evan (2002). "A matter of life and death." Cancer Cell **1**(1): 19-30.

Griffith, J. D., L. Comeau, et al. (1999). "Mammalian telomeres end in a large duplex loop." Cell **97**(4): 503-514.

Haake, A. R., I. Roublevskaia, et al. (1998). "Apoptosis: a role in skin aging?" J Investig Dermatol Symp Proc **3**(1): 28-35.

Hamilton, M. L., H. Van Remmen, et al. (2001). "Does oxidative damage to DNA increase with age?" Proc Natl Acad Sci U S A **98**(18): 10469-10474.

Hampel, B., F. Malisan, et al. (2004). "Differential regulation of apoptotic cell death in senescent human cells." Exp Gerontol **39**(11-12): 1713-1721.

Hansen, M., S. Taubert, et al. (2007). "Lifespan extension by conditions that inhibit translation in Caenorhabditis elegans." Aging Cell **6**(1): 95-110.

Hara, H., J. Araya, et al. (2013). "Mitochondrial fragmentation in cigarette smoke-induced bronchial epithelial cell senescence." Am J Physiol Lung Cell Mol Physiol **305**(10): L737-746.

Hara, H., J. Araya, et al. (2012). "Involvement of creatine kinase B in cigarette smoke-induced bronchial epithelial cell senescence." Am J Respir Cell Mol Biol **46**(3): 306-312.

Harley, C. B., A. B. Futcher, et al. (1990). "Telomeres shorten during ageing of human fibroblasts." Nature **345**(6274): 458-460.

Harman, D. (1956). "Aging: a theory based on free radical and radiation chemistry." J Gerontol **11**(3): 298-300.

Harman, D. (1972). "Free radical theory of aging: dietary implications." Am J Clin Nutr **25**(8): 839-843.

Harper, J. W., G. R. Adami, et al. (1993). "The p21 Cdk-interacting protein Cip1 is a potent inhibitor of G1 cyclin-dependent kinases." Cell **75**(4): 805-816.

Harrison, D. E., R. Strong, et al. (2009). "Rapamycin fed late in life extends lifespan in genetically heterogeneous mice." Nature **460**(7253): 392-395.

Hayflick, L. (1965). "The Limited in Vitro Lifetime of Human Diploid Cell Strains." Exp Cell Res **37**: 614-636.

Hayflick, L. and P. S. Moorhead (1961). "The serial cultivation of human diploid cell strains." Exp Cell Res **25**: 585-621.

Helt, C. E., W. A. Cliby, et al. (2005). "Ataxia telangiectasia mutated (ATM) and ATM and Rad3-related protein exhibit selective target specificities in response to different forms of DNA damage." J Biol Chem **280**(2): 1186-1192.

Hemann, M. T., M. A. Strong, et al. (2001). "The shortest telomere, not average telomere length, is critical for cell viability and chromosome stability." Cell **107**(1): 67-77.

Henle, E. S., Z. Han, et al. (1999). "Sequence-specific DNA cleavage by Fe2+-mediated fenton reactions has possible biological implications." J Biol Chem **274**(2): 962-971.

Herbig, U., M. Ferreira, et al. (2006). "Cellular senescence in aging primates." Science **311**(5765): 1257.

Herbig, U., W. A. Jobling, et al. (2004). "Telomere shortening triggers senescence of human cells through a pathway involving ATM, p53, and p21(CIP1), but not p16(INK4a)." Mol Cell **14**(4): 501-513.

Herbig, U., W. Wei, et al. (2003). "Real-time imaging of transcriptional activation in live cells reveals rapid up-regulation of the cyclin-dependent kinase inhibitor gene CDKN1A in replicative cellular senescence." Aging Cell **2**(6): 295-304.

Hewitt, G., D. Jurk, et al. (2012). "Telomeres are favoured targets of a persistent DNA damage response in ageing and stress-induced senescence." Nat Commun **3**: 708.

Hinojosa, C. A., V. Mgbemena, et al. (2012). "Enteric-delivered rapamycin enhances resistance of aged mice to pneumococcal pneumonia through reduced cellular senescence." Exp Gerontol **47**(12): 958-965.

Hodge, S., G. Hodge, et al. (2005). "Increased airway epithelial and T-cell apoptosis in COPD remains despite smoking cessation." Eur Respir J **25**(3): 447-454.

Hogg, J. C. and W. Timens (2009). "The pathology of chronic obstructive pulmonary disease." Annu Rev Pathol **4**: 435-459.

Holz, O., I. Zuhlke, et al. (2004). "Lung fibroblasts from patients with emphysema show a reduced proliferation rate in culture." Eur Respir J **24**(4): 575-579.

Hong, K. U., S. D. Reynolds, et al. (2004). "Basal cells are a multipotent progenitor capable of renewing the bronchial epithelium." Am J Pathol **164**(2): 577-588.

Houben, J. M., E. M. Mercken, et al. (2009). "Telomere shortening in chronic obstructive pulmonary disease." Respir Med **103**(2): 230-236.

Howard, B. H. (1996). "Replicative senescence: considerations relating to the stability of heterochromatin domains." Exp Gerontol **31**(1-2): 281-293.

Howitz, K. T., K. J. Bitterman, et al. (2003). "Small molecule activators of sirtuins extend Saccharomyces cerevisiae lifespan." Nature **425**(6954): 191-196.

Huang, J., M. Okuka, et al. (2013). "Telomere shortening and DNA damage of embryonic stem cells induced by cigarette smoke." Reprod Toxicol **35**: 89-95.

Hutter, E., K. Renner, et al. (2004). "Senescence-associated changes in respiration and oxidative phosphorylation in primary human fibroblasts." Biochem J **380**(Pt 3): 919-928.

Huyen, Y., O. Zgheib, et al. (2004). "Methylated lysine 79 of histone H3 targets 53BP1 to DNA double-strand breaks." Nature **432**(7015): 406-411.

Hwang, J. W., S. Chung, et al. (2010). "Cigarette smoke-induced autophagy is regulated by SIRT1-PARP-1-dependent mechanism: implication in pathogenesis of COPD." Arch Biochem Biophys **500**(2): 203-209.

Igishi, T., Y. Hitsuda, et al. (2003). "Elevated urinary 8-hydroxydeoxyguanosine, a biomarker of oxidative stress, and lack of association with antioxidant vitamins in chronic obstructive pulmonary disease." Respirology **8**(4): 455-460.

Ishii, T., T. Matsuse, et al. (2001). "Tobacco smoke reduces viability in human lung fibroblasts: protective effect of glutathione S-transferase P1." Am J Physiol Lung Cell Mol Physiol **280**(6): L1189-1195.

Itahana, K., Y. Zou, et al. (2003). "Control of the replicative life span of human fibroblasts by p16 and the polycomb protein Bmi-1." Mol Cell Biol **23**(1): 389-401.

Ito, K. and P. J. Barnes (2009). "COPD as a disease of accelerated lung aging." Chest **135**(1): 173-180.

Ito, K., A. Hirao, et al. (2006). "Reactive oxygen species act through p38 MAPK to limit the lifespan of hematopoietic stem cells." Nat Med **12**(4): 446-451.

Ivanov, A., J. Pawlikowski, et al. (2013). "Lysosome-mediated processing of chromatin in senescence." J Cell Biol **202**(1): 129-143.

Iwasa, H., J. Han, et al. (2003). "Mitogen-activated protein kinase p38 defines the common senescence-signalling pathway." Genes Cells **8**(2): 131-144.

Jackson, J. G. and O. M. Pereira-Smith (2006). "p53 is preferentially recruited to the promoters of growth arrest genes p21 and GADD45 during replicative senescence of normal human fibroblasts." Cancer Res **66**(17): 8356-8360.

Jacobs, J. J. and T. de Lange (2004). "Significant role for p16INK4a in p53-independent telomere-directed senescence." Curr Biol **14**(24): 2302-2308.

Janssens, J. P., J. C. Pache, et al. (1999). "Physiological changes in respiratory function associated with ageing." Eur Respir J **13**(1): 197-205.

Jazayeri, A., J. Falck, et al. (2006). "ATM- and cell cycle-dependent regulation of ATR in response to DNA double-strand breaks." Nat Cell Biol **8**(1): 37-45.

Jeyapalan, J. C., M. Ferreira, et al. (2007). "Accumulation of senescent cells in mitotic tissue of aging primates." Mech Ageing Dev **128**(1): 36-44.

Jia, K., D. Chen, et al. (2004). "The TOR pathway interacts with the insulin signaling pathway to regulate C. elegans larval development, metabolism and life span." Development **131**(16): 3897-3906.

Johnson, S. C., P. S. Rabinovitch, et al. (2013). "mTOR is a key modulator of ageing and age-related disease." Nature **493**(7432): 338-345.

Johnson, S. C., M. E. Yanos, et al. (2013). "mTOR inhibition alleviates mitochondrial disease in a mouse model of Leigh syndrome." Science **342**(6165): 1524-1528.

Jun, J. I. and L. F. Lau (2010). "The matricellular protein CCN1 induces fibroblast senescence and restricts fibrosis in cutaneous wound healing." Nat Cell Biol **12**(7): 676-685.

Jurk, D., C. Wang, et al. (2012). "Postmitotic neurons develop a p21-dependent senescence-like phenotype driven by a DNA damage response." Aging Cell **11**(6): 996-1004.

Jurk, D., C. Wilson, et al. (2014). "Chronic inflammation induces telomere dysfunction and accelerates ageing in mice." Nat Commun **2**: 4172.

Kaeberlein, M., R. W. Powers, 3rd, et al. (2005). "Regulation of yeast replicative life span by TOR and Sch9 in response to nutrients." Science **310**(5751): 1193-1196.

Kanaji, N., H. Basma, et al. (2014). "Fibroblasts that resist cigarette smoke-induced senescence acquire profibrotic phenotypes." Am J Physiol Lung Cell Mol Physiol **307**(5): L364-373.

Kang, H. T., H. I. Lee, et al. (2006). "Nicotinamide extends replicative lifespan of human cells." Aging Cell **5**(5): 423-436.

Kang, T. W., T. Yevsa, et al. (2011). "Senescence surveillance of pre-malignant hepatocytes limits liver cancer development." Nature **479**(7374): 547-551.

Kapahi, P., B. M. Zid, et al. (2004). "Regulation of lifespan in Drosophila by modulation of genes in the TOR signaling pathway." Curr Biol **14**(10): 885-890.

Kaplon, J., L. Zheng, et al. (2013). "A key role for mitochondrial gatekeeper pyruvate dehydrogenase in oncogene-induced senescence." Nature **498**(7452): 109-112.

Kasahara, Y., R. M. Tuder, et al. (2001). "Endothelial cell death and decreased expression of vascular endothelial growth factor and vascular endothelial growth factor receptor 2 in emphysema." Am J Respir Crit Care Med **163**(3 Pt 1): 737-744.

Kasai, H. (1997). "Analysis of a form of oxidative DNA damage, 8-hydroxy-2'-deoxyguanosine, as a marker of cellular oxidative stress during carcinogenesis." Mutat Res **387**(3): 147-163.

Kaul, Z., A. J. Cesare, et al. (2012). "Five dysfunctional telomeres predict onset of senescence in human cells." EMBO Rep **13**(1): 52-59.

Keatings, V. M., P. D. Collins, et al. (1996). "Differences in interleukin-8 and tumor necrosis factor-alpha in induced sputum from patients with chronic obstructive pulmonary disease or asthma." Am J Respir Crit Care Med **153**(2): 530-534.

Kennedy, A. L., J. P. Morton, et al. (2011). "Activation of the PIK3CA/AKT pathway suppresses senescence induced by an activated RAS oncogene to promote tumorigenesis." Mol Cell **42**(1): 36-49.

Kenyon, C. J. (2010). "The genetics of ageing." Nature **464**(7288): 504-512.

Kim, H., X. Liu, et al. (2004). "Reversible cigarette smoke extract-induced DNA damage in human lung fibroblasts." Am J Respir Cell Mol Biol **31**(5): 483-490.

King, P. (2011). "Pathogenesis of bronchiectasis." Paediatr Respir Rev **12**(2): 104-110.

Kiyono, T., S. A. Foster, et al. (1998). "Both Rb/p16INK4a inactivation and telomerase activity are required to immortalize human epithelial cells." Nature **396**(6706): 84-88.

Kolesnichenko, M., L. Hong, et al. (2012). "Attenuation of TORC1 signaling delays replicative and oncogenic RAS-induced senescence." Cell Cycle **11**(12): 2391-2401.

Korotchkina, L. G., O. V. Leontieva, et al. (2010). "The choice between p53-induced senescence and quiescence is determined in part by the mTOR pathway." Aging (Albany NY) **2**(6): 344-352.

Kowald, A. and T. B. Kirkwood (2011). "The evolution and role of mitochondrial fusion and fission in aging and disease." Commun Integr Biol **4**(5): 627-629.

Kranenburg, A. R., W. I. De Boer, et al. (2002). "Enhanced expression of fibroblast growth factors and receptor FGFR-1 during vascular remodeling in chronic obstructive pulmonary disease." Am J Respir Cell Mol Biol **27**(5): 517-525.

Kreiling, J. A., M. Tamamori-Adachi, et al. (2011). "Age-associated increase in heterochromatic marks in murine and primate tissues." Aging Cell **10**(2): 292-304.

Krimpenfort, P., K. C. Quon, et al. (2001). "Loss of p16Ink4a confers susceptibility to metastatic melanoma in mice." Nature **413**(6851): 83-86.

Krishnamurthy, J., C. Torrice, et al. (2004). "Ink4a/Arf expression is a biomarker of aging." J Clin Invest **114**(9): 1299-1307.

Krizhanovsky, V., M. Yon, et al. (2008). "Senescence of activated stellate cells limits liver fibrosis." Cell **134**(4): 657-667.

Krtolica, A., S. Parrinello, et al. (2001). "Senescent fibroblasts promote epithelial cell growth and tumorigenesis: a link between cancer and aging." Proc Natl Acad Sci U S A **98**(21): 12072-12077.

Kuilman, T., C. Michaloglou, et al. (2010). "The essence of senescence." <u>Genes Dev</u> **24**(22): 2463-2479.

Kuilman, T., C. Michaloglou, et al. (2008). "Oncogene-induced senescence relayed by an interleukin-dependent inflammatory network." <u>Cell</u> **133**(6): 1019-1031.

Kuilman, T. and D. S. Peeper (2009). "Senescence-messaging secretome: SMS-ing cellular stress." <u>Nat Rev Cancer</u> **9**(2): 81-94.

Kumar, M., W. Seeger, et al. (2014). "Senescence-associated secretory phenotype and its possible role in chronic obstructive pulmonary disease." <u>Am J Respir Cell Mol Biol</u> **51**(3): 323-333.

Laberge, R. M., P. Awad, et al. (2012). "Epithelial-mesenchymal transition induced by senescent fibroblasts." <u>Cancer Microenviron</u> **5**(1): 39-44.

Lanna, A., S. M. Henson, et al. (2014). "The kinase p38 activated by the metabolic regulator AMPK and scaffold TAB1 drives the senescence of human T cells." <u>Nat Immunol</u>.

Lansdorp, P. M., N. P. Verwoerd, et al. (1996). "Heterogeneity in telomere length of human chromosomes." <u>Hum Mol Genet</u> **5**(5): 685-691.

Laplante, M. and D. M. Sabatini (2012). "mTOR signaling in growth control and disease." <u>Cell</u> **149**(2): 274-293.

Lawless, C., C. Wang, et al. (2010). "Quantitative assessment of markers for cell senescence." <u>Exp Gerontol</u> **45**(10): 772-778.

Lazzerini Denchi, E., C. Attwooll, et al. (2005). "Deregulated E2F activity induces hyperplasia and senescence-like features in the mouse pituitary gland." <u>Mol Cell Biol</u> **25**(7): 2660-2672.

Lechel, A., A. Satyanarayana, et al. (2005). "The cellular level of telomere dysfunction determines induction of senescence or apoptosis in vivo." <u>EMBO Rep</u> **6**(3): 275-281.

Lee, B. Y., J. A. Han, et al. (2006). "Senescence-associated beta-galactosidase is lysosomal beta-galactosidase." <u>Aging Cell</u> **5**(2): 187-195.

Lee, H. W., M. A. Blasco, et al. (1998). "Essential role of mouse telomerase in highly proliferative organs." <u>Nature</u> **392**(6676): 569-574.

Lee, J., R. Reddy, et al. (2009). "Lung alveolar integrity is compromised by telomere shortening in telomerase-null mice." <u>Am J Physiol Lung Cell Mol Physiol</u> **296**(1): L57-70.

Lee, J., A. Sandford, et al. (2011). "Is the aging process accelerated in chronic obstructive pulmonary disease?" <u>Curr Opin Pulm Med</u> **17**(2): 90-97.

Lee, J. H. and T. T. Paull (2005). "ATM activation by DNA double-strand breaks through the Mre11-Rad50-Nbs1 complex." <u>Science</u> **308**(5721): 551-554.

Lerner, C., A. Bitto, et al. (2013). "Reduced mammalian target of rapamycin activity facilitates mitochondrial retrograde signaling and increases life span in normal human fibroblasts." <u>Aging Cell</u> **12**(6): 966-977.

Li, M., C. L. Brooks, et al. (2003). "Mono- versus polyubiquitination: differential control of p53 fate by Mdm2." <u>Science</u> **302**(5652): 1972-1975.

Lin, A. W., M. Barradas, et al. (1998). "Premature senescence involving p53 and p16 is activated in response to constitutive MEK/MAPK mitogenic signaling." <u>Genes Dev</u> **12**(19): 3008-3019.

Lin, S. J., P. A. Defossez, et al. (2000). "Requirement of NAD and SIR2 for life-span extension by calorie restriction in Saccharomyces cerevisiae." <u>Science</u> **289**(5487): 2126-2128.

Liu, X., H. Conner, et al. (2005). "Cigarette smoke extract induces DNA damage but not apoptosis in human bronchial epithelial cells." <u>Am J Respir Cell Mol Biol</u> **33**(2): 121-129.

Liu, Y., H. K. Sanoff, et al. (2009). "Expression of p16(INK4a) in peripheral blood T-cells is a biomarker of human aging." <u>Aging Cell</u> **8**(4): 439-448.

Lokke, A., P. Lange, et al. (2006). "Developing COPD: a 25 year follow up study of the general population." <u>Thorax</u> **61**(11): 935-939.

Lopez-Otin, C., M. A. Blasco, et al. (2013). "The hallmarks of aging." <u>Cell</u> **153**(6): 1194-1217.

Lujambio, A., L. Akkari, et al. (2013). "Non-cell-autonomous tumor suppression by p53." <u>Cell</u> **153**(2): 449-460.

Macaluso, M., M. Montanari, et al. (2006). "Rb family proteins as modulators of gene expression and new aspects regarding the interaction with chromatin remodeling enzymes." <u>Oncogene</u> **25**(38): 5263-5267.

Macip, S., M. Igarashi, et al. (2002). "Inhibition of p21-mediated ROS accumulation can rescue p21-induced senescence." <u>EMBO J</u> **21**(9): 2180-2188.

MacNee, W. (2001). "Oxidants/antioxidants and chronic obstructive pulmonary disease: pathogenesis to therapy." <u>Novartis Found Symp</u> **234**: 169-185; discussion 185-168.

MacNee, W. (2009). "Accelerated lung aging: a novel pathogenic mechanism of chronic obstructive pulmonary disease (COPD)." <u>Biochem Soc Trans</u> **37**(Pt 4): 819-823.

Majumder, S., A. Richardson, et al. (2011). "Inducing autophagy by rapamycin before, but not after, the formation of plaques and tangles ameliorates cognitive deficits." <u>PLoS One</u> **6**(9): e25416.

Mannino, D. M. and A. S. Buist (2007). "Global burden of COPD: risk factors, prevalence, and future trends." <u>Lancet</u> **370**(9589): 765-773.

Martens, J. W., A. M. Sieuwerts, et al. (2003). "Aging of stromal-derived human breast fibroblasts might contribute to breast cancer progression." <u>Thromb Haemost</u> **89**(2): 393-404.

Martin-Ruiz, C., G. Saretzki, et al. (2004). "Stochastic variation in telomere shortening rate causes heterogeneity of human fibroblast replicative life span." <u>J Biol Chem</u> **279**(17): 17826-17833.

Mason, D. X., T. J. Jackson, et al. (2004). "Molecular signature of oncogenic ras-induced senescence." <u>Oncogene</u> **23**(57): 9238-9246.

Maya, R., M. Balass, et al. (2001). "ATM-dependent phosphorylation of Mdm2 on serine 395: role in p53 activation by DNA damage." <u>Genes Dev</u> **15**(9): 1067-1077.

McConnell, B. B., M. Starborg, et al. (1998). "Inhibitors of cyclin-dependent kinases induce features of replicative senescence in early passage human diploid fibroblasts." <u>Curr Biol</u> **8**(6): 351-354.

McCool, K. W. and S. Miyamoto (2012). "DNA damage-dependent NF-kappaB activation: NEMO turns nuclear signaling inside out." <u>Immunol Rev</u> **246**(1): 311-326.

McMullen, J. R., M. C. Sherwood, et al. (2004). "Inhibition of mTOR signaling with rapamycin regresses established cardiac hypertrophy induced by pressure overload." <u>Circulation</u> **109**(24): 3050-3055.

McShane, P. J., E. T. Naureckas, et al. (2013). "Non-cystic fibrosis bronchiectasis." <u>Am J Respir Crit Care Med</u> **188**(6): 647-656.

McShea, A., P. L. Harris, et al. (1997). "Abnormal expression of the cell cycle regulators P16 and CDK4 in Alzheimer's disease." Am J Pathol **150**(6): 1933-1939.

Mehta, I. S., M. Figgitt, et al. (2007). "Alterations to nuclear architecture and genome behavior in senescent cells." Ann N Y Acad Sci **1100**: 250-263.

Melk, A., W. Kittikowit, et al. (2003). "Cell senescence in rat kidneys in vivo increases with growth and age despite lack of telomere shortening." Kidney Int **63**(6): 2134-2143.

Meng, A., Y. Wang, et al. (2003). "Ionizing radiation and busulfan induce premature senescence in murine bone marrow hematopoietic cells." Cancer Res **63**(17): 5414-5419.

Mercer, R. R., M. L. Russell, et al. (1994). "Cell number and distribution in human and rat airways." Am J Respir Cell Mol Biol **10**(6): 613-624.

Michaloglou, C., L. C. Vredeveld, et al. (2005). "BRAFE600-associated senescence-like cell cycle arrest of human naevi." Nature **436**(7051): 720-724.

Michan, S. and D. Sinclair (2007). "Sirtuins in mammals: insights into their biological function." Biochem J **404**(1): 1-13.

Miller, R. A., D. E. Harrison, et al. (2011). "Rapamycin, but not resveratrol or simvastatin, extends life span of genetically heterogeneous mice." J Gerontol A Biol Sci Med Sci **66**(2): 191-201.

Millis, A. J., M. Hoyle, et al. (1992). "Differential expression of metalloproteinase and tissue inhibitor of metalloproteinase genes in aged human fibroblasts." Exp Cell Res **201**(2): 373-379.

Minagawa, S., J. Araya, et al. (2011). "Accelerated epithelial cell senescence in IPF and the inhibitory role of SIRT6 in TGF-beta-induced senescence of human bronchial epithelial cells." Am J Physiol Lung Cell Mol Physiol **300**(3): L391-401.

Mio, T., D. J. Romberger, et al. (1997). "Cigarette smoke induces interleukin-8 release from human bronchial epithelial cells." Am J Respir Crit Care Med **155**(5): 1770-1776.

Moiseeva, O., V. Bourdeau, et al. (2009). "Mitochondrial dysfunction contributes to oncogene-induced senescence." Mol Cell Biol **29**(16): 4495-4507.

Moiseeva, O., F. A. Mallette, et al. (2006). "DNA damage signaling and p53-dependent senescence after prolonged beta-interferon stimulation." Mol Biol Cell **17**(4): 1583-1592.

Moon, H. G., Y. Zheng, et al. (2013). "CCN1 secretion induced by cigarette smoking extracts augments IL-8 release from bronchial epithelial cells." PLoS One **8**(7): e68199.

Morla, M., X. Busquets, et al. (2006). "Telomere shortening in smokers with and without COPD." Eur Respir J **27**(3): 525-528.

Mui, T. S., J. M. Man, et al. (2009). "Telomere length and chronic obstructive pulmonary disease: evidence of accelerated aging." J Am Geriatr Soc **57**(12): 2372-2374.

Muller, K. C., L. Welker, et al. (2006). "Lung fibroblasts from patients with emphysema show markers of senescence in vitro." Respir Res **7**: 32.

Munoz-Espin, D., M. Canamero, et al. (2013). "Programmed cell senescence during mammalian embryonic development." Cell **155**(5): 1104-1118.

Munro, J., N. I. Barr, et al. (2004). "Histone deacetylase inhibitors induce a senescence-like state in human cells by a p16-dependent mechanism that is independent of a mitotic clock." Exp Cell Res **295**(2): 525-538.

Muskhelishvili, L., J. R. Latendresse, et al. (2003). "Evaluation of cell proliferation in rat tissues with BrdU, PCNA, Ki-67(MIB-5) immunohistochemistry and in situ hybridization for histone mRNA." J Histochem Cytochem **51**(12): 1681-1688.

Nakajima, M., O. Kawanami, et al. (1998). "Immunohistochemical and ultrastructural studies of basal cells, Clara cells and bronchiolar cuboidal cells in normal human airways." Pathol Int **48**(12): 944-953.

Nakamaru, Y., C. Vuppusetty, et al. (2009). "A protein deacetylase SIRT1 is a negative regulator of metalloproteinase-9." FASEB J **23**(9): 2810-2819.

Nakamura, A. J., Y. J. Chiang, et al. (2008). "Both telomeric and non-telomeric DNA damage are determinants of mammalian cellular senescence." Epigenetics Chromatin **1**(1): 6.

Nakamura, K., W. Sakai, et al. (2006). "Genetic dissection of vertebrate 53BP1: a major role in non-homologous end joining of DNA double strand breaks." DNA Repair (Amst) **5**(6): 741-749.

Nakamura, M., S. Ohsawa, et al. (2014). "Mitochondrial defects trigger proliferation of neighbouring cells via a senescence-associated secretory phenotype in Drosophila." Nat Commun **5**: 5264.

Nakamura, Y., D. J. Romberger, et al. (1995). "Cigarette smoke inhibits lung fibroblast proliferation and chemotaxis." Am J Respir Crit Care Med **151**(5): 1497-1503.

Namiki, Y. and L. Zou (2006). "ATRIP associates with replication protein A-coated ssDNA through multiple interactions." Proc Natl Acad Sci U S A **103**(3): 580-585.

Narita, M., S. Nunez, et al. (2003). "Rb-mediated heterochromatin formation and silencing of E2F target genes during cellular senescence." Cell **113**(6): 703-716.

Naylor, R. M., D. J. Baker, et al. (2013). "Senescent cells: a novel therapeutic target for aging and age-related diseases." Clin Pharmacol Ther **93**(1): 105-116.

Neelsen, K. J., I. M. Zanini, et al. (2013). "Oncogenes induce genotoxic stress by mitotic processing of unusual replication intermediates." J Cell Biol **200**(6): 699-708.

Nelson, G., J. Wordsworth, et al. (2012). "A senescent cell bystander effect: senescence-induced senescence." Aging Cell **11**(2): 345-349.

Nikota, J. K., P. Shen, et al. (2014). "Cigarette smoke primes the pulmonary environment to IL-1alpha/CXCR-2-dependent nontypeable Haemophilus influenzae-exacerbated neutrophilia in mice." J Immunol **193**(6): 3134-3145.

Nobukuni, S., K. Watanabe, et al. (2002). "Cigarette smoke inhibits the growth of lung fibroblasts from patients with pulmonary emphysema." Respirology **7**(3): 217-223.

Nocker, R. E., D. F. Schoonbrood, et al. (1996). "Interleukin-8 in airway inflammation in patients with asthma and chronic obstructive pulmonary disease." Int Arch Allergy Immunol **109**(2): 183-191.

Noureddine, H., G. Gary-Bobo, et al. (2011). "Pulmonary artery smooth muscle cell senescence is a pathogenic mechanism for pulmonary hypertension in chronic lung disease." Circ Res **109**(5): 543-553.

Nyunoya, T., M. M. Monick, et al. (2006). "Cigarette smoke induces cellular senescence." Am J Respir Cell Mol Biol **35**(6): 681-688.

Nyunoya, T., M. M. Monick, et al. (2009). "Cigarette smoke induces cellular senescence via Werner's syndrome protein down-regulation." Am J Respir Crit Care Med **179**(4): 279-287.

O'Shaughnessy, T. C., T. W. Ansari, et al. (1997). "Inflammation in bronchial biopsies of subjects with chronic bronchitis: inverse relationship of CD8+ T lymphocytes with FEV1." Am J Respir Crit Care Med **155**(3): 852-857.

Ogryzko, V. V., T. H. Hirai, et al. (1996). "Human fibroblast commitment to a senescence-like state in response to histone deacetylase inhibitors is cell cycle dependent." Mol Cell Biol **16**(9): 5210-5218.

Olovnikov, A. M. (1971). "[Principle of marginotomy in template synthesis of polynucleotides]." Dokl Akad Nauk SSSR **201**(6): 1496-1499.

Osorio, F. G., C. Barcena, et al. (2012). "Nuclear lamina defects cause ATM-dependent NF-kappaB activation and link accelerated aging to a systemic inflammatory response." Genes Dev **26**(20): 2311-2324.

Ovadya, Y. and V. Krizhanovsky (2014). "Senescent cells: SASPected drivers of age-related pathologies." Biogerontology.

Pahl, H. L. (1999). "Activators and target genes of Rel/NF-kappaB transcription factors." Oncogene **18**(49): 6853-6866.

Pang, J. H. and K. Y. Chen (1994). "Global change of gene expression at late G1/S boundary may occur in human IMR-90 diploid fibroblasts during senescence." J Cell Physiol **160**(3): 531-538.

Papi, A., G. Casoni, et al. (2004). "COPD increases the risk of squamous histological subtype in smokers who develop non-small cell lung carcinoma." Thorax **59**(8): 679-681.

Parrinello, S., J. P. Coppe, et al. (2005). "Stromal-epithelial interactions in aging and cancer: senescent fibroblasts alter epithelial cell differentiation." J Cell Sci **118**(Pt 3): 485-496.

Parrinello, S., E. Samper, et al. (2003). "Oxygen sensitivity severely limits the replicative lifespan of murine fibroblasts." Nat Cell Biol **5**(8): 741-747.

Passos, J. F., G. Nelson, et al. (2010). "Feedback between p21 and reactive oxygen production is necessary for cell senescence." Mol Syst Biol **6**: 347.

Passos, J. F., G. Saretzki, et al. (2007). "Mitochondrial dysfunction accounts for the stochastic heterogeneity in telomere-dependent senescence." PLoS Biol **5**(5): e110.

Pasteur, M. C., S. M. Helliwell, et al. (2000). "An investigation into causative factors in patients with bronchiectasis." Am J Respir Crit Care Med **162**(4 Pt 1): 1277-1284.

Patel, I. S., I. Vlahos, et al. (2004). "Bronchiectasis, exacerbation indices, and inflammation in chronic obstructive pulmonary disease." Am J Respir Crit Care Med **170**(4): 400-407.

Pesci, A., B. Balbi, et al. (1998). "Inflammatory cells and mediators in bronchial lavage of patients with chronic obstructive pulmonary disease." Eur Respir J **12**(2): 380-386.

Petersen, S., G. Saretzki, et al. (1998). "Preferential accumulation of single-stranded regions in telomeres of human fibroblasts." Exp Cell Res **239**(1): 152-160.

Pospelova, T. V., O. V. Leontieva, et al. (2012). "Suppression of replicative senescence by rapamycin in rodent embryonic cells." Cell Cycle **11**(12): 2402-2407.

Powers, R. W., 3rd, M. Kaeberlein, et al. (2006). "Extension of chronological life span in yeast by decreased TOR pathway signaling." Genes Dev **20**(2): 174-184.

Price, J. S., J. G. Waters, et al. (2002). "The role of chondrocyte senescence in osteoarthritis." Aging Cell **1**(1): 57-65.

Rabe, K. F., S. Hurd, et al. (2007). "Global strategy for the diagnosis, management, and prevention of chronic obstructive pulmonary disease: GOLD executive summary." Am J Respir Crit Care Med **176**(6): 532-555.

Raghu, G., D. Weycker, et al. (2006). "Incidence and prevalence of idiopathic pulmonary fibrosis." Am J Respir Crit Care Med **174**(7): 810-816.

Rahman, I. and I. M. Adcock (2006). "Oxidative stress and redox regulation of lung inflammation in COPD." Eur Respir J **28**(1): 219-242.

Rahman, I., A. A. van Schadewijk, et al. (2002). "4-Hydroxy-2-nonenal, a specific lipid peroxidation product, is elevated in lungs of patients with chronic obstructive pulmonary disease." Am J Respir Crit Care Med **166**(4): 490-495.

Rai, P., T. T. Onder, et al. (2009). "Continuous elimination of oxidized nucleotides is necessary to prevent rapid onset of cellular senescence." Proc Natl Acad Sci U S A **106**(1): 169-174.

Rajendrasozhan, S., S. R. Yang, et al. (2008). "SIRT1, an antiinflammatory and antiaging protein, is decreased in lungs of patients with chronic obstructive pulmonary disease." Am J Respir Crit Care Med **177**(8): 861-870.

Ramirez, R. D., C. P. Morales, et al. (2001). "Putative telomere-independent mechanisms of replicative aging reflect inadequate growth conditions." Genes Dev **15**(4): 398-403.

Ramos, F. J., S. C. Chen, et al. (2012). "Rapamycin reverses elevated mTORC1 signaling in lamin A/C-deficient mice, rescues cardiac and skeletal muscle function, and extends survival." Sci Transl Med **4**(144): 144ra103.

Richter, T. and T. von Zglinicki (2007). "A continuous correlation between oxidative stress and telomere shortening in fibroblasts." Exp Gerontol **42**(11): 1039-1042.

Rinaldi, M., K. Maes, et al. (2012). "Long-term nose-only cigarette smoke exposure induces emphysema and mild skeletal muscle dysfunction in mice." Dis Model Mech **5**(3): 333-341.

Ringshausen, F. C., A. de Roux, et al. (2013). "Bronchiectasis-associated hospitalizations in Germany, 2005-2011: a population-based study of disease burden and trends." PLoS One **8**(8): e71109.

Robida-Stubbs, S., K. Glover-Cutter, et al. (2012). "TOR signaling and rapamycin influence longevity by regulating SKN-1/Nrf and DAF-16/FoxO." Cell Metab **15**(5): 713-724.

Robles, S. J. and G. R. Adami (1998). "Agents that cause DNA double strand breaks lead to p16INK4a enrichment and the premature senescence of normal fibroblasts." Oncogene **16**(9): 1113-1123.

Rock, J. R., S. H. Randell, et al. (2010). "Airway basal stem cells: a perspective on their roles in epithelial homeostasis and remodeling." Dis Model Mech **3**(9-10): 545-556.

Rode, L., S. E. Bojesen, et al. (2013). "Short telomere length, lung function and chronic obstructive pulmonary disease in 46,396 individuals." Thorax **68**(5): 429-435.

Rodier, F. and J. Campisi (2011). "Four faces of cellular senescence." J Cell Biol **192**(4): 547-556.

Rodier, F., J. P. Coppe, et al. (2009). "Persistent DNA damage signalling triggers senescence-associated inflammatory cytokine secretion." Nat Cell Biol **11**(8): 973-979.

Rodier, F., D. P. Munoz, et al. (2011). "DNA-SCARS: distinct nuclear structures that sustain damage-induced senescence growth arrest and inflammatory cytokine secretion." J Cell Sci **124**(Pt 1): 68-81.

Rogakou, E. P., C. Boon, et al. (1999). "Megabase chromatin domains involved in DNA double-strand breaks in vivo." J Cell Biol **146**(5): 905-916.

Rogakou, E. P., D. R. Pilch, et al. (1998). "DNA double-stranded breaks induce histone H2AX phosphorylation on serine 139." J Biol Chem **273**(10): 5858-5868.

Romanov, V. S., M. V. Abramova, et al. (2010). "p21(Waf1) is required for cellular senescence but not for cell cycle arrest induced by the HDAC inhibitor sodium butyrate." Cell Cycle **9**(19): 3945-3955.

Roninson, I. B. (2003). "Tumor cell senescence in cancer treatment." Cancer Res **63**(11): 2705-2715.

Roper, J. M., D. J. Mazzatti, et al. (2004). "In vivo exposure to hyperoxia induces DNA damage in a population of alveolar type II epithelial cells." Am J Physiol Lung Cell Mol Physiol **286**(5): L1045-1054.

Rovillain, E., L. Mansfield, et al. (2011). "Activation of nuclear factor-kappa B signalling promotes cellular senescence." Oncogene **30**(20): 2356-2366.

Rufini, A., P. Tucci, et al. (2013). "Senescence and aging: the critical roles of p53." Oncogene **32**(43): 5129-5143.

Russell, R. E., S. V. Culpitt, et al. (2002). "Release and activity of matrix metalloproteinase-9 and tissue inhibitor of metalloproteinase-1 by alveolar macrophages from patients with chronic obstructive pulmonary disease." Am J Respir Cell Mol Biol **26**(5): 602-609.

Rycroft, C. E., A. Heyes, et al. (2012). "Epidemiology of chronic obstructive pulmonary disease: a literature review." Int J Chron Obstruct Pulmon Dis **7**: 457-494.

Sabatini, D. M., H. Erdjument-Bromage, et al. (1994). "RAFT1: a mammalian protein that binds to FKBP12 in a rapamycin-dependent fashion and is homologous to yeast TORs." Cell **78**(1): 35-43.

Saetta, M., S. Baraldo, et al. (1999). "CD8+ve cells in the lungs of smokers with chronic obstructive pulmonary disease." Am J Respir Crit Care Med **160**(2): 711-717.

Sagiv, A. and V. Krizhanovsky (2013). "Immunosurveillance of senescent cells: the bright side of the senescence program." Biogerontology **14**(6): 617-628.

Salem, A. F., M. S. Al-Zoubi, et al. (2013). "Cigarette smoke metabolically promotes cancer, via autophagy and premature aging in the host stromal microenvironment." Cell Cycle **12**(5): 818-825.

Sanders, Y. Y., H. Liu, et al. (2013). "Histone modifications in senescence-associated resistance to apoptosis by oxidative stress." Redox Biol **1**(1): 8-16.

Sarbassov, D. D., S. M. Ali, et al. (2006). "Prolonged rapamycin treatment inhibits mTORC2 assembly and Akt/PKB." Mol Cell **22**(2): 159-168.

Saretzki, G., M. P. Murphy, et al. (2003). "MitoQ counteracts telomere shortening and elongates lifespan of fibroblasts under mild oxidative stress." Aging Cell **2**(2): 141-143.

Sasaki, T., B. Maier, et al. (2006). "Progressive loss of SIRT1 with cell cycle withdrawal." Aging Cell **5**(5): 413-422.

Satoh, A., C. S. Brace, et al. (2013). "Sirt1 extends life span and delays aging in mice through the regulation of Nk2 homeobox 1 in the DMH and LH." Cell Metab **18**(3): 416-430.

Savale, L., A. Chaouat, et al. (2009). "Shortened telomeres in circulating leukocytes of patients with chronic obstructive pulmonary disease." Am J Respir Crit Care Med **179**(7): 566-571.

Schmitt, C. A., J. S. Fridman, et al. (2002). "A senescence program controlled by p53 and p16INK4a contributes to the outcome of cancer therapy." Cell **109**(3): 335-346.

Schulz, C., K. Wolf, et al. (2003). "Expression and release of interleukin-8 by human bronchial epithelial cells from patients with chronic obstructive pulmonary disease, smokers, and never-smokers." Respiration **70**(3): 254-261.

Sedelnikova, O. A., I. Horikawa, et al. (2004). "Senescing human cells and ageing mice accumulate DNA lesions with unrepairable double-strand breaks." Nat Cell Biol **6**(2): 168-170.

Seluanov, A., V. Gorbunova, et al. (2001). "Change of the death pathway in senescent human fibroblasts in response to DNA damage is caused by an inability to stabilize p53." Mol Cell Biol **21**(5): 1552-1564.

Serra, V., T. von Zglinicki, et al. (2003). "Extracellular superoxide dismutase is a major antioxidant in human fibroblasts and slows telomere shortening." J Biol Chem **278**(9): 6824-6830.

Serrano, M., G. J. Hannon, et al. (1993). "A new regulatory motif in cell-cycle control causing specific inhibition of cyclin D/CDK4." Nature **366**(6456): 704-707.

Serrano, M., A. W. Lin, et al. (1997). "Oncogenic ras provokes premature cell senescence associated with accumulation of p53 and p16INK4a." Cell **88**(5): 593-602.

Seshadri, T. and J. Campisi (1990). "Repression of c-fos transcription and an altered genetic program in senescent human fibroblasts." Science **247**(4939): 205-209.

Shah, P. P., G. Donahue, et al. (2013). "Lamin B1 depletion in senescent cells triggers large-scale changes in gene expression and the chromatin landscape." Genes Dev **27**(16): 1787-1799.

Shapiro, S. D., N. M. Goldstein, et al. (2003). "Neutrophil elastase contributes to cigarette smoke-induced emphysema in mice." Am J Pathol **163**(6): 2329-2335.

Shelton, D. N., E. Chang, et al. (1999). "Microarray analysis of replicative senescence." Curr Biol **9**(17): 939-945.

Shen, T. and S. Huang (2012). "The role of Cdc25A in the regulation of cell proliferation and apoptosis." Anticancer Agents Med Chem **12**(6): 631-639.

Sherr, C. J. (1994). "G1 phase progression: cycling on cue." Cell **79**(4): 551-555.

Shiloh, Y. (2003). "ATM and related protein kinases: safeguarding genome integrity." Nat Rev Cancer **3**(3): 155-168.

Shimi, T., V. Butin-Israeli, et al. (2011). "The role of nuclear lamin B1 in cell proliferation and senescence." Genes Dev **25**(24): 2579-2593.

Shioi, T., J. R. McMullen, et al. (2003). "Rapamycin attenuates load-induced cardiac hypertrophy in mice." Circulation **107**(12): 1664-1670.

Shivshankar, P., A. R. Boyd, et al. (2011). "Cellular senescence increases expression of bacterial ligands in the lungs and is positively correlated with increased susceptibility to pneumococcal pneumonia." Aging Cell **10**(5): 798-806.

Smogorzewska, A. and T. de Lange (2002). "Different telomere damage signaling pathways in human and mouse cells." EMBO J **21**(16): 4338-4348.

Soler, N., S. Ewig, et al. (1999). "Airway inflammation and bronchial microbial patterns in patients with stable chronic obstructive pulmonary disease." Eur Respir J **14**(5): 1015-1022.

Sone, H. and Y. Kagawa (2005). "Pancreatic beta cell senescence contributes to the pathogenesis of type 2 diabetes in high-fat diet-induced diabetic mice." Diabetologia **48**(1): 58-67.

Song, W., J. Zhao, et al. (2001). "Interleukin-6 in bronchoalveolar lavage fluid from patients with COPD." Chin Med J (Engl) **114**(11): 1140-1142.

Spallarossa, P., P. Altieri, et al. (2010). "p38 MAPK and JNK antagonistically control senescence and cytoplasmic p16INK4A expression in doxorubicin-treated endothelial progenitor cells." PLoS One **5**(12): e15583.

Spilman, P., N. Podlutskaya, et al. (2010). "Inhibition of mTOR by rapamycin abolishes cognitive deficits and reduces amyloid-beta levels in a mouse model of Alzheimer's disease." PLoS One **5**(4): e9979.

Stein, G. H., M. Beeson, et al. (1990). "Failure to phosphorylate the retinoblastoma gene product in senescent human fibroblasts." Science **249**(4969): 666-669.

Stein, G. H., L. F. Drullinger, et al. (1991). "Senescent cells fail to express cdc2, cycA, and cycB in response to mitogen stimulation." Proc Natl Acad Sci U S A **88**(24): 11012-11016.

Stein, G. H., L. F. Drullinger, et al. (1999). "Differential roles for cyclin-dependent kinase inhibitors p21 and p16 in the mechanisms of senescence and differentiation in human fibroblasts." Mol Cell Biol **19**(3): 2109-2117.

Storer, M., A. Mas, et al. (2013). "Senescence is a developmental mechanism that contributes to embryonic growth and patterning." Cell **155**(5): 1119-1130.

Stucki, M. and S. P. Jackson (2006). "gammaH2AX and MDC1: anchoring the DNA-damage-response machinery to broken chromosomes." DNA Repair (Amst) **5**(5): 534-543.

Suga, T., M. Kurabayashi, et al. (2000). "Disruption of the klotho gene causes pulmonary emphysema in mice. Defect in maintenance of pulmonary integrity during postnatal life." Am J Respir Cell Mol Biol **22**(1): 26-33.

Suram, A. and U. Herbig (2014). "The replicometer is broken: telomeres activate cellular senescence in response to genotoxic stresses." Aging Cell.

Suram, A., J. Kaplunov, et al. (2012). "Oncogene-induced telomere dysfunction enforces cellular senescence in human cancer precursor lesions." EMBO J **31**(13): 2839-2851.

Takahashi, A., N. Ohtani, et al. (2006). "Mitogenic signalling and the p16INK4a-Rb pathway cooperate to enforce irreversible cellular senescence." Nat Cell Biol **8**(11): 1291-1297.

Takai, H., A. Smogorzewska, et al. (2003). "DNA damage foci at dysfunctional telomeres." Curr Biol **13**(17): 1549-1556.

Takizawa, H., M. Tanaka, et al. (2001). "Increased expression of transforming growth factor-beta1 in small airway epithelium from tobacco smokers and patients with chronic obstructive pulmonary disease (COPD)." Am J Respir Crit Care Med **163**(6): 1476-1483.

Tchkonia, T., Y. Zhu, et al. (2013). "Cellular senescence and the senescent secretory phenotype: therapeutic opportunities." J Clin Invest **123**(3): 966-972.

te Poele, R. H., A. L. Okorokov, et al. (2002). "DNA damage is able to induce senescence in tumor cells in vitro and in vivo." Cancer Res **62**(6): 1876-1883.

Tilstra, J. S., A. R. Robinson, et al. (2012). "NF-kappaB inhibition delays DNA damage-induced senescence and aging in mice." J Clin Invest **122**(7): 2601-2612.

Tissenbaum, H. A. and L. Guarente (2001). "Increased dosage of a sir-2 gene extends lifespan in Caenorhabditis elegans." Nature **410**(6825): 227-230.

Toledo, F. and G. M. Wahl (2006). "Regulating the p53 pathway: in vitro hypotheses, in vivo veritas." Nat Rev Cancer **6**(12): 909-923.

Trougakos, I. P., A. Saridaki, et al. (2006). "Identification of differentially expressed proteins in senescent human embryonic fibroblasts." Mech Ageing Dev **127**(1): 88-92.

Tsuji, T., K. Aoshiba, et al. (2004). "Cigarette smoke induces senescence in alveolar epithelial cells." Am J Respir Cell Mol Biol **31**(6): 643-649.

Tsuji, T., K. Aoshiba, et al. (2006). "Alveolar cell senescence in patients with pulmonary emphysema." Am J Respir Crit Care Med **174**(8): 886-893.

Tsuji, T., K. Aoshiba, et al. (2010). "Alveolar cell senescence exacerbates pulmonary inflammation in patients with chronic obstructive pulmonary disease." Respiration **80**(1): 59-70.

Tzortzaki, E. G., K. Dimakou, et al. (2012). "Oxidative DNA damage and somatic mutations: a link to the molecular pathogenesis of chronic inflammatory airway diseases." Chest **141**(5): 1243-1250.

Uziel, T., Y. Lerenthal, et al. (2003). "Requirement of the MRN complex for ATM activation by DNA damage." EMBO J **22**(20): 5612-5621.

Valdes, A. M., T. Andrew, et al. (2005). "Obesity, cigarette smoking, and telomere length in women." Lancet **366**(9486): 662-664.

van den Bosch, M., R. T. Bree, et al. (2003). "The MRN complex: coordinating and mediating the response to broken chromosomes." EMBO Rep **4**(9): 844-849.

van Deursen, J. M. (2014). "The role of senescent cells in ageing." Nature **509**(7501): 439-446.

van Steensel, B., A. Smogorzewska, et al. (1998). "TRF2 protects human telomeres from end-to-end fusions." Cell **92**(3): 401-413.

Vasile, E., Y. Tomita, et al. (2001). "Differential expression of thymosin beta-10 by early passage and senescent vascular endothelium is modulated by VPF/VEGF: evidence for senescent endothelial cells in vivo at sites of atherosclerosis." FASEB J **15**(2): 458-466.

Vassallo, P. F., S. Simoncini, et al. (2014). "Accelerated senescence of cord blood endothelial progenitor cells in premature neonates is driven by SIRT1 decreased expression." Blood **123**(13): 2116-2126.

Vaziri, H., M. D. West, et al. (1997). "ATM-dependent telomere loss in aging human diploid fibroblasts and DNA damage lead to the post-translational activation of p53 protein involving poly(ADP-ribose) polymerase." EMBO J **16**(19): 6018-6033.

Vellai, T., K. Takacs-Vellai, et al. (2003). "Genetics: influence of TOR kinase on lifespan in C. elegans." Nature **426**(6967): 620.

Vera, E., B. Bernardes de Jesus, et al. (2013). "Telomerase reverse transcriptase synergizes with calorie restriction to increase health span and extend mouse longevity." PLoS One **8**(1): e53760.

Vezina, C., A. Kudelski, et al. (1975). "Rapamycin (AY-22,989), a new antifungal antibiotic. I. Taxonomy of the producing streptomycete and isolation of the active principle." J Antibiot (Tokyo) **28**(10): 721-726.

von Zglinicki, T. (2002). "Oxidative stress shortens telomeres." Trends Biochem Sci **27**(7): 339-344.

von Zglinicki, T., R. Pilger, et al. (2000). "Accumulation of single-strand breaks is the major cause of telomere shortening in human fibroblasts." <u>Free Radic Biol Med</u> **28**(1): 64-74.

von Zglinicki, T., G. Saretzki, et al. (1995). "Mild hyperoxia shortens telomeres and inhibits proliferation of fibroblasts: a model for senescence?" <u>Exp Cell Res</u> **220**(1): 186-193.

Waaijer, M. E., W. E. Parish, et al. (2012). "The number of p16INK4a positive cells in human skin reflects biological age." <u>Aging Cell</u> **11**(4): 722-725.

Wada, T., N. Joza, et al. (2004). "MKK7 couples stress signalling to G2/M cell-cycle progression and cellular senescence." <u>Nat Cell Biol</u> **6**(3): 215-226.

Waga, S., G. J. Hannon, et al. (1994). "The p21 inhibitor of cyclin-dependent kinases controls DNA replication by interaction with PCNA." <u>Nature</u> **369**(6481): 574-578.

Walters, M. S., B. P. De, et al. (2014). "Smoking accelerates aging of the small airway epithelium." <u>Respir Res</u> **15**(1): 94.

Wang, B., S. Matsuoka, et al. (2002). "53BP1, a mediator of the DNA damage checkpoint." <u>Science</u> **298**(5597): 1435-1438.

Wang, C., D. Jurk, et al. (2009). "DNA damage response and cellular senescence in tissues of aging mice." <u>Aging Cell</u> **8**(3): 311-323.

Wang, C., M. Maddick, et al. (2010). "Adult-onset, short-term dietary restriction reduces cell senescence in mice." <u>Aging (Albany NY)</u> **2**(9): 555-566.

Wang, E. (1995). "Senescent human fibroblasts resist programmed cell death, and failure to suppress bcl2 is involved." <u>Cancer Res</u> **55**(11): 2284-2292.

Wang, J., Q. Sun, et al. (2012). "A differentiation checkpoint limits hematopoietic stem cell self-renewal in response to DNA damage." <u>Cell</u> **148**(5): 1001-1014.

Wang, X. Q., J. L. Redpath, et al. (2006). "ATR dependent activation of Chk2." <u>J Cell Physiol</u> **208**(3): 613-619.

Watson, J. D. (1972). "Origin of concatemeric T7 DNA." <u>Nat New Biol</u> **239**(94): 197-201.

Webley, K., J. A. Bond, et al. (2000). "Posttranslational modifications of p53 in replicative senescence overlapping but distinct from those induced by DNA damage." <u>Mol Cell Biol</u> **20**(8): 2803-2808.

Weibel, E. R. (1963). "Principles and methods for the morphometric study of the lung and other organs." <u>Lab Invest</u> **12**: 131-155.

Weinberg, R. A. (1995). "The retinoblastoma protein and cell cycle control." <u>Cell</u> **81**(3): 323-330.

West, M. D., O. M. Pereira-Smith, et al. (1989). "Replicative senescence of human skin fibroblasts correlates with a loss of regulation and overexpression of collagenase activity." <u>Exp Cell Res</u> **184**(1): 138-147.

Wilkinson, J. E., L. Burmeister, et al. (2012). "Rapamycin slows aging in mice." <u>Aging Cell</u> **11**(4): 675-682.

Willemse, B. W., N. H. ten Hacken, et al. (2005). "Effect of 1-year smoking cessation on airway inflammation in COPD and asymptomatic smokers." <u>Eur Respir J</u> **26**(5): 835-845.

Williams, G. C. (1957). "Pleiotropy, natural selection, and the evolution of senescence " <u>Evolution </u>**11**: 398-411.

Wong, K. K., R. S. Maser, et al. (2003). "Telomere dysfunction and Atm deficiency compromises organ homeostasis and accelerates ageing." <u>Nature</u> **421**(6923): 643-648.

Wu, J. J., J. Liu, et al. (2013). "Increased mammalian lifespan and a segmental and tissue-specific slowing of aging after genetic reduction of mTOR expression." Cell Rep **4**(5): 913-920.

Wu, Z. H., Y. Shi, et al. (2006). "Molecular linkage between the kinase ATM and NF-kappaB signaling in response to genotoxic stimuli." Science **311**(5764): 1141-1146.

Xiong, Y., G. J. Hannon, et al. (1993). "p21 is a universal inhibitor of cyclin kinases." Nature **366**(6456): 701-704.

Xiong, Y., H. Zhang, et al. (1992). "D type cyclins associate with multiple protein kinases and the DNA replication and repair factor PCNA." Cell **71**(3): 505-514.

Xue, W., L. Zender, et al. (2007). "Senescence and tumour clearance is triggered by p53 restoration in murine liver carcinomas." Nature **445**(7128): 656-660.

Yang, S. R., J. Wright, et al. (2007). "Sirtuin regulates cigarette smoke-induced proinflammatory mediator release via RelA/p65 NF-kappaB in macrophages in vitro and in rat lungs in vivo: implications for chronic inflammation and aging." Am J Physiol Lung Cell Mol Physiol **292**(2): L567-576.

Yao, H., S. Chung, et al. (2012). "SIRT1 protects against emphysema via FOXO3-mediated reduction of premature senescence in mice." J Clin Invest **122**(6): 2032-2045.

Yao, H., I. K. Sundar, et al. (2013). "P21-PARP-1 pathway is involved in cigarette smoke-induced lung DNA damage and cellular senescence." PLoS One **8**(11): e80007.

Yao, H., S. R. Yang, et al. (2008). "Disruption of p21 attenuates lung inflammation induced by cigarette smoke, LPS, and fMLP in mice." Am J Respir Cell Mol Biol **39**(1): 7-18.

Yeung, F., J. E. Hoberg, et al. (2004). "Modulation of NF-kappaB-dependent transcription and cell survival by the SIRT1 deacetylase." EMBO J **23**(12): 2369-2380.

Yoshida, T., I. Mett, et al. (2010). "Rtp801, a suppressor of mTOR signaling, is an essential mediator of cigarette smoke-induced pulmonary injury and emphysema." Nat Med **16**(7): 767-773.

Young, R. P. and R. J. Hopkins (2010). "Link between COPD and lung cancer." Respir Med **104**(5): 758-759.

Zeman, M. K. and K. A. Cimprich (2014). "Causes and consequences of replication stress." Nat Cell Biol **16**(1): 2-9.

Zhang, H., K. H. Pan, et al. (2003). "Senescence-specific gene expression fingerprints reveal cell-type-dependent physical clustering of up-regulated chromosomal loci." Proc Natl Acad Sci U S A **100**(6): 3251-3256.

Zhang, J., C. R. Pickering, et al. (2006). "p16INK4a modulates p53 in primary human mammary epithelial cells." Cancer Res **66**(21): 10325-10331.

Zhang, R., W. Chen, et al. (2007). "Molecular dissection of formation of senescence-associated heterochromatin foci." Mol Cell Biol **27**(6): 2343-2358.

Zhang, R., M. V. Poustovoitov, et al. (2005). "Formation of MacroH2A-containing senescence-associated heterochromatin foci and senescence driven by ASF1a and HIRA." Dev Cell **8**(1): 19-30.

Zhou, F., S. Onizawa, et al. (2011). "Epithelial cell senescence impairs repair process and exacerbates inflammation after airway injury." Respir Res **12**: 78.

Zhu, J., D. Woods, et al. (1998). "Senescence of human fibroblasts induced by oncogenic Raf." <u>Genes Dev</u> **12**(19): 2997-3007.

Zou, L. and S. J. Elledge (2003). "Sensing DNA damage through ATRIP recognition of RPA-ssDNA complexes." <u>Science</u> **300**(5625): 1542-1548.